DISSERTATION

NUMERICAL MODEL FOR SEDIMENT FLUSHING AT THE NAKDONG RIVER ESTUARY BARRAGE

Submitted by

Un Ji

Department of Civil and Environmental Engineering

In partial fulfillment of the requirements

For the Degree of Doctor of Philosophy

Colorado State University

Fort Collins, Colorado

Fall 2006

COLORADO STATE UNIVERSITY

October 20, 2006

WE HEREBY RECOMMEND THAT THE DISSERTATION PREPARED UNDER OUR SUPERVISION BY UN JI ENTITLED NUMERICAL MODEL FOR SEDIMENT FLUSHING AT THE NAKDONG RIVER ESTUARY BARRAGE AS FULFILLING IN PART REQUIREMENTS FOR THE DEGREE DOCTOR OF PHILOSOPHY.

Committee on Graduate Work

Dr. Chester C. Watson

Dr. Chih T. Yang

Dr. Ellen E. Wohl

Dr. Pierre Y. Julien
(Advisor)

Dr. Luis A. Garcia
(Department Head)

ABSTRACT OF DISSERTATION

NUMERICAL MODEL FOR SEDIMENT FLUSHING
AT THE NAKDONG RIVER ESTUARY BARRAGE

The Nakdong River is located in the southeastern region of South Korea and flows 521.5 km from the Taebaek Mountains to the East Sea. The Nakdong River is the second largest river in Korea and flows through major cities, including Daegu and Busan. The Nakdong River Estuary Barrage (NREB), a hydraulic structure, was built in 1983-87 at the river mouth to prevent salt-water intrusion. The upstream channel of the NREB near Busan has experienced sedimentation problems requiring annual dredging operation after the construction. The main purpose of sediment dredging is to prevent flooding during late summer. According to the past records, the annual average dredging volume is about 665,000 m^3 in the upstream channel of the NREB.

This dissertation documents the evaluation and development of sediment control and flushing methods that reduce and possibly eliminate the need for dredging operations at the NREB. Two numerical models, a steady state model and a quasi-steady state model with variable discharge, were developed. The upstream model simulation spans 40 km upstream of the NREB. This model simulates sediment transport capacity and bed elevation changes.

Sediment flushing curves have been developed with respect to upstream discharge and downstream flow depth using the steady state model. The analysis of flushing curves and past records of annual dredging sediments (665,000 m^3) indicate that sediment flushing is possible at the NREB.

Annual simulation scenarios of sediment flushing are developed and analyzed based on flow, stage, and tide level data to evaluate the feasibility of the flushing technique. Annual simulations for the period from 1998 to 2003 were performed using the quasi-steady state model. Flushing simulation results indicate that an average 54% of the annual dredging volume with redeposition in the upstream bed can be eliminated by flushing, with the maximum amount of flushing being 80% in the 2003 simulation. The total flushed amount of sediment without redeposition should be in excess of the annual dredging volume. Therefore, sediment flushing controlled by water level operations including tidal effects should be effective at NREB. Optimization and generalization of the sediment flushing procedure can be accomplished by comparing steady-state sediment flushing curves, flow duration curves from 1998 to 2003, and quasi-steady state sediment flushing simulations based on a numerical model.

Simulations of sediment transport and water level variations with and without dredging operations are conducted. Quasi-steady state simulations indicate that at high flow, the water level differences with and without dredging are very small. However, water level changes can be significant at low flow because of tidal effects. Numerical simulations indicate that the sediment deposits can be effectively sluiced during the early flood season without sediment dredging. It is also found that the absence of dredging operations at the NREB would not cause significant water level changes against the levees during major floods.

The effects of the sediment flushing technique on the sediment concentration changes are examined. Higher sediment concentrations generally occur during the early flood season. The average increase in sediment concentration by the flushing technique

is not significant. The differences between flushing and non-flushing simulations are 58.8 ppm in 2002 and 49.5 ppm in 2003. However, flushing will increase peak sediment concentration. For example, the maximum sediment concentration difference between flushing and non-flushing simulations at a discharge of 1,924 cms in 2002 is 911.3 ppm.

Un Ji
Civil and Environmental Engineering Department
Colorado State University
Fort Collins, CO 80523
Fall 2006

ACKNOWLEDGEMENTS

I would like to thank my advisor Dr. Pierre Julien for the support, guidance, and encouragement throughout my time at CSU. I also would like to extend my appreciation to my committee members; Dr. Chester Watson, Dr. Ted Yang, and Dr. Ellen Wohl for their helpful comments and generous assistance during my study.

My deepest thanks go to Max Shih, Seema Shah-Fairbank, and Mark Velleux not only for their support and encouragement throughout my studies but also for their true friendship. They have made my life at CSU wonderful and successful. I would also like to extend my appreciation to other members of Dr. Julien's Dream Team; James Halgren, Hyunsik Kim, Jaehoon Kim, Amanda Larsen, Kyoungmo Lim, and Youngho Shin. In addition, I would like to thank Korean visiting professors; Dr. Sangkil Park, Dr. Hyunsuk Shin, and Dr. Sukhwan Jang. Special thanks to Seema Shah-Fairbank, Amanda Larsen, and David Dust for reviewing my draft and Amanda Cox for providing graphs for this study. I also would like to thank other CSU members including Jenifer Davis, Laurie Alburn, Linda Hinshaw, Mary Casey, Gloria Garza, and Karen Holm for their patience and kindness to my questions. My deepest thanks extends to Jeehyun Yoo for her friendship and prayers for me. Jeehyun! You are more than just a friend. Thanks to all colleagues and friends whom I met in Fort Collins.

I would also like to thank the Myoungji University, Dr. Jungho Sonu, Dr. Woonkwang Yeo, Dr. Chongkun Pyun, and Dr. Byungman Yoon who supported and provided the opportunity to study at CSU.

Finally, I would like to thank my family including Youjung, Sanghwa, Ian, Hyoung, especially my mom and dad for their unconditional love and support, I love you. Thanks to my boyfriend, Yoonsung for the support, love, and patience to wait for me in Korea since summer 2003.

Lord God! Thank you for giving me everything I could ever want and much more.

TABLE OF CONTENTS

LIST OF FIGURES

LIST OF TABLES

LIST OF SYMBOLS

A	channel cross sectional area
c	celerity
c_B	Brownlie equation coefficient
C	Chezy coefficient
$C, C_{ppm}, C_{mg/l}$	sediment concentration
d_*	dimensionless particle diameter
d_s, d_{50}	grain size
D	diffusion coefficient
f	Darcy-Weisbach friction factor
Fr	Froude number
g	gravity acceleration
G	specific gravity
h	flow depth
h_c	critical depth
h_n	normal depth
H	water stage
L	total length of the reservoir
n	Manning coefficient
p_o	porosity of bed material
q	unit discharge

$\hat{q}_{tx}$, $\hat{q}_{ty}$, $\hat{q}_{tz}$	total unit sediment discharge
Q, Q_p, Q_m	flow discharge, peak flow discharge, minimum peak flow discharge
Q_s	sediment discharge
R_b	hydraulic radius related to the bed
R_h	hydraulic radius
S_0	bed slope
S_f	friction slope
t	time
T	transport-stage parameter
T_w	top width
T_E, T_{Ei}	trap efficiency
u_*	shear velocity
v_x , $v_{y,}$, v_z	flow velocity in the x-, y-, and z-direction
V	cross section averaged velocity
V_c	critical velocity
W	channel width
X	distance
X_c, X_{ci}	settling distance
γ_{mdl}	dry specific weight of sediment deposits
γ_s	specific weight of particle
α	weighting factor

β	resistance exponent
$\varepsilon_x, \varepsilon_y, \varepsilon_z$	dispersion (mixing) coefficient
ν	kinematic viscosity
ν_m	fluid mixture kinematic viscosity
ρ	mass density of water
ρ_m	fluid mixture mass density of water
ω, ω_i	fall velocity
σ_g	geometric standard deviation of the bed material
τ_*	Shields parameter
τ_{*c}	Shields dimensionless critical shear stress
τ_0	bed shear stress
τ_c	critical shear stress

CHAPTER 1: INTRODUCTION

1.1 LOWER NAKDONG RIVER AND NAKDONG RIVER ESTUARY BARRAGE

The Nakdong River is located in the southeastern region of South Korea and has a drainage area of about 23,817 square kilometers (KOWACO, 2003). The Lower Nakdong River is affected by annual frequent typhoons and has large floods with high water levels from June to September. The strongest typhoon to ever reach the Korean Peninsula was Typhoon Rusa (Kim et al., 2004). It occurred on August 31, 2002 and resulted in record precipitation and flooding in South Korea. The floods caused by Typhoon Rusa killed 213 people and left another 33 missing. The estimated damage caused by the typhoon was approximately $5.5 billion. Typhoon Maemi, on September 12, 2003, was another catastrophic typhoon that hit South Korea. It caused widespread damage from the Nakdong River basin to the port of Busan in populated areas in the southeastern part of the peninsula. More than 110 people were killed in Korea. The Gupo Bridge collapsed and about 18,000 buildings were either destroyed or damaged by the typhoon (Ji and Julien, 2005). Also, the estimated damage caused by Typhoon Maemi was approximately $4 billion.

Near the Nakdong Estuary, there are wetlands, sand islands and deltas, which provide an ideal habitat for migratory birds and waterfowls. The Nakdong River Estuary Barrage (NREB) was built in 1983-87 near the Eulsuk Island to prevent salt-water intrusion in the estuary. The 2.3-km-long barrage includes 510 m of 10 gates section and 1,720 m of a closed dam section with a navigation lock, fish ladder, and other related structures. The NREB provides the control of the upstream water level and the local road for auto-traffic, and prevents salt-water intrusion into the Lower Nakdong River.

Since the construction of the barrage, the Lower Nakdong River has experienced sedimentation problems requiring dredging. The main purpose of dredging sediments is to maintain the flood conveyance capacity of the upstream channel on the Lower Nakdong River during typhoons and floods, which are coupled with high water levels. Historical records indicate an average of 665,000 m^3 per year of dredging with an annual cost estimated at $2 million. The material dredged is primarily non-cohesive fine sand. Most of the sedimentation occurs after floods and during low flows. The gates cause a backwater effects upstream of the barrage, which results in sediment deposition.

1.2 OBJECTIVES

To reduce and possibly eliminate the dredging operation at the NREB, sediment routing and flushing methods can be substituted as a control method. Therefore, numerical modeling is required to simulate and analyze the feasibility of these methods. The main objectives of this research are to:

1) use a numerical model to develop sediment flushing curves to describe the flushed sediment volumes at a given discharge and flow depth,
2) examine the feasibility of sediment flushing at the NREB using numerical model calibrated with field data,
3) determine water surface changes with and without dredging, and
4) analyze sediment flushing effects on sediment concentration.

1.3 APPROACH AND METHODOLOGY

The primary purpose of the model is to simulate the sediment deposition and to quantify the possible amounts of sluiced sediments under different conditions considering the flow rate and tidal effects. This model is based on available field data. The model reach is sufficiently long to describe the backwater effects, which is up to 40 km upstream of the NREB. Also, the sediment transport rate and bed elevation changes are simulated by a numerical model. The upstream boundary condition was determined from the stream gauging records of Samryangjin Station. The downstream boundary condition was determined by the water level of the NREB, while considering the gate operations and tidal records. The steady state model was used to determine sediment deposition and flushing under constant upstream discharge and downstream water depth. A quasi-steady state model with variable discharge was developed to analyze the different gate operation strategies to effectively sluice the sediment without dredging operation. This model was calibrated, validated and applied for a five year period, which included major typhoons. The modeling results were used primarily to evaluate the present dredging operation and to analyze the feasibility of sediment flushing.

This dissertation consists of seven chapters. An introduction is presented in Chapter 1. Chapter 2 presents a literature review for the reservoir sedimentation, the control methods for reservoir sedimentation, and previous studies about sediment flushing. The site descriptions and characteristics of the Lower Nakdong River and NREB are described in Chapter 3. The numerical model development and methods are documented in Chapter 4. Chapters 5 and 6 describe numerical simulation results of the steady state model and the quasi-steady state model with variable discharge. Finally, Chapter 7 presents the conclusions of this study.

CHAPTER 2: LITERATURE REVIEW

About 1% of the total storage capacity in the world's reservoirs is lost annually due to sedimentation (Mahmood, 1987 and Yoon, 1992). This amount is equal to replacing approximately 300 large dams annually worldwide, at an estimated cost of $ 9 billion to replace existing storage capacity (Annandale, 2001). Similarly, flood conveyance and navigation capacity of the Lower Nakdong River has been lost due to sedimentation and the annual cost of sediment dredging has been $ 2 million. This chapter presents a literature review of reservoir sedimentation studies with focus on dredging and flushing operations.

2.1 RESERVOIR SEDIMENTATION

2.1.1 Reservoir sediment deposition

Sediment particles are transported by flows and deposit throughout a reservoir due to decreased velocities. Typical flows and deposition type are shown in Figure 2-1. The longitudinal deposition consists of three main zones; *Topset bed, Foreset bed,* and *Bottomset bed* (Morris and Fan, 1997). The coarse and fine material form delta deposits of *Topset bed* and *Bottomset bed.* The finer particles are carried by density current. The slope of *Foreset bed* depends on the particles of deltas. Deltas of coarse material have steeper slopes than deltas of fine material.

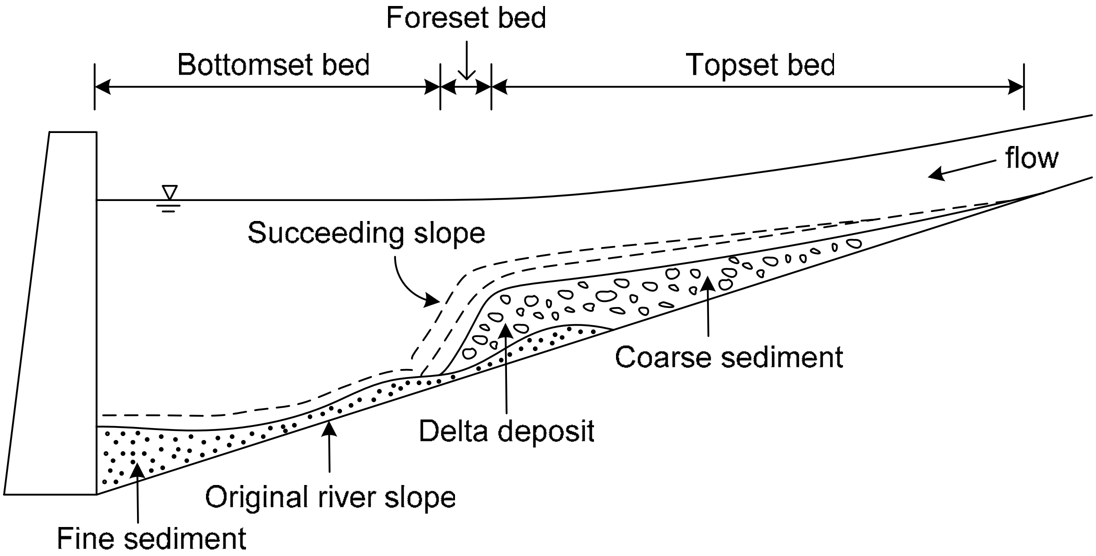

Figure 2-1. Typical flow and deposition of reservoir

Borland (1971) examined the relationship between *Topset bed* slope and original stream slope of a reservoir delta. He used field measurements of existing reservoirs and found that *Topset* slope is approximately one-half of the original bed slope. However, there are many variations in slope and shape of delta formations under different condition. Thus, numerical modeling and empirical methods using geometric data are necessary to estimate reservoir sedimentation. To determine reservoir sediment deposition patterns, Borland and Miller (1962) and Borland (1975) presented the area increment method and empirical relationship using field data of 30 reservoirs in the U.S. Mathematical and numerical models regarding sediment deposition patterns of a reservoir were studied by Frenette and Julien (1986), Graf (1971 and 1984), Lopez (1978), Rice (1981), Simons et al. (1982), and Yücel and Graf (1973). Fan and Morris (1992a) described the patterns of sediment deposition using field measurements from China and described four general types of longitudinal deposit geometries.

In 1997, Morris and Fan presented the four general types of longitudinal deposits, which are shown in Figure 2-2. Delta type has a mainly coarse fraction of inflowing sediment or a large fraction of finer sediment such as silt. If sediment deposition occurs in high sediment laden flows or small reservoirs which have a large inflow of fine sediment, the deposition pattern is a wedge-shaped. If the water is passed regularly through the gate of a reservoir or barrage, the apex of the delta migrates to the dam and the deposition appears wedge-shaped, which is considered as the equilibrium state for certain reservoirs over a long time period (Lai and Shen, 1996). Tapering deposits are a common pattern in a long reservoir which has fine deposition, and uniform deposits can be found in a narrow reservoir with frequent water fluctuation and a small load of fine sediments.

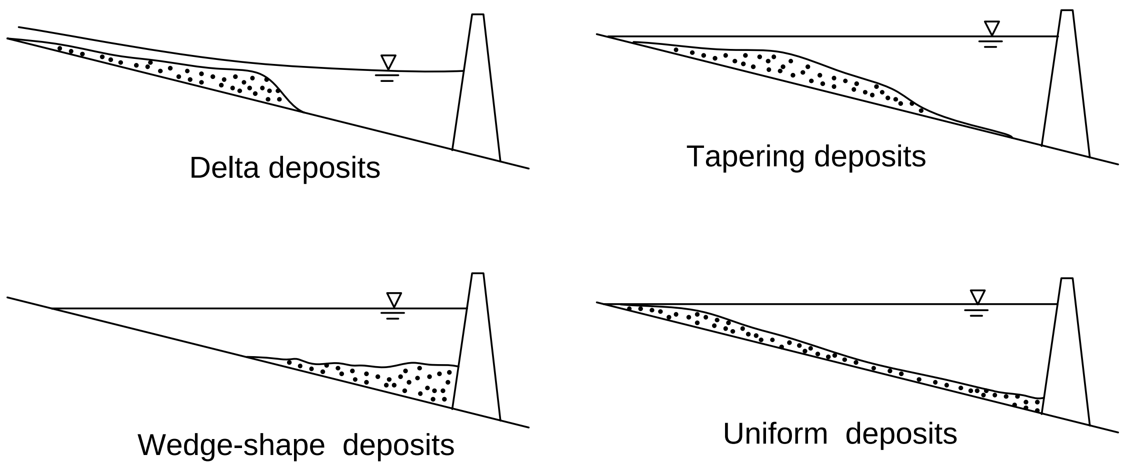

Figure 2-2. Basic types of longitudinal deposit

These geometries depend on inflowing sediment characteristics and reservoir operation (Morris and Fan, 1997). However, the deposition pattern of reservoir sedimentation in nature is more complex by the interaction between water discharge, particle size of sediments, geometry, and reservoir operation.

2.1.2 Reservoir trap efficiency

To predict the amount of sediment deposits in reservoirs, the trap efficiency has been widely used. Trap efficiency is the ratio of the deposited sediments to the total inflowing sediments. It depends on several factors such as particle size, sediment load, flow characteristics, and detention time, which can change due to reservoir operations and characteristics. Churchill (1948) and Brune (1953) provided empirical methods to determine the trap efficiency. Brune (1953) developed the empirical relationship using field records from 44 reservoirs in the U.S. Brune's method presents the relationship between the sediment trapped in percent and the capacity inflow ratio (Figure 2-3).

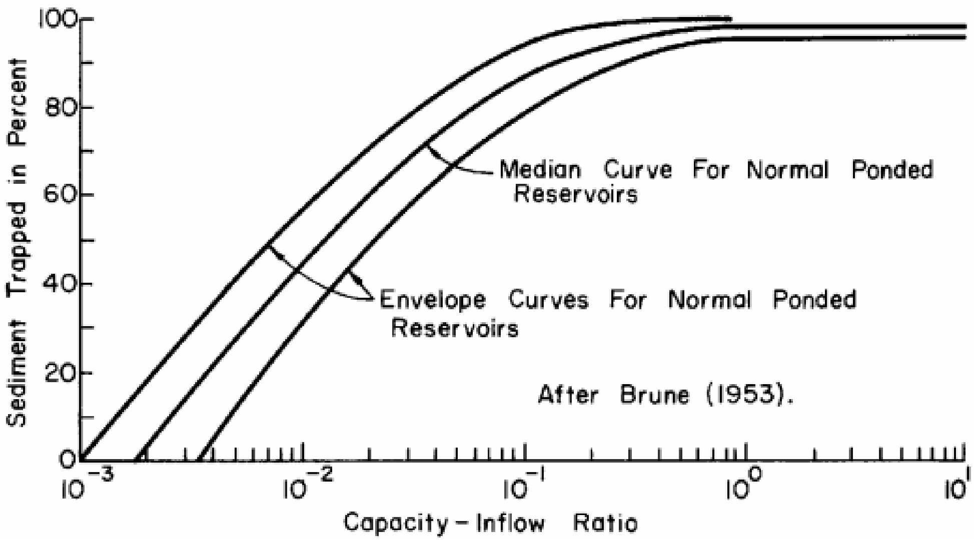

Figure 2-3. Brune's curve for trap efficiency

The capacity inflow ratio is based on the mean annual water inflow. Due to the very limited data, Borland (1971) indicated that Brune's curve is not recommended for use on desilting basins, flood retarding structures, or semidry reservoirs; however, the Churchill curve is more applicable for estimating the trap efficiency for desilting basins and semidry reservoirs.

Churchill (1948) presented a logarithmic relationship using reservoir data from the Tennessee Valley Authority. His analysis relates the percentage of incoming sediments passing through a reservoir to the sedimentation index of a reservoir (Figure 2-4). The sediment index is the ratio of the retention time to the mean velocity of water through the reservoir. The retention time is calculated as the reservoir capacity (cubic feet) divided by the mean daily inflow (cubic feet per second).

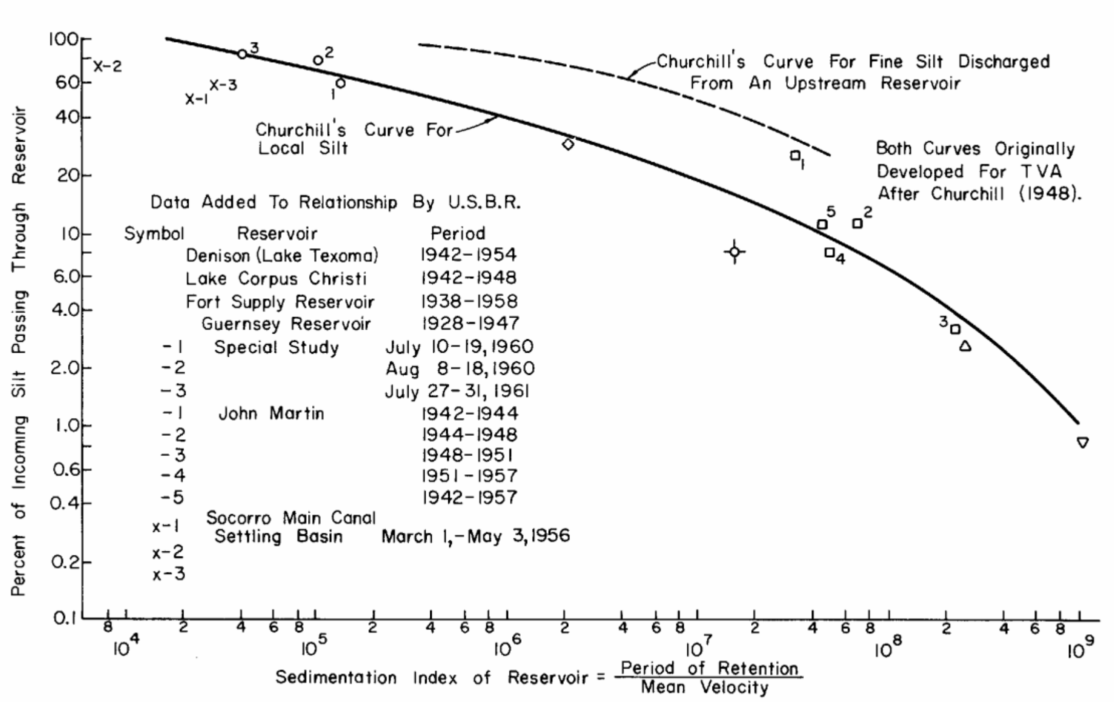

Figure 2-4. Churchill's curve for trap efficiency

Alternative methods for estimating the trap efficiency have been developed by Brown (1958), Chen (1975), Karaushev (1966) and Borland (1971). Brown (1958) suggested that sediment trapped in percent is related to the ratio of the original storage capacity of a reservoir and the watershed area. Chen (1975) developed a sediment trap efficiency curve relating the ratio of basin area and outflow rate to the different particle sizes. Karaushev (1966) developed a trap efficiency equation for a specific size category of sediment calculated from actual data. This method is based on theoretical derivation and empirical observation. Borland (1971) introduced a new procedure to compute the trap efficiency applying the fraction of deposited material and the settling velocity of the suspended material as follows:

$$T_E = 1 - e^{\frac{-1.055 L\omega}{Vh}} \tag{2.1}$$

where T_E = trap efficiency

L = total length of the reservoir

ω = fall velocity of the sediment

V = cross section averaged velocity

h = flow depth

Julien (1998) presented the similar equation for the trap efficiency with the percentage of settled sediment fraction i within a given distance X and the distance X_{C_i} to settle the 99% of sediment in suspension:

$$T_{Ei} = 1 - e^{\frac{-X\omega_i}{Vh}} \tag{2.2}$$

$$X_{C_i} = 4.6 \frac{Vh}{\omega_i} \tag{2.3}$$

where T_{Ei} = trap efficiency

ω_i = fall velocity of the sediment fraction i

Also, as part of a sedimentation study of the Peligre Reservoir in Haiti, Frenette and Julien (1986) found that the Brune, Churchill, and other empirical methods underestimated trap efficiencies compared to actual measurements. Julien (1998) suggests that careful consideration is needed when calculating trap efficiencies for silt and clay particles because of density currents and possible flocculation effects.

2.2 CONTROL METHODS FOR RESERVOIR SEDIMENTATION

To maintain the reservoir's storage capacity, the appropriate methods to control sedimentation for each reservoir are necessary. Reviews about different control methods for reservoir sedimentation have been presented by Brown (1943), Fan (1985a, 1985b), and Brabben (1988). Morris and Fan (1997) described three strategies used to control reservoir sedimentation: (1) reduction of sediment yield; (2) sediment excavating; and (3) hydraulic regime methods such as sediment routing and flushing. Through the review of control methods for reservoir sedimentation, the most effective method can be considered to mitigate sedimentation problems for the NREB.

2.2.1 Reduction in sediment yield

A reduction in sediment yield entering a reservoir cannot totally solve the reservoir sedimentation problem, but can delay the sediment accumulation rate by erosion control and upstream sediment trapping (Fan and Morris, 1992b). Many kinds of management practices to reduce sediment yield are used across the world. For erosion control, structural or mechanical measures are used to reduce the flow velocity, to increase the storage of surface water, and to dispose of runoff (Morgan, 1995). Also, vegetative agronomic measures and operational measures to minimize erosion potential as nonstructural controls can be applied to erosion control. Hydraulic structures to trap sediment at the upstream area include a check dam, debris basin, sediment detention basin, etc. Sediment trapping can be a highly effective method to reduce sediment yield but there are still many weakness such as high cost, silting, sustainability, and limited benefits. Therefore, the watershed management with erosion control would be executed widely to reduce the sediment yield.

2.2.2 Sediment dredging

To preserve the reservoir capacity and maintain the navigation channel, dredging operations have been used widely in lakes, reservoirs, and barrages, even though it costs highly. The feasibility and method of dredging operation are determined depending on the size of sediment volume, the location to dredge, the particle size and geometry of deposits, and the water level.

There are several methods to dredge sediment, which can be classified into hydraulic and mechanical dredging. Hydraulic dredging appropriates the water to transport sediments and mechanical dredging involves digging and lifting sediments to the surface. Hydraulic dredging is efficient to handle variously distributed size materials from fine to coarse sand. Hydraulic suction dredging with a cutterhead is the most popular type. To dredge sediments of about 665,000 cubic meters per year at the upstream channel of the NREB, hydraulic suction dredging with a cutterhead and a large pump has been used over 10 years. Siphon dredging is a hydraulic dredging method and doesn't have a pump and a discharge line. The head differences between the water surface in the reservoir and the possibly lowest discharge point on the dam allow sediment transport downstream of reservoirs. Many small siphon dredges are used in Chinese reservoirs (Morris and Fan, 1997). However, this method has a few limitations about head differences and water level of a reservoir. Also, a cable-suspended dredge pump, which is one of the specialized hydraulic dredging systems, is used for precision dredging with a submerged video monitor. A submerged hydraulic or pneumatic pump creates a suction vortex without a cutterhead. The disadvantage of a cable-suspended dredging pump system is the high cost to operate. A cable-suspended pneumatic pump was used to dredge 550,000 cubic meters of silt from Gibraltar Reservoir at Santa Barbara (Morris and Fan, 1997). Mechanical dredging removes the sediment with a closed or unclosed bucket. Compared to hydraulic dredging, mechanical dredging carries the sediment with low water contents, and excavated amounts are relatively small. It may be suitable for gravel or large materials of a reservoir.

2.2.3 Sediment routing

During the rising water level of a flood, the outflow of sediment discharge becomes smaller than the inflow because of a decrease in flow velocity and the backwater effect (Fan, 1985a). Although sediment routing and flushing aim to remove sediment in reservoirs, they are fundamentally different techniques. Sediment routing primarily minimizes sediment deposits and balances deposition and scouring during floods. Sediment flushing focuses on the elimination of already deposited sediments.

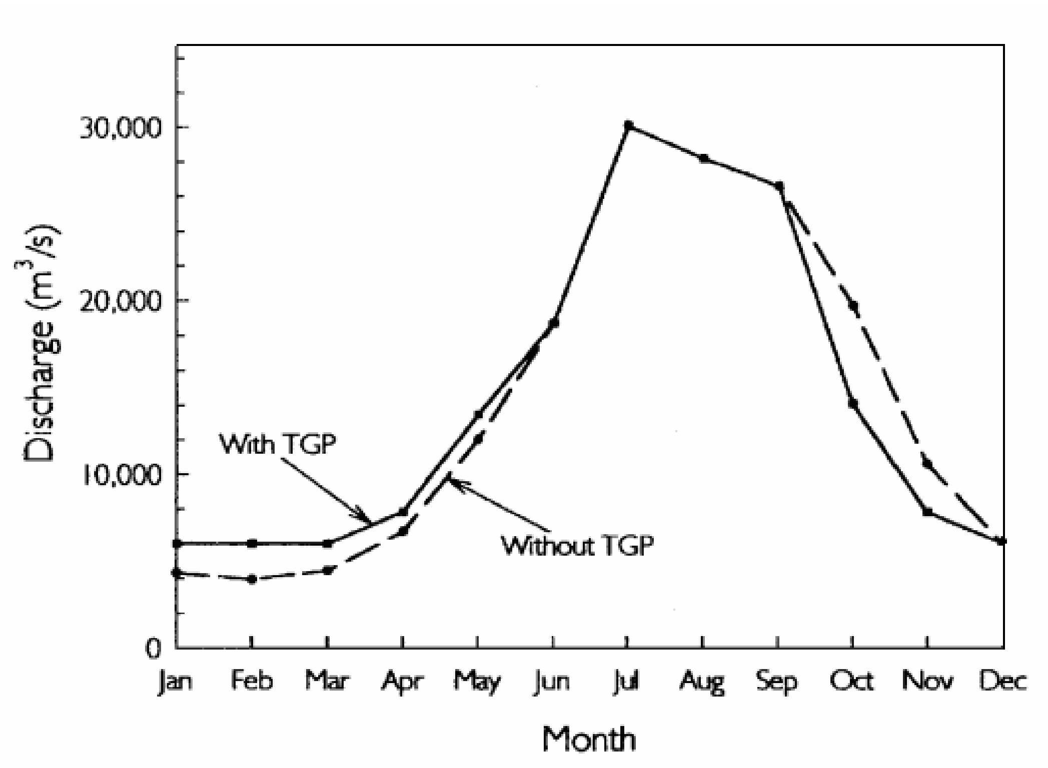

Figure 2-5. Hydrograph of Yangtze River below Three Gorges Project (Chen, 1994)

The distinguishing characteristic of sediment routing compared to sediment flushing is to preserve the natural hydrograph and the timewise pattern of sediment transport. Because the incoming sediment concentration is higher at the rising limb of the hydrograph than the decreasing limb, the water after the flood peak contains less sediment (Fan and Morris, 1992b). Therefore, it is wise to start impoundment as late as possible in order to reduce the contained sediment in the water (Basson, 1997). Partial drawdown, which is one of the techniques for sediment routing, has been applied to the hydrograph of the Yangtze River below Three Gorges Project. Figure 2-5 shows that the reservoir has a very little effect on the natural hydrograph (Chen, 1994). Increased effectiveness in sediment routing can be found in small reservoirs or in estuary barrages, which can release a large amount of water during floods. However, in some cases, sediment routing requires supplemental methods such as flushing and dredging, because sediment routing could not remove the accumulated sediment.

Sediment routing techniques are classified into *Sediment Pass-Through* and *Sediment Bypass* methods. The *Sediment Bypass* method requires proper topographic conditions and additional constructions for the by pass channel. Nagle Reservoir in South Africa is an example of the *Sediment Bypass* method (Annandale, 1987). *Sediment Pass-Through* consists of seasonal drawdown, flood drawdown by hydrograph prediction, flood drawdown by rule curves, and venting turbid density currents. Due to the various hydraulic, hydrologic, and sedimentation conditions of a reservoir or barrage, different techniques of sediment routing are applied to the different sites. For the Nakdong River Estuary Barrage (NREB), flood drawdown techniques can be applied to reduce the inflow of sediments rather than the seasonal emptying drawdown, because the downstream tidal water level at the NREB should be considered. Especially, flood drawdown by rule curves may be the most appropriate technique for the barrage, which has the large gate capacity and the limitation of lowering water level. Rule curves consist of discharge measurements and water elevations at the barrage or dam with gate operations. Figure 2-

6 shows the case of rule curves at Cowlitz Falls Dam in USA (after Locher and Wang, 1995, ref. Morris and Fan, 1997).

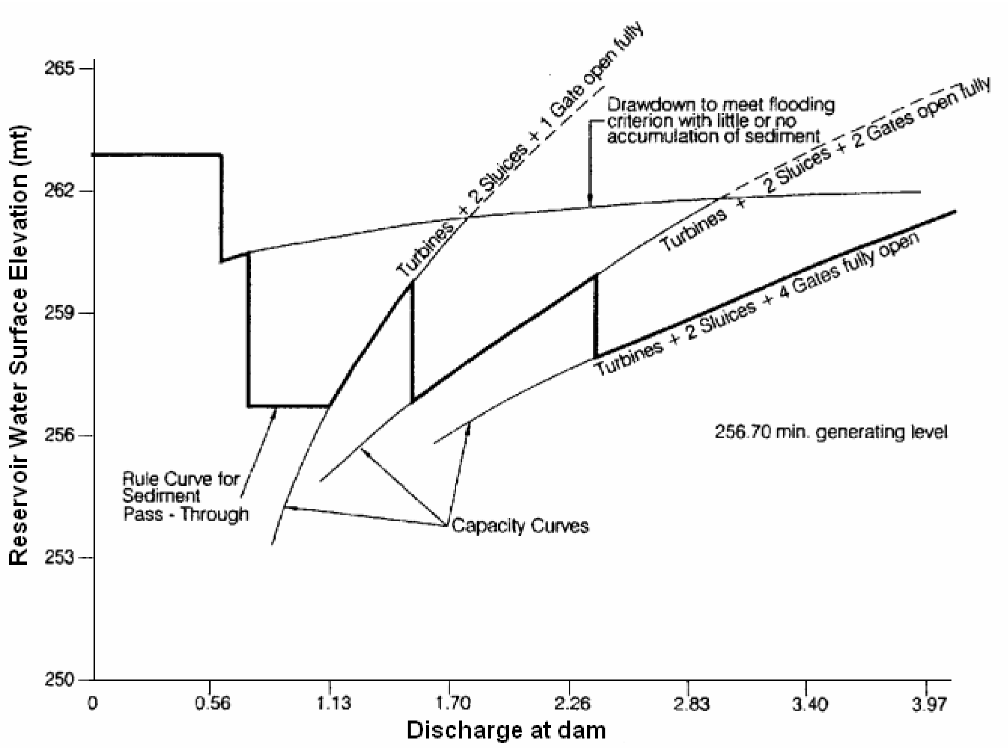

Figure 2-6. Rule curve for sediment pass-through operation at Cowlitz Falls Dam in the U.S. (after Locher and Wang, 1995, ref Morris and Fan, 1997)

Many case studies for sediment routing, especially using sluicing, were executed by Zyrjanov (1973) for the Ouchi-Kurgan Reservoir of USSR, Xia and Ren (1980) for the Heisonglin Reservoir of China, Wei (1986), Hong and Chen (1992), and Qian et al. (1993) for the Sanmenxia Reservoir of China, and Lin (1992), Hu (1995), and Su (1995) about sluicing activity in China (Brandt 1999).

2.2.4 Sediment flushing

Although drawdown and emptying skills are applied to sediment flushing, the flushing operation differs from sediment routing regarding the removal of previously deposited sediments. Another different characteristic of flushing, compared to

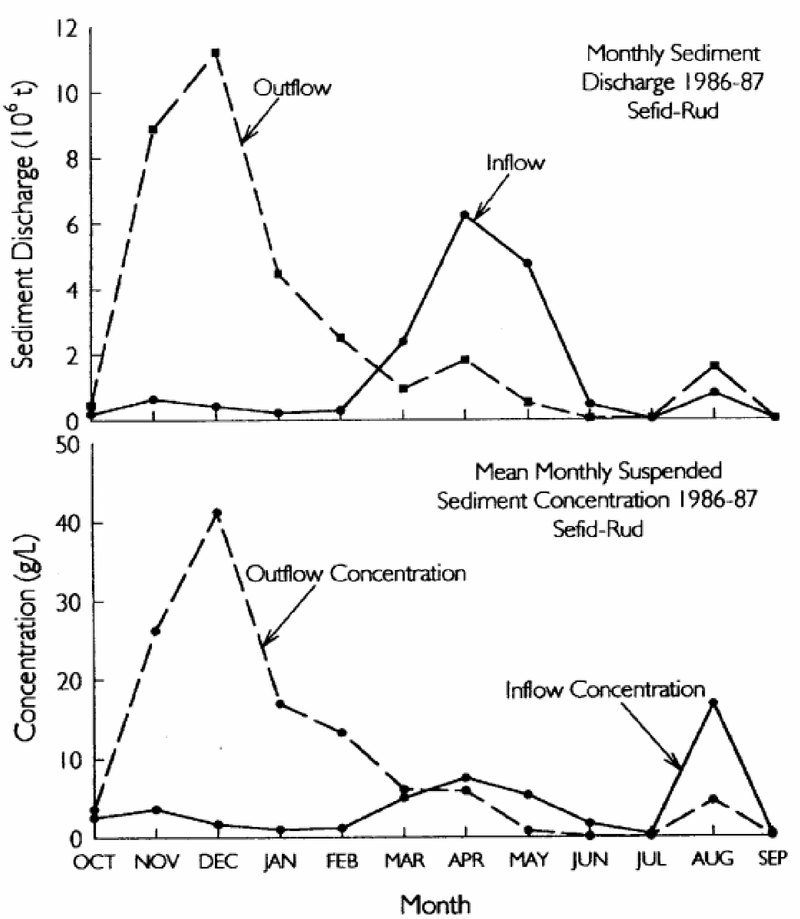

Figure 2-7. Change in the seasonality of sediment delivery below Sefid-Rud Reservoir, Iran caused by flushing (data from Tolouie, 1993, ref. Morris and Fan, 1997)

sediment routing, is that the timewise patterns of sediment inflow and release are significantly different (Figure 2-7).

The flushing process is generated by opening the outlet such as sluice gates to erode accumulated sediments. The longitudinal profile of the flushing processes is illustrated in Figure 2-8. This figure describes the flushing processes corresponding to the drawdown operation with various water levels (Lai and Shen, 1996). Assuming enough sluicing capacity and no sediment clogging, the apex of the delta can move retrogressively in the upstream direction, if the water level of a dam or barrage is lowered enough to scour the apex of the delta. Then, the sediments scoured from the delta move to the vicinity of a dam or barrage and settle before they can be flushed out. If drawdown flushing is operated with wedge-shaped deposition, the operation with gate opening within a very short period of time under pressurized flow is appropriate to remove the sediments in the vicinity of a dam or barrage.

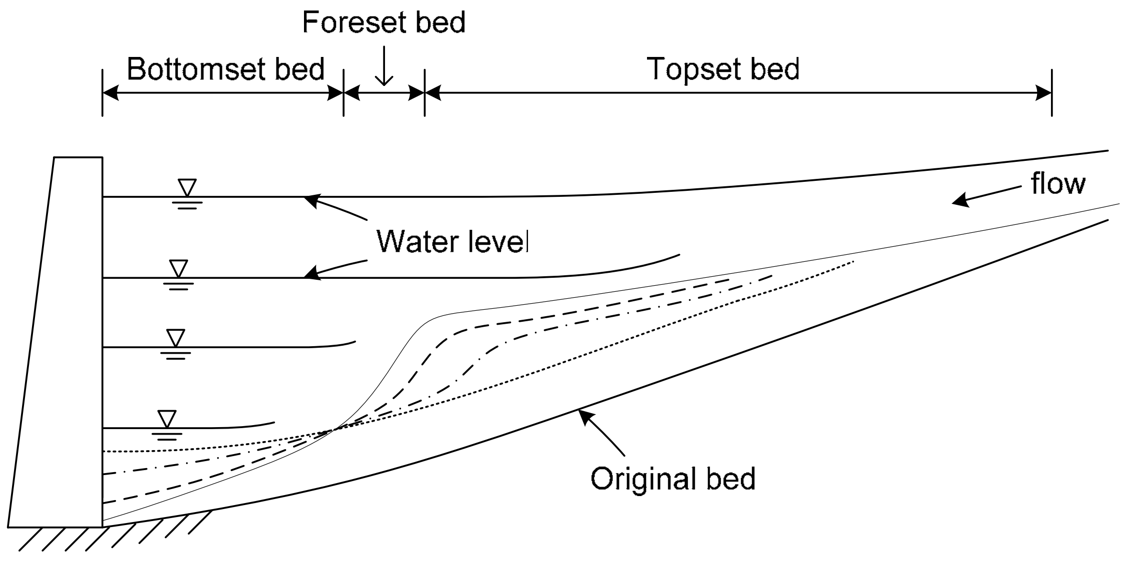

Figure 2-8. Longitudinal profile of flushing process

Fan (1985a) classified flushing into two categories; empty or free-flow flushing and pressure flushing. Empty or free-flow flushing should be emptied with riverine flow through the impoundment. The free-flow condition is used when the sluices are clear of sediment and usually begins when the water level is already low (Wu, 1989). In China, some irrigation reservoirs are emptied during the first part of the flood season for flushing and refilled during the latter part of the flood season. If the water demand is limited in a special season, seasonal emptying is also feasible. For example, Jing (1956) recommended flushing methods to remove the sediments for the Jensanpei Reservoir in Taiwan which was constructed to operate only 6 months of the year. Flushing can also be used during the nonflood season, but will typically require a longer flushing period due to the low discharge. Flushing under pressure is to release the water through the bottom outlets after lowering the water level. However, this technique results in only a very limited area being scoured.

Because of the complexity of flushing operations, it is difficult to describe the general rules to apply for a certain reservoir. However, Shen (1999) suggested the following general rules for flushing operations.

1. Water level in reservoir should be drawn down to improve the efficiency of flushing.
2. Flushing sediment is more efficient in narrow reservoirs than wide reservoirs.
3. For wide reservoirs, or when the total lateral width of flushing outlets is much less than the reservoir width, a distinct flushing channel is formed and retrogressive erosion occurs mainly inside this flushing channel. Sediment may be deposited outside the width of this flushing channel.
4. Flushing channel widths were found to be approximately 11 to 12 times the square root of the bankfull discharge inside the flushing channel as determined by Atkinson (1996) from field data, and Lai and Shen (1996) and Janssen (1999) from

laboratory data. This relationship agrees well with the "empirical regime formulae" presented by Yalin (1992).

2.3 PREVIOUS STUDY OF SEDIMENT FLUSHING

Sediment flushing is widely used to restore the storage volume. Oldest known practice of flushing in Spain in the 16th century was reported by D'Rohan (1911, ref. Talebbeydokhti and Naghshineh, 2004). Another early example of flushing was reported by Jordana (1925) in Peña Reservoir, Spain. Also, Atkinson (1996) reported that flushing has proved to be highly effective at some sites and listed example cases. According to his reports, at the Mangahao reservoir in New Zealand, 59% of the original operating storage had been lost by 1958, 34 years after the reservoir was first impounded. The reservoir was flushed in 1969, when 75% of accumulated sediments were removed

Table 2-1. Examples of reservoirs that have been successfully flushed (Atkinson, 1996)

Reservoir	Country	Reference
Baira	India	Jaggi and Kashyap (1984)
Gebidem	Switzerland	Dawans et al (1982)
Gmud	Austria	Rienossal and Schnelle (1982)
Hengshan	China	IRTCES (1985)
Honglingjin	China	IRTCES (1985)
Mangahao	New Zealand	Jowett (1984)
Naodehai	China	IRTCES (1985)
Palagneda	Switzerland	Swiss Nat. Committee on Large Dam (1982)
Santo Domingo	Venezuela	Krumdieck and Chamot (1979)

in a month (Jowett, 1984). Table 2-1 presents examples of reservoirs where maintenance of storage volumes in excess of about 50% of their original capacity was achieved through flushing (Atkinson, 1996).

Besides the studies already mentioned, there are several additional studies about sediment flushing. In this chapter, recently executed studies using flume experiments and physical models, and analytical and numerical models, are reviewed.

2.3.1 Flume experiments and physical model studies

Hotchkiss and Parker (1988, ref. Hotchkiss and Parker, 1990) carried out experiments of reservoir sedimentation and sluicing in a laboratory flume. A depositional delta formed at the upstream area of the sluice gate and the simulated reservoir was drained using sluice gates. As a result, the progressing degradation was produced. Due to the short distance of the flume, deltas moved downstream too rapidly with the steep topset slopes. Hotchkiss and Parker (1990) indicated that sluicing in the laboratory model must be done very carefully to avoid extremely unsteady features not observed in the field. Informational feedback between physical and mathematical models in this case produces a rational representation of reservoir sedimentation and sluicing.

Lai and Shen (1995, 1996) showed that the understanding of flushing processes has been improved through laboratory experiments using noncohesive uniform size lightweight walnut shell grits. The results of experiments were that the pressure flushing formed a flushing cone in a very short period of time and a small amount of sediment was scoured. However, after increasing the height of the opening, retrogressive erosion occurred in the upstream direction. As a result, a large amount of sediment was flushed through the reservoir.

Janssen and Shen (1997) performed physical models for the flushing test during drawdown with uniformly sized noncohesive sediments and no incoming sediment load. The results showed that, when the flow through the reservoir achieves riverine conditions, the flushing channel widens and incises rapidly, because of steeper water-surface slopes. When the flow through the reservoir is confined to the flushing channel, the channel incises more slowly into the sediment bed, and widens intermittently by bank failure processes. The rate of widening and incision decrease until an equilibrium state is reached.

Talebbeydokhti and Naghshineh (2004) modeled a one-dimensional reservoir in a flume in the hydraulic laboratory of Shiraz University to investigate flushing operation processes using polymer particles, which behave as very fine and non-cohesive particles. They showed the result that the rate of sediment flushing is strongly associated with outflow rate, water surface gradient with the dam section, and the width of the flushing channel.

Among the physical models simulating prototype reservoirs, the experiment for the Jensanpei Reservoir in Taiwan was performed in 1:50 scale by Wu (1989). In addition, Cassidy (1990) did the physical model for sluicing at the Cowlitz Falls project in the U.S. and Wang (1992) simulated sediment flushing in a reservoir at Beijing, China. Other studies about physical models were performed by Shah and Kulkarni (1993) for simulating flushing at the Baira Reservoir, India; Tu et al. (1995) for the Rock creek and Cresta Dam reservoirs in the U.S. using two physical models in scale 1:50; Dum et al.

(1996) for the Kreuzbergmaut hydropower station on the river Salzach, Austria in scale 1:50; and Heigerth and Medved (1996) of the Dionysen Reservoir, Austria in scale 1:40 to determine positions of groynes for best efficiency of flushing (Brandt, 1999).

2.3.2 Analytical and numerical studies

Many analytical and numerical studies have been used to simulate the process of sediment flushing since 1980. Wang and Locher (1989) used one-dimensional HEC-6 model to develop operational procedures to minimize the accumulation of sediment in the Cowlitz Falls reservoir in the U.S. Also, Morris and Hu (1992) used the HEC-6 model to analyze the impacts of different gate operations for the Loíza Reservoir during floods. Ju (1992) presented one-dimensional diffusion models using the unit stream power equation for sediment transport to study analytically or numerically the simulation of removed sediments volume and bed profile changes. Shen et al. (1993) developed a one-dimensional diffusion equation to simulate bed-profile changes. Also, they described a two-dimensional mobile-bed model to predict bed evolution in a reservoir and showed that the models can simulate the lateral variation of bed elevation.

Jin (1995) used a two-dimensional model to analyze reservoir erosion in order to improve the navigation possibilities. The quasi two-dimensional FLUVIAL-12 model was used for a series of tests at Rock and Cresta Dams in the U.S. by Tu et al. (1995). Chang et al. (1996) used FLUVIAL-12 numerical modeling to evaluate the feasibility and effectiveness of Sediment-Pass-Through (SPT) for the reservoirs on the North Fork Feather River. Chang and Fan (1996) presented tests and calibration of the FLUVIAL-12 model for the reservoir. Lai and Shen (1996) presented a one dimensional diffusion model only to simulate the general trend of bed profile evolution and the amount of reservoir sediment removal during flushing for evaluating the applicability and limitations of this model.

In 1999, Olsen used a two-dimensional numerical model to simulate flushing of sediments from reservoirs. This model solves the depth-averaged Navier-Stokes equations on a two-dimensional grid and was compared with data from physical model studies. The main features of the erosion pattern were reproduced and the deviation between the calculation and the measurement of the scour volume was small. Olsen (1999) indicated that most of the simplifications made on the numerical model were reasonable. Molino et al. (2001) applied a two-dimensional numerical model to the case study site of Abbey-stead Reservoir, U.K. The model analyzed two management scenarios and had a clear difference. Also, it showed a good agreement between the numerical simulations and field data.

Chang et al. (2003) used the genetic algorithm to optimize and determine the operation rule curves and flushing schedule in a reservoir. The sediment-flushing model is developed to calculate the amount of the flushed sediments and modified the elevation-storage curve. The models were successfully applied to Tapu Reservoir in Taiwan. Wu and Chou (2004) presented a simulation approach to evaluating flushing flows and exploring the tradeoffs associated with non-inferior flushing options. The results indicated that flushing efficiency is higher for the larger flow, but flushing duration is less sensitive to the flow discharge. Liu et al. (2004) developed the one-dimensional model which consists of a flow movement module and sediment transport module in which the bed material load is taken as sediment mixture. The model predicted the amounts of the flushed and deposited sediment and was calibrated on the case of field data at Dashidaira and Unazuki reservoirs on the Kurobe River in Japan.

CHAPTER 3: NAKDONG RIVER ESTUARY BARRAGE (NREB)

3.1 BACKGROUND AND SITE DESCRIPTION

The Nakdong River has a drainage area of about 23,384 square kilometers and spans 510 km from the north across South Korea (Figure 3-1). An estuary barrage was built in 1983-87 to prevent salt-water intrusion and provide the stable water level in the upstream channel of the NREB (Figure 3-2). Since the construction of the NREB, the Lower Nakong River has experienced sedimentation problems requiring dredging operation. The main purpose of dredging sediments is to provide the flood conveyance capacity of the upstream channel of the Lower Nakdong River for large floods.

Every year, the Lower Nakdong River has annually frequent typhoons and large floods with high water level from June to September. Typhoon Rusa, which occurred in August 31, 2002 for 2 days, caused historical precipitation and flooding in Korea (Kim et al., 2004). The rainfall amount was 880 mm for 24 hours, exceeding the PMP (840 mm within 25 km^2). Especially, Typhoon Maemi of September 12, 2003 hit the Lower Nakdong River and caused extensive damage over a large area with an extremely flashy hydrograph of over 400mm of local precipitation and a severe storm surge. The water level at Gupo Bridge significantly exceeded normal levels and reached a maximum stage of 5.06 m. The flood level exceeded the warning stage of 4 m, and the dangerous stage of 5 m corresponds to 70% of the project flood (19,370 cubic meters per second) for the Nakdong River (Ji and Julien, 2005). Typical damage on the Lower Nakdong River was the bridge collapse shown in Figure 3-3. At this time, September 14, the

Figure 3-1. Nakdong River basin and Lower Nakdong River

Figure 3-2. Nakdong River Estuary Barrage (NREB)

Figure 3-3. Gupo Bridge failure after Typhoon Maemi

1.06 km-long Gupo Bridge partially collapsed with the loss of the 19th pier. The discharge of the Nakdong River peaked on September 14 at a value around 13,000 cubic meters per second.

The average width of the Nakdong River is approximately 45 m and reaches 250 m in the Lower Nakdong River. Based on the Mulgeum station, the average water depth is 2 – 3 m on the Lower Nakdong River (from the NREB to Samryangjin). The Lower

Nakdong River has a very mild bed slope (S_0) of approximately 0.0001 m/m and has one tributary, the Yangsan River. Due to this mild slope, salt water intrudes up to 40 km from the river mouth. Sediments carried from upstream deposit in the estuary near the NREB. Therefore, in this study, the upstream boundary for numerical model development should be extended to Samryangjin to analyze sediment problems and consider backwater effects.

3.2 HYDRAULIC AND HYDROLOGIC CHARACTERISTICS OF THE LOWER NAKDONG RIVER

Much of South Korea, including the Nakdong River basin, is underlain by granite, which limits the extent to which rainfall can infiltrate. The climate of South Korea is dominated by monsoons, which result in over 50% of total precipitation for a year during June to September (Park, 1998). Also, the average annual frequency of typhoons over the 30-year period from 1971 to 2000 is 26.7 per year. Several typhoons flood the Nakdong River basin annually (Ji and Julien, 2005). Due to seasonally concentrated rainfall by monsoons and typhoons, the coefficient of river regime, which is the ratio of a river flow volume at its maximum to the minimum flow volume, is 10-100 times greater for the Nakdong River compared to other rivers (Table 3-1). The high coefficient of river regime indicates high possibilities of droughts or floods.

The mean annual discharge of the Nakdong River is 13.8 billion cubic meters per year (about 438 cubic meters per second). Figure 3-4 is the monthly graph of mean daily discharge released from the NREB during the period 1994-2002.

Table 3-1. Comparisons of coefficients of ratio of maximum peak flow and minimum peak flow (Q_p / Q_m)

Name	Q_p / Q_m
Nakdong River	260 (372, before dam construction)
Han River	90 (390, before dam construction)
Yangtze River	22
Thames River	8
Rhine River	18
Seine River	34
Nile River	30
Mississippi River	3

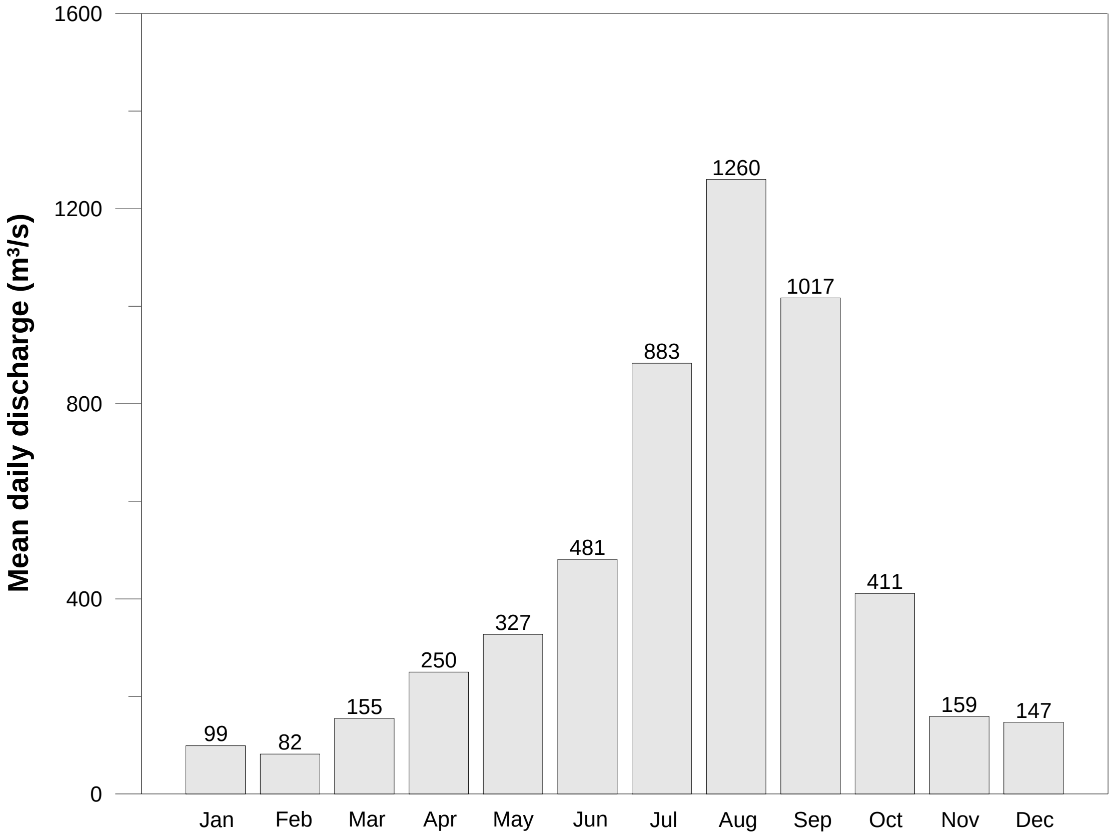

Figure 3-4. Released discharge from the NREB during 1994-2002 periods

The wet season from July to September has a large discharge and the minimum discharge occurs in February. The mean annual precipitation of the Nakdong River is 1,186 mm and the mean annual temperature ranges from 12 to 16 $°C$. Probable precipitation and floods of different frequencies estimated for the Lower Nakdong River from Samryangjin to the NREB are described in Table 3-2. In South Korea, there are two different kinds of flood discharge and level for the flood warning system at most of the stations. One of them is the *warning flood level*, which has a 50% discharge of a design flood, and the other is the *dangerous flood level*, which has a 70% discharge of a design flood. Among the stations located in the Lower Nakdong River, the standard values of warning and dangerous floods for the Jindong and Gupo stations are shown in Table 3-3. At Jindong Station, a peak flood of 20,512 m^3/s was recorded on August 29, 1939. This flood exceeded the design flood conveyance (16,110 m^3/s).

Table 3-2. Probable precipitations and floods of different frequencies on the Lower Nakdong River (source: KMOCT and KOWACO, 2004)

Station name	**days**	**Probable precipitation of different frequencies (mm/day)**				
		50-year	**80-year**	**100-year**	**150-year**	**200-year**
Samryangjin	1	238.3	256.2	264.7	280.1	291
	2	309.7	333.1	344.1	364.2	378.5
Mulgum	1	239.2	257.2	265.8	281.3	292.2
	2	310.6	334.1	345.2	365.4	379.7
Gupo	1	240.6	258.7	267.3	282.9	294
	2	312.1	335.7	346.9	367.2	381.6
NREB	1	240.7	258.9	267.5	283.1	294.2
	2	312.2	335.9	347.1	367.4	381.8
Station		**Probable flood discharge of different frequencies (cms)**				
		50-year	**80-year**	**100-year**	**150-year**	**200-year**
Samryangjin to NREB		17,780	19,360	20,060	21,450	22,350

Table 3-3. Flood stage and discharge of Jindong, Samryangjin and Gupo stations on the Lower Nakdong River (source: KMOCT and KOWACO, 2004)

Station	Flood Stage (m)		Flood Discharge (cms)		Design discharge (cms)
	Warning flood stage	Dangerous flood level	Warning flood discharge	Dangerous flood level	
Jindong	8.5	10.5	8,055	11,277	16,110
Samryangjin	7.0	9.0	8,420	11,788	16,840
Gupo	4.0	5.0	9,685	13,559	19,370

The Jindong Station is located 84.3 km upstream of the river mouth and is the first station without tidal backwater effects (KMOCT and KOWACO, 2004). Therefore, the discharge rating curve at Jindong Station has been well developed using field measurements collected since 1955. Using daily mean discharge data for 35 years (1967-2001) at Jindong Station, the mean annual flow was calculated as 372 m^3/s. This is slightly less than the mean daily discharge at the NREB (438 m^3/s). The mean annual flood at Jindong Station was 5,748 m^3/s.

3.3 SEDIMENTATION CHARACTERISTICS OF THE LOWER NAKDONG RIVER

The bed material distributions of Gupo and Jindong stations are shown in Figures 3-5 and 3-6. The median grain size of bed materials is 0.3 mm at Jindong Station and 0.25 mm at Gupo station. The bed is mainly fine sand. The 0.25 mm of the median particle size for Gupo Station is applied to the numerical modeling of 40 km upstream of the NREB.

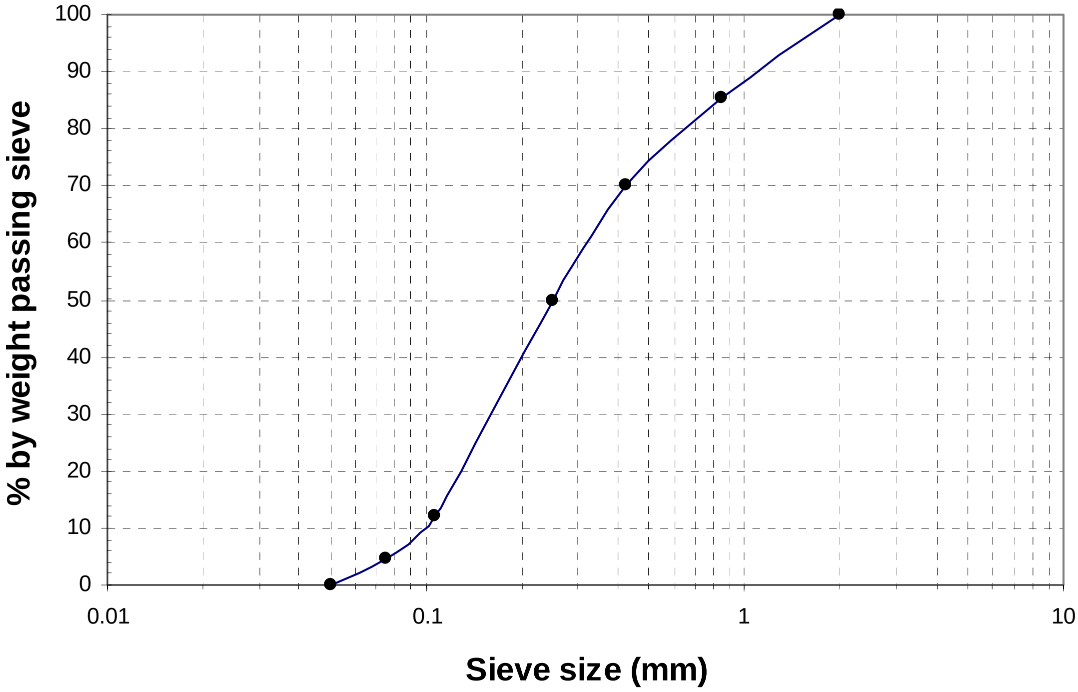

Figure 3-5. Particle size distribution of bed materials at Gupo Station

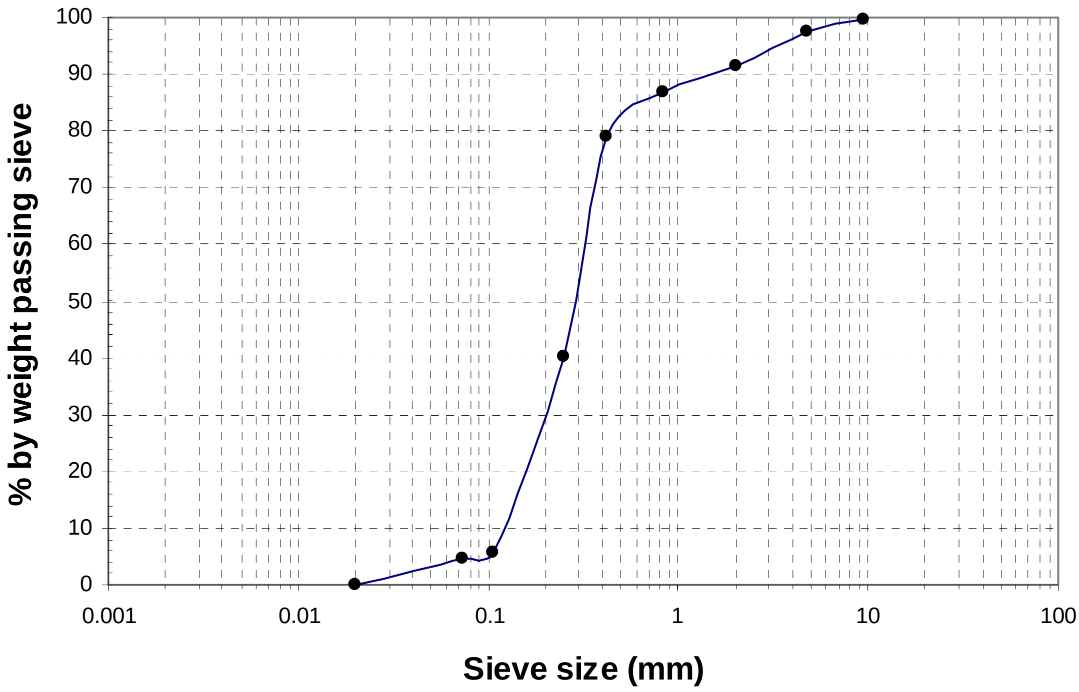

Figure 3-6. Particle size distribution of bed materials at Jindong Station

Although there are not many studies and data about the roughness factor of the Lower Nakdong River, two values suggested in the past reports of the Nakdong River were found. The roughness factor for the Lower Nakdong River, which was determined considering historic flood data, bed materials, and bedforms, is 0.023 for Manning's n, in the Nakdong River Maintenance General Planning Report (KMOCT, 1991). Also, a Darcy-Weisbach friction factor (f) of 0.03 was used to compute the backwater profile of the Lower Nakdong River in the NREB maintenance manual (ISWACO-NEDECO, 1987). If the averaged depth is assumed 3m, which is similar to the averaged depth of the Lower Nakdong River, the following relation equations produce the Darcy-Weisbach friction factor, 0.03 and Manning's n, 0.023.

$$C = \frac{1}{n} h^{1/6} = \frac{1}{0.023} \times 3(m)^{1/6} = 52.214 \tag{3.1}$$

$$f = \frac{8g}{C^2} = \frac{8 \times 9.81(m/s^2)}{52.214^2} = 0.029 \approx 0.03 \tag{3.2}$$

where C = Chezy's coefficient

g = gravity acceleration

h = flow depth

Because resistance to flow depends largely on bedform configurations, three methods (Simons and Richardson (1963, 1966), Bogardi (1974), and van Rijn (1984)) to predict bedform configurations are selected to verify the feasibility of given roughness factors. Simons and Richardson proposed the bedform classification diagram plotting stream power as a function of particle diameter (Julien, 1998). Bogardi used the Shield number (τ_*) and particle diameter to predict the bedform configurations. Van Rijn proposed a bedform classification based on the dimensionless particle diameter (d_*) and the transport-stage parameter (T) (Julien, 1998). Graphs and equations used for the bedform calculations are summarized in Appendix A. The backwater profile was calculated based on the mean daily flow of the Lower Nakdong River, and then the bedform configurations were determined by three methods. The results are shown in Figures 3-7 and 3-8. The calculation results show that the bedform configurations of the Lower Nakdong River consist of ripples and dunes, which is very similar to field observations using the sound navigation ranging, as shown in Figure 3-9.

	A	Y	Z	AA	AB	AC	AD	AE	AF	AG	AH	AI	AJ	AK
1														
2			Simons and Richardson method					Bogardi method			Van Rijn method			
3	XS Distance		Shear stress	Velocity	Shear stress *	Bed form		Shield parameter	Bed form		Grain shear	Grain shear	T	Bed form
4	(m)		lb/ft^2	ft/s	Velocity						velocity	stress		
5	0		0.008693629	1.093613333	0.009507469	Ripples		0.102839266	Ripples		0.013306128	0.177053036	0.060197818	Ripples
6	100		0.008777832	1.098896695	0.00964593	Ripples		0.103835321	Ripples		0.013376834	0.178939694	0.071495172	Ripples
7	200		0.008861246	1.104105672	0.009783752	Ripples		0.104822052	Ripples		0.013446581	0.180810551	0.08269791	Ripples
8	300		0.008943892	1.109242553	0.009920946	Ripples		0.105799696	Ripples		0.013515398	0.18266599	0.093808325	Ripples
9	400		0.009026288	1.114340326	0.010058357	Ripples		0.106774383	Ripples		0.013583726	0.184517599	0.104895804	Ripples
10	500		0.009108758	1.119419387	0.01019652	Ripples		0.107749937	Ripples		0.013651836	0.186372622	0.116003725	Ripples
11	600		0.009191563	1.124496037	0.010335876	Ripples		0.108729461	Ripples		0.013719947	0.188236959	0.127167418	Ripples
12	700		0.00927491	1.129582894	0.01047678	Ripples		0.1097154	Ripples		0.01378823	0.190115277	0.138414835	Ripples
13	800		0.009358969	1.134690063	0.010619529	Ripples		0.110709752	Ripples		0.013856818	0.192011412	0.149768935	Ripples
14	900		0.00944388	1.139825782	0.010764378	Ripples		0.111714187	Ripples		0.013925824	0.193928581	0.161248986	Ripples
15	1000		0.009529764	1.144996902	0.01091155	Ripples		0.112730128	Ripples		0.01399534	0.195869547	0.172871536	Ripples
16	1100		0.009616725	1.150209221	0.011061246	Ripples		0.113758817	Ripples		0.014065445	0.197836733	0.184651096	Ripples
17	1200		0.009704857	1.155467727	0.011213649	Ripples		0.114801356	Ripples		0.014136206	0.199832306	0.196600637	Ripples
18	1300		0.009794244	1.160776778	0.011368931	Ripples		0.115858739	Ripples		0.014207682	0.201858235	0.208731945	Ripples
19	1400		0.009884963	1.166140229	0.011527253	Ripples		0.11693188	Ripples		0.014279928	0.203916335	0.221055895	Ripples
20	1500		0.009977086	1.171561524	0.01168877	Ripples		0.118021621	Ripples		0.014352989	0.2060083	0.233582636	Ripples
21	1600		0.010070679	1.177043773	0.01185363	Ripples		0.119128755	Ripples		0.01442691	0.208135729	0.246321732	Ripples
229	22400		0.054660204	2.742198394	0.149889125	Dunes		0.646590204	Dunes		0.036728569	1.348987785	7.077771167	Dunes
230	22500		0.054997965	2.750657752	0.151280579	Dunes		0.650585666	Dunes		0.036854322	1.358241078	7.13318011	Dunes
231	22600		0.055334536	2.759061522	0.15267139	Dunes		0.654567058	Dunes		0.036979296	1.367468299	7.188432927	Dunes
232	22700		0.055669833	2.767408077	0.154061145	Dunes		0.658533366	Dunes		0.037103463	1.376666989	7.243514902	Dunes
233	22800		0.056003768	2.775695814	0.155449424	Dunes		0.662483578	Dunes		0.037226801	1.385834694	7.298411341	Dunes
234	22900		0.056336258	2.783923156	0.156835812	Dunes		0.666416687	Dunes		0.037349283	1.39496897	7.353107605	Dunes
235	23000		0.056667217	2.792088565	0.15821989	Dunes		0.670331698	Dunes		0.037470887	1.40406739	7.407589159	Dunes
236	23100		0.056996564	2.800190539	0.159601239	Dunes		0.674227627	Dunes		0.037591589	1.413127549	7.461841613	Dunes
237	23200		0.057324216	2.808227622	0.160979446	Dunes		0.678103506	Dunes		0.037711365	1.422147078	7.515850769	Dunes
238	23300		0.057650092	2.816198412	0.162354098	Dunes		0.681958387	Dunes		0.037830195	1.431123645	7.569602667	Dunes
239	23400		0.057974115	2.82410156	0.163724789	Dunes		0.685791341	Dunes		0.037948056	1.440054965	7.623083621	Dunes
240	23500		0.058296208	2.831935775	0.165091117	Dunes		0.689601466	Dunes		0.038064929	1.448938801	7.676280244	Dunes
241	23600		0.058616297	2.839699823	0.166452687	Dunes		0.693387878	Dunes		0.038180793	1.457772969	7.729179457	Dunes
242	23700		0.058934308	2.847392527	0.167809108	Dunes		0.697149721	Dunes		0.038295631	1.466555336	7.781768481	Dunes
243	23800		0.059250172	2.855012758	0.169159996	Dunes		0.700886157	Transition		0.038409424	1.475283814	7.834034814	Dunes
244	23900		0.059563819	2.862559432	0.17050497	Dunes		0.704596369	Transition		0.038522154	1.483956354	7.885966191	Dunes
245	24000		0.05987518	2.870031502	0.171843654	Dunes		0.708279551	Transition		0.038633806	1.492570941	7.937550546	Dunes
246	24100		0.06018419	2.877427952	0.173175672	Dunes		0.711934915	Transition		0.038744362	1.501125589	7.988775983	Dunes
247	24200		0.060490783	2.884747794	0.174500653	Dunes		0.715561681	Transition		0.038853807	1.509618336	8.039630756	Dunes

Figure 3-7. The results of bedform calculations

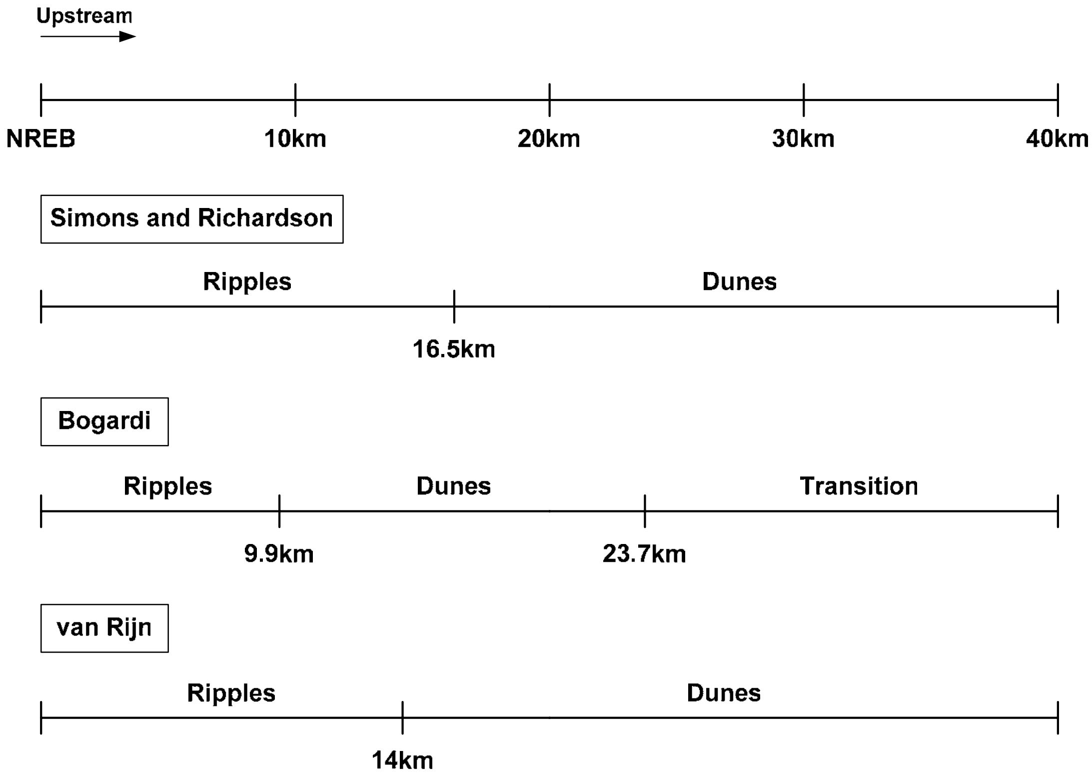

Figure 3-8. The results of bedform calculations diagram on the Lower Nakdong River

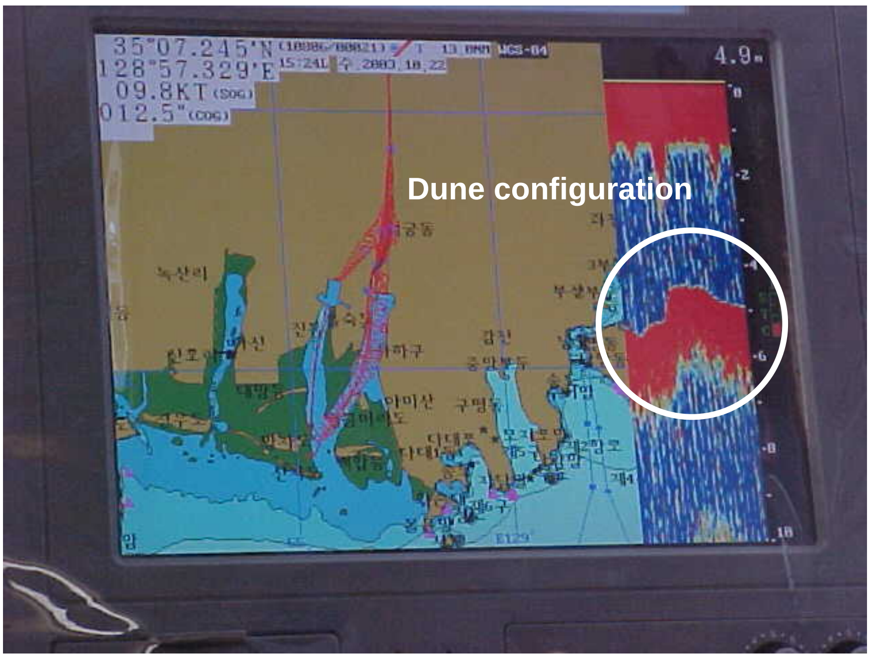

Figure 3-9. Bedform observation using the sound navigation ranging (SONAR)

KOWACO collected sediment field data in 1995 at the NREB and Jindong Station and presented calculated total sediment load of Jindong Station. The total sediment load for the NREB was estimated in this study using sediment field data measured by KOWACO.

Measured sediment field data and the Modified Einstein Procedure (Colby and Hembree, 1995) were used to estimate the total sediment load at Jindong Station (KOWACO, 1995). Because presently used suspended sediment sampler such as point and depth integrated samplers cannot collect the sediments for the entire water column, the unmeasured load must be estimated and added to the measured load to estimate the total load using the Modified Einstein Procedure. Sediment field data were suspended sediment concentrations, and particle size distributions of suspended sediment and bed material. Calculated sediment discharge data of Jindong Station by KOWACO were compared with several total sediment load equations in Figure 3-10. The total sediment load calculated by the Modified Einstein Procedure is referred to as field data in this study. The Engelund and Hansen (1967) method overestimated the total load at Jindong Station. Shen and Hung (1972), Ackers and White (1973), Yang (1979), and Brownlie (1981) equations show relatively good agreement with the field data.

Also, suspended sediment concentrations and particle size distributions of suspended sediment and bed material at the NREB were measured by KOWACO in 1995. In this study, the unmeasured load was estimated and added to the measured load to calculate the total load at the NREB using the Bureau of Reclamation Automated Modified Einstein Procedure (BORAMEP). BORAMEP is a computer model that utilizes the Modified Einstein Procedure to estimate the total sediment load in a hydraulic

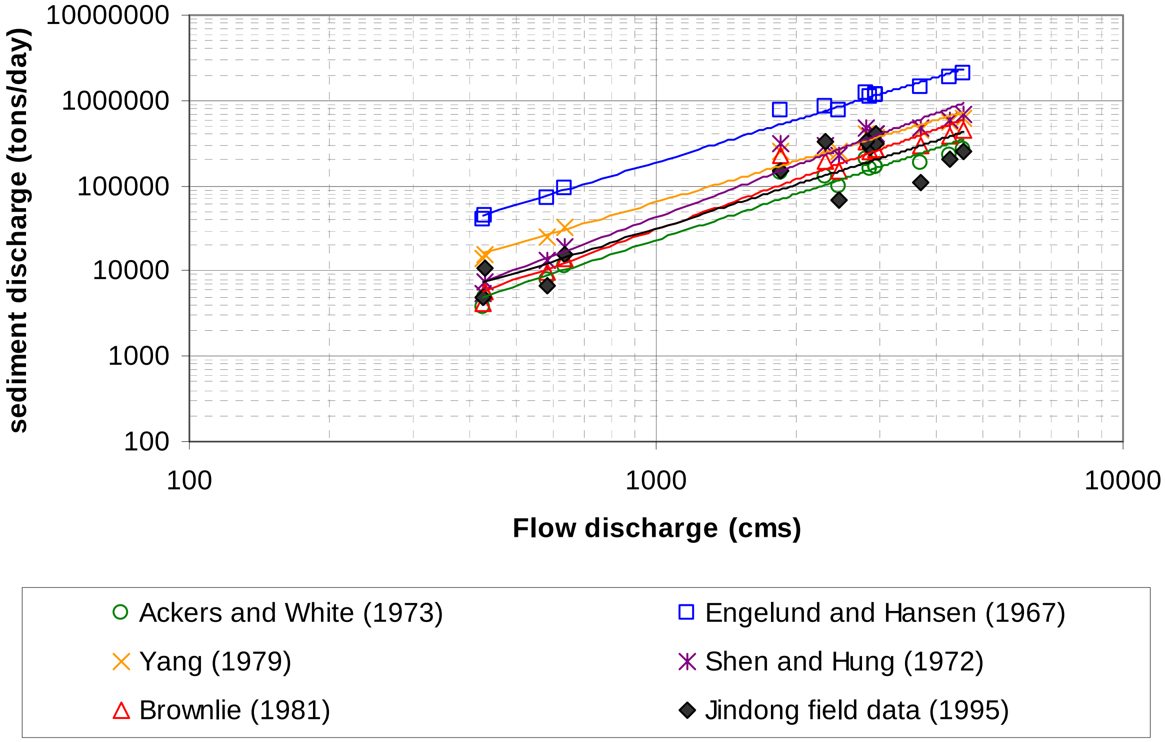

Figure 3-10. Sediment transport equations comparison of Jindong Station

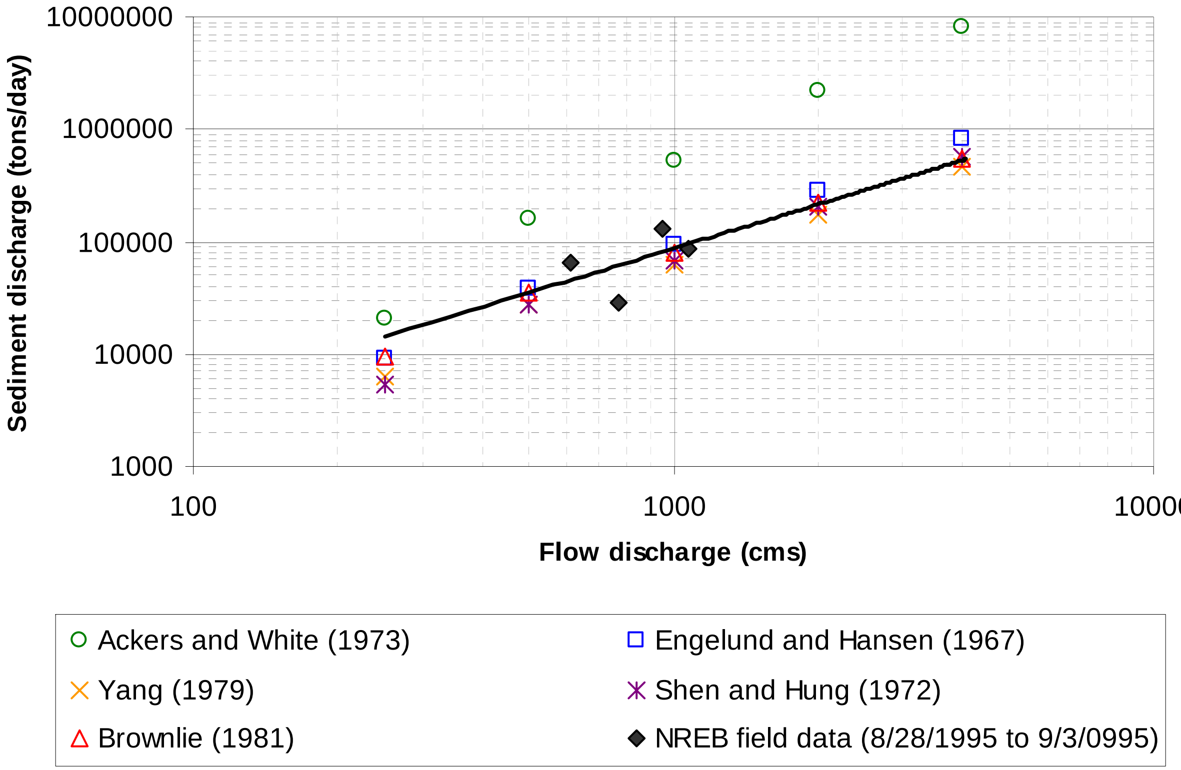

Figure 3-11. Sediment transport equations comparison of the NREB

system (Shah, 2006). Figures of the BORAMEP program and calculation results are presented in Appendix B. Calculated sediment discharge data of the NREB were also compared with several total sediment load equations in Figure 3-11 to analyze the appropriate sediment transport equation for the numerical model. Julien (1998) indicated that Ackers and White's (1973) equation tends to overestimate the sediment transport of fine and very fine sands. Figure 3-8 shows the same trend of the overestimation of Ackers and White's method in the Lower Nakdong River, which has bed material composed of fine sands. Engelund and Hansen (1967), Yang (1979), Shen and Hung (1972) and Brownlie (1981) equations are relatively fitted to the NREB field data.

In this study, the Brownlie equation was adopted as a sediment transport equation for the numerical model of 40 km area from the NREB to the Samryangjin. It is based on the comparisons of sediment transport equations at Jindong Station and the NREB in this chapter and the sensitivity analysis of sediment transport equations in Chapter 5.

3.4 MORPHOLOGICAL CHANGES IN THE LOWER NAKDONG RIVER BED

The morphological bed changes near the NREB were analyzed using historical measured data. Choi (1996) surveyed and analyzed cross sectional changes upstream of the NREB from April 1988 to December 1991. Cross sectional data of 1988 and 1989 were used to compare the morphological changes before and after the barrage construction. The cross sectional geometries measured in 1990 and 1991 provided the morphological variation before and after floods. Surveyed cross sections were located in 0.5 km, 1 km, and 1.5 km upstream of the NREB.

The channel bed on the right bank was more scoured than other parts through time. This indicates that the main flow channel forms on the right bank side during the low flow season

As shown in Figure 3-12 (a), the averaged bed elevation at 0.5 km, 1 km, and 1.5 km upstream of the NREB right after the construction ranged from -5 m to -7m. After 13 months, the cross sectional geometry of three sections wasn’t changed much on comparison to the results of April 1988 (see Figure 3-12 (b)). However, the surveyed results of August 1989 indicated that significant sediments were deposited in these sections after the barrage construction (Figure 3-12 (c)). At this time (August 1989), the bed elevation of the center point was from -2.6 m to -5 m. Particularly, the morphological bed changes are most conspicuous when the cross sections of April 1988 and April 1990 are compared with each other. It is indicated that significant sediments were deposited at 0.5 km to 1.5 km upstream of the NREB in the early period after the construction.

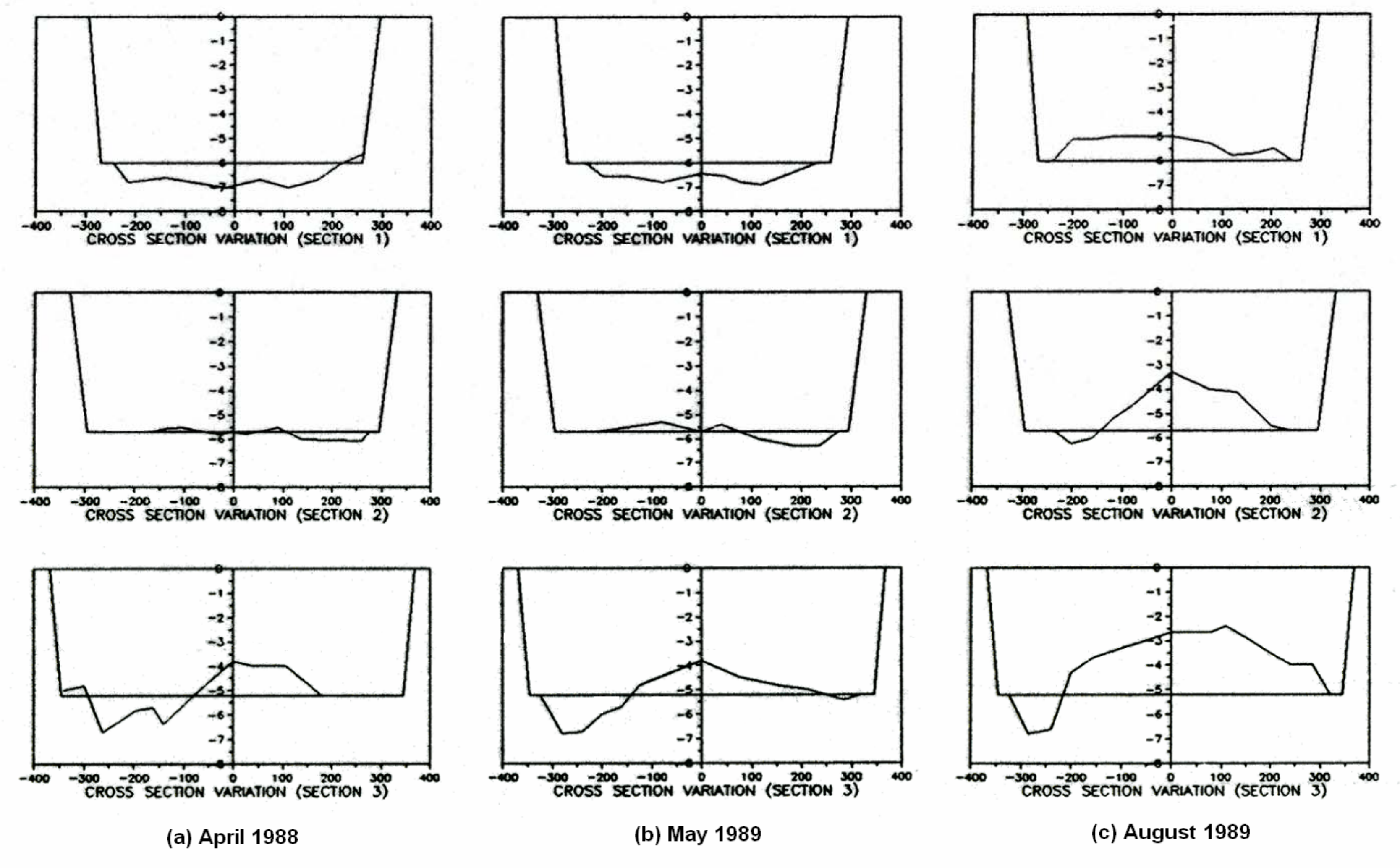

Figure 3-12. Cross sectional variations from 1988 to 1989 (unit: m) (Choi, 1996)

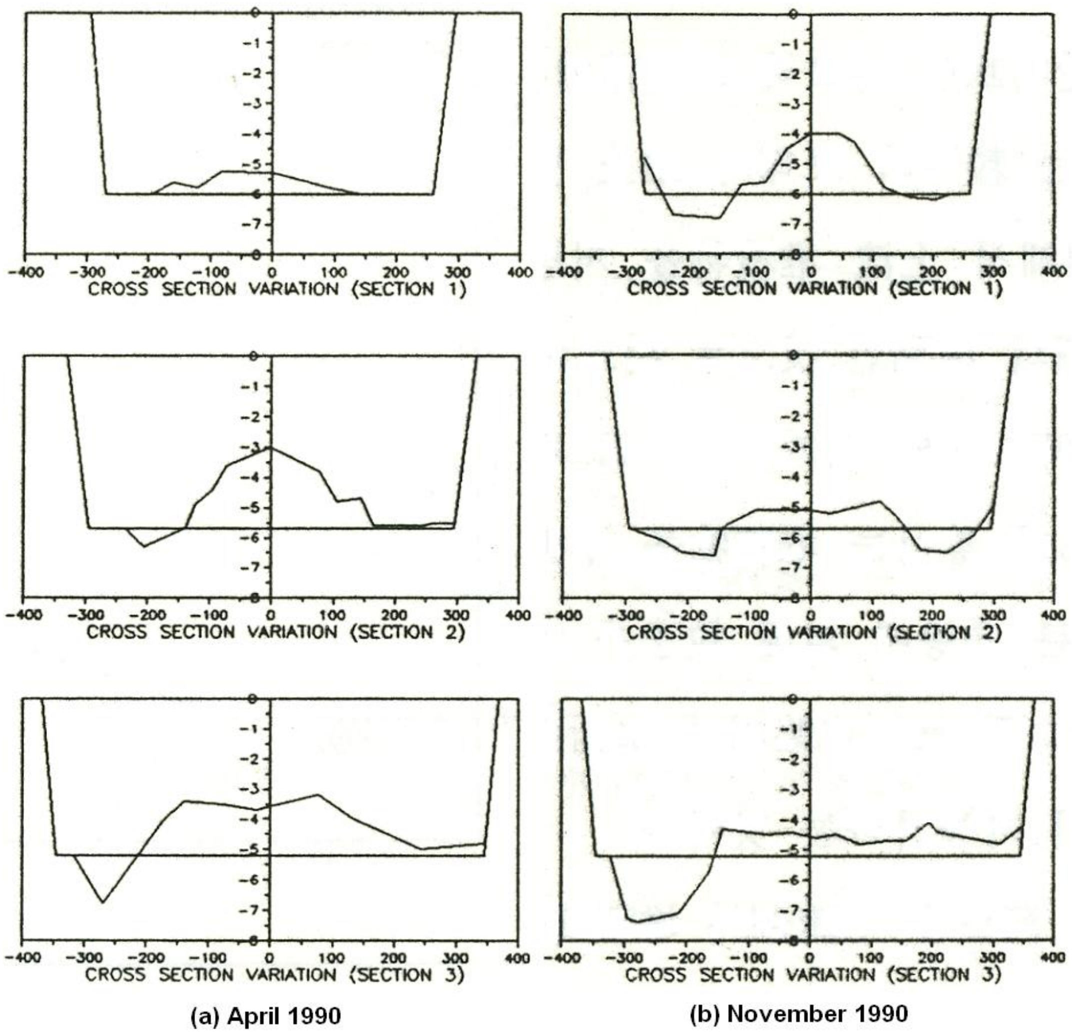

Figure 3-13. Cross sectional variations in 1990 (unit: m) (Choi, 1996)

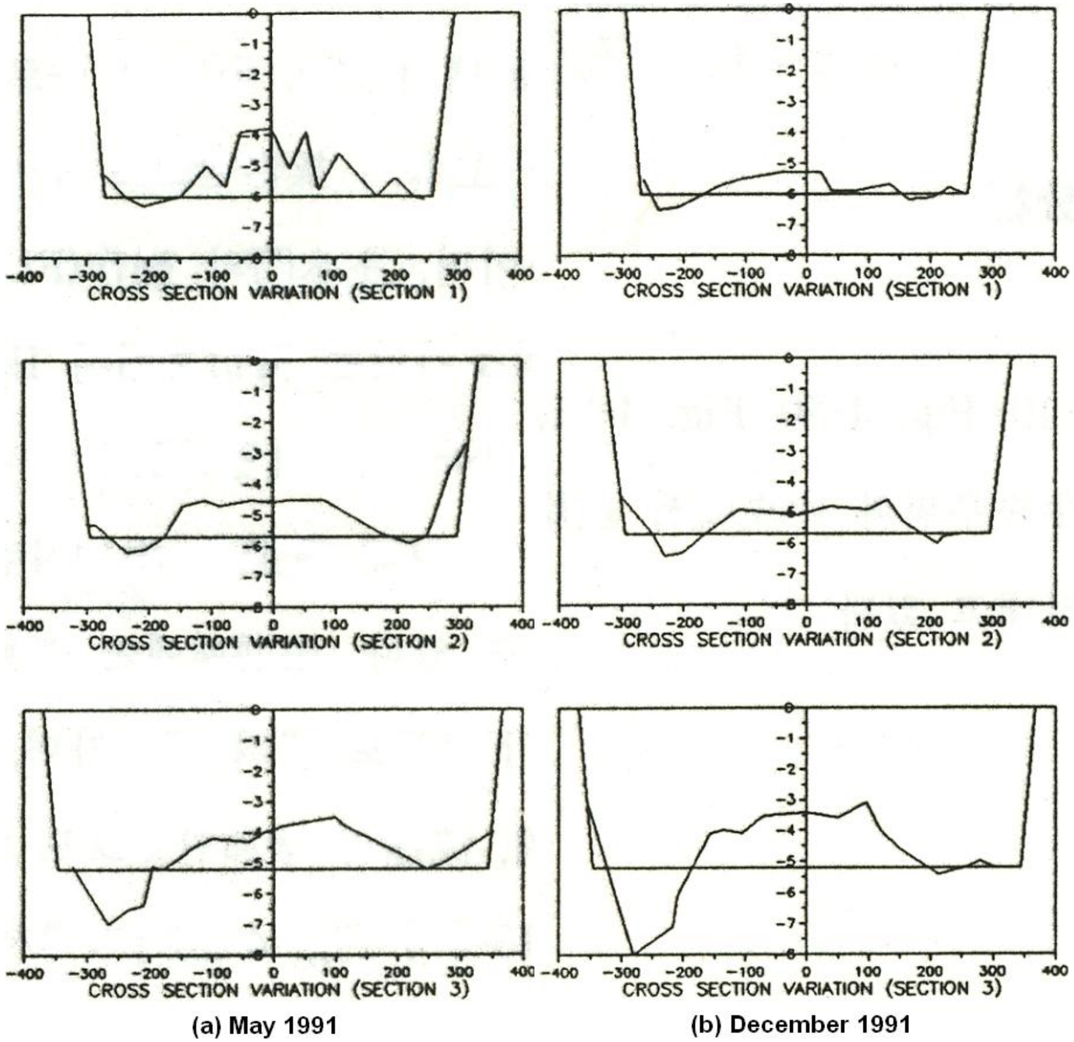

Figure 3-14. Cross sectional variations in 1991 (unit: m) (Choi, 1996)

Figures 3-13 and 3-14 show the surveying results of 1990 and 1991 for cross sectional changes. During the low flow condition, sediments from the upstream channel were deposited near the NREB, as shown in Figures 3-13 (a) and 3-14 (a). The cross sectional changes in Figures 3-13 (b) and 3-14 (b) indicated that sediment deposits were eliminated by high flow rates during the flood season (June to September). Choi (1996) indicated that seasonal differences in sediment deposits implied the possibility and feasibility of gate operation to eliminate sediment deposits in the upstream approach channel of the NREB. Surveyed results also indicated that sediments in the flood season would be sluiced by high flow rates, and velocity increases by gate opening in the low flow condition could prevent sediment deposition.

Figure 3-15 represents the bed elevation changes for 10 years with longitudinal profiles surveyed in 1981 and 1991. The 25 km upstream of the NREB had bed scour and a lot of sediments were deposited 25 km to 45 km upstream of the NREB. It is considered that the morphological changes from the NREB to 45 km upstream of the NREB result from the barrage construction. Therefore, the channel slope in the early stage after the barrage construction (early 90s) became higher than before the barrage construction. It is anticipated that the steeper slope generates the faster velocity so that more sediments are transferred from the upstream channel and deposited near the NREB, especially at present.

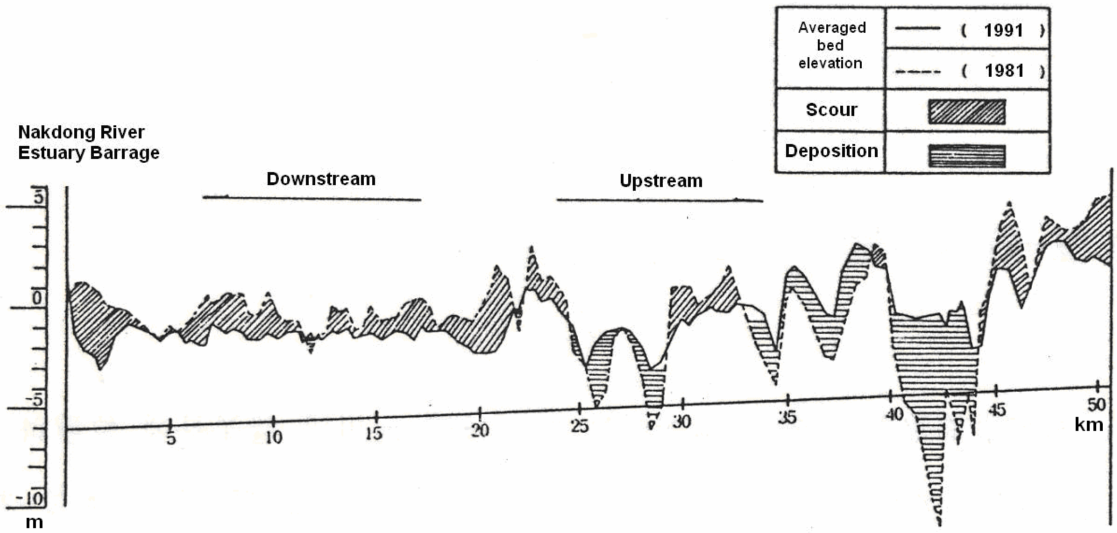

Figure 3-15. Longitudinal profile comparison in 1981 and 1991 (Choi, 1996)

3.5 NREB DESCRIPTION, OPERATION, AND SEDIMENT DREDGING

The Nakdong River Estuary Barrage (NREB) was built in 1983-87 to prevent salt-water intrusion in the estuary. The NREB is equipped with ten gates, four regulating gates and six main gates (ISWACO-NEDECO, 1987). The gates can be used for underflow and overflow. Figure 3-16 shows overflow of the regulation gate. The 2.3-km-long barrage includes 510 m of gate sections and 1,720 m of closed dam section with a navigation lock, a fish ladder, and related structures. The NREB supplies the stable water stage upstream and the local auto-traffic improvement, as well as reducing salt-water intrusion. However, the Lower Nakdong River has been dredged to maintain the conveyance capacity of the channel during large floods with high tides (Figure 3-17).

The historical record for the amount of dredging indicates about 665,000 m^3 per year at an annual cost of about 2 million dollars.

Figure 3-16. Regulation gate

Figure 3-17. Sediment dredging on the Lower Nakdong River

According to the NREB maintenance manual prepared by ISWACO-NEDECO (Industrial Sites and Water Resources Development Corporation - Netherlands Engineering Consultants) in 1987, sediment accumulation in the upstream approach channel (3 km from the barrage) must be limited to the siltation buffer depth of one meter, which equals a deposited sediment volume that ranges from 175 to 450 m^3. In addition, an additional 400 to 500 thousand cubic meters, which is approximately 10 percent of the siltation buffer of 0.2 meter in depth, has to be removed for the upstream part of the reservoir between the upstream end of the approach channel and Samryangjin. ISWACO-NEDECO indicated that the dredging works would have to cover a very long area, removing only small quantities and the dredging works would require much time to cover the full stretch and have to be executed as a continuous job.

Historic records of dredging amounts during the 14 years from 1990 to 2003 are in Tables 3-4 and 3-5, which also show the estimated sediment volumes by surveying. For the upstream channel of the NREB, about 665 thousand cubic meters of sediments per year were dredged. Hydraulic suction dredging with a cutterhead and a large pump has been used over 14 years at the NREB. To protect habitat for migratory birds, dredging must be limited from April to September.

Table 3-4. Sediment deposits and dredging amounts after the construction of the NREB from 1988 to 2000 (KOWACO, 2003)

Survey		Upstream		Downstream		Total amount		Unit: 10^3 m^3
Year	Month	Sediment deposits	Differences	Sediment deposits	Differences	Sediment deposits	Differences	Dredging amount
1988	April	220	220			220	220	
	October	526	306	45	45	571	351	
1989	May	765	239	56	11	821	250	
	August	1993	1228	591	535	2584	1763	
1990	April	1944	-49	580	-11	2524	-60	Upstream: 727
	November	992	-952	835	255	1827	-697	
1991	May	1947	955	808	-27	2755	928	Upstream: 627
	December	1704	-243	1404	596	3108	353	
1992	May	1881	177	1751	347	3632	524	Upstream: 949
	December	790	-1091	2241	490	3031	-601	
1993	June-July	1283	493	1847	-394	3130	99	Upstream: 763
	December	775	-508	2124	277	2899	-231	
1994	May	1182	407	2089	-35	3271	372	Upstream: 938
	December	509	-673	2144	55	2653	-618	
1995	May	708	199	2175	31	2883	230	Upstream: 613
	December	621	-87	2121	-54	2742	-141	
1996	May	882	261	2234	113	3116	374	Upstream: 878
	December	475	-407	2355	121	2830	-286	
1997	April-June	590	115	2387	32	2977	147	Downstream: 1288
	December	723	133	1145	-1242	1868	-1109	
1998	June-July	442	-285	902	-243	1344	-528	Downstream: 330
	October	1614	1172	818	-84	2432	1088	
1999	May	1627	13	745	-73	2372	-60	Upstream: 546
	November	1454	-173	654	-91	2108	-264	
2000	April	1690	236	687	33	2377	269	Upstream: 726
	November	1166	-524	956	269	2122	-255	

Table 3-5. Sediment deposits and dredging amounts after the construction of the NREB from 2001 to 2003 (KOWACO, 2003)

Survey		Upstream		Downstream		Total amount		Unit: 10^3 m^3
Year	**Month**	**Sediment deposits**	**Differences**	**Sediment deposits**	**Differences**	**Sediment deposits**	**Differences**	**Dredging amount**
2001	**April**	1226	60	1005	49	2231	109	Upstream: 480
	October	626	-600	849	-156	1475	-756	
2002	**May**	500	-126	885	36	1385	-90	Upstream: 442
	November	223	-227	296	-589	519	-816	
2003	**May**	294	71	650	354	944	425	Upstream: 294
	December	249	-45	525	-125	774	-170	
Average		988	9	1223	17	2173	26	Upstream: 665

3.5 ENVIRONMENTAL EFFECTS ON THE LOWER NAKDONG RIVER

The Nakdong River has been converted to municipal, agricultural, and industrial water resources for 10 million people. Also, near the Nakdong Estuary, there are wetlands, sand islands and deltas, which provide an ideal place and habitat for migratory birds and waterfowls. However, rapid urbanization and industrialization with population increases have caused significant environmental problems and have affected water quality. Also, during typhoon and flood season, significant sediments are transported from the upstream channel to the Lower Nakdong River (Figure 3-18).

Figure 3-18. Flooded rice field in the Lower Nakdong River

Eulsuk Island is an important wetland area for waterfowl and provides suitable winter habitat to large populations of Taiga Bean Geese (Figure 3-19), White-naped Cranes, and many other species of cranes, geese, ducks and plovers.

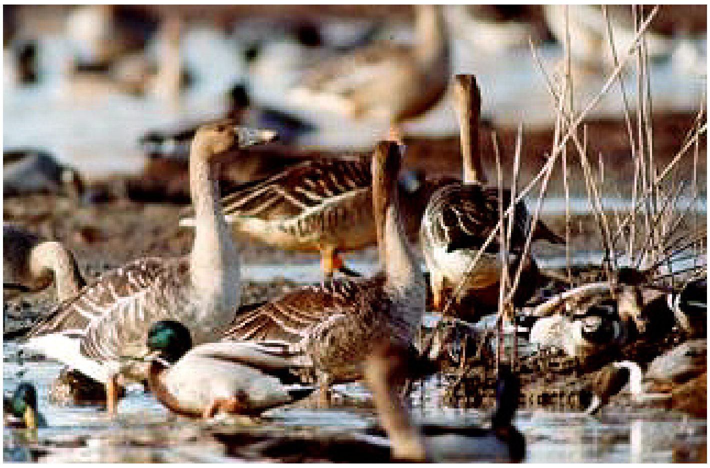

Figure 3-19. Taiga Bean Geese

Eulsuk Island as a bird refuge may be impacted by the quality of sediment. The quality of sediment near Eulsuk Island would be dominated by sediments transported from the upstream channel and affected by gate operations of the Nakdong River Estuary Barrage placed in Eulsuk Island to control the upstream water of the Lower Nakdong River. Therefore, it is essential to analyze the sediment quality near Eulsuk Island and to clarify sediment effects on water quality. One of the water quality components, suspended sediments, is a key indicator of other pollutants, particularly nutrients and metals that are carried on the surfaces of sediment in suspension. Suspended sediments cause a range of environmental water quality problems, including benthic smothering, irritation of fish gills, and transport of contaminants (Davies-Colley and Smith, 2001). The cloudy appearance of silt-laden water results from the intense scattering of light by the fine suspended particles, a phenomenon referred to as 'turbidity' (Kirk, 1985). Turbidity is an important parameter related to sediment concentration and is used to determine the quality of drinking water and to describe water quality conditions.

In addition, salinity impacts water quality of the river and estuary due to flocculated, trapped, and resuspended sediments. Salt-water intrusion and vertical gravitational circulation lead to the ‘trapping’ of the suspended sediment inflowing from the river and the sea (Jiufa and Chen, 1998). Also, the flocculation rate is enhanced by sediment concentration and salinity; i.e., as these quantities increase, both the time to steady state and the steady state floc size decrease (Lick et al., 1993). The flocculated and trapped sediments are apt to resuspend sediments and cause high suspended sediment concentration and high turbidity.

Therefore, in this study, the sediment concentration calculated by the numerical modeling using field data was plotted over a year and analyzed the high concentration period. Also, to analyze the flushing technique effects on the sediment concentration changes, calculated sediment concentration data for flushing and non-flushing simulations were compared in this study (see Chapter 6.3.3.). To consider the prevention of the salt water intrusion in the model, the flushing technique was applied with the regulation. The upstream water level always should be maintained 20 cm above the downstream water level (tide level) of the barrage.

CHAPTER 4: NUMERICAL MODELING FOR THE UPSTREAM NAKDONG RIVER ESTUARY BARRAGE (NREB)

4.1 GENERAL DESCRIPTION OF NUMERICAL MODELING

To simulate sediment deposition and evaluate the feasibility of sediment flushing methods for the NREB, a numerical model of the upstream reach should be used. The model reach should be sufficiently long to describe the backwater effects, which is up to 40 km at Samryangjin. The primary purpose of the model is to simulate the sediment deposition and to quantify possible amounts of sluiced sediments associated with different conditions considering the flow rate and tidal effects.

For the first stage of numerical modeling, a one-dimensional steady flow model with suspended and bed load sediment transport is developed to simulate sediment deposits and to establish sediment flushing curves as a function of upstream discharge and downstream depth. The sediment flushing curves with different discharge represent the relationship between flushed sediment volume and flushing time considering different water depths at the barrage located in the downstream end. In addition, the developed one-dimensional steady model is utilized for the sensitivity analysis of sediment transport equations at the Lower Nakdong River (see Chapter 5.2).

After developing sediment flushing curves, the numerical model was upgraded to a one-dimensional quasi-steady model with variable discharge to analyze different gate operation scenarios and to determine amounts of flushed sediment without dredging under unsteady flows. The discharge data of Samryangjin Station and the observed water stage data of the NREB are used for boundary conditions. The one-dimensional quasi-steady model is calibrated and validated with water stage and discharge field data observed in 2002 and 2003. The different gate operation results in different water depths at the barrage so that the sediment deposits can be sluiced by lowering the water level.

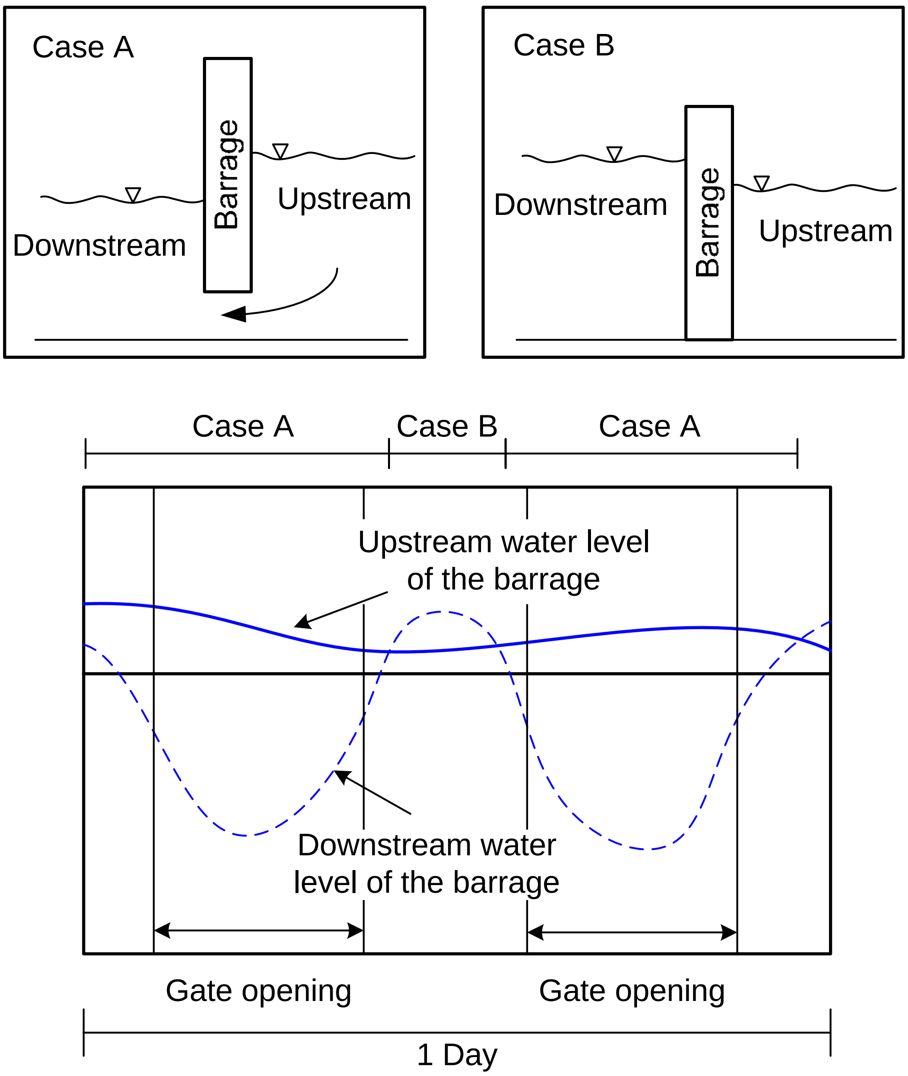

Figure 4-1. Description of possible daily flushing time

To evaluate the effective gate operation scenarios, the possible flushing period (April to June for the NREB) before the flood season and possible daily flushing time considering tidal effects should be considered (Figure 4-1). Figure 4-1 indicates that the gate can be opened only in Case A, which considers the tide condition. ISWACO-NEDECO (1987) also regulated that the gate cannot be operated when the water level difference between the downstream and upstream sides of the barrage is less than 0.2 m above the downstream water level to avoid salt-water intrusion into the upstream channel. Therefore, the upstream water level of the NREB can be controlled by the gate opening as shown in Figure 4-2. The upstream water level should be maintained 0.2 m above the downstream water level for the maximum flushing effect. In the flushing simulation, the adjusted sine curve water level (Figure 4-3) was used as a downstream boundary condition. In other words, the tide effect and gate operation were considered for the flushing simulation using the downstream water level modification in the model.

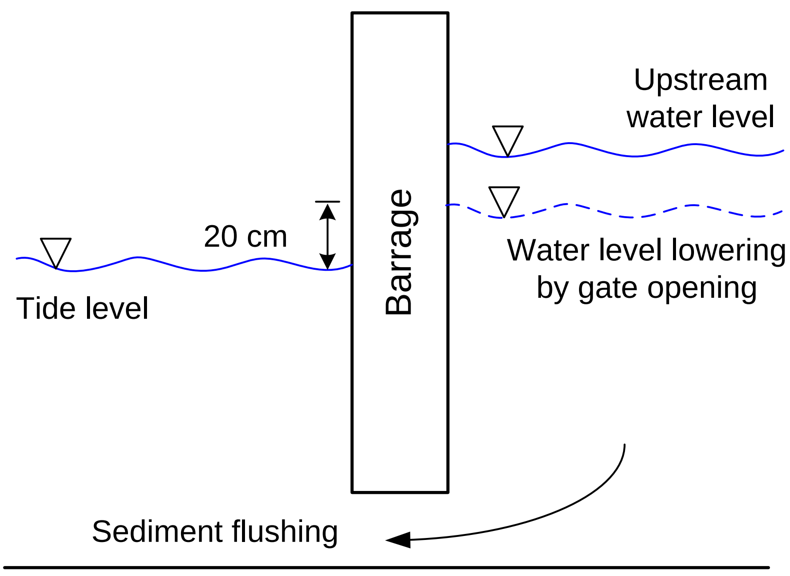

Figure 4-2. The sketch of gate opening for sediment flushing

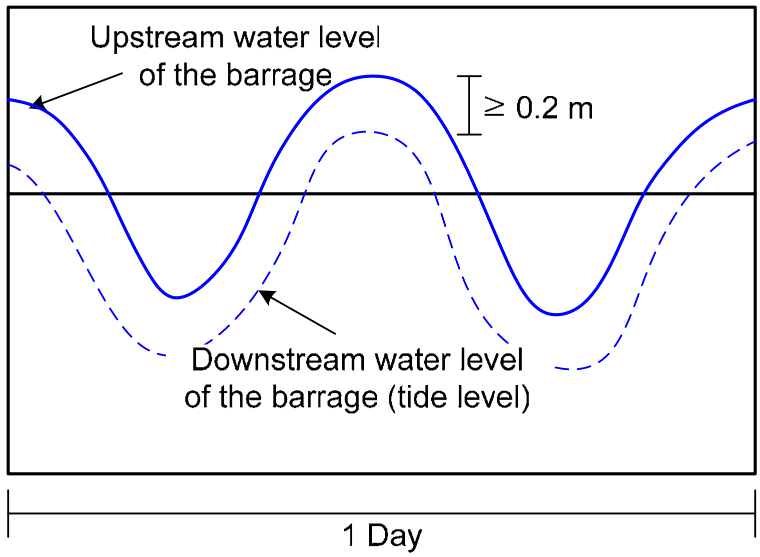

Figure 4-3. Description of water level control by the gate operation

4.2 INPUT PARAMETERS AND SIMPLIFICATION

For the steady state numerical analysis, the flow was considered steady, one-dimensional, and incompressible. The bed was assumed impervious and the cross-sectional geometry was a wide rectangular channel. Also, the median particle size, 0.25 mm at Gupo Station located 15 km upstream of the NREB, was used for the numerical modeling from the NREB to the Samryangjin. For the roughness factor, which was already discussed in Chapter 3.3, the Darcy-Weisbach friction factor (f), 0.03 was used throughout the entire reach. For the quasi-steady state numerical modeling with variable discharge, the channel width and the Darcy-Weisbach friction factor (f) were changed in the high flow conditions to consider floodplain flow.

Two steps of numerical steady state modeling were conducted. First, the simulation of sediment deposition during 134 days was computed for a constant discharge and downstream water depth. To simulate sediment deposition at the upstream channel of the NREB, the initial bed slope was assumed as 0.0002, because the bed slope after the sediment deposition should be around 0.0001 based on field observation, which indicated an aggradation of 1 to 2 m at the delta. The unit discharge of a steady flow was 4 m^2/s and the downstream water depth (h_d) was fixed by 5 m.

Second, the bed elevation changes from the first simulation are used as an initial bed condition for the simulation of sediment sluicing and flushing. Five different unit discharges (1 m^2/s, 2 m^2/s, 4 m^2/s, 8 m^2/s, and 16 m^2/s) are adopted to develop the relations of sediment flushing and downstream water depth at the barrage under different discharges. To estimate the flushed sediment volume, the channel width (W) is assumed as 250 m, which is the average channel width of the Lower Nakdong River as determined by field observations. Among the developed sediment flushing curve, three cases of 100 days for 500 cms, 50 days for 1000 cms, and 30 days for 2000 cms were used for the sediment transport sensitivity analysis.

The stage and discharge hydrograph were annexed to the numerical quasi-steady state modeling. Also, the hourly water stage data were used for the downstream boundary condition instead of the constant water depth in the one-dimensional quasi-steady state model with variable discharge. The detailed additional description of the input parameter and data synthesis for the numerical quasi-steady state model is presented in Chapter 6.1.1.

4.3 METHODS AND EQUATIONS

The governing equations used in modeling are: (1) the continuity equation for gradually-varied flow; (2) the momentum equation for channel flow; (3) a flow resistance equation; (4) the continuity equations for sediment and bed elevation changes; and (5) a sediment transport equation.

4.3.1 Hydraulic process computation

For an impervious channel without rainfall and without lateral inflow, the one-dimensional continuity equation that expresses conservation of mass is (Julien, 2002):

$$\frac{\partial A}{\partial t} + \frac{\partial Q}{\partial x} = 0 \tag{4.1}$$

where: A = channel cross sectional area

Q = flow discharge

The momentum equation can be derived for 2D flows by relating the net forces per unit mass to flow acceleration. The one-dimensional momentum equation for rivers becomes (Julien, 2002):

$$\frac{\partial V}{\partial t} + V\frac{\partial V}{\partial x} = gS_0 - g\frac{\partial h}{\partial x} - \frac{\tau_0}{\rho h} \tag{4.2}$$

where: S_0 = bed slope

V = flow velocity

g = gravity acceleration = 9.81 m/s^2

h = flow depth

τ_0 = bed shear stress

ρ = mass density of water

Equation (4.2) can reduce to the St. Venant equation with the assumptions of a hydrostatic pressure distribution, the bed shear stress in wide-rectangular channels such as $\tau_0 = \rho g h S_f$ (where, S_f = friction slope), and the combination with Equation (4.1). The St. Venant equation has dimensionless form as follows (Julien, 2002):

$$S_f = S_0 - \frac{\partial h}{\partial x} - \frac{V \partial V}{g \partial x} - \frac{1}{g}\frac{\partial V}{\partial t} \tag{4.3}$$

The St. Venant equation is also referred as the dynamic-wave approximation. For all steady flows as well as unsteady flows, the last term, which represents the local-acceleration, can be neglected because it is very small. Also, in the numerical modeling for the Lower Nakdong River, the local-acceleration term was negligible. The details of the calculation results for each term of the St. Venant equation for the Lower Nakdong River are as follows.

The hydraulic condition of Typhoon Maemi at the Lower Nakdong River was adopted to examine each term of the St. Venant equation and to determine which approximation is appropriate for backwater calculation. The discharge of Gupo Station at the Nakdong River peaked at a value of 14,312 cubic meters per second and the water level rose at 2 m per day. At a given discharge, the hydraulic geometry and velocity were calculated by the at-a-station relationship developed for the Nakdong River. Table 4-1 shows the at-a-station hydraulic geometry relationship of the Nakdong River (the details are summarized in Appendix C).

Table 4-1. At-a-station hydraulic geometry relationship of the Nakdong River

Relationship	Equation
Stage - Discharge	$Q = 70.1H^{2.09}$
Width - Discharge	$T_w = 55.2H^{0.236}$
Depth - Discharge	$h = 0.392Q^{0.324}$
Area - Discharge	$A = 10.3Q^{0.648}$
Velocity - Discharge	$V = 0.0461Q^{0.439}$

The continuity equation (Equation (4.1)) can be used to calculate the flow discharge at different cross sections (Julien, 2002). With the given discharge (14,000 cms) at the current cross section, the flow discharge 20 km upstream can be computed by Equation (4.4) knowing that the water level rises at 2m per day.

$$\Delta Q = -\frac{T_w \Delta h}{\Delta t}\Delta x \tag{4.5}$$

The top width was calculated to be 534 m using the width-discharge at-a-station relationship given in Table 4-1. The upstream discharge was determined to be 14,243 cms:

$$Q_2 = 14{,}000cms + \frac{(525m)(2m/day)}{86{,}400s/day}20{,}000m = 14{,}243cms \tag{4.6}$$

Each term of the St. Venant Equation is assigned a number:

$$S_f = S_0 - \frac{\partial h}{\partial x} - \left(\frac{V}{g}\frac{\partial V}{\partial x}\right) - \left(\frac{1}{g}\frac{\partial V}{\partial t}\right) \tag{4.7}$$

$$\qquad 1 \qquad 2 \qquad\quad 3 \qquad\qquad 4$$

Term number 1 is the bed slope and has a value of 0.0002:

$$S_0 = 0.0002 \tag{4.8}$$

Term number 2 represents the free surface slope. The flow depth for the downstream section was determined using the at-a-station depth-discharge relationship:

$$h_{DS} = 0.392Q^{0.324} = 0.392(14{,}000\text{ cms})^{0.324} = 8.64\text{ m} \tag{4.9}$$

It was assumed that a uniform cross-section was applied over the entire reach. Therefore, the hydraulic depth at 20 km upstream was also determined using the at-a-station depth-discharge relationship:

$$h_{US} = 0.392Q^{0.324} = 0.392(14{,}243\text{ cms})^{0.324} = 8.69\text{ m} \tag{4.10}$$

The second term was evaluated using these flow depths and the 20 km change in station information:

$$\frac{\partial h}{\partial x} = \frac{8.64\text{ m} - 8.69\text{ m}}{20{,}000\text{ m}} = -2.5\text{x}10^{-6} \tag{4.11}$$

The third term in the St. Venant Equation was evaluated using the at-a-station velocity relationship:

$$V_{DS} = 0.0461Q^{0.439} = 0.0461(14{,}000\text{ cms})^{0.439} = 3.05\text{ m/s} \tag{4.12}$$

It was assumed that a uniform cross-section was applied over the entire reach. Therefore, the flow velocity at 20 km upstream was also determined using the at-a-station velocity-discharge relationship:

$$V_{US} = 0.0461Q^{0.439} = 0.0461(15{,}250\text{ cms})^{0.439} = 3.07\text{ m/s} \tag{4.13}$$

The third term was evaluated using these velocities and the 20 km change in station information:

$$\frac{V}{g}\frac{\partial V}{\partial x} = \frac{3.05\text{ m/s}}{9.81\text{ m/s}^2}\left(\frac{3.05\text{ m/s} - 3.07\text{ m/s}}{20{,}000\text{ m}}\right) = -3.1\text{x}10^{-7} \tag{4.14}$$

To calculate the change in time for the fourth term, the celerity was calculated using the velocity relationship:

$$c = \beta V = \frac{5}{3}V = \frac{5}{3}(3.05\text{ m/s}) = 5.08\text{ m/s} \tag{4.15}$$

For the 20 km distance, the time of travel for the flood wave $(t = x/c)$ was determined to be 3937 seconds. The fourth term was evaluated using this change in time and previous calculated velocities:

$$\frac{1}{g}\frac{\partial V}{\partial t} = \frac{1}{9.81\text{ m/s}^2}\left(\frac{3.05\text{ m/s} - 3.07\text{ m/s}}{3937\text{ s}}\right) = -5.2\text{x}10^{-7} \tag{4.16}$$

The first term, the bed slope, is two orders of magnitude greater than the second term and three orders of magnitude greater than the third and fourth terms. Therefore, the local acceleration term was negligible and the quasi-steady dynamic-wave approximation, which includes the first four terms of Equation (4.3), was used in the numerical modeling.

$$S_f = S_0 - \frac{\partial h}{\partial x} - \frac{V\partial V}{g\partial x} \tag{4.17}$$

Water surface elevation profile was calculated by applying the quasi-steady dynamic-wave approximation. In the wide rectangular channel, because the hydraulic radius (R_h) equals to the water depth (h), Equation (4.17) becomes:

$$\frac{dh}{dx}=\frac{S_0-S_f}{1-Fr^2}=S_0\frac{\left[1-\left(\frac{h_n}{h}\right)^3\right]}{\left[1-\left(\frac{h_c}{h}\right)^3\right]} \tag{4.18}$$

where: Fr = Froude number

h_n = normal depth

h_c = critical depth

The cross sectional velocity can be calculated using the Chezy equation, which describes flow resistance to solve the continuity and momentum equations for the channel flow (Yang, 1996).

$$V=Ch^{1/2}S_f^{\ 1/2}=\frac{q}{h} \tag{4.19}$$

where: q = unit discharge

The Chezy coefficient, C, can be calculated using friction factor, $f=0.03$ and also remained constant.

$$C=\left(\frac{8g}{f}\right)^{1/2} \tag{4.20}$$

The normal depth and critical depth can be calculated by the following equations.

$$h_n=\left(\frac{q^2}{C^2S_0}\right)^{1/3} \text{ and } h_c=\left(\frac{q^2}{g}\right)^{1/3} \tag{4.21}$$

Therefore, the upstream depth of the i section can be computed by the sum of the water depth of the $i+1$ section (Figure 4-4) and the water depth changes with respect to the x-directional change calculated by Equation (4.18).

$$h_i = h_{i+1} \pm dh \tag{4.22}$$

$$h_i = h_{i+1} \pm \frac{S_0\left[1-\left(\frac{h_n}{h}\right)^3\right]}{\left[1-\left(\frac{h_c}{h}\right)^3\right]}dx \tag{4.23}$$

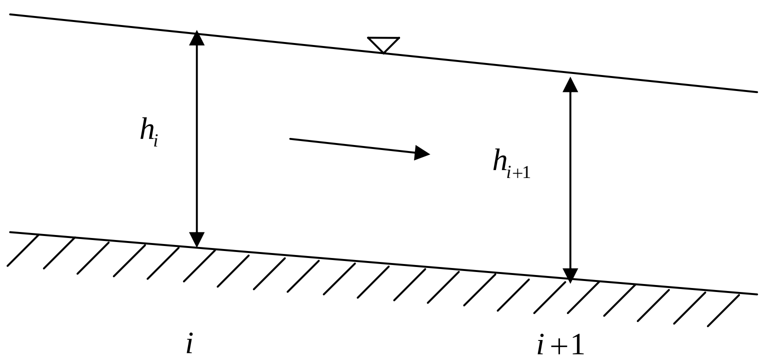

Figure 4-4. Sketch of channel flow

4.3.2 Sediment transport and bed changes computation

The sediment continuity equation for the sediment concentration without sediment source can be derived by conservation of mass (Julien, 1998).

$$\frac{\partial C}{\partial t} + \frac{\partial \hat{q}_{tx}}{\partial x} + \frac{\partial \hat{q}_{ty}}{\partial y} + \frac{\partial \hat{q}_{tz}}{\partial z} = 0 \tag{4.24}$$

where: C = spatial-averaged sediment concentration inside in the flow

$\hat{q}_{tx}$, $\hat{q}_{ty}$, $\hat{q}_{tz}$ = total unit sediment discharge by volume in the x-, y-, and z-directions (mass fluxes)

The sediment mass flux ($\hat{q}_{tx}$, $\hat{q}_{ty}$, and $\hat{q}_{tz}$) can be expressed in a simple mathematical form which has three types of mass fluxes: advective fluxes, diffusive fluxes, and mixing fluxes.

$$\hat{q}_{tx} = v_x C - (\varepsilon_x + D)\frac{\partial C}{\partial x} \tag{4.25}$$

$$\hat{q}_{ty} = v_y C - (\varepsilon_y + D)\frac{\partial C}{\partial y} \tag{4.26}$$

$$\hat{q}_{tz} = v_z C - (\varepsilon_z + D)\frac{\partial C}{\partial z} \tag{4.27}$$

where: v_x , v_y,, v_z = flow velocity in the x-, y-, and z-direction

ε_x, ε_y, ε_z = dispersion (mixing) coefficient in the x-, y-, and z-directions

D = diffusion coefficient

The diffusive and dispersive flux may be negligible because it can be assumed that advective fluxes are dominant in the channel flow of the Lower Nakdong River.

For estimating the bed material discharge, Brownlie's method was used. The following equations are for the concentration, C_{ppm} of Brownlie's method.

$$C_{ppm} = 7115 c_B \left(\frac{V - V_c}{\sqrt{(G-1) g d_s}} \right)^{1.978} S_f^{\ 0.6601} \left(\frac{R_h}{d_s} \right)^{-0.3301} \tag{4.28}$$

where: G = specific gravity

c_B = coefficient, 1 for laboratory data and 1.268 for field data

d_s = particle size

V_c = critical velocity

And the calculation of the critical velocity is the following.

$$\frac{V_c}{\sqrt{(G-1)gd_s}} = 4.596\tau_{*c}^{0.529} S_f^{\ -0.1405} \sigma_g^{\ -0.1606} \tag{4.29}$$

where: τ_{*c} = Shields dimensionless critical shear stress

τ_c = critical shear stress

σ_g = geometric standard deviation of the bed material

The geometric standard deviation of the bed material (σ_g) is 1 for uniform condition and 3 for well graded condition.

$$\sigma_g = \sqrt{\frac{d_{84}}{d_{16}}} \tag{4.30}$$

The sediment size d_{84} and d_{16} are values of grain size for which 84% and 16% of the material weight is finer. The Shields dimensionless critical shear stress τ_{*c} is a function of the critical shear stress, τ_c , which can be determined using a graph or table.

$$\tau_{*c} = \frac{\tau_c}{(\gamma_s - \gamma)d_s} \tag{4.31}$$

where: γ_s = specific weight of particle

Also, the following conversion equations for sediment concentration and discharge were used in the computation program.

$$C_{mg/l} = \frac{1mg/lGC_{ppm}}{G + (1-G)10^{-6}C_{ppm}} \tag{4.32}$$

$$Q_s \text{ (metric tons / day) } = 0.0864 C_{mg/l} Q\,(m^3/s) \tag{4.33}$$

where: Q_s = sediment discharge

The bed surface elevation can be estimated by the sediment continuity equation. Julien (1998) derived the riverbed aggradation and degradation equation from Equation (4.24) assuming a steady sediment supply without lateral sediment inflow. Based on the assumptions, Equation (4.24) reduces to:

$$\frac{\partial \hat{q}_{tx}}{\partial x} + \frac{\partial \hat{q}_{tz}}{\partial z} = 0 \tag{4.34}$$

Because the diffusive and dispersion fluxes are small and negligible compared with advective fluxes and the settling velocity is dominant in the z-direction, Equation (4.34) becomes:

$$\frac{\partial v_x C}{\partial x} - \frac{\partial \omega C}{\partial z} = 0 \tag{4.35}$$

where: ω = fall (settling) velocity

For the gradually varied flow, the further approximation ($\partial v_x / \partial x \to 0$) is applicable.

$$v_x \frac{\partial C}{\partial x} - \frac{\omega C}{h} = 0 \tag{4.36}$$

Using Equation (4.36), the sediment concentration for particle size of a given fraction i can be described with the upstream sediment concentration C_{0i} of fraction i.

$$C_i = C_{0i} e^{-\Delta x \omega_i / hV} \tag{4.37}$$

The trap efficiency T_{Ei} represents the percentage of sediment fraction i settled within a given distance Δx .

$$T_{Ei} = \frac{C_{0i} - C_i}{C_{0i}} = 1 - e^{(-\Delta x \omega)/q} \tag{4.38}$$

Bed changes of aggradation and degradation were computed using the followed continuity equation of sediment, which is the integrated form of Equation (4.34).

$$\frac{\partial z}{\partial t} = -\frac{T_{Ei}}{(1 - p_0)} \frac{\partial Q_s}{W \partial x} \tag{4.39}$$

where: p_o = porosity of bed material = $1 - \frac{\gamma_{mdl}}{\gamma_s}$

γ_{mdl} = dry specific weight of sediment deposits

Q_s = sediment discharge

W = channel width

d_* = dimensionless particle diameter = $d_s \left[\frac{(G-1)g}{\nu^2} \right]^{1/3}$

ν = kinematic viscosity

An explicit scheme is used for the finite difference scheme of this equation. The domain of the scheme is Figure 4-5. Calculated bed elevation changes split using the weighting factor, α , which is between 0 and 1 ($0 < \alpha < 1$), and affects the stability of a scheme. The stability depends on the hydrodynamic conditions and the type of sediment-transport equation. Because the sediment transport relationship is more proportional to the velocity than the flow depth in the Brownlie's method used in the developed numerical model, a backward difference (Equation (4.40)) and the weighting factor of 0 were used to consider the stability of explicit scheme.

$$\Delta z_{i+1} = -\frac{T_{Ei}}{(1-p_0)}\frac{(Q_{si+1} - Q_{si})}{W\Delta x}\Delta t \tag{4.40}$$

where: Δt = time step

The calculation of new bed slope for the next time step is

$$S_{0i} = \frac{z_i - z_{i+1}}{\Delta x} \tag{4.41}$$

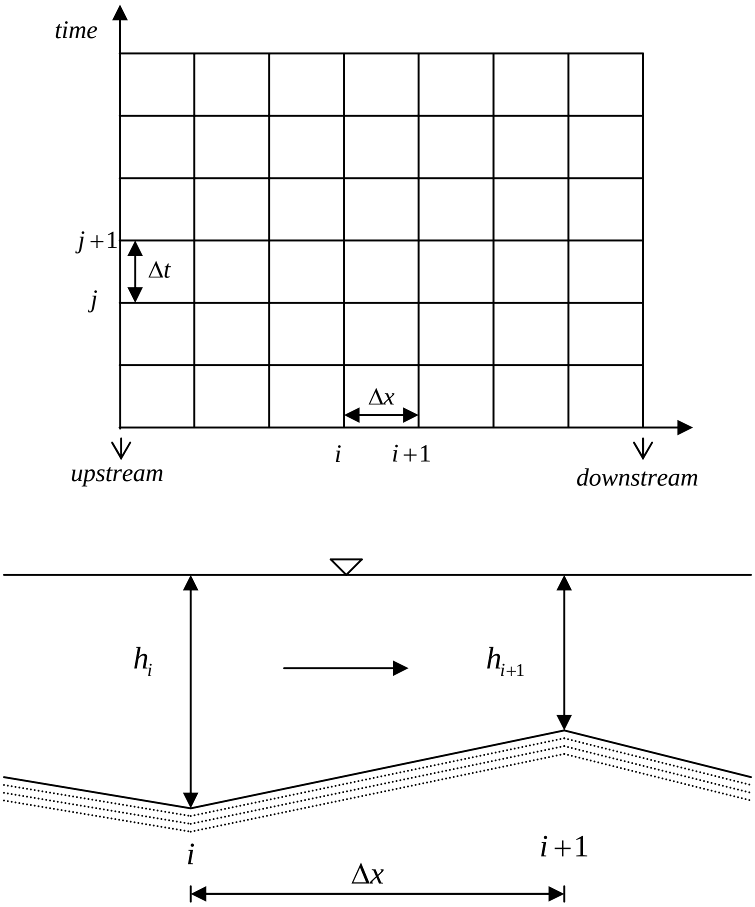

Figure 4-5. Domain sketch of numerical scheme

4.4 COMPUTER PROGRAM CODING DESCRIPTION

Excel with Visual Basic Application was used for programming the numerical model. The program for the steady state model has four parts in Excel sheets: *Input data, Initial Computation, Computation sheet, and Graphs*. For the quasi-steady state model with variable discharge, which is the upgraded version of the original steady state model, two parts were added in Excel sheets: (1) *Hydrograph* for additional input data part; (2) *Water surface level changes* for the output data file.

Two different types of computer program codes, which are the *Excel with Visual Basic Application* and *Excel spread sheet with Visual Basic Application*, were made. The *Excel with Visual Basic Application* was coded at the beginning and mostly made by Visual Basic code. However, the initially developed program was modified to the second version of *Excel spread sheet with Visual Basic Application* to reduce the operation time. The second code simultaneously used Excel spreadsheets for calculations and Visual Basic code for time iterations and input data transformation so that calculation time was able to decrease, especially when the calculation of the long time period was conducted. Mostly, the later program of the *Excel spread sheet with Visual Basic Application* was used for simulations in order to reduce the operating time for the long time period. Figures and program codes of the numerical model are presented in Appendix D.

CHAPTER 5: STEADY STATE MODEL SIMULATION

5.1 SEDIMENT DEPOSITION AND FLUSHING SIMULATION

The numerical analysis of the steady state model was conducted to simulate sediment deposition at the upstream channel of the NREB and to predict the flushed sediment volume by downstream water depth drawdown, which can be determined by the gate operation of the barrage. The unit discharge for the simulation of sediment deposition was 4 m^2/s. Assuming a channel width of 250 m, the flow discharge was 1000 m^3/s. The time duration of the simulation was 134 days, and the downstream water depth (h_d) was 5 m. Other conditions for input parameters were the same as mentioned in Chapter 4.2.

Figure 5-1 presents the results of the sediment deposition model. Model results are similar to field observations. The maximum height of sediment deposits along the channel was 60 cm and the deposited sediment volume was about 2,660,000 m^3 for 134 days assuming the channel width of 250 m. The bed elevation after simulating sediment deposition was considered as the new initial bed condition for the next simulation for sediment flushing.

One of the simulated results for sediment flushing is shown in Figure 5-2. The downstream water depth (h_d) was fixed at 3 m during 100 days of flushing periods. After 100 days with 3 m of the downstream water depth, the maximum eroded height was 34 cm, and the flushed sediment volume was estimated at 710,476 m^3. This is above the

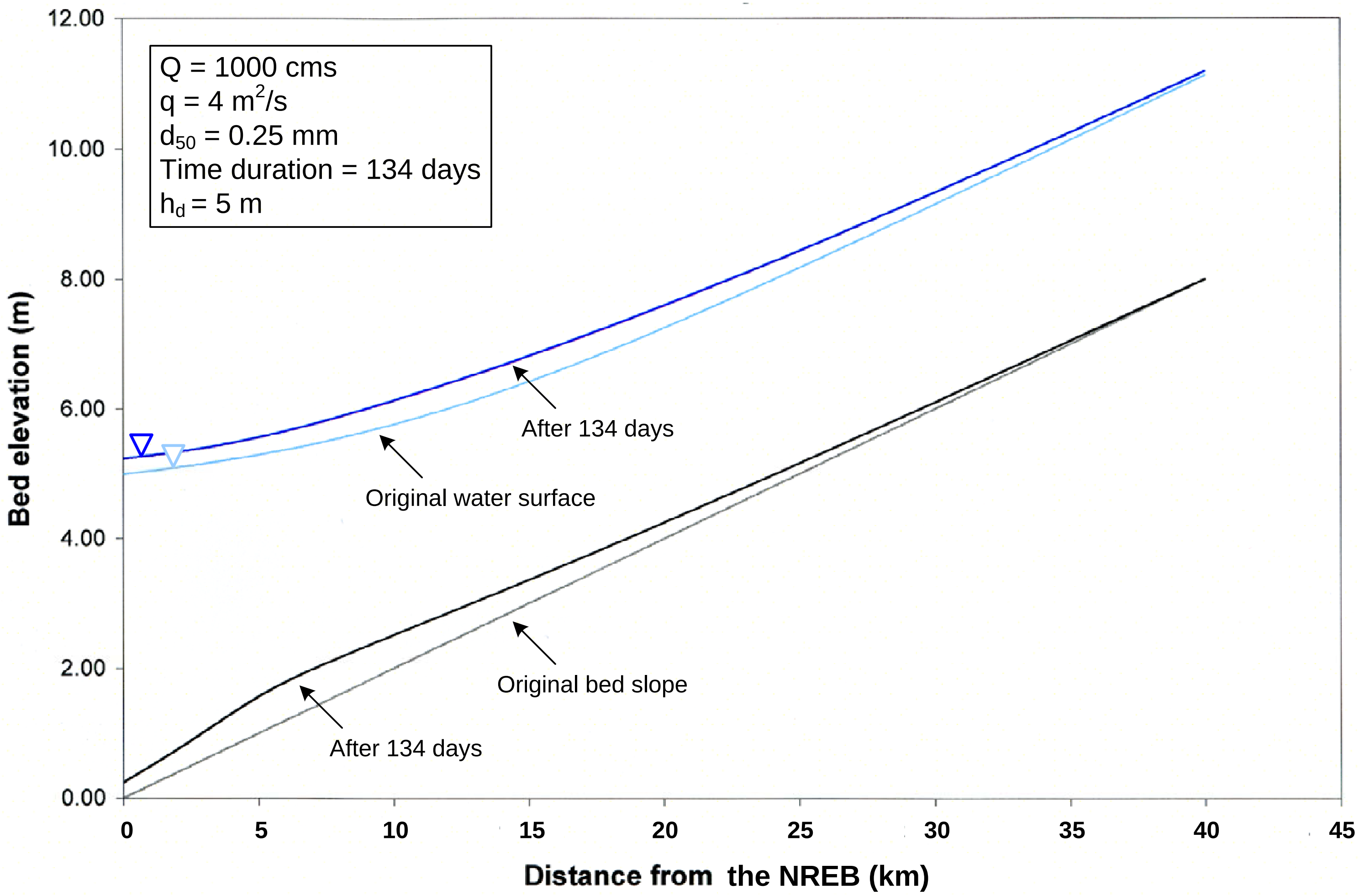

Figure 5-1. Results of sediment deposition modeling

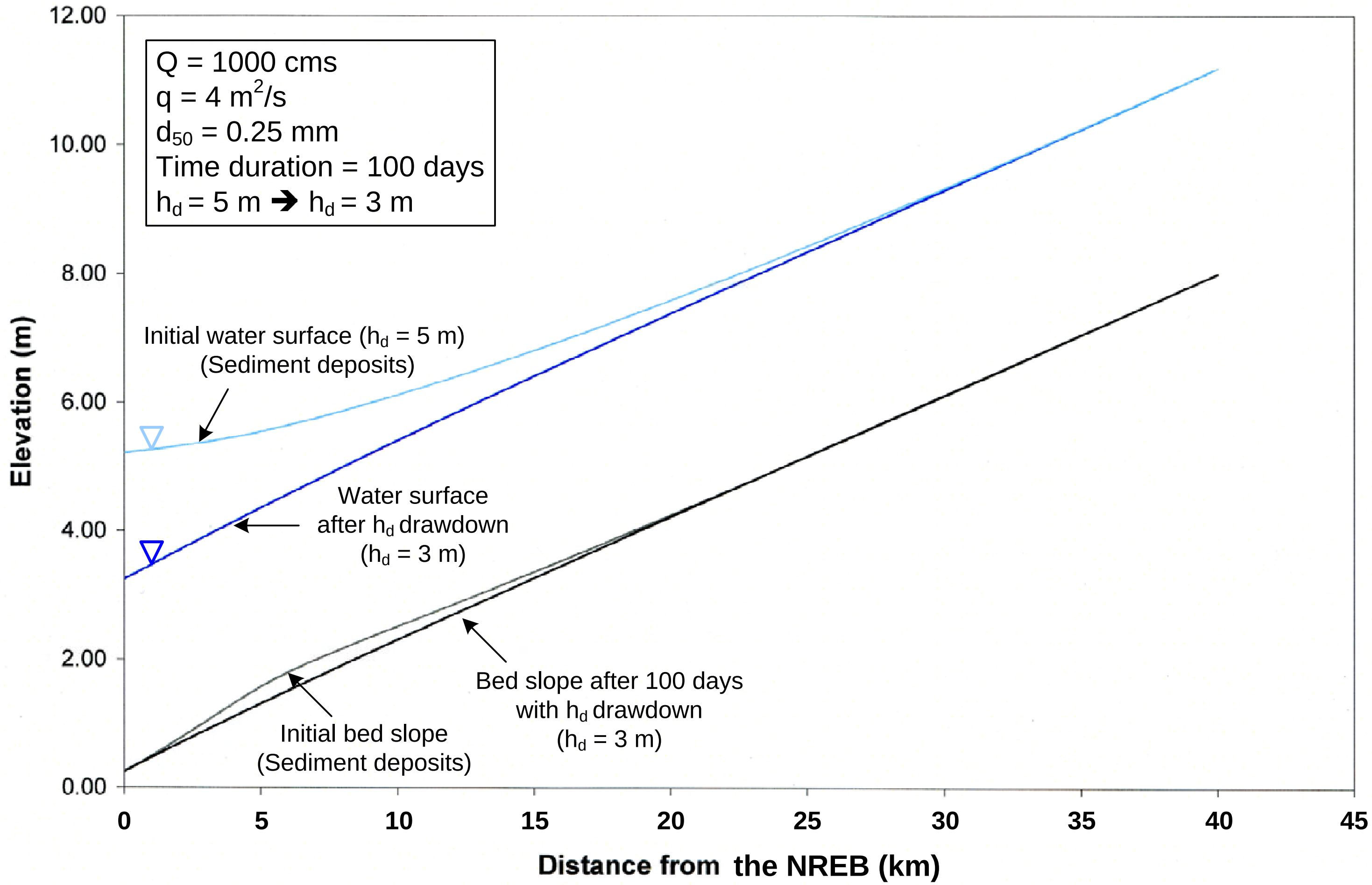

Figure 5-2. Results of sediment flushing modeling with downstream water depth drawdown

annual dredged volume of 665,000 m^3 at the NREB. The flushed sediment volumes resulting from different time durations were also calculated by model simulation.

Figure 5-3 describes bed elevation changes by different flushing times with a flow discharge of 1000 m^3/s and the downstream water depth (h_d) of 3 m. The amounts of flushed sediments at various downstream drawdown depths are shown in Table 5-1 and plotted in Figure 5-4. About 26 days are required to remove the same volume of sediment (665,000 m^3) averaged annually at the NREB assuming a downstream water depth of 2.7 m and flow rate of 1000 m^3/s.

Table 5-1. Calculated volume of flushed sediments with different drawdown and durations (q = 4 m^2/s, Q = 1000 m^3/s)

Q=1000cms	**Sediment volume (m^3)**			
days	h_d = 2.7 m	h_d = 2.8 m	h_d = 2.9 m	h_d = 3.0 m
0	0	0	0	0
10	249,818	178,278	119,557	71,039
20	500,168	356,957	239,496	142,513
30	750,201	535,338	359,148	213,778
50	1,251,823	893,052	597,997	355,978
70	1,749,203	1,247,861	836,119	497,963
100	2,489,220	1,775,902	1,191,789	710,476
150	3,699,133	2,639,491	1,772,284	1,058,156
200	4,871,175	3,476,328	2,335,265	1,396,063
300	7,072,680	5,044,379	3,394,057	2,033,751

Five different unit flow discharges (1 m^2/s, 2 m^2/s, 4 m^2/s, 8 m^2/s, and 16 m^2/s) were used to establish the relationship between flushed sediment volume and flushing

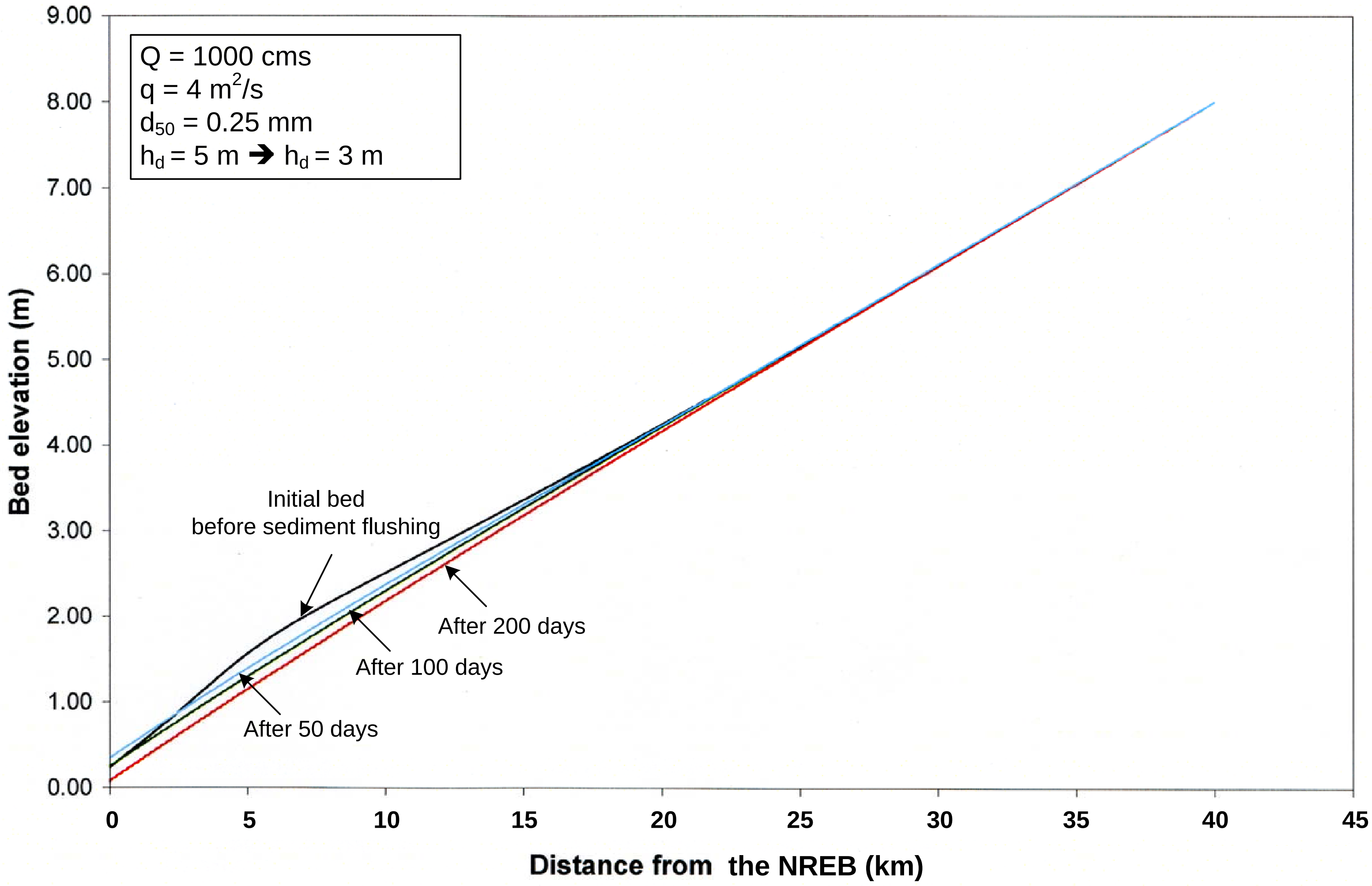

Figure 5-3. Bed elevation changes by sediment flushing with different time durations

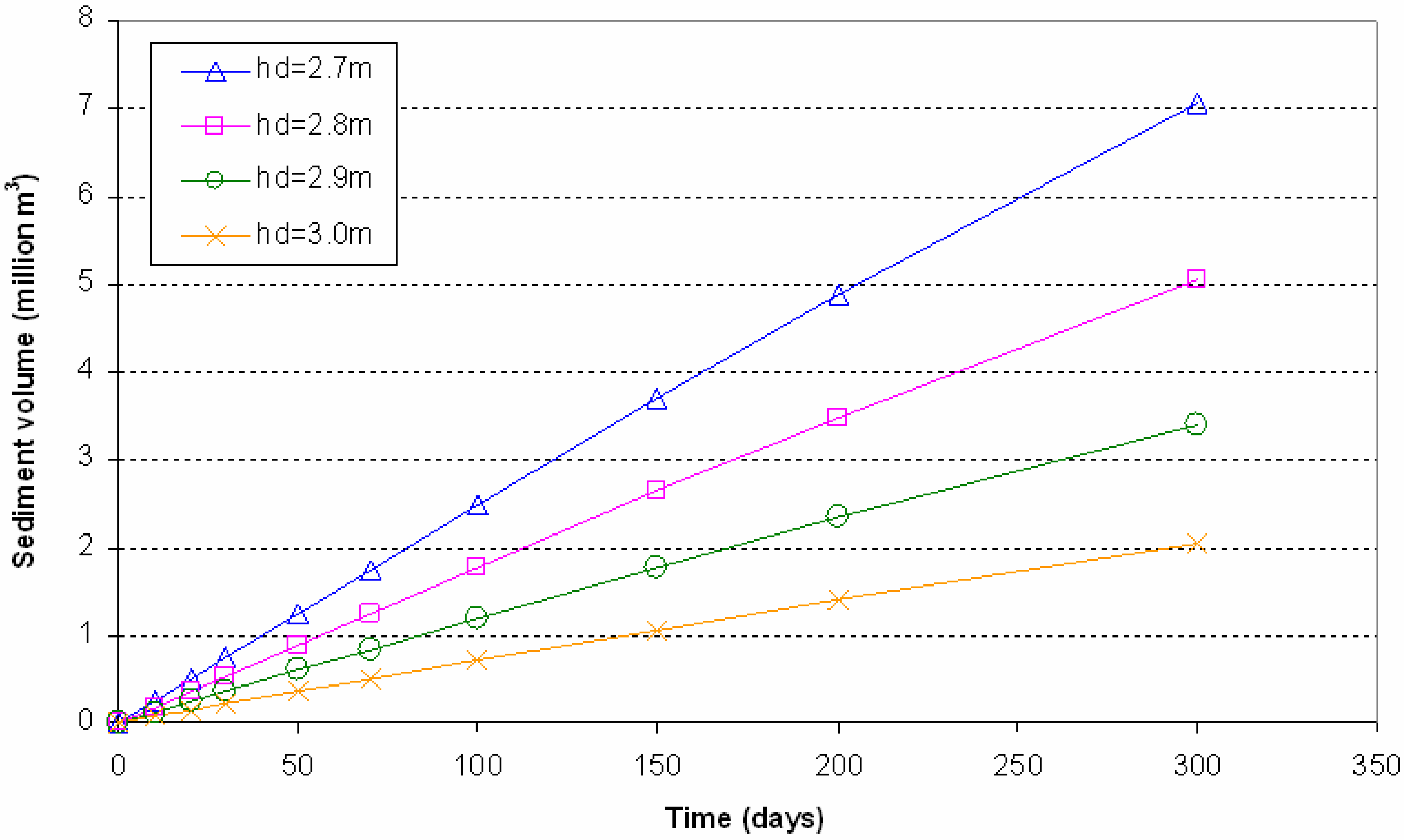

Figure 5-4. Flushed sediment volume of different downstream water depths for $Q = 1000$ m^3/s

time considering different water depths at the barrage located downstream. The results of each case, which are called sediment flushing curves, are described in Figures 5-5 to 5-9. The sediment curve can be used as a fundamental criterion for sediment flushing with different gate operation conditions in the field. These flushing curves were also compared to the dredged sediment volume of the NREB. The unit flow discharge of 1 m^2/s and 2 m^2/s represents low flow conditions and 8 m^2/s and 16 m^2/s can be considered relatively high flow conditions in the Lower Nakdong River.

To flush the sediment deposits equal to the annual dredging volume (665,000 m^3), it took 48 to 180 days at the low flow conditions (1m^2/s and 2 m^2/s). However, for the relatively high flow conditions, it took less than 25 days to flush sediment deposits of 665,000 m^3. In particular, it took only 13 days with 16 m^2/s of unit discharge and 7.6 m of downstream water depth to flush the annual dredging volume of 665,000 m^3. The developed sediment flushing curves indicate the feasibility of sediment flushing at the NREB.

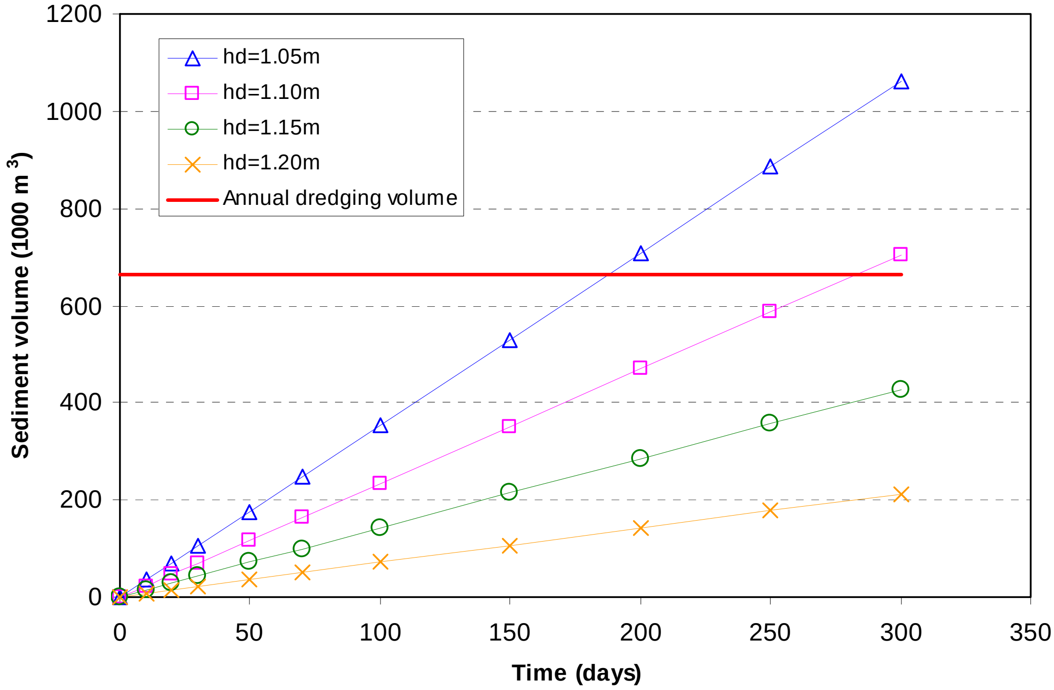

Figure 5-5. Flushed sediment volume for $Q = 250$ m^3/s

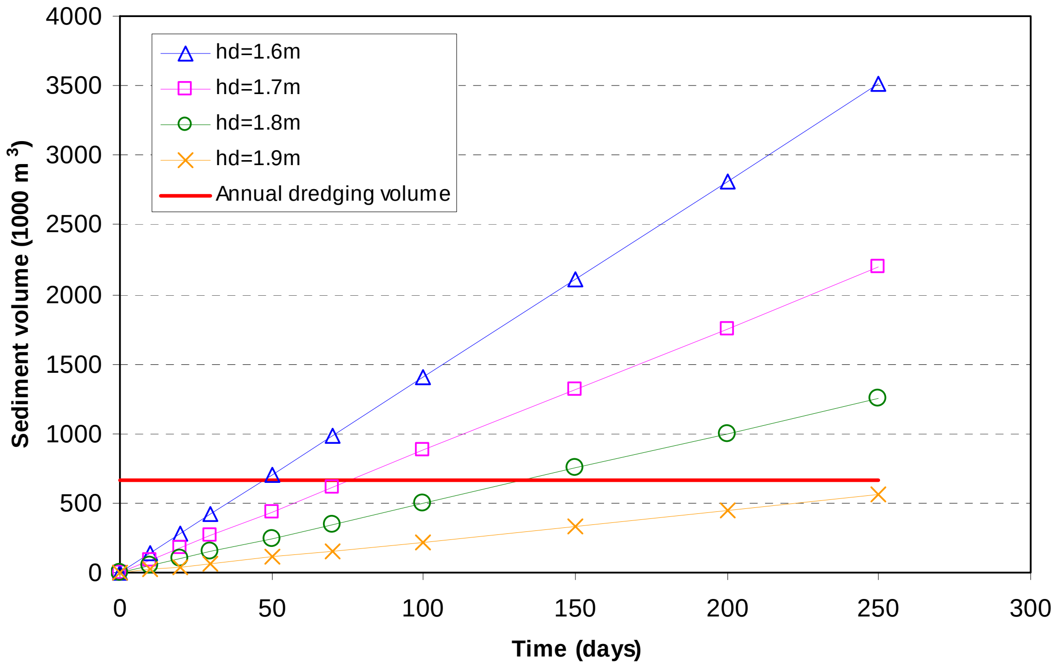

Figure 5-6. Flushed sediment volume for $Q = 500$ m^3/s

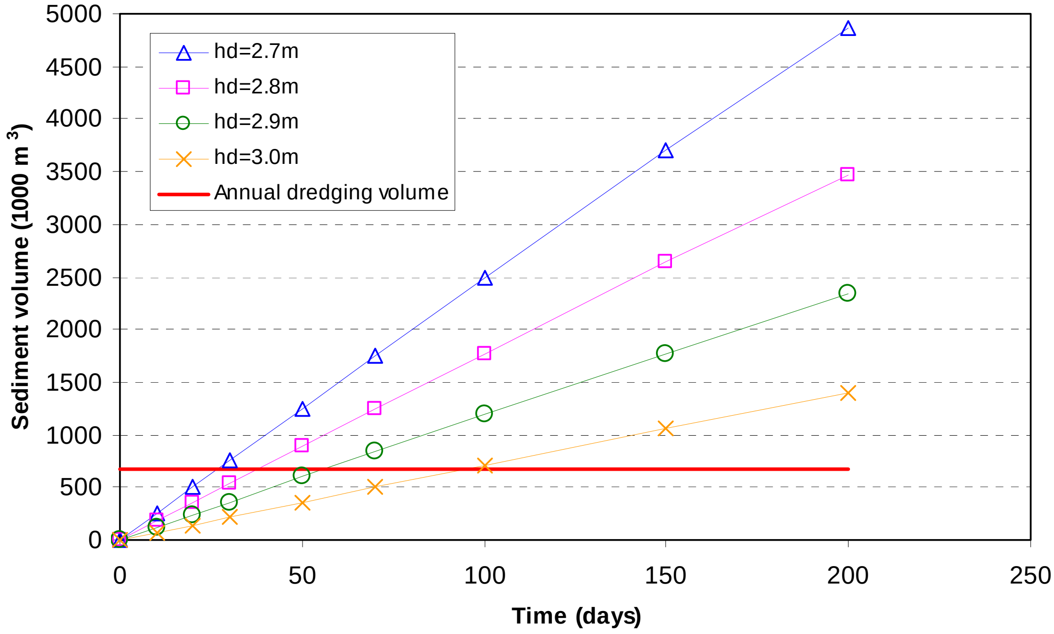

Figure 5-7. Flushed sediment volume for $Q = 1000$ m^3/s

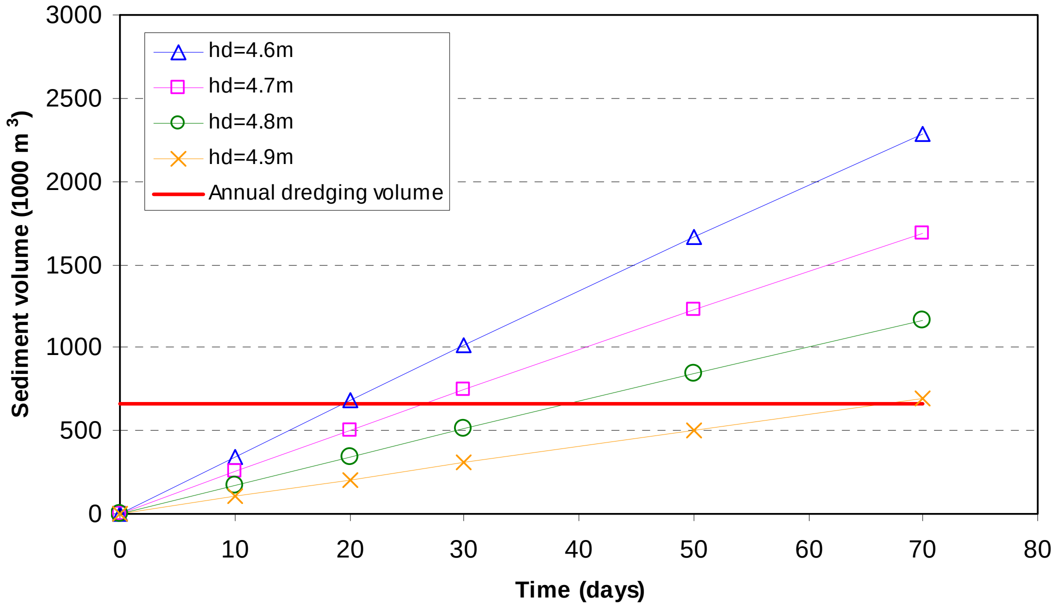

Figure 5-8. Flushed sediment volume for $Q = 2000$ m^3/s

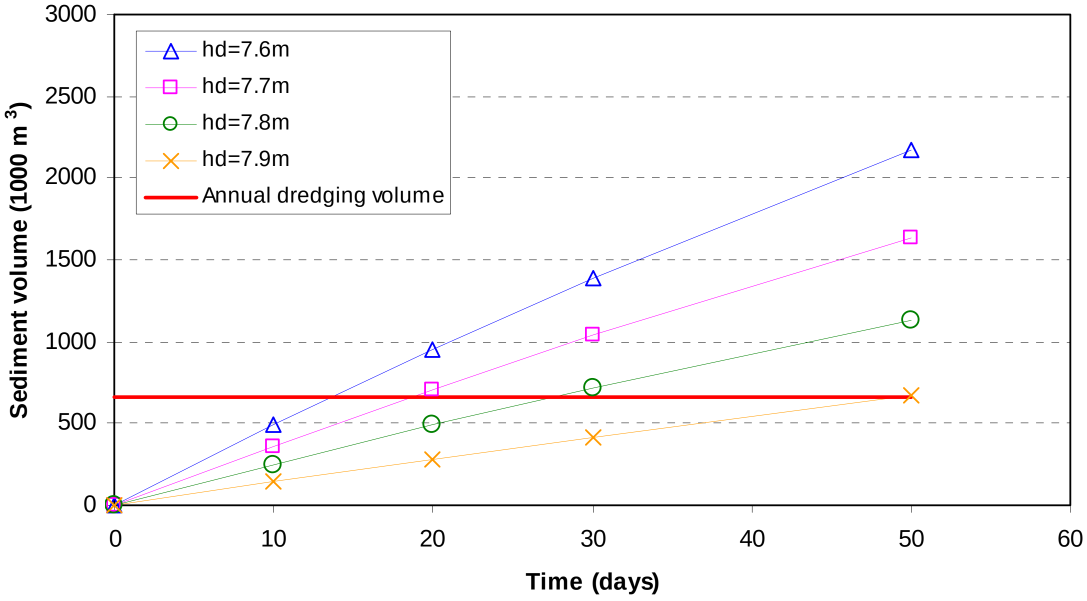

Figure 5-9. Flushed sediment volume for $Q = 4000\ m^3/s$

5.2 SENSITIVITY ANALYSIS OF SEDIMENT TRANSPORT EQUATIONS

Observation of sediment outflow data can be used for the calibration to adjust and evaluate sediment transport equations. Because none of the proposed sediment transport equations can be accepted as a universal equation (Yang, 1996), the comparison of several formulas with field observations is strongly recommended to select the most appropriate sediment transport equation for a given field site. In this study, the sediment transport capacity of Jindong Station and the NREB using field data in 1995 was compared to total sediment load estimated by five different sediment transport equations. Table 5-2 shows the calculation results of the NREB (see Chapter 3.3). Engelund and Hansen (1967), Shen and Hung (1972), Yang (1979), and Brownlie (1981) show a good agreement with the NREB field data, and the Shen and Hung, Ackers and White, Yang, and Brownlie equations are well fitted with Jindong Station field data.

However, it was anticipated that variations in computed sediment capacities associated with various transport equations would have significant influence on the sediment flushing computations; hence, sensitivity analyses were performed. Due to the absence of field measurements for comparison of flushed sediments, it is very important to analyze the sensitivity of the sediment flushing estimation of various sediment transport equations.

To analyze sensitivity of sediment transport equations for sediment flushing calculation, the steady state models, which have four different sediment transport equations such as Ackers and White, Engelund and Hansen, Yang, and Brownlie, were built. Three cases among the developed flushing curves were selected, as shown in Figure 5-10, to compare the flushed sediment volume computed by various sediment transport equations. Four different downstream water depths with 100 days for 500 cms, 50 days for 1000 cms, and 30 days for 2000 cms were used for boundary conditions and

Table 5-2. Sediment transport capacity comparisons of the NREB

Discharge (Q) ➔	**Sediment transport capacity (tons/day)**				
	250 cms	**500 cms**	**1000 cms**	**2000 cms**	**4000 cms**
Ackers and White	20,263	158,271	519,548	2,176,815	81,704,279
Brownlie	9,377	35,649	80,666	218,264	556,270
Engelund and Hansen	9,021	38,486	95,205	288,902	827,381
Shen and Hung	5,367	27,303	67,144	204,813	572,416
Yang	6,182	27,388	61,910	175,220	457,585
Regression equation of NREB field data	14,197	35,115	86,852	214,821	531,342

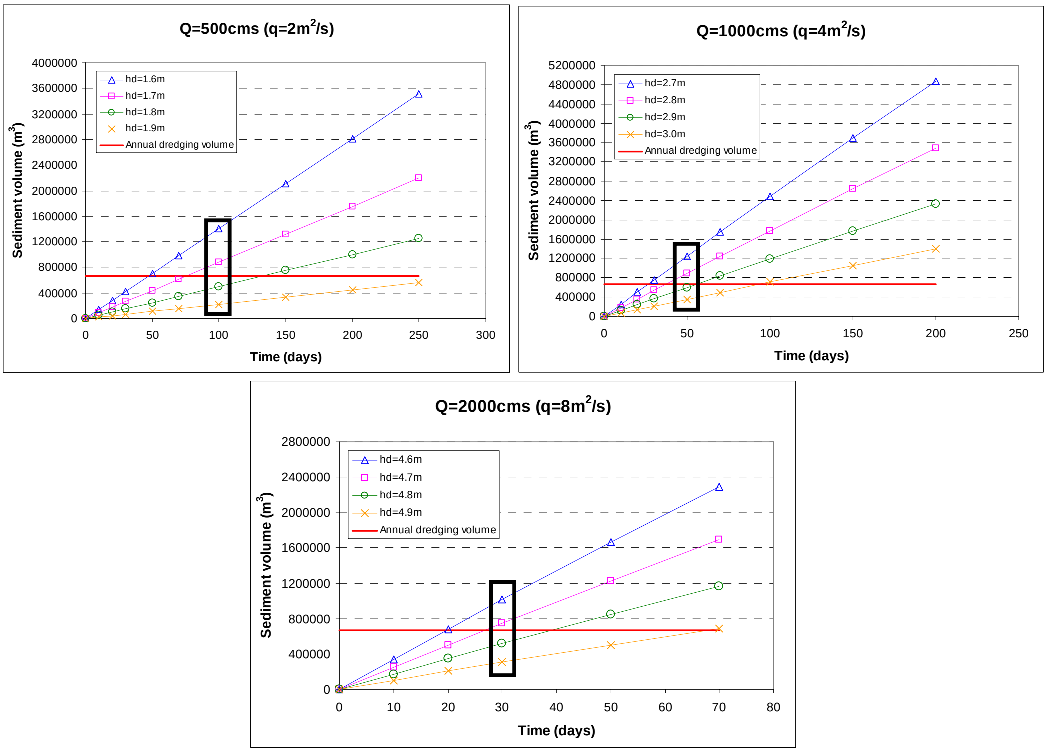

Figure 5-10. Selected cases for sensitivity analysis of sediment transport equations

total flushing simulation time. Table 5-3 and Figures 5-11 to 5-13 present the sensitivity analysis results of three different cases. For the flow conditions of 500 cms and 1000 cms, Engelund and Hansen's (1967) equation produced a relatively high flushed sediment volume from the upstream channel of the NREB. On the other hand, Yang's (1979) equation estimated lower values of sediment flushing than other equations. The variation between highest calculated values and computation results of Yang's equation ranged approximately from 200,000 m^3 to 700,000 m^3. Also, computation results of the Ackers and White (1973), Engelund and Hansen (1967), and Brownlie (1981) equations varied widely in the relatively high flow discharge, whereas variations of flushed sediments by those three equations in the low flows were very small.

The differences in the results of sensitivity analyses are attributable to different approaches and applied field data to develop sediment transport formulas. Model results of sensitivity analyses indicated that the sediment flushing estimation by Brownlie's method stands for the average value at the Lower Nakdong River. In this study, the Brownlie equation was selected as a sediment transport equation for the numerical model of 40 km area from the NREB and the Samryangjin.

Table 5-3. Sensitivity analysis results of sediment transport equations for sediment flushing computation

Q=500cms 100 days	**Flushed sediment volume (m^3)**			
	h_d = 1.6 m	h_d = 1.7 m	h_d = 1.8 m	h_d = 1.9 m
Engelund and Hansen (1967)	1386745	853476	479104	210986
Brownlie (1981)	1404262	876773	498088	221619
Ackers and White (1973)	1332935	828104	467966	206997
Yang (1979)	683339	410890	225488	97232
Q=1000cms 50 days	**Flushed sediment volume (m^3)**			
	h_d = 2.7 m	h_d = 2.8 m	h_d = 2.9 m	h_d = 3.0 m
Engelund and Hansen (1967)	1351870	955234	635297	375299
Brownlie (1981)	1251823	893052	597997	355978
Ackers and White (1973)	1110128	791579	530641	315616
Yang (1979)	622396	435960	287341	168162
Q=2000cms 30 days	**Flushed sediment volume (m^3)**			
	h_d = 4.6 m	h_d = 4.7 m	h_d = 4.8 m	h_d = 4.9 m
Engelund and Hansen (1967)	1202379	883287	603082	356416
Brownlie (1981)	1012437	750174	513294	304583
Ackers and White (1973)	833141	615952	422934	251050
Yang (1979)	519009	380250	258732	152094

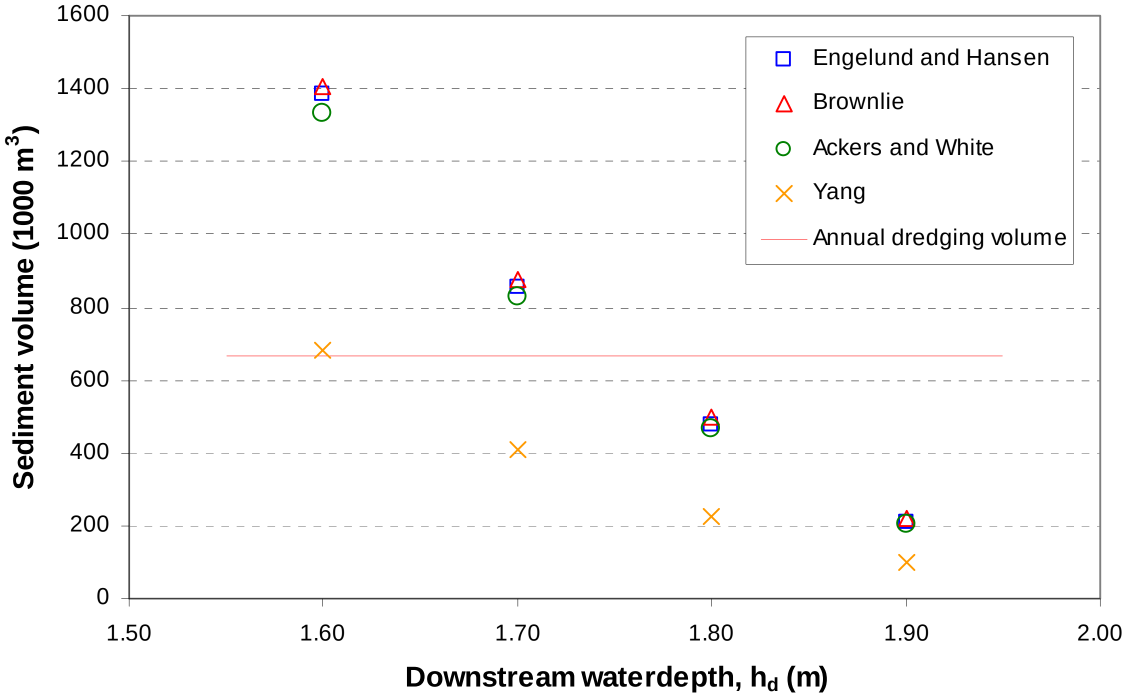

Figure 5-11. Sensitivity analysis result of $Q = 500$ cms and 100 days

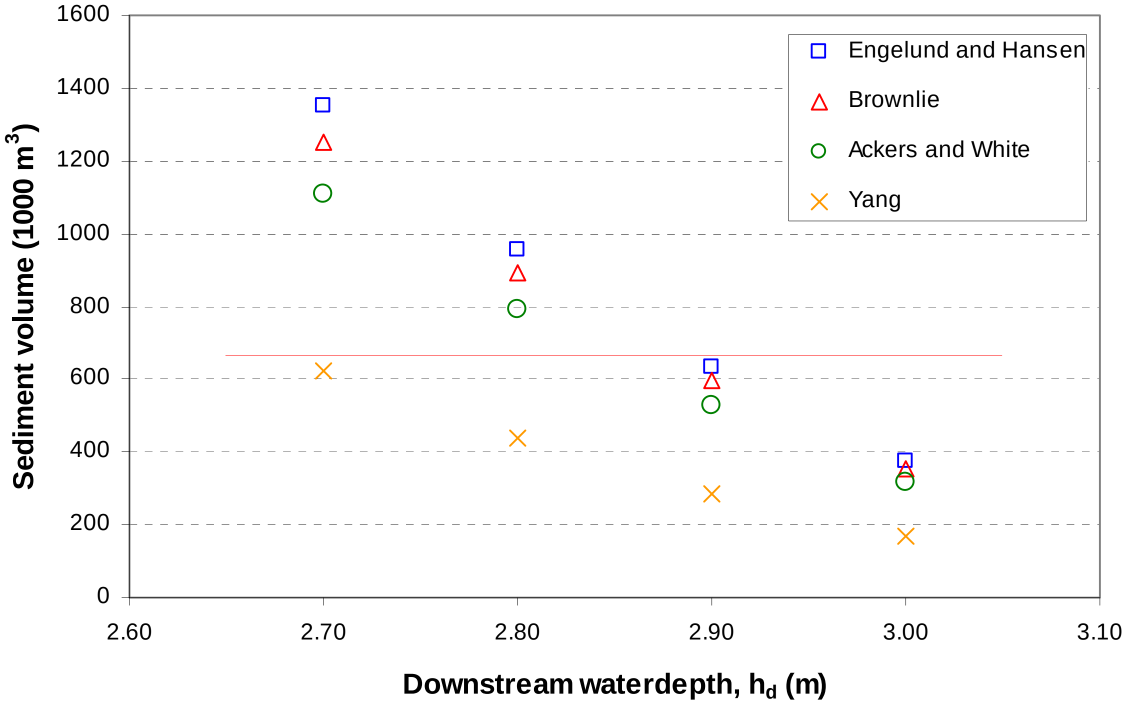

Figure 5-12. Sensitivity analysis result of $Q = 1000$ cms and 50 days

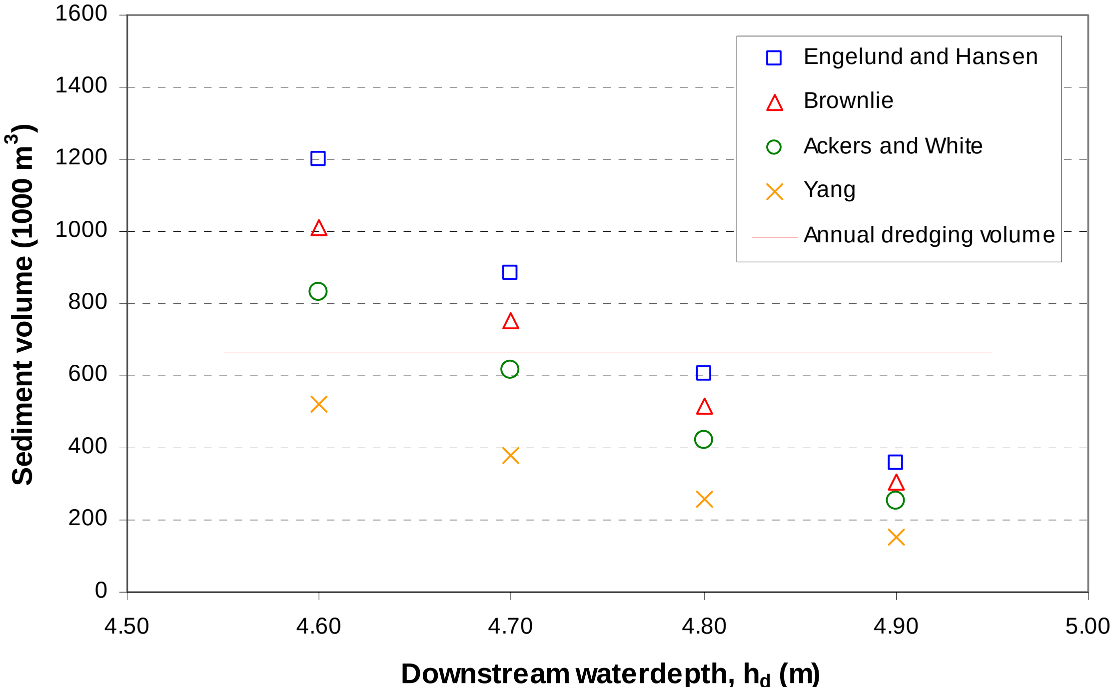

Figure 5-13. Sensitivity analysis result of $Q = 2000$ cms and 30 days

CHAPTER 6: QUASI-STEADY STATE MODEL APPLICATION

The quasi-steady state model with variable discharge was developed primarily to simulate sediment flushing and to evaluate the feasibility of the flushing technique at the NREB using field data. Also, it was used to simulate sediment transport and water level variation with and without dredging operations. The model organization and field data synthesis were conducted to demonstrate the sediment and bed change processes under the sediment control methods including existing dredging operation and suggested flushing technique for the NREB and Lower Nakdong River. For a more accurate simulation when comparing with physical hydraulic and sediment transport process, a model calibration stage is also necessary. A calibration stage for the sediment transport calculation and a sensitivity analysis for the sediment flushing calculation were conducted earlier in the Chapter 3 and 5 using the developed steady state model. In this chapter, hydraulic parameters were adjusted to calibrate the model with stage and discharge data in the field.

6.1 MODEL AND INPUT DATA ORGANIZATION

The quasi-steady state model was developed to use the stage and discharge hydrographs and tide level data observed in the field rather than fixed downstream depth and constant discharge in the original steady state model.

The stage and discharge data from Samryangjin Station, the hourly stage data gauged at the NREB, and the tide data observed at Busan Harbor were collected and synthesized for the boundary condition. The stage and discharge data were obtained from the Nakdong River Flood Control Office and reformed into hourly data to match the tide level data. Tides near the Nakdong River Estuary have been recorded in the coastal area near Busan City by the National Oceanographic Research Institute (NORI) in Korea since 1956. The historic tide data were obtained from the internet website of the Marine Data Center, a subsidiary department of the NORI.

The stage, discharge, and tide data for 2002 and 2003 were plotted in Figures 6-1 and 6-2. Also, Figures 6-3 and 6-4 describe the difference between tide level and upstream water level at the NREB. The differences in water level varied approximately from -1 m to 2 m in 2002 and 2003. The negative value of the water level differences means that the tide level of the downstream side at the barrage is higher than the water stage level of the upstream side. The gate cannot be opened in this situation. However, except in special cases, for example September-1-2003 and May-6-2003 (see Figures 6-3 and 6-4), the upstream water level was higher than tide level most of the year. This indicated that lowering the water level by opening the gate could be applied to eliminate the sediment deposits in the upstream channel. Figure 6-5 describes the concept of lowering the water level by opening the gate. This concept was applied to the numerical simulation for sediment flushing. In the sediment flushing model, the upstream water level is fitted to the new water level, 20 cm above the downstream tide level (historic data), as shown in Figure 6-6. The dotted line in Figure 6-6 represents the adjusted upstream water stage in the sediment flushing model. The gate must be operated to match this line in the field. However, in the model calibration and dredging simulation, the observed downstream water level was used without water level adjustment.

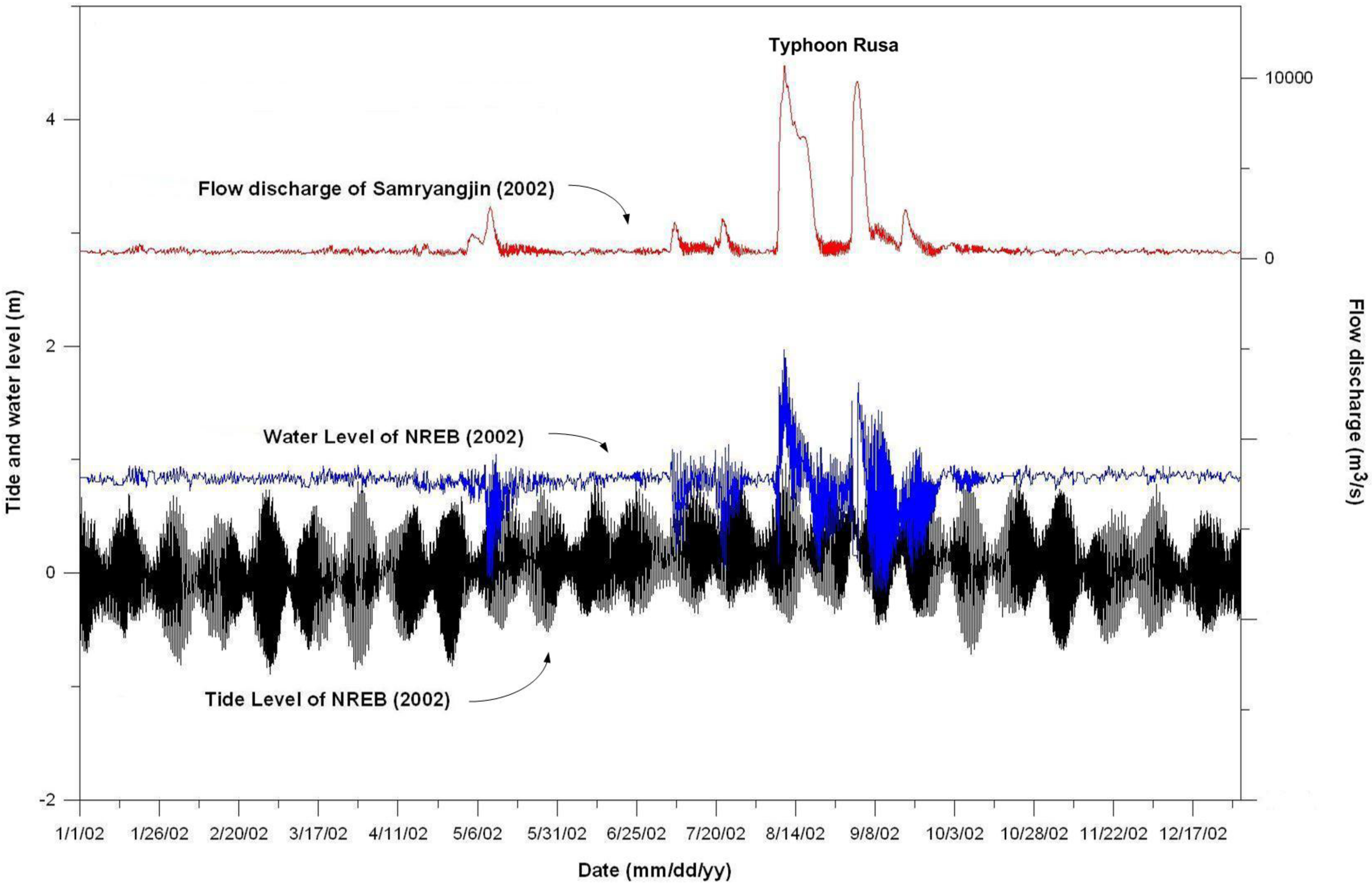

Figure 6-1. Water level, discharge, and tide data (2002) at the NREB

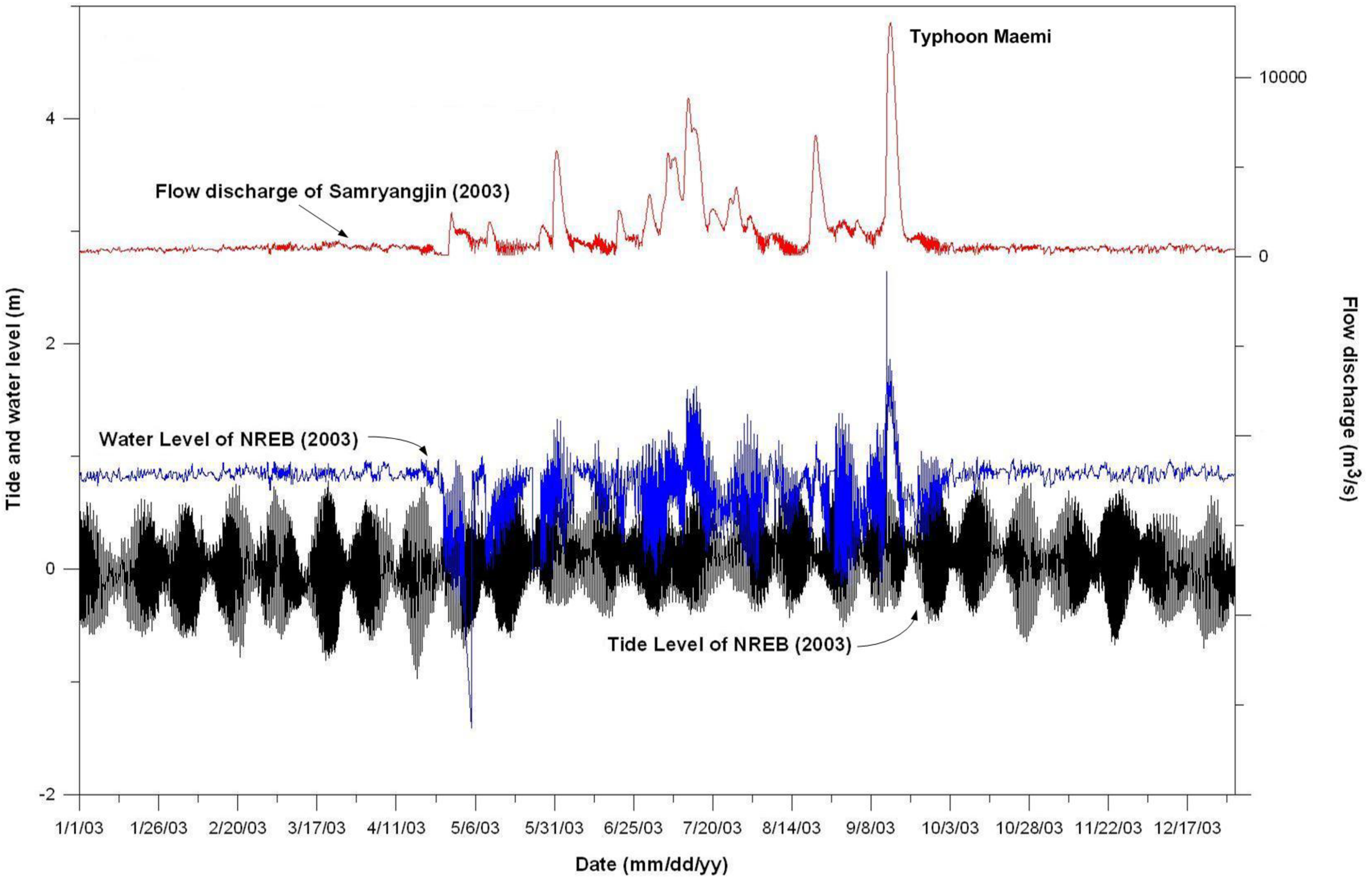

Figure 6-2. Water level, discharge, and tide data (2003) at the NREB

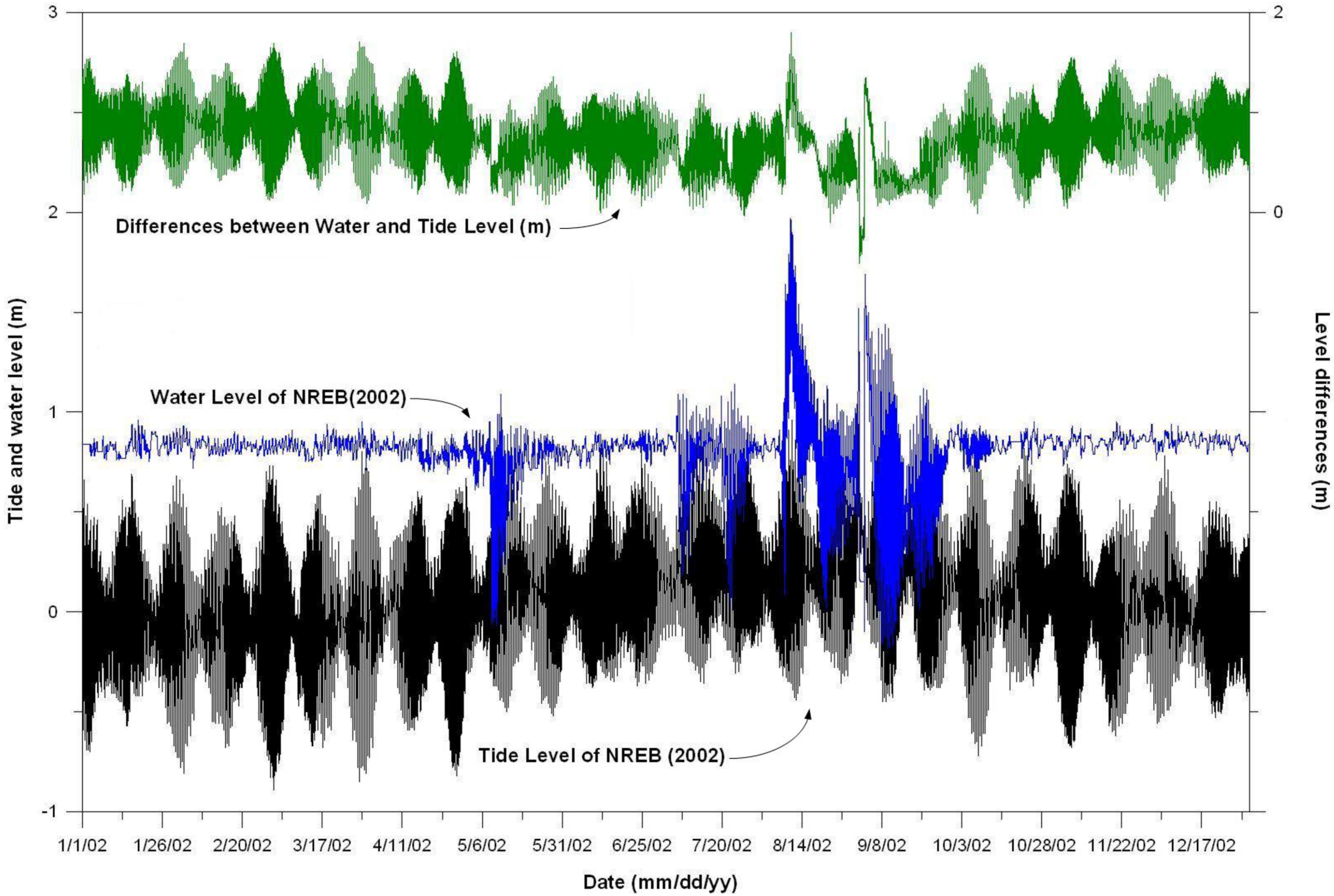

Figure 6-3. Level differences of upstream side water stage of the NREB and downstream side tide level (2002)

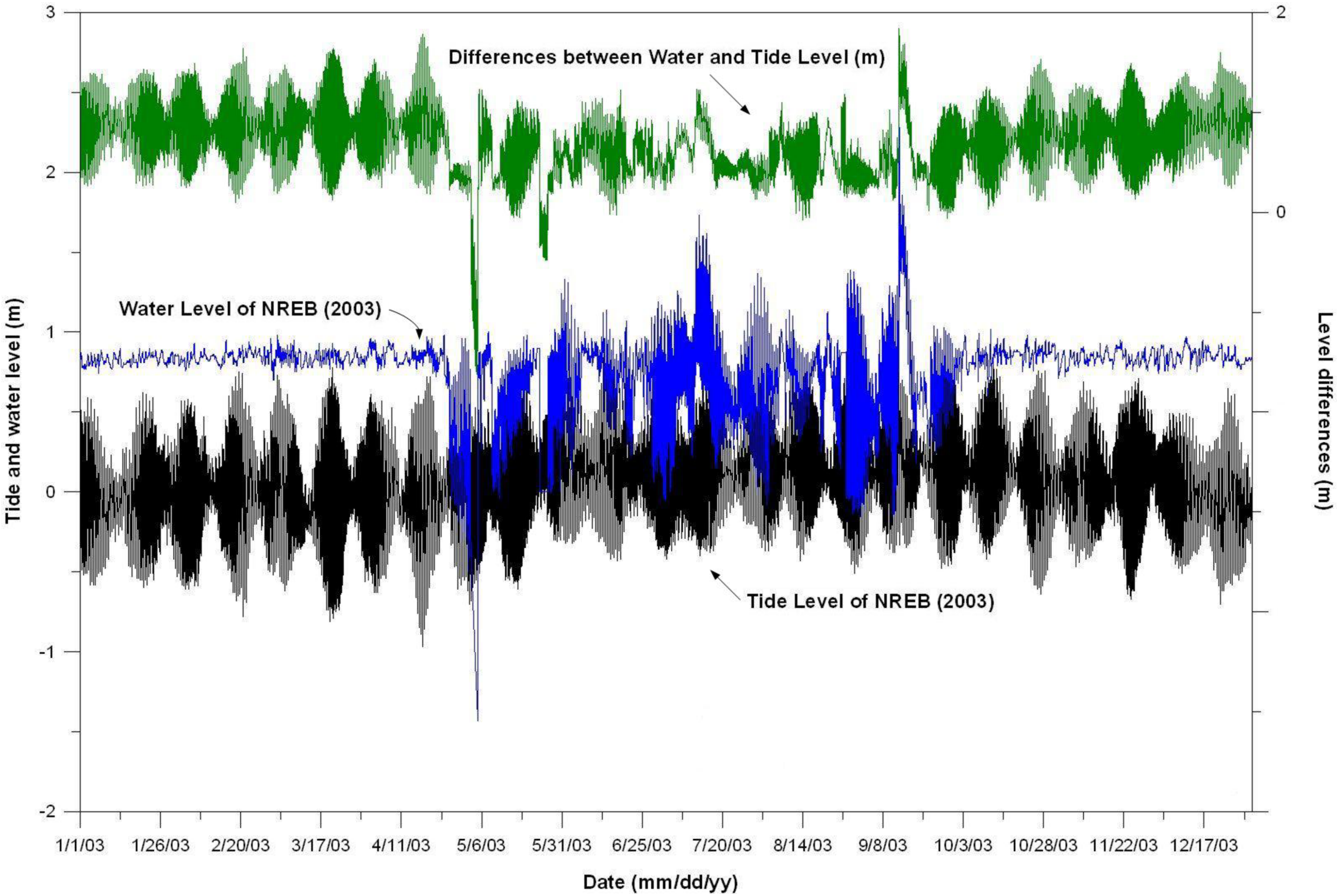

Figure 6-4. Level differences of upstream side water stage of the NREB and downstream side tide level (2002)

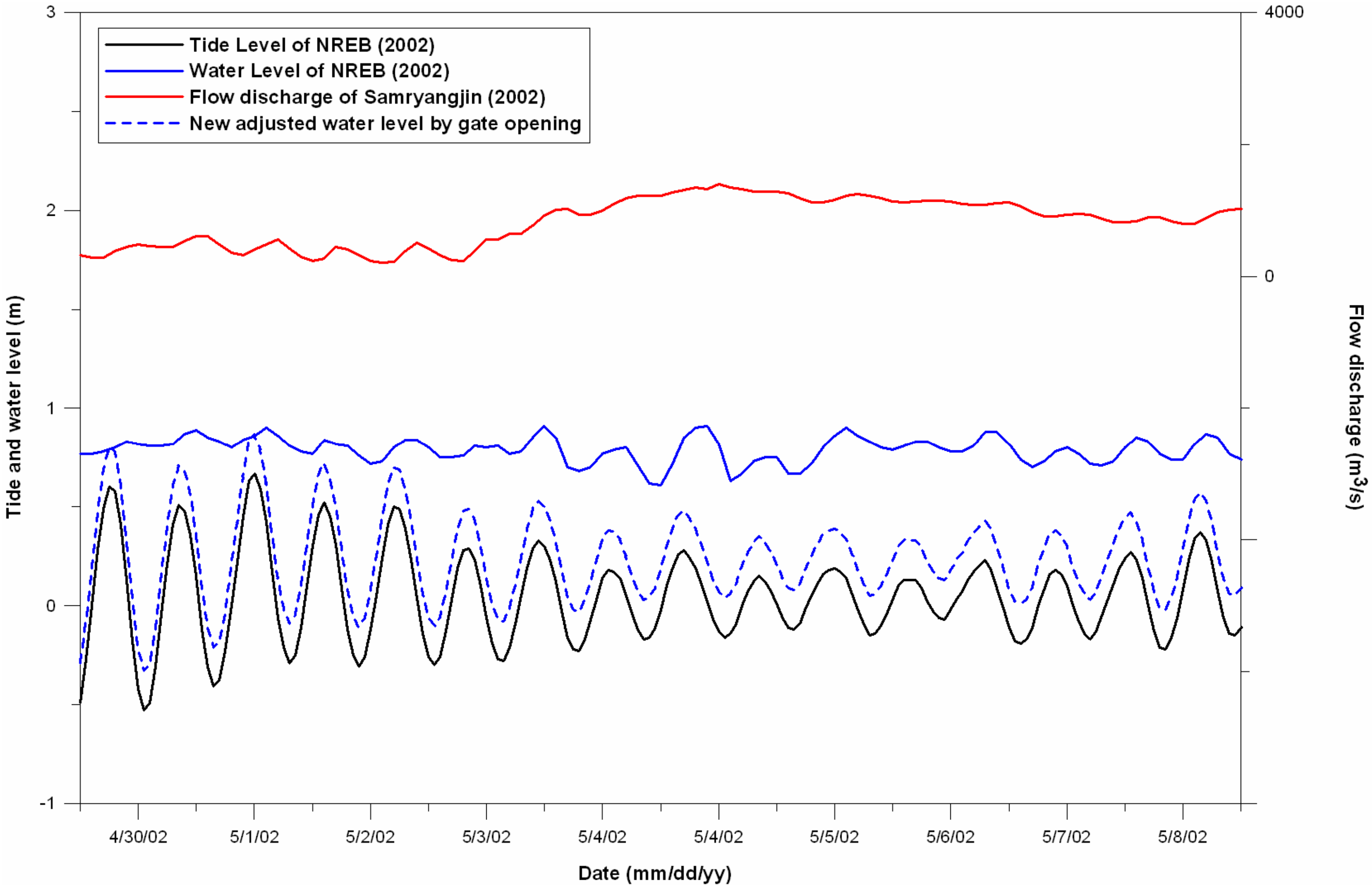

Figure 6-5. Water level lowering for sediment flushing in the numerical modeling

6.2 MODEL CALIBRATION AND VALIDATION

The purpose of model calibration is to obtain a set of parameters so that the model will respond like the physical system it represents (Hoggan, 1997). The stage and discharge field data in 2002 were used to calibrate the model. Calibration parameters of bed roughness and channel width were adjusted until a suitable fit was obtained.

It was determined that the Gupo Station was not representative of the Lower Nakdong River because of significant bed form changes caused by frequent bridge and highway construction and repair work. Therefore, it was not appropriate to compare the simulated stage with the observed stage at the Gupo Station for model calibration. Consequently, a stage graph computed by the quasi-steady state model with a given hydrograph was compared to the observed stage graph at Samryangjin Station.

Simulation results of the stage hydrograph calibration were well matched with field data. The model calibration results from 2002 are described in Figure 6-6. The percent difference was -8.8 % between observed and simulated water stages for the first peak of major floods (August 10, 2002) and -7.3 % for the second peak (September 2, 2002). Also, for the low flow conditions from January to April and from November to December, the percent differences were +7.5 % and +3.8 %, respectively.

The calibrated model was validated with the stage hydrograph of Samryangjin Station in 2003 and the validation performance was also good, as shown in Figure 6-7. The percent difference ranged from +2.9 % to +5.9 % for the peak flow during July to September. Although the validation performance for the low flow condition was less than the calibration performance, the validation results were generally satisfied.

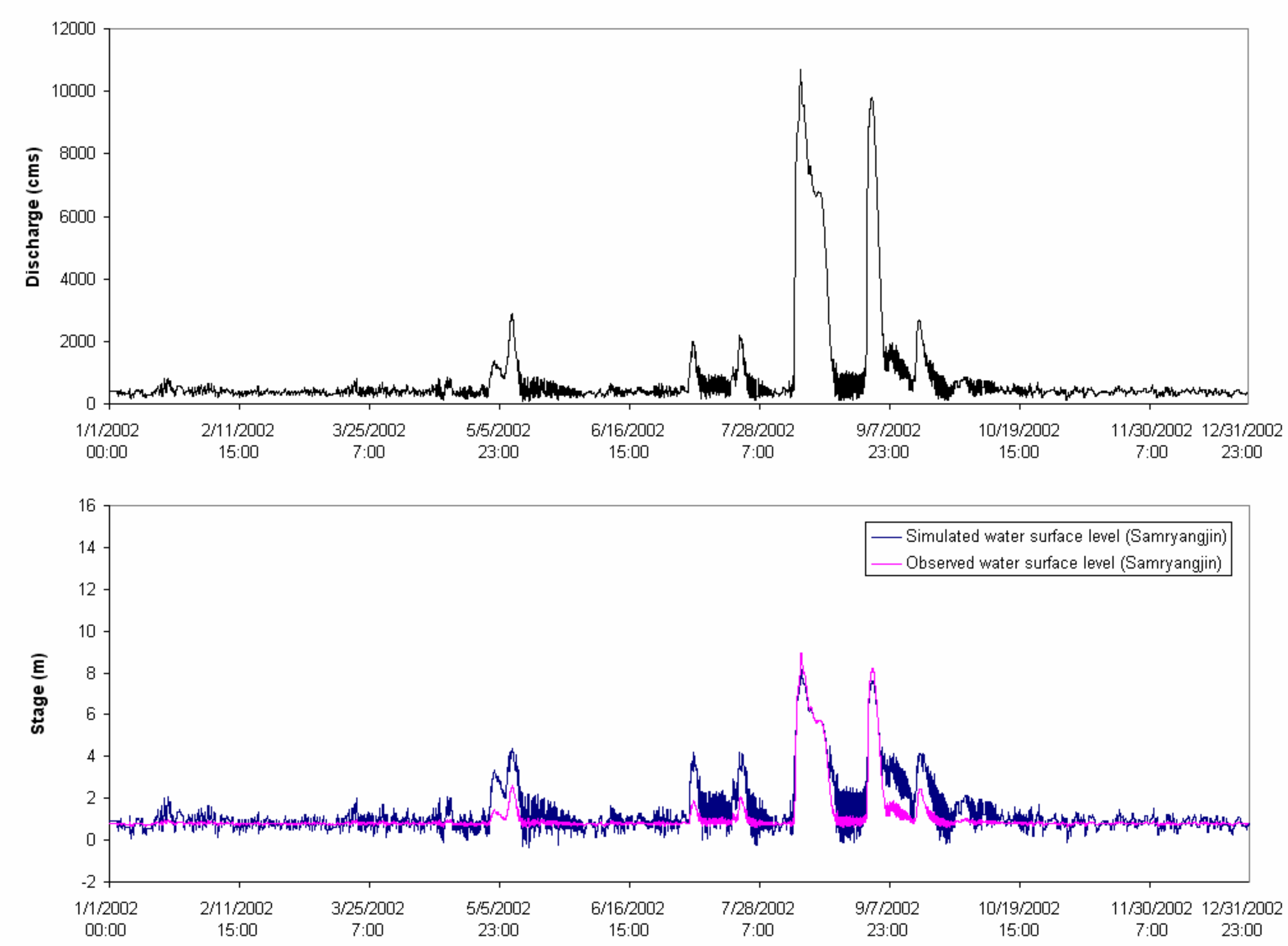

Figure 6-6. Model calibration with 2002 field data

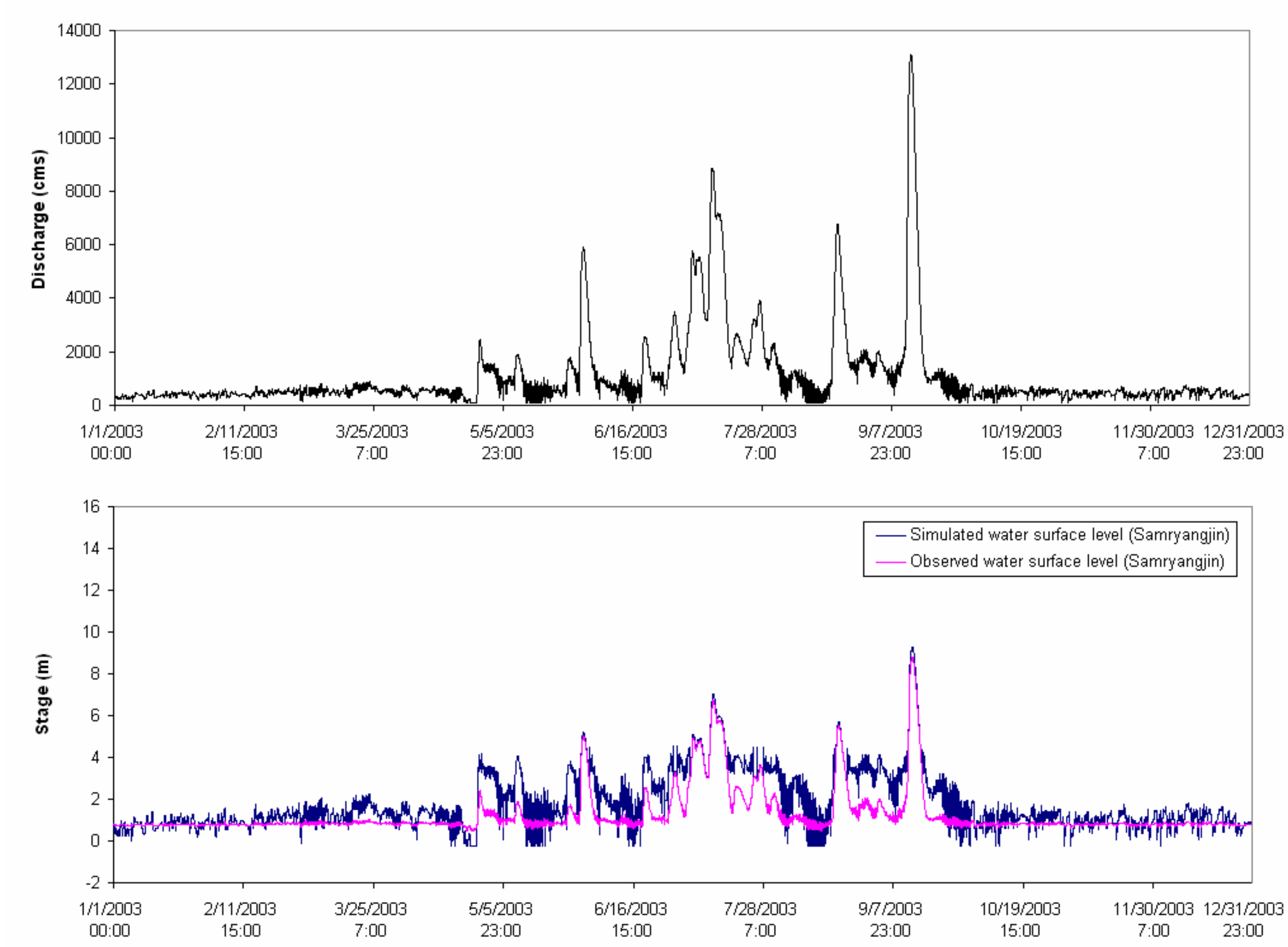

Figure 6-7. Model validation with 2003 field data

The calibration and validation results are evaluated in Table 6-1.

The water surface level at the NREB has relatively large oscillations when compared to the observed upstream water level at Samryangjin Station because the water level at the NREB is sensitive to changes in gate operations. This phenomenon is localized near the barrage and isn't significantly transmitted to the Samryangjin Station in the field. However, the calculated water level of Samryangjin Station in the model had larger oscillation than the observed water level during the calibration and validation processes because the NREB water level was used for the downstream boundary condition in the model. The most important factor for the calibration and validation was the agreement of the simulated and observed peak stage during the flood and typhoon season because the safety of the levee should be considered under any circumstance and situation.

Table 6-1. Model calibration and validation results

Samryangjin water stage Calibration	Observed stage m	Simulated stage m	Difference m	Percent difference %
1st peak stage (8/10/2002)	8.93	8.14	-0.79	-8.8%
2nd peak stage (9/2/2002)	8.17	7.57	-0.6	-7.3%
Low flow condition from January to April	0.8	0.86	0.06	7.5%
Low flow condition from November to December	0.8	0.83	0.03	3.8%
Samryangjin water stage Validation	**Observed stage m**	**Simulated stage m**	**Difference m**	**Percent difference %**
1st peak stage (7/12/2003)	6.71	7.03	0.32	4.8%
2nd peak stage (8/21/2003)	5.54	5.7	0.16	2.9%
3rd peak stage (9/14/2003)	8.78	9.3	0.52	5.9%
Low flow condition from January to April	0.82	1.09	0.27	32.9%
Low flow condition from November to December	0.8	0.97	0.17	21.2%

6.3 MODEL APPLICATION AND SIMULATION RESULTS

The developed and calibrated quasi-steady state model was used to simulate the sediment transport and water level variations with and without the dredging operation to evaluate the effectiveness of the present dredging method on the Lower Nakdong River. Also, the sediment flushing was simulated and demonstrated with the numerical model using the field data to evaluate the feasibility of flushing technique at the NREB. The calculated sediment concentration from the numerical modeling was used to analyze the high concentration period over a year and the flushing technique effects on sediment concentration changes for the environmental aspect.

6.3.1 With and without dredging operation

Before the sediment flushing simulation, performing a numerical analysis of the present dredging operation was necessary. The main purpose of the dredging operation at the Lower Nakdong River is to remove the sediment deposits and to maintain the conveyance capacity of the channel during large floods with high tides. The changes of the hydraulic condition, especially the water level rising during large floods, were examined under the assumption of the absence of the dredging operation and compared to the hydraulic condition with the present dredging operation. This numerical analysis will be helpful to determine whether the dredging operation is the best way to eliminate the deposited sediments at the Lower Nakdong River.

The field data of 2002 to 2003 were selected for the dredging simulation. To apply the bed condition with the present dredging operation to the numerical modeling, the initial bed elevation was fixed with the original bed condition (Figure 5-1) that was used for the sediment deposition simulation of the steady state modeling. The original bed condition represents no deposition in the upstream channel. Even though some deposition in the upstream channel was anticipated in the numerical analysis during January to April of each year, the bed deposition right before the first flood wasn't exceeded and even reached the usual bed condition after the dredging operation in the field. This could be considered the maximum dredging effect for the extreme case. Also, the bed elevation result after the sediment deposition simulation (Figure 5-1) of the steady state model was selected as the initial bed condition for the non dredging simulation.

Computed results with and without the dredging operation for the water stage are compared in Figures 6-8 to 6-11. As shown in Figures 6-8 and 6-10, simulation results indicated that water level differences between two simulations were much smaller in the flood season than in the pre-flood season. The averaged value of water level differences was 27.6 cm in 2002 and 6.8 cm in 2003 when the flow discharge exceeded 10,000 cms. Although the maximum differences of the water stage were estimated as 46.8 cm in 2002 and 47.8 cm in 2003, those differences occurred in the low flood condition which was less than 2000 cms. Also, the successive simulation without dredging for two years (2002 and 2003) was conducted to examine whether water level differences would accumulate year after year. As shown in Figure 6-12 (two-year simulation), water level differences in 2003 during major floods are almost the same as in Figure 6-10 (single year simulation). The 6.8 cm of water stage differences in 2003 of the single year simulation was similar to 6.7 cm in 2003 of the two-year successive simulation, when the

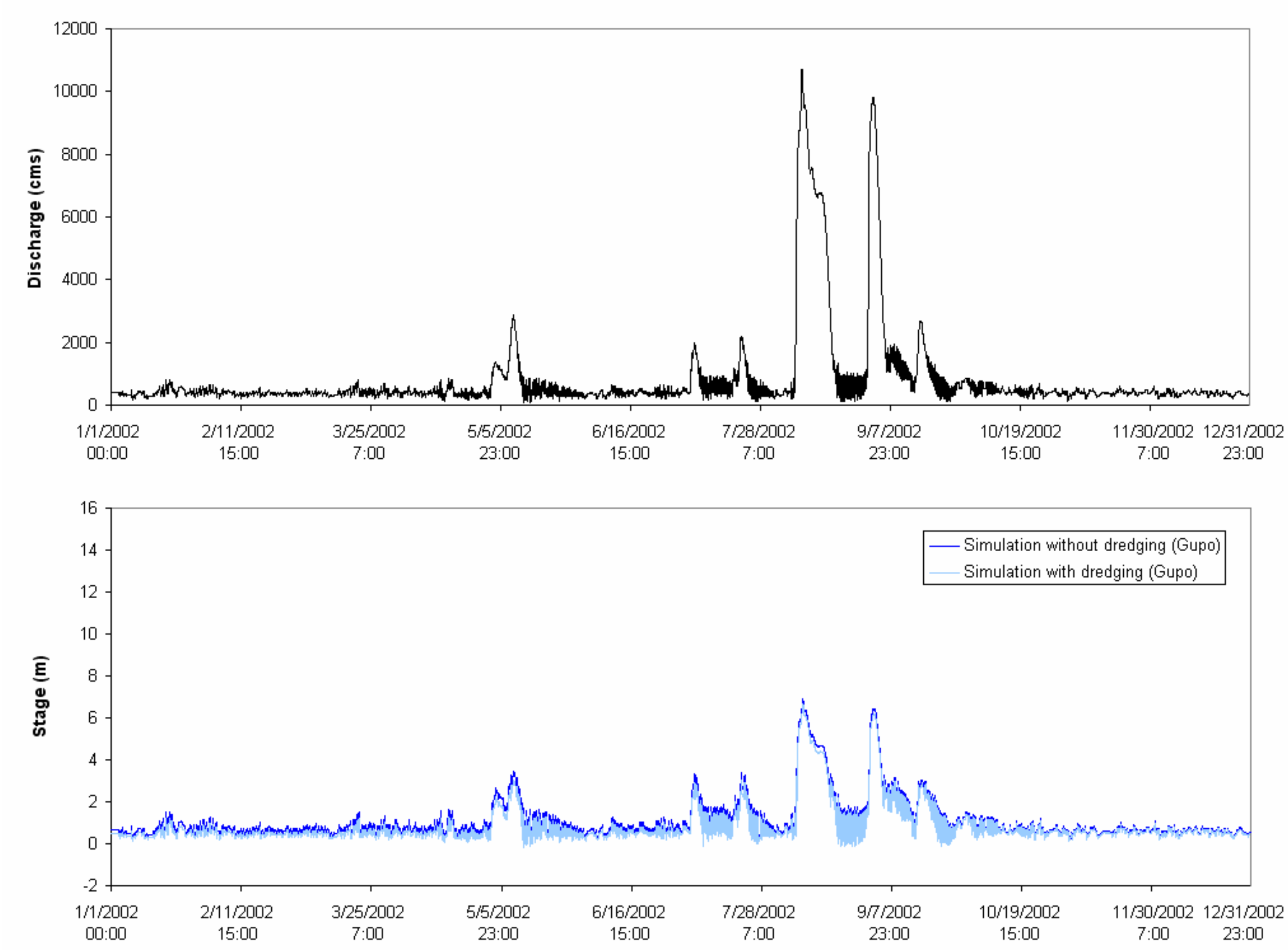

Figure 6-8. Numerical simulations with and without dredging operation (2002)

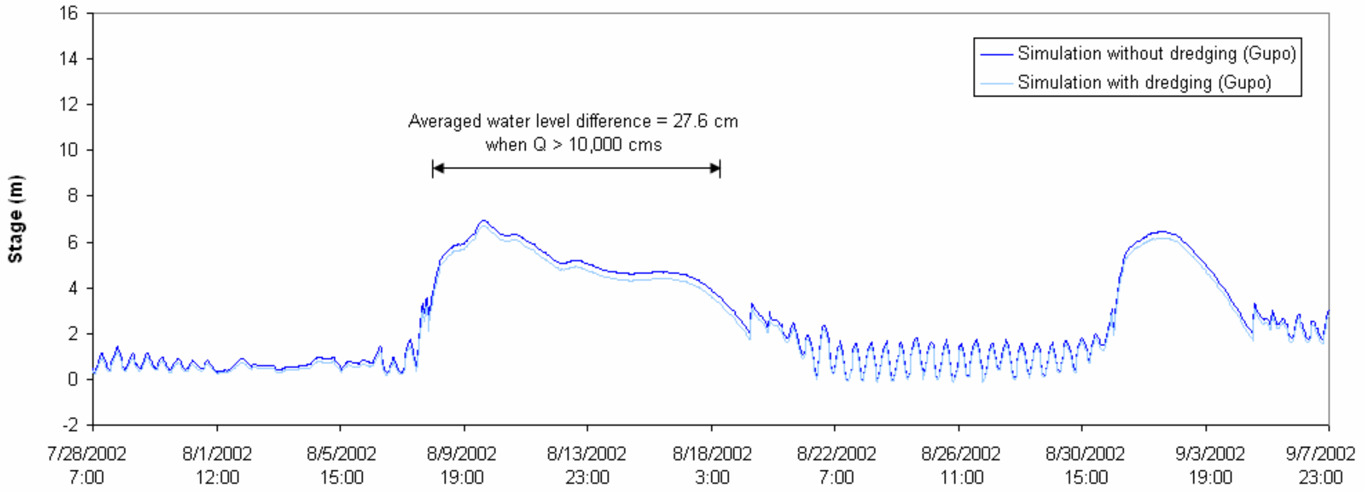

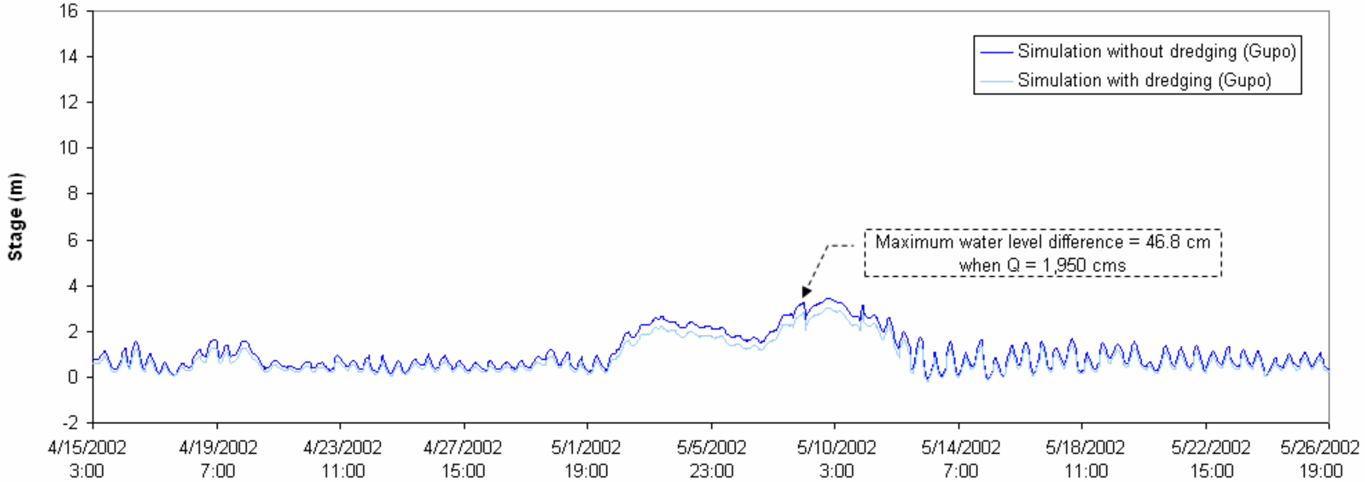

Figure 6-9. Water level differences with and without dredging operation (2002)

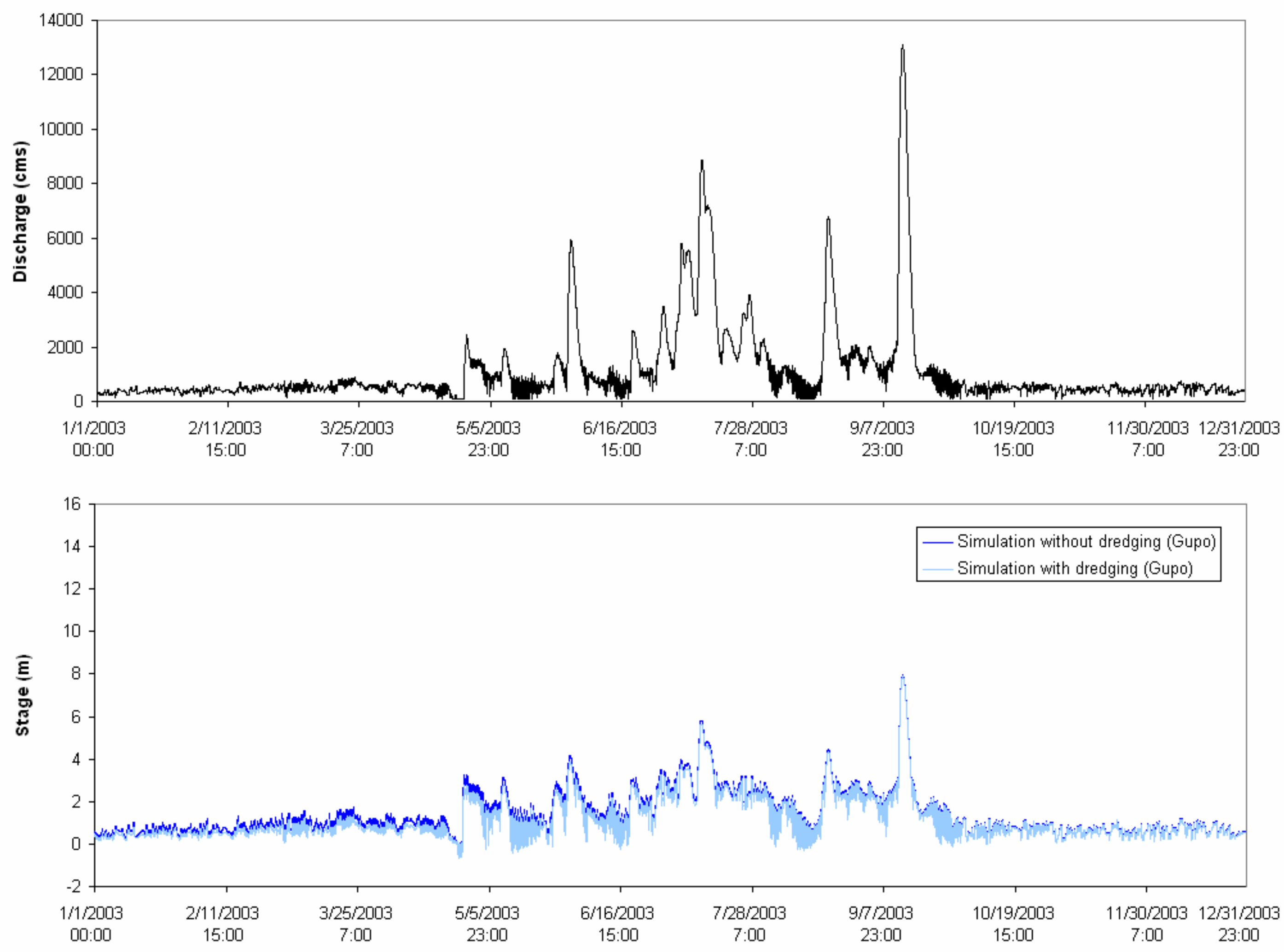

Figure 6-10. Numerical simulations with and without dredging operation (2003)

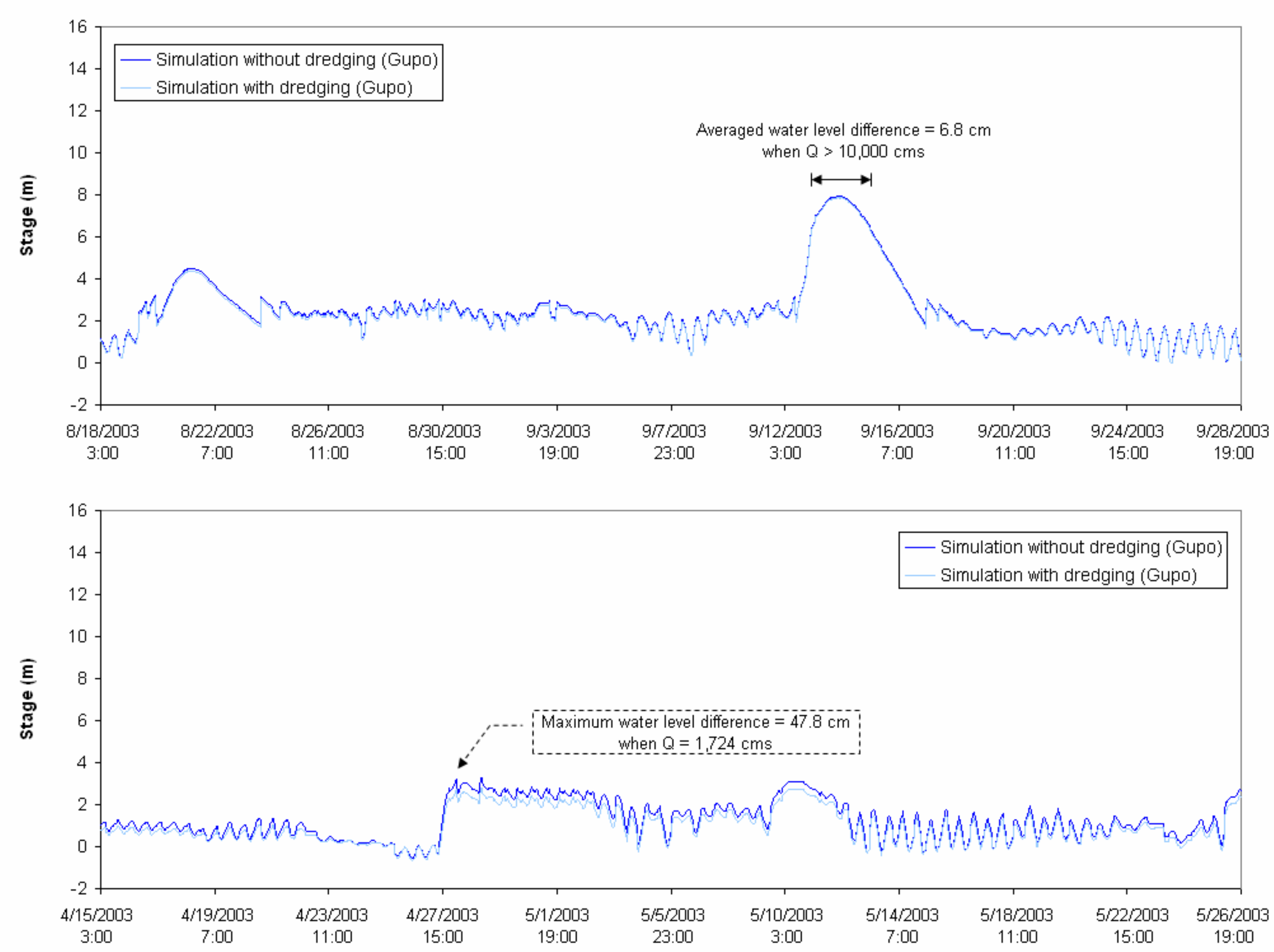

Figure 6-11. Water level differences with and without dredging operation (2003)

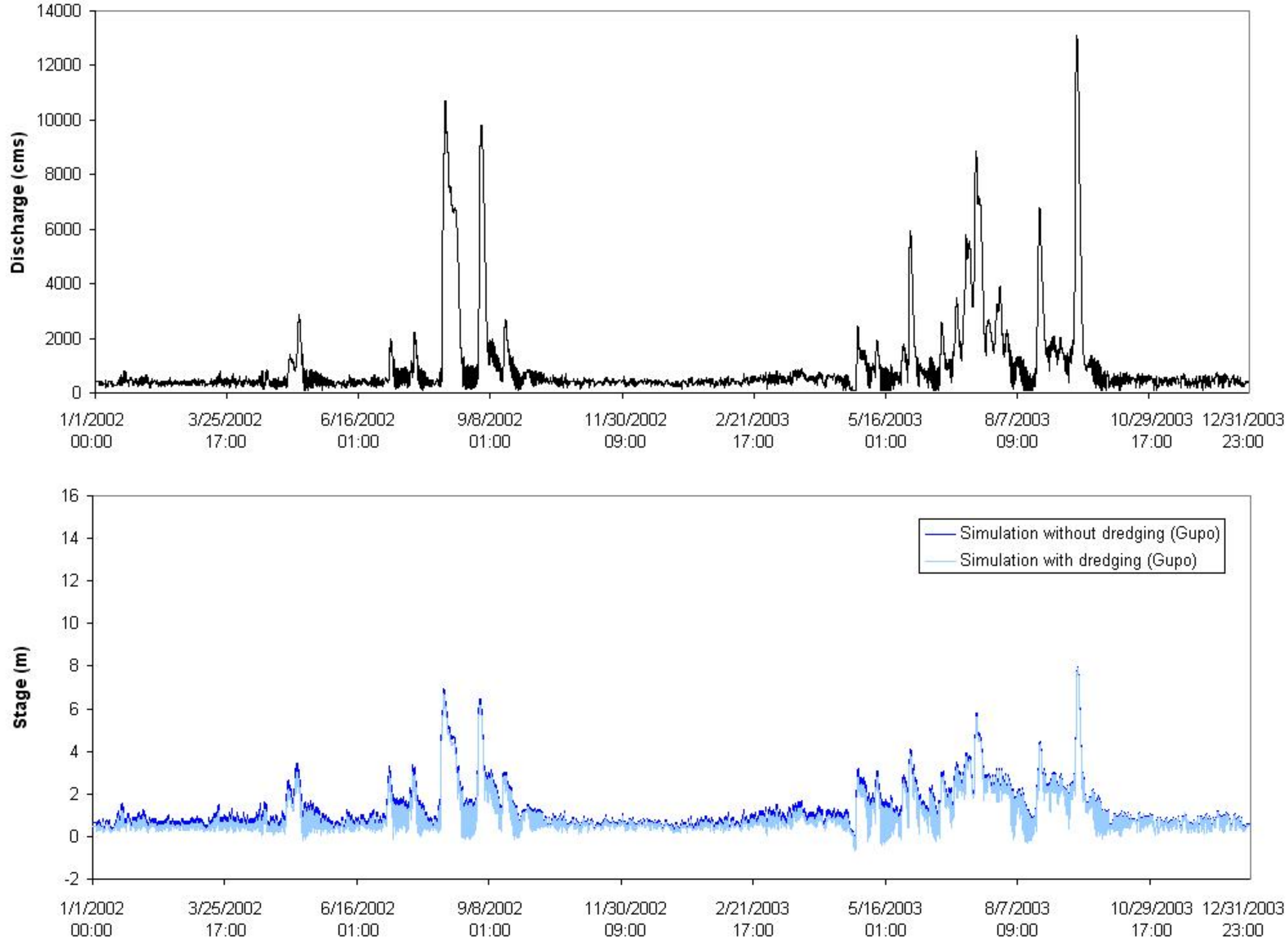

Figure 6-12. Water level differences of two-year successive simulation with and without dredging operation (2002 and 2003)

flow discharge exceeded 10,000 cms. The two-year successive simulation result indicated that the water level differences were not accumulated and could not affect the safety of the levees.

The numerical simulation has found that deposited sediments can be sufficiently flushed and eliminated by the hydraulic power during the early flood season without the sediment dredging. Also, it is found that the absence of the dredging operation at the NREB would not cause significant water level changes against the levees.

6.3.2 Sediment flushing simulation

In sediment flushing simulations, profiles for bed elevation, flushed sediment volumes, and maximum eroded heights were computed for each year of 1998 to 2003. Discharge hydrographs from 1998 to 2003 were used to make several flushing scenarios. Also, the NREB water surface level was adjusted by the water level drawdown within possible ranges of 20 cm above the tide in the sediment flushing model.

Selected possible flushing periods ranged from 13 to 44 days in the early flood season (April to June), depending on the hydrologic conditions. With the exception of 2002, most years had intermediate flows between May to June before a major flood season. The term “intermediate flows” was used in this study to describe the flow discharge over 1000 cms and below the discharge of major floods in the early flood season (April to June). The establishment of possible flushing periods depended on how long and how often the intermediate flow lasted before the major flood and typhoon season in the hydrograph. Therefore, determined sediment flushing periods are various in starting date and duration by hydrograph characteristics of each year.

Simulation results are summarized in Tables 6-2 and 6-3 and plotted in Figures 6-13 to 6-16. In flushing simulations from 1998 to 2003, the delta deposits were eliminated or reduced by flushing. The average amount of the flushed sediments from 1998 to 2003 was around 360,000 m^3 per year. This overall average amount approximately corresponds to 54% of the annual dredging volume of 665,000 m^3. Especially, bed materials of 528,517 m^3 were flushed by water level drawdown at the NREB during 44 days in 2003. Because the intermediate flow discharge lased for a relatively long time in 2003, 80% of mean annual dredged sediments could be eliminated in the upstream bed with the maximum eroded height of 24 cm, as shown in Figure 6-13. Also, flushed sediments were increased as the flushing periods became longer. When the intermediate flows exist for a relatively long period or occur frequently before the major flood season, much sediment can be flushed in the upstream channel and longer flushing time can sluice more sediments. If the intermediate flows are produced only in a short period, but occur more frequently, flushing at these periods will be more effective.

As shown in the hydrograph of 2002 (see Table 6-2 or Appendix E), the intermediate flow for 2002 occurred in May once. The second peak of the intermediate flows for 2002 was in July. Due to the 2-month interval, the total flushed sediments after the first intermediate flow became smaller as the flushing period got longer. The sediment volume of 236,160 m^3 sluiced for 13 days was reduced to 189,524 m^3 for 20 days and 131,732 m^3 for 31 days, which indicated that around 100,000 m^3 of sediment were re-deposited for 2 weeks. In these 2 weeks, there was the low flow condition without an intermediate flow. Also, the difference between flushed sediments from 1998 between the 16-day and 36-day was approximately 200,000 m^3 (Table 6-3).

Table 6-2. Sediment flushing simulation results from 2001 to 2003

		2003	2002	2001
Hydrograph		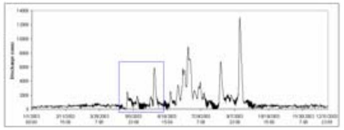	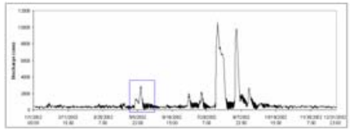	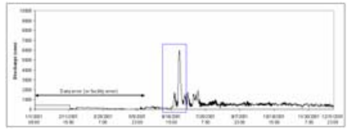
Sediment flushing period I	Period date (days)	4/27/03 to 5/15/03 (19 days)	5/2/02 to 5/14/02 (13 days)	6/1/01 to 6/30/01 (30 days)
	Flushed amount	279,110 m^3	236,160 m^3	131,712 m^3
	% of mean annual dredging (665,000 m^3)	42 %	35.5 %	19.8 %
	Maximum erosion	15 cm	12.5 cm	11 cm
Sediment flushing period II	Period date (days)	4/27/03 to 5/29/03 (33 days)	5/1/02 to 5/20/02 (20 days)	6/16/01 to 6/30/01 (15 days)
	Flushed amount	253,709 m^3	189,524 m^3	317,918 m^3
	% of mean annual dredging (665,000 m^3)	38 %	28.5 %	47.8 %
	Maximum erosion	15.6 cm	11.3 cm	17 cm
Sediment flushing period III	Period date (days)	4/27/03 to 6/9/03 (44 days)	5/1/02 to 5/31/02 (31 days)	
	Flushed amount	528,517 m^3	131,732 m^3	
	% of mean annual dredging (665,000 m^3)	80 %	19.8 %	
	Maximum erosion	24 cm	10.8 cm	

Table 6-3. Sediment flushing simulation results from 1998 to 2000

		2000	1999	1998
Hydrograph		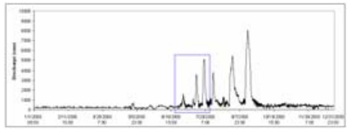	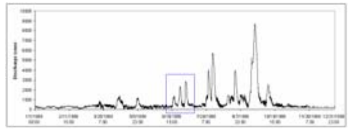	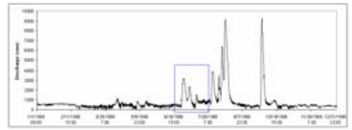
Sediment flushing period I	Period date (days)	6/28/00 to 7/31/00 (34 days)	6/17/99 to 7/6/99 (20 days)	6/25/98 to 7/10/98 (16 days)
	Flushed amount	377,124 m^3	232,309 m^3	430,477 m^3
	% of mean annual dredging (665,000 m^3)	56.7 %	34.9 %	64.7 %
	Maximum erosion	20 cm	13.3 cm	20.1 cm
Sediment flushing period II	Period date (days)	7/12/00 to 7/31/00 (20 days)		6/25/98 to 7/14/98 (20 days)
	Flushed amount	409,023 m^3		424,203 m^3
	% of mean annual dredging (665,000 m^3)	61.5 %		63.8 %
	Maximum erosion	20 cm		20.1 cm
Sediment flushing period III	Period date (days)			6/25/98 to 7/31/98 (36 days)
	Flushed amount			226,201 m^3
	% of mean annual dredging (665,000 m^3)			34 %
	Maximum erosion			14.4 cm

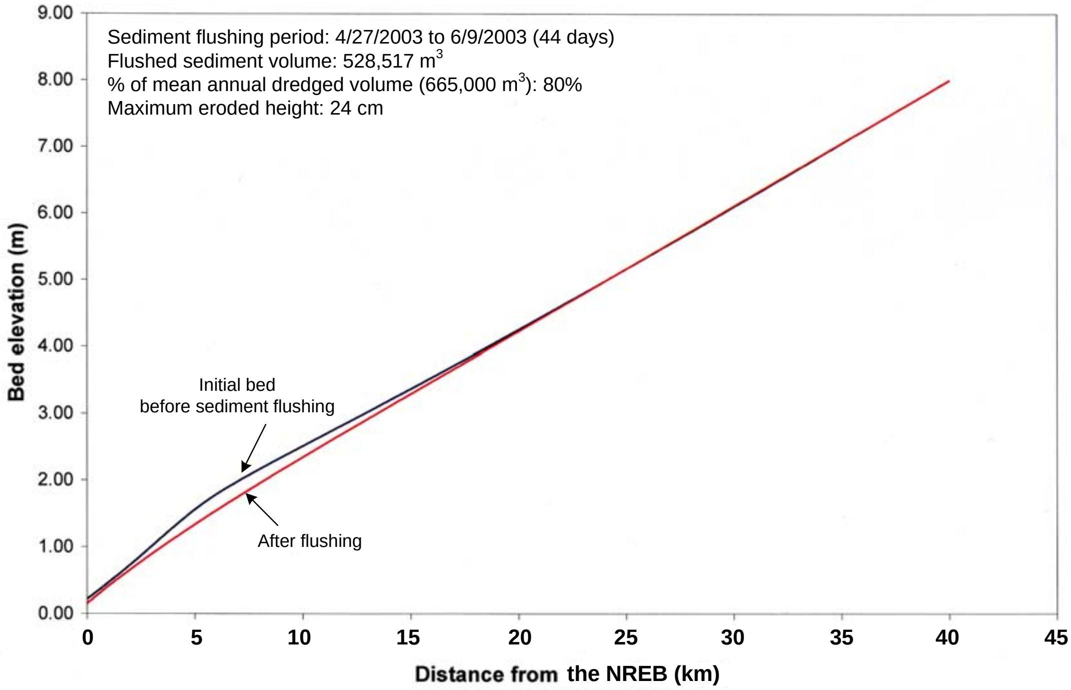

Figure 6-13. Bed elevation changes after sediment flushing (2003)

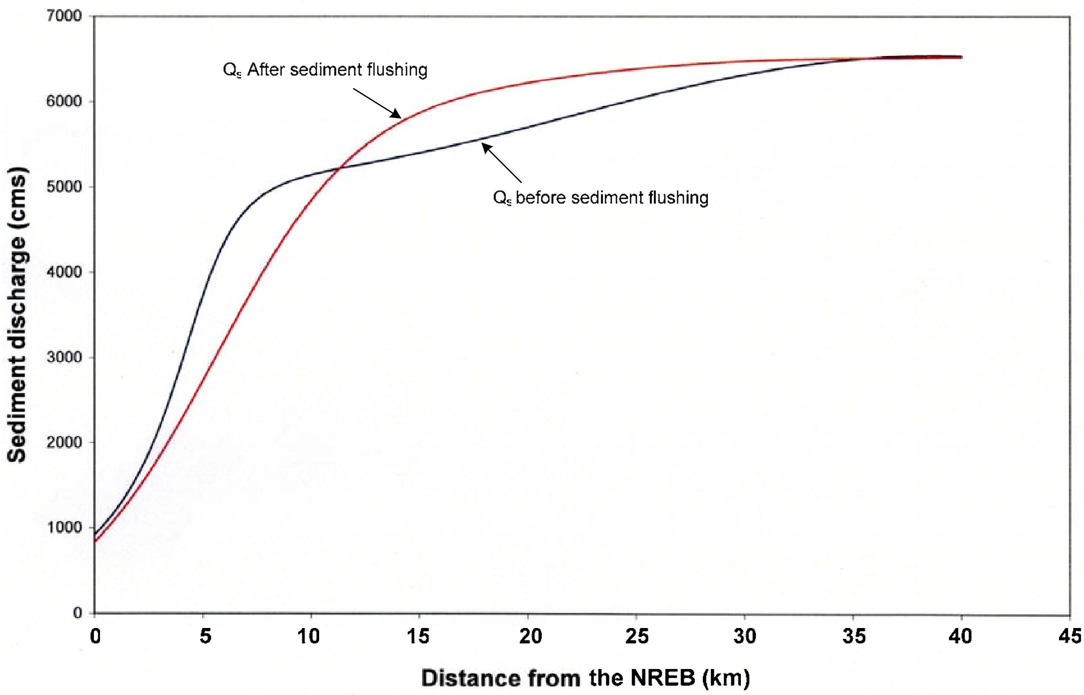

Figure 6-14. Sediment discharge before and after sediment flushing (2003)

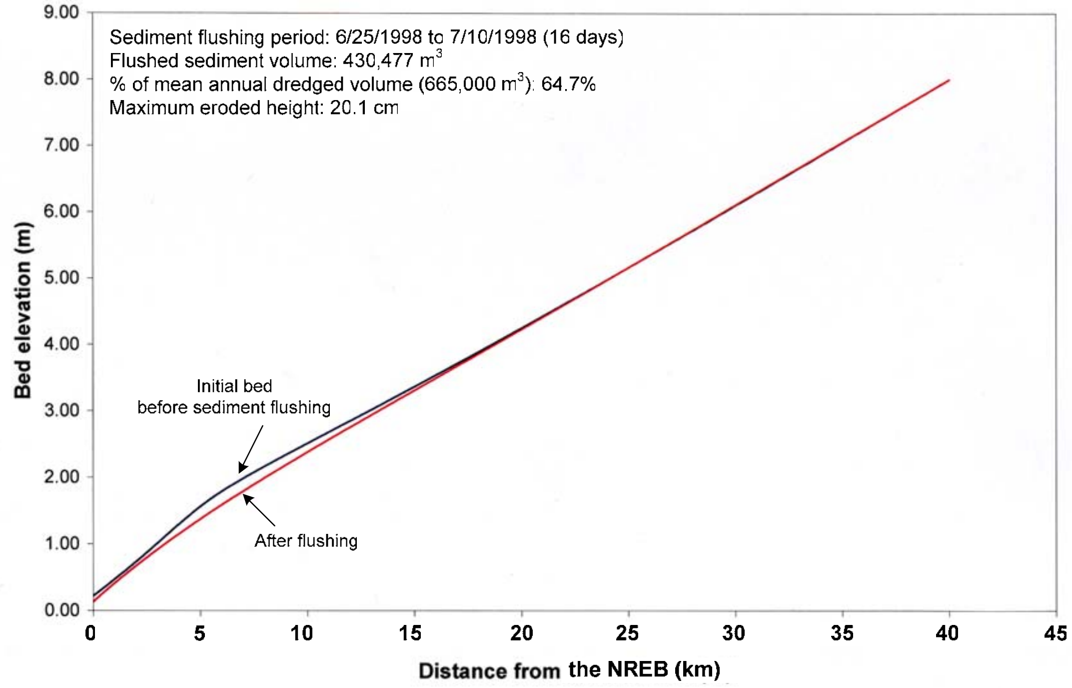

Figure 6-15. Bed elevation changes after sediment flushing (1998)

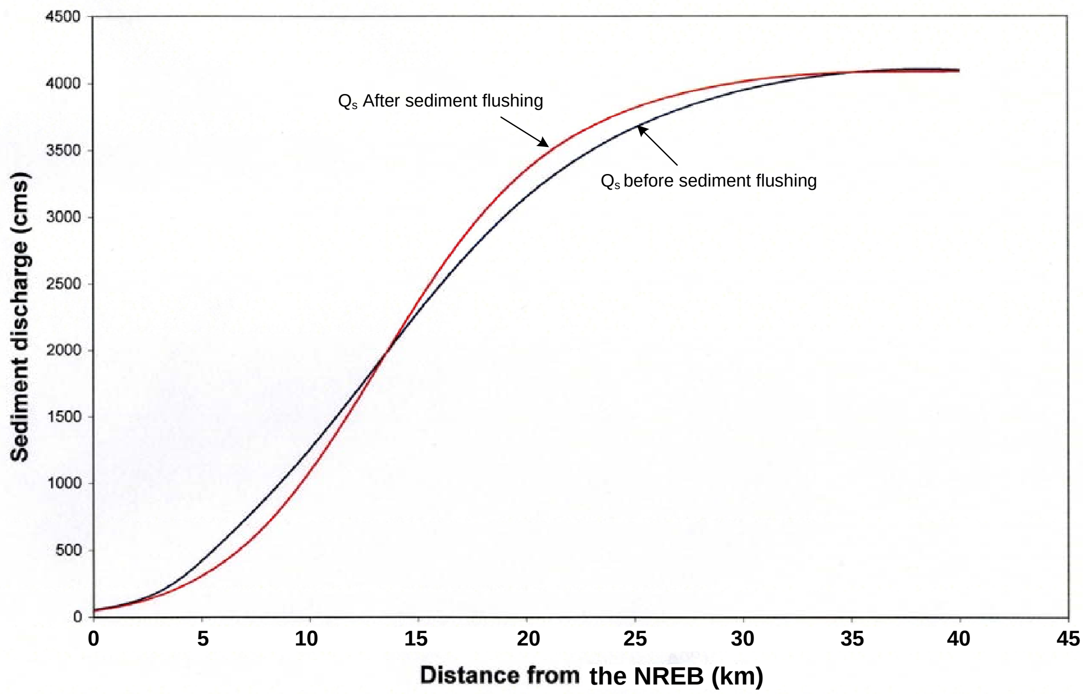

Figure 6-16. Sediment discharge before and after sediment flushing (1998)

Because there were no intermediate flows after 16 days (June, 25 to July, 10) of flushing time in 1998, sediments were re-deposited with time till the end of July. Although it seems that the short flushing time is more effective than the long period in some cases, sediment flushing during the low flow condition, especially the intervals between two intermediate flows, prevents a lot of re-deposited sediments at that time. Sediment flushing during the low flow conditions minimizes re-deposited sediments compared to dredging, which cannot minimize sediment deposits during the intervals between two intermediate flows.

As indicated in the overall flushing simulation, it is anticipated that the river bed has a large amount of re-deposited sediments immediately after dredging works used for sediment removal in April and May at the Lower Nakdong River. Although sediments eliminated by flushing are approximately 54 % of mean annual dredging in the numerical analysis, the overall sediment volume removed by flushing can actually exceed the annual dredging volume, because the redeposition of sediments following dredging operations is much greater than after the flushing events. Note that sediment flushing in the numerical model was operated in the low flow condition as well as in the high flow condition. If the first intermediate flow occurs much later after the dredging operation, a lot of sediments will be re-deposited during the low flow condition. Therefore, the total flushed amount of sediment without redeposition should be in excess of the annual dredging volume. Because it is not easy to predict how much and when the intermediate discharge is going to occur, the flushing method is considered more effective than the dredging method to prevent and remove sediment deposits.

Flushing can be operated using hydraulic power whenever the upstream water level is 20 cm higher than the tide level, whereas sediment dredging only can be operated at one time during the low flow season. The real time observation of flow discharge changes at Samrynagjin Station and water stage changes at the NREB will be the only important conditions to consider before executing a flushing technique in the field. In conclusion, sediment flushing can be applied effectively in the field because this method is only controlled by water level drawdown considering the upstream water surface level and downstream tide level.

6.3.3 Sediment concentration comparison

According to the EPA National Water Quality Inventory - 2000 Report (U.S. EPA, 2003), excessive sediment was the leading cause of impairment for rivers and streams, followed by lakes, reservoirs, ponds, and estuaries. Severity of effect caused by sediments is a function of many factors such as sediment concentration, duration, particle size, etc. As mentioned in Chapter 3.5, sediment concentration can be a very important indicator of other pollutants. Transported sediments cause a range of environmental water quality problems, including benthic smothering, irritation of fish gills, and transport of contaminants. Sediment concentration is related to the turbidity parameter, which is used to determine the quality of drinking water and to describe water quality conditions. For that reason, sediment concentration was computed and analyzed to describe indirectly the effects on the environmental water quality by the numerical modeling.

First, the sediment concentration variation over a year was calculated by the numerical model and plotted in Figures 6-17 and 6-18 for 2002 and 2003. It was assumed that there were not any dredging and flushing operations in order to analyze the high concentration period over a year. Second, to analyze the flushing technique effects on the sediment concentration changes, sediment concentration for flushing and non-flushing simulations was calculated and compared in Figures 6-19 and 6-20.

As flood frequency was increased from May to September, sediment concentration generally became smaller. Also, 2000 cms or more flow discharge caused rapid increases in the sediment concentration distribution. The highest concentrations of sediment did not always coincide with the occurrence of maximum flow rates. Especially, the first peak of the intermediate flow caused relatively higher sediment concentration, reflecting the greater availability of sediment at that time. In 2002, a higher sediment concentration was produced in the first intermediate flow than in the maximum flow rate that occurred in September 2, 2002. Also, the maximum flow rate occurred in September 14, 2003, but the highest sediment concentration of 2003 was generated much earlier before the maximum flow rate. Therefore, further studies and research on the environmental effects on the Nakdong River and Estuary should be focused on the period of the early flood season rather than the major flood.

Figures 6-19 and 6-20 are the results of flushing and non-flushing simulations to compare sediment concentration during the flushing time. In the 2002 simulation, the average sediment concentration difference was 58.8 ppm during the flushing time (May 1, 2002 – May 31, 2002) and the maximum difference was 911.3 ppm at 1,924 cms of flow discharge. Also, the averaged sediment concentration difference for the 2003 simulation was 49.5 ppm during the flushing time (April 27, 2002 – May 29, 2002) and the maximum difference was 673.2 ppm at 2,419 cms of flow discharge. The mean increase

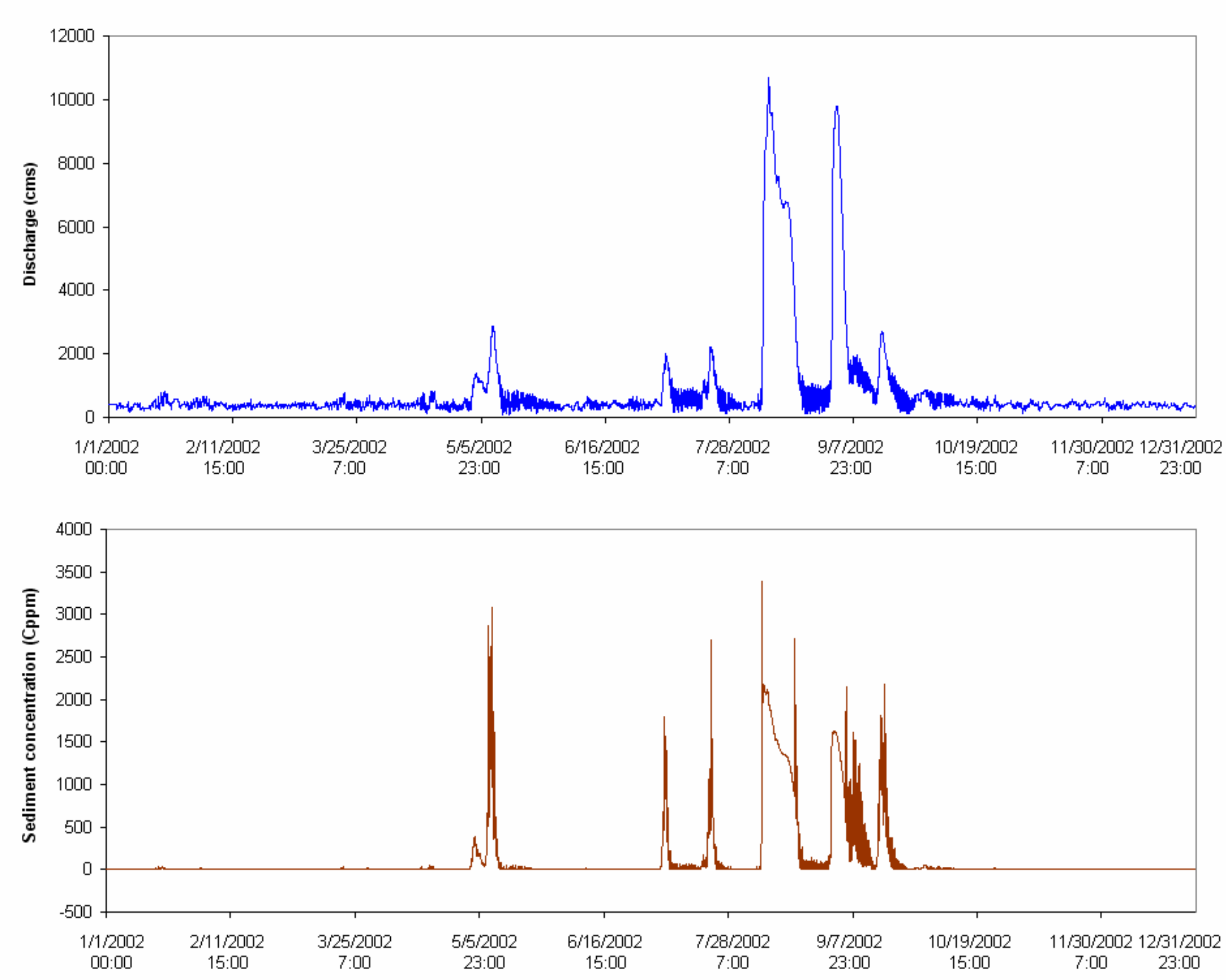

Figure 6-17. Simulation results of Sediment concentration (Cppm) in 2002

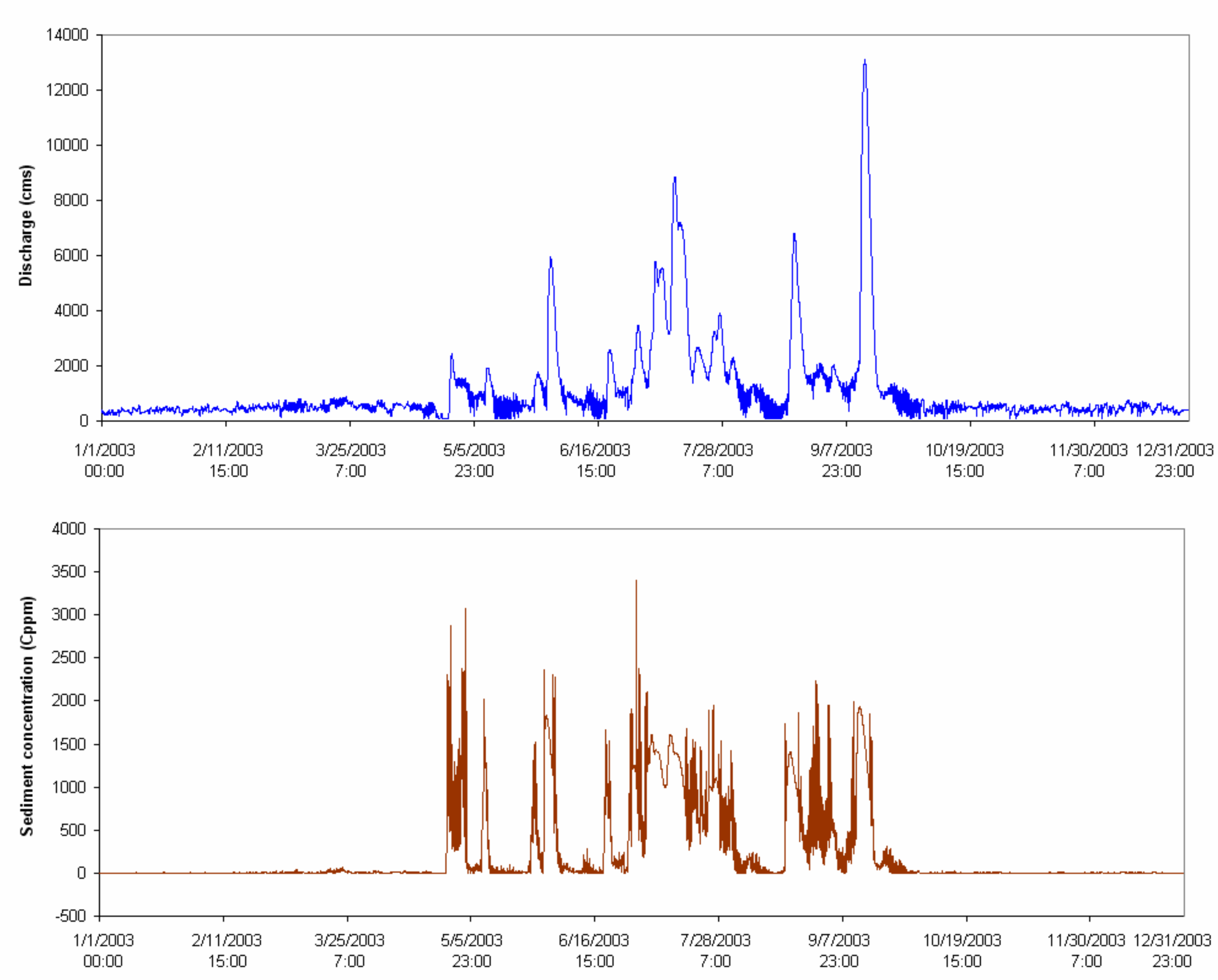

Figure 6-18. Simulation results of Sediment concentration (Cppm) in 2003

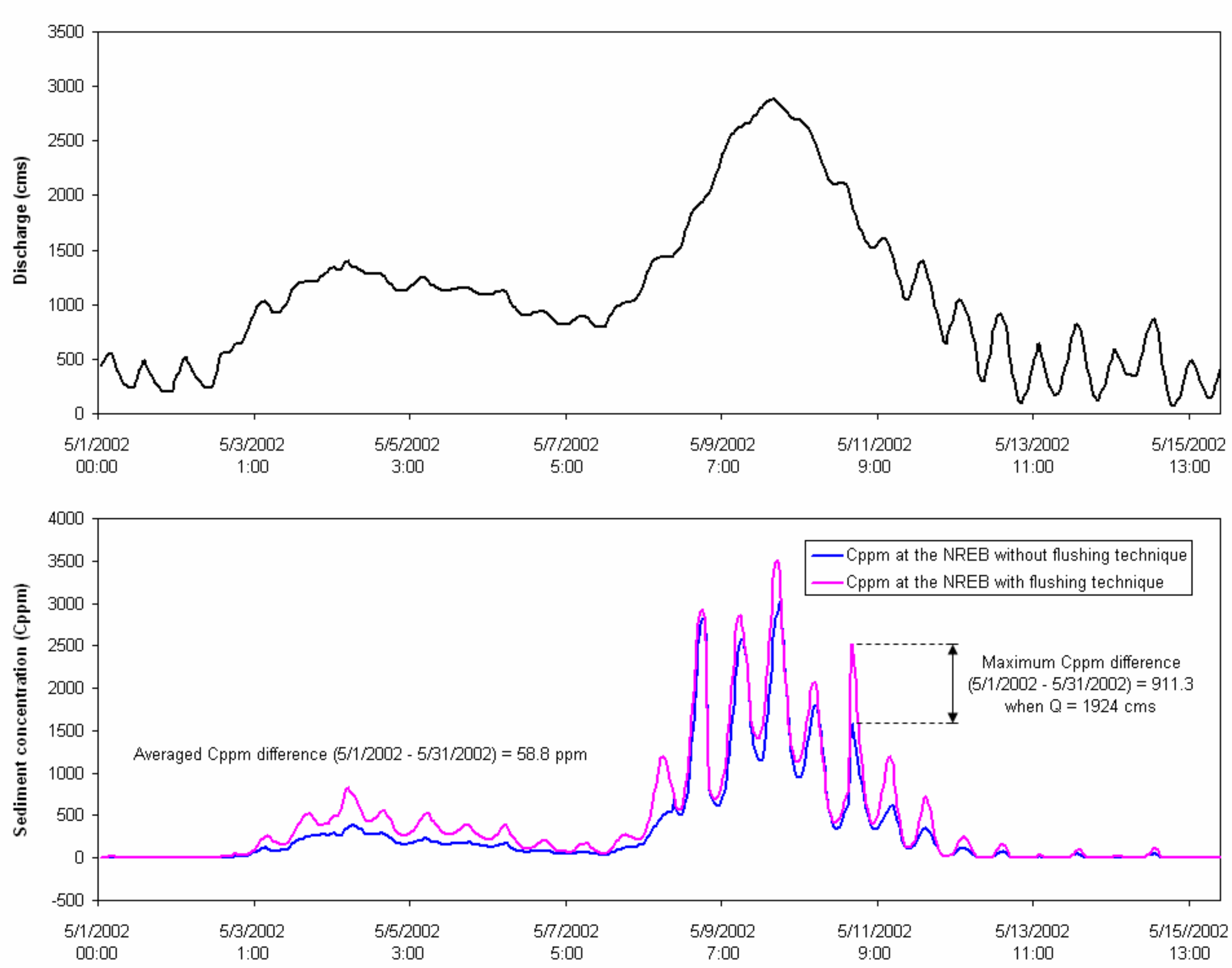

Figure 6-19. Sediment concentration comparison between with and without flushing simulations (2002)

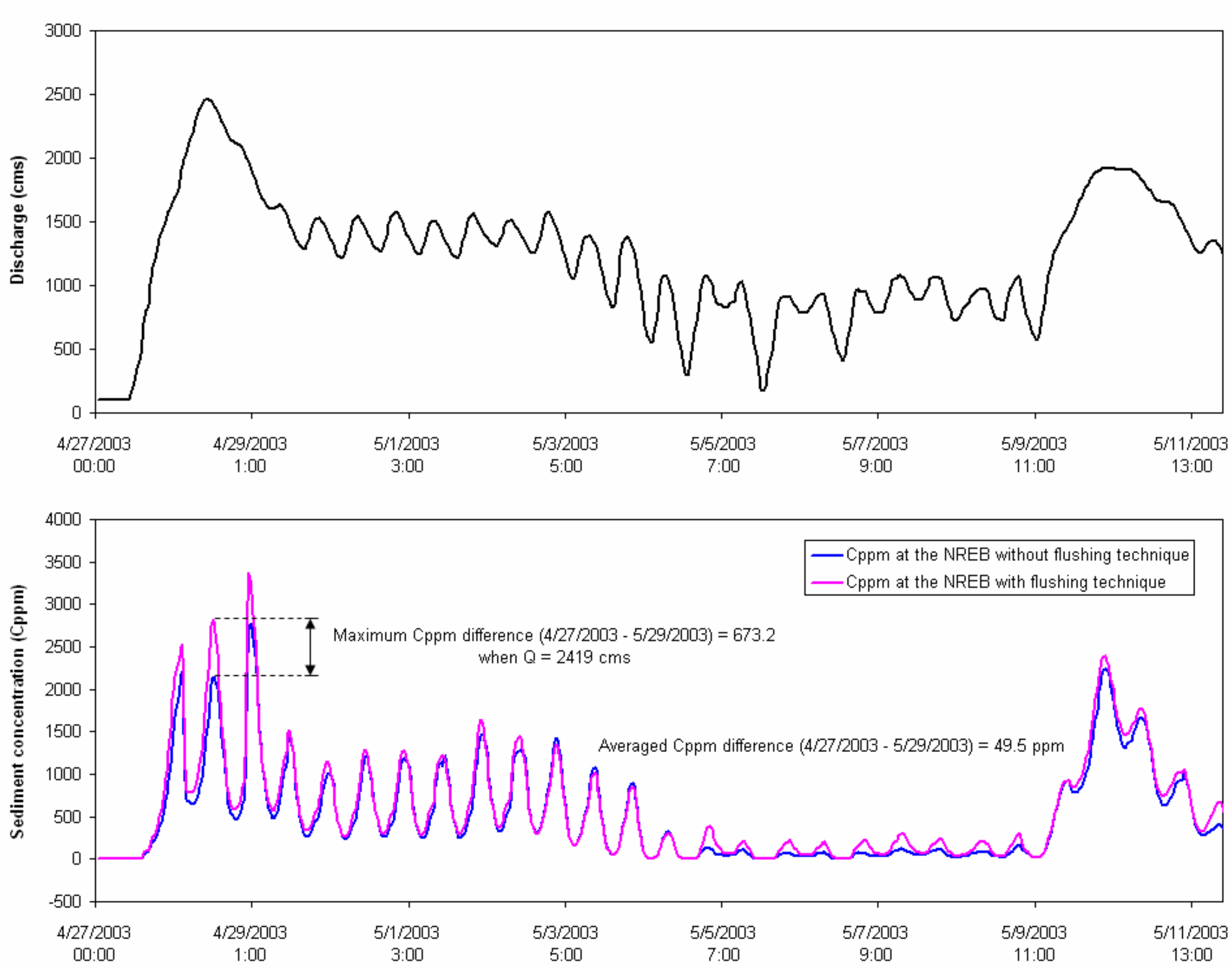

Figure 6-20. Sediment concentration comparison between with and without flushing simulations (2003)

in sediment concentration by sediment flushing was less than 60 ppm of the mean value. It was not a significant increase. Therefore, it is concluded that the flushing operation at the Lower Nakdong River does not considerably influence the increment of sediment concentration.

6.4 SEDIMENT FLUSHING METHOD OPTIMIZATION

More details of the sediment flushing procedure are essential to apply flushing technique in the field. Optimization and generalization of the sediment flushing procedure was accomplished by:

- Steady-state sediment flushing curves (see Chapter 5.1.)
- Flow duration curves from 1998 to 2003
- Quasi-steady state sediment flushing simulations

All analysis is based on the case of the Nakdong River Estuary Barrage.

The flushing time to sluice the same amount of annual dredging sediments from the upstream channel of the NREB are plotted with respect to flow discharge in Figure 6-21. It is indicated that the relation between a discharge and flushing time becomes much steeper as the discharge is greater than 1000 cms. The discharge greater than 1000 cms can flush the same amount of annual dredging sediments within a relatively short time period (within a month). In addition, the flow duration curves from 1998 to 2003 are mostly higher than the results of sediment flushing curves (Figure 6-21). Even though the flow duration curves of 2001 and 2002 are lower than the sediment flushing curve results at high flow conditions, sediment flushing is still feasible as shown in Table 6-2.

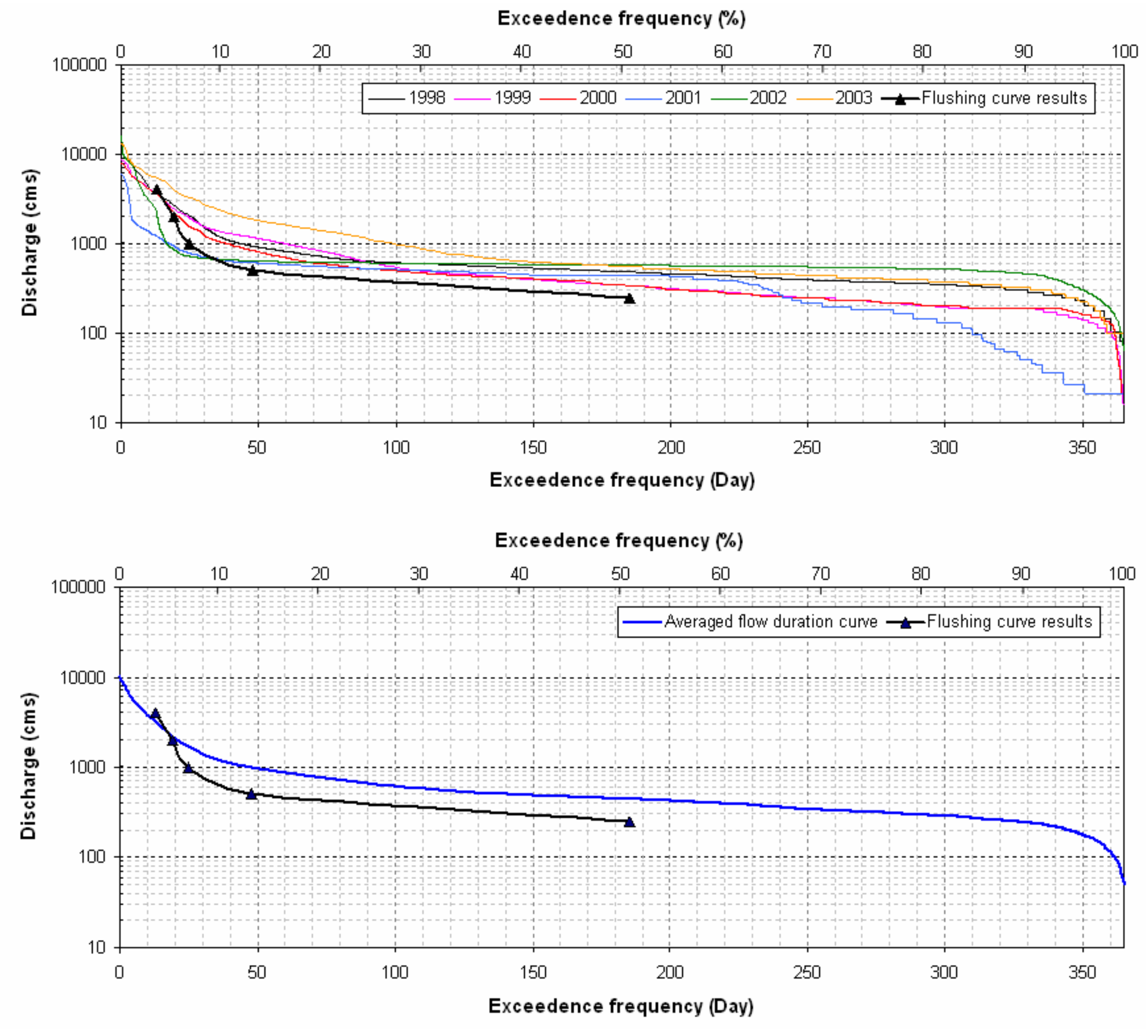

Figure 6-21. Flow duration curves and sediment flushing curve results

The water level at the estuary barrage cannot be lowered to downstream water depths of sediment flushing curves for low flows (see Figures 5-5 and 5-6) because of the tide effect and sustained water level maintenance. Therefore, it is most effective to flush sediment deposition during relatively high flows events. The discharge greater than 1000 cms was defined as an intermediate flow for the Lower Nakdong River. The quasi-steady state model is used for sediment flushing simulations under the intermediate flow conditions. Consequently, the flow discharge of 1000 cms at Samryangjin Station is the criteria for the sediment flushing method at the Nakdong River Estuary Barrage. The flow discharge corresponding to the inflection point in the graph of flushing curve results would be approximately the criteria to apply sediment flushing for the estuary barrage. To verify the discharge criteria of sediment flushing for the estuary barrage, the flushing simulation based on a numerical model with field data, especially tide levels, will be necessary as well as the analysis of flow duration and sediment flushing curves.

The procedure to apply sediment flushing at the estuary barrage is recommended as follows:

Step 1. Simulate the hydraulic and sedimentation process using a numerical for the applied upstream channel of the estuary barrage using a numerical model.

Step 2. Change the flow discharge and downstream water depth (level) in the numerical simulation to develop sediment flushing curves.

Step 3. Compare and analyze results of sediment flushing curves and flow duration curves for several years and find out the discharge of the inflection point in the graph of flushing curve results.

Step 4. Determine the criteria for the flow discharge based on the analysis of *Step 3*. The numerical modeling of sediment flushing using field data such as the discharge and water stage hydrographs and tide level graph will be helpful to verify the determined discharge criteria.

CHAPTER 7: CONCLUSIONS AND RECOMMENDATIONS

7.1 CONCLUSIONS

The numerical model was developed to simulate sediment transport and to analyze the feasibility of sediment flushing at the Nakdong River Estuary Barrage. Historic field data were used to demonstrate various applications and scenarios for the Lower Nakdong River and NREB. The developed numerical model provided simulations that were successfully calibrated and validated. The primary conclusions of the dissertation are summarized as follows:

1. The sediment flushing curves were established using the steady state model at the NREB, which describes the flushed sediment volumes at a given discharge and flow depth. The developed sediment flushing curves indicate that sediment flushing for the NREB should be effective. For the example shown in Figure 5-9, it took only 13 days with 4000 m^3/s of flow discharge and 7.6 m of downstream water depth to flush annual dredging sediment volume (665,000 m^3).
2. To evaluate the feasibility of the flushing technique, annual simulation scenarios of sediment flushing were developed and analyzed based on flow, stage, and tide level data. Annual simulations for the period from 1998 to 2003 were performed using the quasi-steady state model. Based on annual simulations, the average amount of flushed sediments with redeposition was approximately 360,000 m^3 per year, corresponding to 54% of the annual dredging volume (665,000 m^3). In the

2003 simulation (see Figure 6-13.), 80% of mean annual dredged sediments could be eliminated in the upstream bed with the maximum eroded height of 24 cm. The total flushed amount of sediment without redeposition should be in excess of the annual dredging volume. It is concluded that sediment flushing controlled by lowering the water level through gate operation should be effective at NREB. More details of the sediment flushing procedure are presented in Chapter 6.4. Optimization and generalization of the sediment flushing procedure can be accomplished by comparing steady-state sediment flushing curves, flow duration curves from 1998 to 2003, and quasi-steady state sediment flushing simulations based on a numerical model.

3. Simulations of sediment transport and water level variations with and without dredging operations were conducted. Quasi-steady state simulations indicated that at high flow, the water level differences with and without dredging were very small. For instant, the average value of water level differences with and without dredging was 27.6 cm in 2002 and 6.8 cm in 2003 when the flow discharge exceeded 10,000 cms (Figures 6-9 and 6-11). However, water level changes can be significant at low flow because of tidal effects. Also, the simulation of two successive years (2002 and 2003) without dredging was conducted to examine whether water level differences would accumulate year after year. In 2003 when the flow discharge exceeded 10,000 cms, the 6.8 cm of water stage differences for a single-year simulation was similar to the 6.7 cm difference from the two-year simulation, when the flow discharge exceeded 10,000 cms. The two-year simulation result without dredging indicated that the water level differences were

not accumulating year after year. Based on the simulation of two successive years, it is concluded that the absence of dredging operations at NREB should not cause a significant water level change and affect the safety of the levees during major floods.

4. Flushing does not significantly increase the average sediment concentration. As shown in Figures 6-19 and 6-20, the sediment concentration differences between flushing and non-flushing simulations are 58.8 ppm in 2002 and 49.5 ppm in 2003. However, flushing will increase peak sediment concentration. For example, the maximum sediment concentration difference between flushing and non-flushing simulations at a discharge of 1,924 cms in 2002 was 911.3 ppm (see Figure 6-19.).

7.2 RECOMMENDATIONS FOR FUTURE WORK

The recommendations for future work to complete the feasibility analysis of sediment flushing at the NREB and to reduce the sedimentation problems on the Lower Nakdong River are:

1. Bathymetric surveys of the channel bed during both low and high flow conditions are essential to examine bed changes after 1991. Most importantly, bathymetric surveys should be conducted before and after dredging operations and after the first intermediate flow to allow further validation of the numerical modeling.
2. A two-dimensional NREB downstream model will be needed to show the downstream effect of changes in gate operations and the suspended sediment concentrations and turbidity at the downstream end of the 5 km reach operated by

NREB. It will also be helpful to analyze where sediments will deposit downstream and how much sediment concentration affects the aquatic habitat for migratory birds at Eulsuk Island.

REFERENCES

Ackers, P., and White, W.R., 1973. Sediment transport: New approach and analysis. J. Hyd. Div. ASCE, 99, no. HY11:2041-60.

Annandale, G.W., 1987. Reservoir Sedimentation. Elsevier Science Publishers, New York.

Annandale, G.W., 2001. Reservoir Conservation and Sediment Management. Water week 2001. Water Bank Group, Washington, D.C., US.

Atkinson, E., 1996. The Feasibility of Flushing Sediment from Reservoirs. Report OD 137, HR Wallingford, Wallingford.

Basson, G.R., 1997. Hydraulic Measures to deal with Reservoir Sedimentation: Flood Flushing, Sluicing and Density Current Venting. Third International Conference on River Flood Hydraulics, Stellenbosch, South Africa.

Bogardi, J., 1974. Sediment Transport in Alluvial Streams. Budapest: Akademiai Kiado.

Borland, W.M., 1971. "Reservoir sedimentation", Chap. 29. In H.W. Shen (editor), River mechanics. Water Resources Publications, Fort Collins, Colo.

Borland, W.M., 1975. Sedimentation Engineering. American Society of Civil Engineering, Manual No.54, pp.587-605.

Borland, W.M. and Miller, C.R., 1962. Stabilization of Five Mile and Muddy Creek. American Society of Civil Engineering Meeting, Omaha, Neb.

Brabben, T.E., 1988. Reservoir Desilting Methods. Technical Note OD/TN 32 HR Wallingford, Wallingford.

Brandt, S.A., 1999: Reservoir Desiltation by Means of Hydraulic Flushing: Sedimentological and Geomorphological Effects in Reservoirs and Downstream Reaches As Illustrated by the Cachí Reservoir and the Reventazón River, Costa Rica. Ph.D. thesis submitted to Institute of Geography, University of Copenhagen.

Brown, C.B., 1943. The Control of Reservoir Silting. United State Department of Agriculture, Miscellaneous Publication No. 521, Washington, D.C.

Brown, C.B., 1958. Sediment Transportation. Engineering Hydraulics Wiley, New York.

Brownlie, W.R., 1981. Prediction of flow depth and sediment discharge in open-channels. Report no. KH-R-43A. Pasadena, California Institute of Technology, W. M. Keck Laboratory.

Brune, G.M., 1953. Trap Efficiency of Reservoirs. Trans. Am. Geophysical Union, 34(3):407-418

Cassidy, J.J., 1990. Impact of artificial reservoirs on hydrological equilibrium. Hydrology in Mountainous Regions II: Artificial Reservoirs, Water and Slopes, Proceedings of the Lausanne Symposia, 27 Aug. - 1 Sep., 1990, R.O. IAHS Publication No. 194, pp. 223-233.

Chang, F.J., Lai, J.S., and Kao, L.S., 2003. Optimization of operation rule curves and flushing schedule in a reservoir. Hydrological Processes 17(8):1623-1640.

Chang, H.H., Harrison, L.L., Lee, W., and Tu, S., 1996. Numerical modeling for sediment-pass-through reservoirs. *Journal of Hydraulic Engineering*, 122(7):381-388.

Chang, H.H., and Fan, S.S., 1996. Reservoir erosion and sedimentation for model calibration. Reservoir Sedimentation, Proceedings of the St Petersburg Workshop May 1994, S. Bruk and H. Zebidi, eds, IHP-V, Technical Documents in Hydrology NO. 2, UNESCO, Paris.

Chen, Y.H., 1975. Design of Sediment Retention Curve. Urban Hydrology and Sediment Control Symposium, Lexington.

Chen, J., 1994. Sedimentation Studies at Three Gorges. Intl. Water Power and Dam Construction (August):54-58.

Choi, B.S., 1996. A Study on the Estuary Hydraulic Characteristics in the vicinity of the Nakdong River Estuary. Ph.D. Dissertation. Pusan National University, Busan, Korea.

Churchill, M.A., 1948. Discussion of "Analysis and Use of Reservoir Sedimentation Data" by L.C. Gottschalk. Proc. Federal Inter-Agency Sedimentation Conf., Denver.

Colby, B.R., and Hembree C.H., 1955. Computation of Total Sediment Discharge, Niobrara River near Cody, Nebraska. U.S. Geological Survey, Water-Supply Paper 1357.

Davies-Colley, R.J. and Smith D.G., 2001. Turbidity, Suspended Sediment, and Water Clarity: A Review. Journal of the American Water Resources Association 37:1085-1101.

Dawans, P.H., Charpie, J., Giezendanner, W., and Rufwenacht, H.P., 1982. Le degravement de la retenue de Gebidem. 14th Congress on Large Dams, ICOLD, Rio de Janeiro 1982. Q54, R25.

D'Rohan, W., 1911. The silting up of reservoirs and canals and some methods for preventing same. Engin. and Contract, Vol. 35, pp. 56-58.

Dum, T., Kresnik, E., and Keller, H., 1996. Entwicklung eines Ausschotterungsbeckens (Development of a debris detention basin). Internationales Symposium Verlandung von Stauseen und Stauhaltungen, Sedimentprobleme in Leitungen und Kanälen, 2. Teil, 28./29. März 1996 an der ETH Zürich. Mitteilungen 143, Versuchanstalt für Wasserbau, Hydrologie und Glaziologie der Eidgenössischen Technischen Hochschule Zürich, D. Vischer, ed., pp. 145-159 (in German).

Engelund, F., and Hansen, E., 1967. A Monograph on Sediment Transport to Alluvial Streams. Copenhagen, Teknik Vorlag.

Fan, J., 1985a. Methods of preserving reservoir capacity. Methods of Computing Sedimentation in Lake and Reservoir. A contribution to the International Hydrological Programme, IHP-II Project A. 2.6.1 Panel, S. Bruk, ed., Unesco, Paris, pp. 65-164.

Fan, J., 1985b. Methods of preserving reservoir capacity. Lecture Notes of the Training Course on Reservoir Sedimentation. Series of Publication IRTCES, Beijing, pp. II.1-II.96.

Fan, J. and Morris, G.L., 1992a. Reservoir Sedimentation. I: Delta and Density Current Deposits. Journal of Hydraulic Engineering, ASCE, 118(3):354-369

Fan, J. and Morris, G.L., 1992b. Reservoir Sedimentation. II: Reservoir Desiltation and Long-term Storage Capacity. Journal of Hydraulic Engineering, ASCE, 118(3):370-384

Frenette, M. and Julien, P.Y., 1986. Advances in Predicting Reservoir Sedimentation. Proceedings 3rd International Symposium, River Sedimentation, U. Mississippi, Oxford.

Graf, W.H., 1971. Hydraulic of Sediment Transport. McGraw Hill, New York.

Graf, W.H., 1984. Hydraulics of Reservoir Sedimentation. Communication du Laboratoire d'hydraulique #51, EPFL, Lausanne, 40 p.

Heigerth, G. and Medved, N., 1996. Untersuchungen zur Steuerung der Spülung von verlandeten Flussstauräumen (Investigations for control sediment scouring in river reservoirs). Internationales Symposium Verlandung von Stauseen und Stauhaltungen, Sedimentprobleme in Leitungen und Kanälen, 2. Teil, 28./29. März 1996 an der ETH Zürich. Mitteilungen 143, Versuchanstalt für Wasserbau, Hydrologie und Glaziologie der Eidgenössischen Technischen Hochschule Zürich, D. Vischer, ed., pp. 161-174 (in German).

Hoggan, D.H., 1997. Computer-assisted floodplain hydrology and hydraulics. McGraw Hill, New York.

Hong, S. and Chen, Z., 1992. Erosional and depositional changes and their effects during different operation periods at the Sanmenxia Reservoir. Sediment Management, Proceedings of the 5th International Symposium on River Sedimentation, Karlsruhe, 1992, University of Karlsruhe, Institute of Hydraulic Structures and Agricultural Engineering, Vol. 2, pp. 943-952.

Hotchkiss, R. and Parker, G., 1988. Reservoir sediment sluicing - laboratory study. Hydraulic Engineering, Proceedings of the 1988 National Conference, Colorado Aug. 1988, pp. 1073-1078.

Hotchkiss, R. and Parker, G., 1990. Laboratory modelling of reservoir sedimentation and sluicing: scale considerations. International Conference on Physical Modelling of Transport and Suspension, ASCE, pp. 14B.25-14B.30.

Hu, C., 1995. Controlling reservoir sedimentation in China. Hydropower and Dams, March, pp. 50-52.

IRTCES, 1985. Lecture notes of the training course on reservoir sedimentation. International Research and Training Centre on Erosion and Sedimentation, Tsinghua University, Beijing, China.

ISWACO-NEDECO, 1987. Nakdong River Estuary Barrage and Reclamation Project: Operation Manual. Republic of Korea Industrial Sites and Water Resources Development Corporation and Netherlands Engineering Consultants, 1987, Busan, Korea.

Jaggi, A.L. and Kashyap, B. R, 1984. Desilting of Baira reservoir of Baira Siul project. Irrigation and Power, October 1984.

Janssen, R., 1999. An Experimental Investigation of Flushing Channel Formation during Reservoir Drawdown. Ph.D. dissertation, University of Berkeley.

Janssen, R.H.A. and Shen, H.W., 1997. The development of equilibrium profiles for flushing channels. Energy and Water: Sustainable Development, Proceedings of Theme D, Water for a Changing Global Community, 27th Congress of the IAHR, San Francisco, California Aug. 10-15, pp. 108-113.

Ji, U. and Julien, P.Y., 2005. The Impact of Typhoon Maemi on the Nakdong River, South Korea. Hydrology Days, Colorado State University, March 7, 2005, pp. 103-110.

Jiufa L. and Chen Z., 1998. Sediment resuspension and implications for turbidity maximum in the Changjiang Estuary. International Journal of Marine Geology 148:117-124.

Jin, L., 1995. Effect of Jiaosi sluice to the riverbed deformation before Jiaosi project. Sixth International Symposium on River Sedimentation, Management of Sediment: Philosophy, Aims, and Techniques, New Delhi, 7-11 November, 1995, Balkema, Rotterdam, pp. 853-857.

Jing, C., 1956. A Report on the Experiment of Sediment Flushing of Jensanpei Reservoir. Taiwan Sugar Company, Taipei.

Jordana, J., 1925. El pantano de la peña en 1924 (The Peña Reservoir in 1924). Revista de Obras Públicas, Vol. 73, pp. 39-42 (in Spanish).

Jowett, I., 1984. Sedimentation in New Zealand hydroelectric schemes. Water International, Vol. 9, pp.172-173.

Ju, J., 1992. Unit stream power and riverbed evolution. Sediment Management, Proceedings of the 5th International Symposium on River Sedimentation, Karlsruhe, 1992, University of Karlsruhe, Institute of Hydraulic Structures and Agricultural Engineering, Vol. 1, pp. 403-408.

Julien, P.Y., 1998. Erosion and Sedimentation. Cambridge University Press, Cambridge, UK.

Julien, P.Y., 2002. River Mechanics. Cambridge University Press, Cambridge, UK.

Karaushev, A., 1966. A Method of Calculating Sedimentation in Reservoirs. Soviett Hydrology, AGU, NO. 3.

Kim, C.W., Woo, H., Kim, W., Lee, D.H., and Yoon, K.S., 2004. Re-Channelization of Stream Channels Affected by an Extreme Flood Due to the 2002 Typhoon Rusa in Korea. World Water Congress 2004, Salt Lake City, Utah.

Kirk, J.T.O., 1985. Effects of Suspensolids (Turbidity) on Penetration of Solar Radiation in Aquatic Ecosystems. Hydrobiologia 125:195-208.

KMOCT, 1991. The Nakdong River Maintenance General planning Report. Korean Ministry of Coonstruction and Transportation (KMOCT), Korea.

KMOCT and KOWACO, 2004. Investigation of Nakdong River basin. Korean Ministry of Transportation and Communications and Korean Water Resources Corporation, Korea.

KOWACO, 1995. A Study on Sedimentation Characteristics in Nakdong Estuary Barrage. Korea Water Resources Corporation (KOWACO), Korea.

KOWACO, 2003. Nakdong River Estuary Barrage Annual Maintenance Report. Korea Water Resources Corporation, Korea.

Krumdieck, A. and Chamot, P., 1979. Sediment flushing at the Santo Domingo reservoir. Water Power and Dam Construction.

Lai, J.S. and Shen, H.W., 1995. Degradation flushing processes in reservoir. HYDRA 2000, Proceedings of the XXVIth Congress of the IAHR, Volume 4, the Hydraulics of Water Resources and Their Development, London.

Lai, J.S. and Shen, H.W., 1996. Flushing Sediment Through Reservoirs. Journal of Hydraulic Research, 34(2):237-255.

Lick W., Huang H.N., and Jepsen R., 1993. Flocculation of fine-grained sediments due to differential settling. Journal of Geophysical Research – Oceans 98 (C6):10279-10288.

Lin, B., 1992. Watershed and sediment management in China. Sediment Management, Proceedings of the 5th International Symposium on River Sedimentation, Karlsruhe, 1992, University of Karlsruhe, Institute of Hydraulic Structures and Agricultural Engineering, Vol. 1, pp. 5-18.

Liu, J., Minami, S., Otsuki, H., Liu, B., and Ashida, K., 2004. Prediction of Concerted Sediment Flushing. Journal of Hydraulic Research, ASCE, 130(11):1089-1096.

Locher, F.A. and Wang, J.S., 1995. Operation Procedures for Sediment Bypassing at Cowlitz Falls Dam. In 15th Annual USCOLD Lecture Series, USCOLO, Denver.

Lopez, J.L., 1978. Mathematical Modeling of Sediment Deposition in Reservoir. Ph.D. dissertation, Colorado State University, Fort Collins, Colorado.

Mahmood, K., 1987. Reservoir sedimentation: IMPACT, Extent, and Mitigation. World Bank Technical Paper Number 71, Washington, D.C.

Molino, B., Greco, M., and Rowan, J.S., 2001. A 2-D Reservoir Routing Model: Sedimentation History of Abbeystead Reservoir, U.K. Water Resources Management, 15:109-122, Kluwer Academic Publishers.

Morgan, R.P.C., 1995. Soil Erosion and Conservation, 2nd ed. Longman Group, Essex, UK.

Morris, G.L. and Fan, J., 1997. Reservoir Sedimentation Handbook: Design and Management of Dams, Reservoir, and Watersheds for Sustainable Use. McGraw Hill, New York.

Morris, G.L. and Hu, G., 1992. HEC-6 modeling of sediment management in Loíza Reservoir, Puerto Rica. Hydraulic Engineering: Saving A Threatened Resource - in Search of Solutions, Proceedings of the Hydraulic Engineering Sessions at Water Forum '92, ASCE, pp. 630-635.

Olsen, N.R.B., 1999. Two-dimensional numerical modeling of flushing process in water reservoirs. Journal of Hydraulics Research, 37(1):3-16.

Park, S.B., 1998. Basic water quality of the mid to lower part of Nakdong River and the influences of the early rainfall during monsoon on the water quality. M.S. thesis, Pusan National University, Busan, South Korea.

Qian, Y., Cheng, X., Fu, C., and Shang, H., 1993. Influence of the upstream reservoirs on the adjustment of downstream alluvial channel. International Journal of Sediment Research, 8(3):1-20.

Rice, T.L., 1981. Reservoir Sedimentation Modeling. Ph.D. Dissertation, Colorado State University, Fort Collins, Colorado.

Rienossal, K. and Schnelle, P., 1982. Sedimentation of small reservoirs in the high alps. 14th Congress on large Dams, ICOLD, Rio de Janeiro, 1982.

Shah, C.M. and Kulkarni, V.K., 1993. Sediment regulation - case studies. Proceedings of XXV Congress of IAHR, 30 Aug.-3 Sep., 1993, Tokyo, Japan, Technical Session A, Flood and Drought, pp. 744-752.

Shah, S.C., 2006. Variability in Total Sediment Load Using BORAMEP on the Rio Grande Low Flow Conveyance Channel. M.S. Thesis. Colorado State University, Fort Collins, CO.

Shen, H.W., 1999. Flushing sediment through reservoirs. Journal of Hydraulic Research, Vol. 37, NO. 6 pp. 743-757.

Shen, H.W., and Hung, C.S., 1972. An engineering approach to total bed-material load by regression analysis. Proc. sedimentation Symposium, ed. H.W. Shen. Berkeley, Calif.: Water Resources Pub., chap 14.
Remodified Einstein procedure for sediment load. J. Hyd. Div. ASCE, 109, no. 4 (1983): 565-78.

Shen, H.W., Lai, J.S., and Zhao, D., 1993. Hydraulic desiltation for noncohesive sediment. Proceedings of the 1993 Annual ASCE Hydraulic Engineering Conference, San Francisco.

Simons, D.B. and Richardson, E.V., 1963. Form of bed roughness in alluvial channels. Trans. ASCE, 128(1963): 284-323

Simons, D.B. and Richardson, E.V., 1966. Resistance to flow in alluvial channels. Professional Paper 422-J. Washington, D.C., U.S. Geological Survey.

Simons, Li and Ass., 1982. Engineering Analysis of Fluvial Systems, Fort Collins, Colorado.

Su, Y., 1995. Operational mode of the reservoirs in heavily sediment-laden rivers in China. HYDRA 2000, Proceedings of the XXVIth Congress of the IAHR, Volume 4, the Hydraulics of Water Resources and Their Development, London, 11-15 Sep., 1995, pp. 278-283.

Swiss national Committee on Large Dams, 1982. General paper. 14th Congress on Large Dams, ICOLD, Rio de Janeiro, 1982.

Talebbeydokhti, N. and Naghshineh, A., 2004. Flushing sediment through reservoirs. Iranian Journal of Science & Technology. Transaction B. Vol. 28. No. B1:119-136.

Tolouie, E., 1993. Reservoir Sedimentation and Desiltation. Ph.D. Thesis, University of Birmingham, UK.

Tu, S., Geary, G., Lee, W., and Chang, H., 1995. Development of reservoir operation rules to control sedimentation: a numerical model study for Rock Creek and Cresta dams. Sediment Management and Erosion Control on Water Resources Projects, Fifteenth Annual USCOLD Lecture Series, San Francisco, California, May 15-19, 1995, pp. 267-281.

U.S. EPA, 2003. Developing Water Quality Criteria for Suspended and Bedded Sediments (SABS), Office of Water. In draft August, 2003.

van Rijn, L.C., 1984. Sediment transport, Part III: Bedforms and alluvial roughness. J. Hyd. Div. ASCE, 110, no 12: 1733-54.

Wang, Z., 1992. Model of non-Newtonian fluid flow. Sediment Management, Proceedings of the 5th International Symposium on River Sedimentation, Karlsruhe, 1992, University of Karlsruhe, Institute of Hydraulic Structures and Agricultural Engineering, Vol. 1, pp. 409-415.

Wang, J.S. and Locher, F.A., 1989. Design aspects for operation to bypass sediment at Cowlitz Falls reservoir. Design of Hydraulic Structures 89, Proceedings of the Second International Symposium on Design of Hydraulic Structures, Fort Collins.

Wei, Y., 1986.The silt problem in San Men Gorge Dam and its remodifying project. Journal of Wate Resources, 5(2):188-192.

Wu, C.M., 1989. Hydraulic properties of reservoir desilting. Proceedings of XXIII

Congress of the IAHR, Hydraulics and the Environment, Technical Session B: Fluvial Hydraulics, Ottawa 1989, pp. B587-B593.

Wu, F-C. and Chou, Y-J., 2004. Tradeoffs associated with sediment-maintenance flushing flows: a simulation approach to exploring non-inferior options. River research and applications, John Wiley & Sons Ltd: Journal Administration Department, UK, 20(5):591-604.

Xia, M. and Ren, Z., 1980. Methods of sluicing sediment from Heisonglin Reservoir and its utilization downstream. International Symposium on River Sedimentation, Beijing 1980, pp. 717-726.

Yalin, M.S., 1992. River Mechanics. Pergamon Press.

Yang, C.T., 1996. Sediment Transport Theory and Practice. McGraw-Hill, New York.

Yang, C.T., 1979. Unit Stream Power Equation for Total Load. J. Hyd. Div. ASCE, vol. 40: 123-138.

Yoon, Y.N., 1992. The state and the perspective of the direct sediment removal methods from reservoirs. International Journal of Sediment Research, 7(2):99-116.

Yücel, Ö. and Graf, W.H., 1973. Bed Load Deposition in Reservoir. Preceedings XV Congress of International Association of Hydraulic Engineering and Research, Istanbul, Turkey.

Zyrjanov, A.G., 1973. Dynamics of reservoir silting of Ouchi-Kurgan Hydroelectric Station and experience of preventing of sediment siltation. Hydrotechnical Construction, No. 1, pp. 32-37 (in Russian).

APPENDIX A: BEDFORM CALCULATION OF THE LOWER NAKDONG RIVER

Graphs and equations used to predict bedform calculations are summarized in this section. Simons and Richardson (1963, 1966, from Julien 1998) proposed the bedform classification graph (Figure A-1) plotting the stream power $\gamma q S_f$ as a function of particle diameter d_s based on the extensive laboratory experiments and some canal field observations.

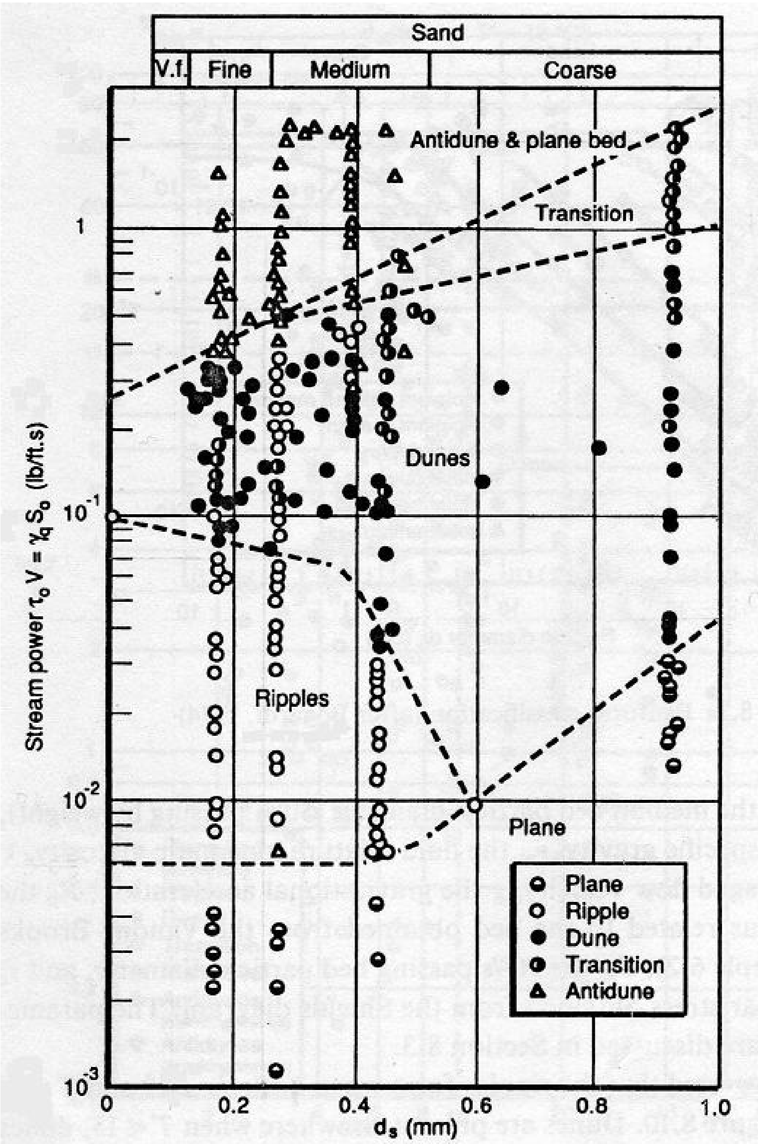

Figure A-1. Bedform classification (after Simons and Richardson, 1963, 1966)

Bogardi (1974) plotted a particle stability factor $\frac{gd_s}{u_*^2}$ against particle diameter d_s.

Figure A-2 shows the Bogardi's graph of the bedform classification.

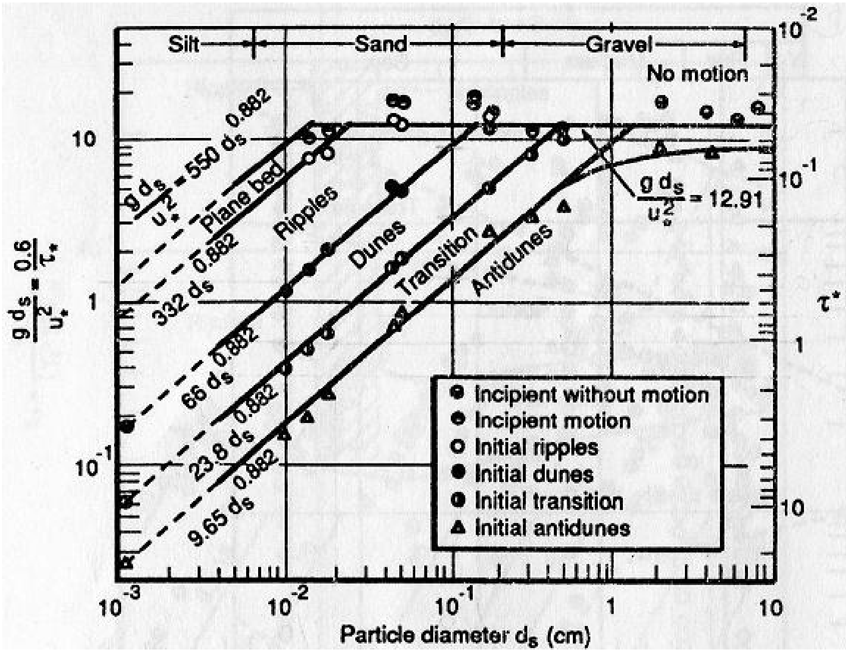

Figure A-2. Bedform classification (after Bogardi, 1974)

van Rijn (1984) proposed a bedform classification based on the dimensionless particle diameter d_* and the transport-stage parameter T as following.

$$d_* = d_{50}\left[\frac{(G-1)g}{\nu_m^2}\right]^{1/3}$$

$$T = \frac{\tau_*^{'} - \tau_{*c}}{\tau_{*c}} = \frac{(u_*^{'})^2 - u_{*c}^2}{u_{*c}^2} = \frac{\rho_m V^2}{\tau_c\left[5.75\log(4R_b/d_{90})\right]^2} - 1$$

where: ν_m = fluid mixture kinematic viscosity

R_b = hydraulic radius related to the bed

τ_* = Shields parameter

$\tau_*^{'}$ = grain Shield parameter

u_* = shear velocity

$u_*^{'}$ = grain shear velocity

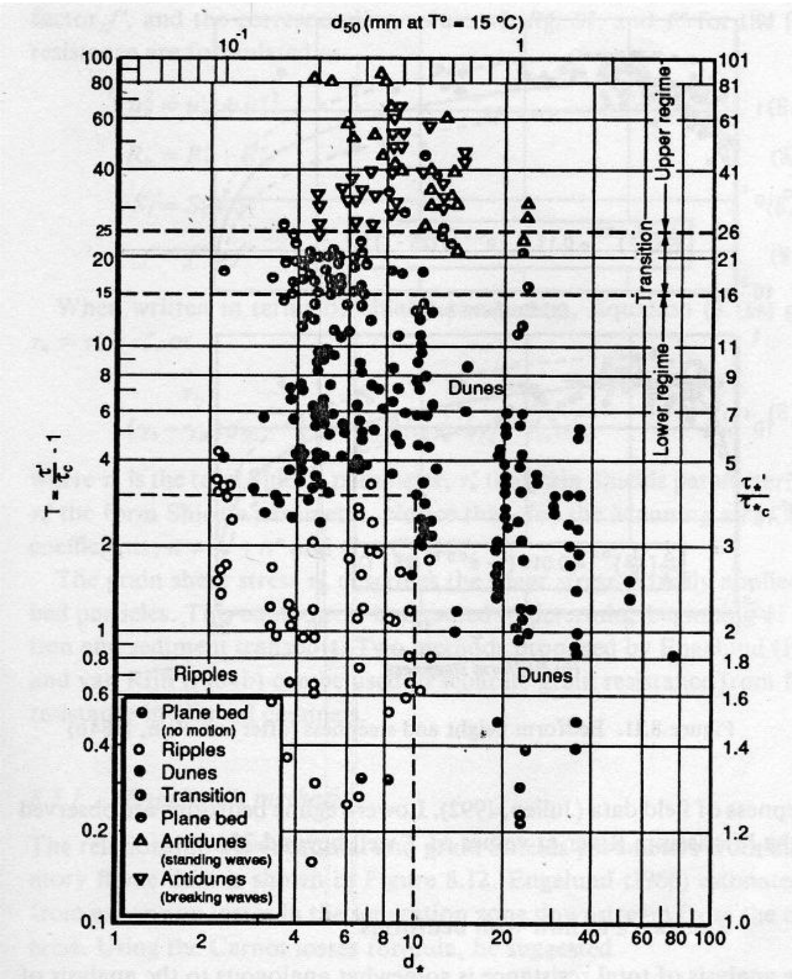

Figure A-3. Bedform classification (after van Rijn, 1984)

Using the three methods, the bedform classification of the Lower Nakdong River was predicted as shown in Figures A-4 to A-13.

XS Distance (m)	Simons and Richardson method: Shear stress lb/ft^2	Velocity ft/s	Shear stress * Velocity	Bed form	Bogardi method: Shield parameter	Bed form	Van Rijn method: Grain shear velocity	Grain shear stress	T	Bed form
0	0.008693629	1.093613333	0.009507469	Ripples	0.102839266	Ripples	0.013306128	0.177053036	0.060197818	Ripples
100	0.008777832	1.098896695	0.00964593	Ripples	0.103835321	Ripples	0.013376834	0.178939694	0.071495172	Ripples
200	0.008861246	1.104105672	0.009783752	Ripples	0.104822052	Ripples	0.013446581	0.180810551	0.08269791	Ripples
300	0.008943892	1.109242553	0.009920946	Ripples	0.105799696	Ripples	0.013515398	0.18266599	0.093808325	Ripples
400	0.009026288	1.114340326	0.010058357	Ripples	0.106774383	Ripples	0.013583726	0.184517599	0.104895804	Ripples
500	0.009108758	1.119419387	0.01019652	Ripples	0.107749937	Ripples	0.013651836	0.186372622	0.116003725	Ripples
600	0.009191563	1.124496037	0.010335876	Ripples	0.108729461	Ripples	0.013719947	0.188236959	0.127167418	Ripples
700	0.00927491	1.129582894	0.01047678	Ripples	0.1097154	Ripples	0.01378823	0.190115277	0.138414835	Ripples
800	0.009358969	1.134690063	0.010619529	Ripples	0.110709752	Ripples	0.013856818	0.192011412	0.149768935	Ripples
900	0.00944388	1.139825782	0.010764378	Ripples	0.111714187	Ripples	0.013925824	0.193928581	0.161248986	Ripples
1000	0.009529764	1.144996902	0.01091155	Ripples	0.112730128	Ripples	0.01399534	0.195869547	0.172871536	Ripples
1100	0.009616725	1.150209221	0.011061246	Ripples	0.113758817	Ripples	0.014065445	0.197836733	0.184651096	Ripples
1200	0.009704857	1.155467727	0.011213649	Ripples	0.114801356	Ripples	0.014136206	0.199832306	0.196600637	Ripples
1300	0.009794244	1.160776778	0.011368931	Ripples	0.115858739	Ripples	0.014207682	0.201858235	0.208731945	Ripples
1400	0.009884963	1.166140229	0.011527253	Ripples	0.11693188	Ripples	0.014279928	0.203916335	0.221055895	Ripples
1500	0.009977086	1.171561524	0.01168877	Ripples	0.118021621	Ripples	0.014352989	0.2060083	0.233582636	Ripples
1600	0.010070679	1.177043773	0.01185363	Ripples	0.119128755	Ripples	0.01442691	0.208135729	0.246321732	Ripples
1700	0.010165805	1.182589792	0.012021977	Ripples	0.120254027	Ripples	0.014501729	0.210300138	0.259282263	Ripples
1800	0.010262524	1.188202142	0.012193953	Ripples	0.121398141	Ripples	0.014577482	0.212502972	0.272472885	Ripples
1900	0.010360892	1.193883145	0.012369694	Ripples	0.122561768	Ripples	0.014654201	0.214745612	0.285901867	Ripples
2000	0.010460964	1.199634898	0.012549337	Ripples	0.123745541	Ripples	0.014731917	0.217029376	0.2995771	Ripples
2100	0.010562789	1.205459267	0.012733011	Ripples	0.124950056	Ripples	0.014810655	0.219355516	0.313506085	Ripples
2200	0.010666414	1.211357884	0.012920845	Ripples	0.126175873	Ripples	0.01489044	0.221725216	0.327695902	Ripples
2300	0.010771884	1.217332128	0.013112961	Ripples	0.127423504	Ripples	0.014971292	0.224139578	0.342153159	Ripples
2400	0.010879238	1.223383103	0.013309475	Ripples	0.128693417	Ripples	0.015053226	0.226599614	0.356883916	Ripples
2500	0.010988509	1.229511605	0.013510499	Ripples	0.129986018	Ripples	0.015136256	0.229106231	0.371893597	Ripples
2600	0.011099727	1.235718091	0.013716134	Ripples	0.131301651	Ripples	0.015220388	0.231660209	0.387186882	Ripples
2700	0.011212915	1.242002636	0.01392647	Ripples	0.13264058	Ripples	0.015305626	0.234262185	0.402767575	Ripples
2800	0.011328087	1.248364884	0.014141587	Ripples	0.134002982	Ripples	0.015391966	0.236912624	0.418638469	Ripples
2900	0.01144525	1.254804004	0.014361546	Ripples	0.135388934	Ripples	0.015479399	0.239611797	0.434801179	Ripples
3000	0.011564401	1.261318633	0.014586394	Ripples	0.136798394	Ripples	0.015567908	0.242359749	0.451255985	Ripples
3100	0.011685524	1.267906833	0.014816156	Ripples	0.138231195	Ripples	0.015657467	0.245156276	0.46800165	Ripples
3200	0.011808594	1.274566036	0.015050833	Ripples	0.139687022	Ripples	0.015748044	0.248000888	0.485035255	Ripples
3300	0.011933571	1.281293004	0.015290401	Ripples	0.141165407	Ripples	0.015839596	0.250892789	0.502352027	Ripples
3400	0.012060401	1.288083798	0.015534807	Ripples	0.142665713	Ripples	0.01593207	0.253830848	0.5199452	Ripples
3500	0.012189015	1.294933755	0.015783967	Ripples	0.144187124	Ripples	0.016025404	0.256813584	0.537805891	Ripples
3600	0.012319329	1.301837484	0.016037764	Ripples	0.145728643	Ripples	0.016119527	0.259839145	0.555923023	Ripples
3700	0.012451243	1.308788882	0.016296048	Ripples	0.147289087	Ripples	0.016214355	0.26290531	0.574283294	Ripples
3800	0.012584641	1.315781171	0.016558634	Ripples	0.148867094	Ripples	0.016309797	0.266009492	0.592871212	Ripples
3900	0.012719395	1.32280696	0.016825304	Ripples	0.15046113	Ripples	0.016405754	0.269148755	0.611669192	Ripples
4000	0.012855361	1.329858333	0.017095808	Ripples	0.152069506	Ripples	0.016502116	0.272319842	0.630657735	Ripples

Figure A-4. Bedform calculation for the Lower Nakdong River (0 to 4 km)

	XS Distance (m)	Simons and Richardson method: Shear stress lb/ft^2	Velocity ft/s	Shear stress * Velocity	Bed form	Bogardi method: Shield parameter	Bed form	Van Rijn method: Grain shear velocity	Grain shear stress	T	Bed form
46	4100	0.012992385	1.336926962	0.017369869	Ripples	0.1536904	Ripples	0.016598772	0.275519218	0.649815676	Ripples
47	4200	0.013130304	1.344004237	0.017647184	Ripples	0.155321885	Ripples	0.016695602	0.278743126	0.669120513	Ripples
48	4300	0.01326895	1.351081425	0.017927432	Ripples	0.156961963	Ripples	0.016792488	0.281987649	0.688548794	Ripples
49	4400	0.01340815	1.358149828	0.018210277	Ripples	0.158608604	Ripples	0.01688931	0.285248786	0.708076562	Ripples
50	4500	0.013547734	1.365200958	0.01849538	Ripples	0.160259781	Ripples	0.016985951	0.288522532	0.727679834	Ripples
51	4600	0.013687535	1.372226705	0.018782401	Ripples	0.161913518	Ripples	0.0170823	0.29180496	0.747335092	Ripples
52	4700	0.013827392	1.379219495	0.019071009	Ripples	0.163567927	Ripples	0.017178251	0.295092301	0.767019769	Ripples
53	4800	0.013967157	1.386172437	0.019360889	Ripples	0.165221247	Ripples	0.017273709	0.298381023	0.786712713	Ripples
54	4900	0.014106695	1.39307944	0.019651747	Ripples	0.166871873	Ripples	0.017368589	0.301667896	0.80639459	Ripples
55	5000	0.014245885	1.399935309	0.019943318	Ripples	0.168518394	Ripples	0.017462819	0.304950055	0.826048231	Ripples
56	5100	0.014384627	1.406735809	0.020235369	Ripples	0.170159602	Ripples	0.017556339	0.308225037	0.845658901	Ripples
57	5200	0.014522836	1.413477696	0.020527704	Ripples	0.171794516	Ripples	0.017649102	0.311490818	0.865214478	Ripples
58	5300	0.014660449	1.420158722	0.020820165	Ripples	0.173422382	Ripples	0.017741077	0.314745827	0.884705548	Ripples
59	5400	0.014797423	1.426777606	0.021112631	Ripples	0.175042676	Ripples	0.017832245	0.317988945	0.904125417	Ripples
60	5500	0.01493373	1.433333987	0.021405023	Ripples	0.176655098	Ripples	0.017922597	0.321219498	0.923470046	Ripples
61	5600	0.015069365	1.439828351	0.021697299	Ripples	0.178259555	Ripples	0.018012141	0.324437232	0.942737917	Ripples
62	5700	0.015204335	1.446261947	0.021989451	Ripples	0.179856151	Ripples	0.018100892	0.327642284	0.961929846	Ripples
63	5800	0.015338664	1.452636692	0.022281506	Ripples	0.181445163	Ripples	0.018188874	0.330835143	0.981048762	Ripples
64	5900	0.015472388	1.458955069	0.022573519	Ripples	0.183027021	Ripples	0.018276121	0.334016608	1.00009945	Ripples
65	6000	0.015605554	1.465220027	0.022865571	Ripples	0.184602283	Ripples	0.018362673	0.337187743	1.019088283	Ripples
66	6100	0.01573822	1.471434881	0.023157765	Ripples	0.186171617	Ripples	0.018448573	0.340349834	1.03802296	Ripples
67	6200	0.015870447	1.477603222	0.023450224	Ripples	0.187735773	Ripples	0.01853387	0.343504344	1.05691224	Ripples
68	6300	0.016002306	1.483728824	0.023743083	Ripples	0.189295567	Ripples	0.018618616	0.346652872	1.0757657	Ripples
69	6400	0.016133869	1.489815578	0.02403649	Ripples	0.190851861	Ripples	0.018702864	0.349797116	1.094593506	Ripples
70	6500	0.016265211	1.495867418	0.0243306	Ripples	0.192405544	Ripples	0.018786667	0.352938838	1.113406218	Ripples
71	6600	0.01639641	1.501888269	0.024625575	Ripples	0.193957522	Ripples	0.018870078	0.35607984	1.132214608	Ripples
72	6700	0.01652754	1.507882	0.02492158	Ripples	0.195508701	Ripples	0.018953151	0.35922193	1.151029522	Ripples
73	6800	0.016658679	1.513852388	0.025218781	Ripples	0.197059981	Ripples	0.019035937	0.362366912	1.169861749	Ripples
74	6900	0.016789902	1.519803088	0.025517344	Ripples	0.198612245	Ripples	0.019118487	0.365516562	1.188721927	Ripples
75	7000	0.01692128	1.525737617	0.025817434	Ripples	0.200166356	Ripples	0.019200849	0.368672618	1.207620467	Ripples
76	7100	0.017052885	1.531659334	0.026119211	Ripples	0.201723149	Ripples	0.01928307	0.371836772	1.226567494	Ripples
77	7200	0.017184785	1.537571435	0.026422835	Ripples	0.20328343	Ripples	0.019365192	0.375010659	1.245572811	Ripples
78	7300	0.017317046	1.543476949	0.026728461	Ripples	0.204847973	Ripples	0.019447258	0.37819586	1.264645867	Ripples
79	7400	0.017449729	1.549378736	0.027036239	Ripples	0.206417521	Ripples	0.019529308	0.38139389	1.283795747	Ripples
80	7500	0.017582896	1.555279491	0.027346317	Ripples	0.207992783	Ripples	0.019611379	0.384606205	1.303031166	Ripples
81	7600	0.017716602	1.561181746	0.027658836	Ripples	0.209574436	Ripples	0.019693507	0.387834199	1.322360471	Ripples
82	7700	0.017850904	1.567087879	0.027973935	Ripples	0.211163124	Ripples	0.019775723	0.391079205	1.341791648	Ripples
83	7800	0.017985852	1.573000118	0.028291747	Ripples	0.212759464	Ripples	0.019858059	0.3943425	1.361332334	Ripples
84	7900	0.018121497	1.578920551	0.028612403	Ripples	0.214364039	Ripples	0.019940544	0.397625302	1.380989832	Ripples
85	8000	0.018257885	1.584851131	0.028936029	Ripples	0.215977408	Ripples	0.020023206	0.400928779	1.400771131	Ripples

Figure A-5. Bedform calculation for the Lower Nakdong River (4 to 8 km)

	A	Y	Z	AA	AB	AC	AD	AE	AF	AG	AH	AI	AJ	AK
1														
2			Simons and Richardson method					Bogardi method			Van Rijn method			
3	XS Distance		Shear stress	Velocity	Shear stress *	Bed form		Shield parameter	Bed form		Grain shear	Grain shear	T	Bed form
4	(m)		lb/ft^2	ft/s	Velocity						velocity	stress		
86	8100		0.018395061	1.59079369	0.029262747	Ripples		0.217600102	Ripples		0.02010607	0.404254047	1.420682917	Ripples
87	8200		0.018533068	1.596749939	0.029592676	Ripples		0.219232629	Ripples		0.02018916	0.407602177	1.440731598	Ripples
88	8300		0.018671948	1.602721484	0.029925932	Ripples		0.220875473	Ripples		0.020272498	0.410974194	1.460923319	Ripples
89	8400		0.018811739	1.608709826	0.030262629	Ripples		0.222529097	Ripples		0.020356107	0.414371085	1.481263983	Ripples
90	8500		0.018952478	1.614716375	0.030602877	Ripples		0.224193943	Ripples		0.020440005	0.417793797	1.501759265	Ripples
91	8600		0.019094202	1.620742452	0.030946785	Ripples		0.225870437	Ripples		0.020524211	0.421243244	1.522414632	Ripples
92	8700		0.019236946	1.626789298	0.031294458	Ripples		0.227558986	Ripples		0.020608743	0.424720305	1.543235358	Ripples
93	8800		0.019380741	1.632858079	0.031646	Ripples		0.229259982	Ripples		0.020693618	0.428225832	1.564226541	Ripples
94	8900		0.019525621	1.638949891	0.032001515	Ripples		0.230973804	Ripples		0.020778851	0.43176065	1.585393115	Ripples
95	9000		0.019671616	1.645065766	0.032361102	Ripples		0.232700816	Ripples		0.020864457	0.435325557	1.606739863	Ripples
96	9100		0.019818755	1.651206677	0.032724861	Ripples		0.234441369	Ripples		0.020950449	0.438921329	1.628271434	Ripples
97	9200		0.019967069	1.657373544	0.033092891	Ripples		0.236195805	Ripples		0.021036842	0.442548722	1.649992349	Ripples
98	9300		0.020116583	1.663567231	0.033465289	Ripples		0.237964455	Ripples		0.021123647	0.446208471	1.671907014	Ripples
99	9400		0.020267327	1.669788561	0.03384215	Ripples		0.239747639	Ripples		0.021210877	0.449901295	1.694019733	Ripples
100	9500		0.020419325	1.676038308	0.034223571	Ripples		0.241545671	Ripples		0.021298542	0.453627897	1.71633471	Ripples
101	9600		0.020572605	1.682317207	0.034609647	Ripples		0.243358853	Ripples		0.021386654	0.457388963	1.738856065	Ripples
102	9700		0.02072719	1.688625957	0.035000471	Ripples		0.245187484	Ripples		0.021475222	0.461185168	1.761587834	Ripples
103	9800		0.020883106	1.694965219	0.035396138	Ripples		0.247031854	Ripples		0.021564257	0.465017175	1.784533982	Ripples
104	9900		0.021040376	1.701335621	0.035796741	Ripples		0.248892246	Ripples		0.021653767	0.468885634	1.807698408	Ripples
105	10000		0.021199024	1.707737763	0.036202374	Ripples		0.250768938	Dunes		0.021743762	0.472791186	1.831084947	Ripples
106	10100		0.021359073	1.714172213	0.03661313	Ripples		0.252662202	Dunes		0.02183425	0.476734462	1.85469738	Ripples
107	10200		0.021520546	1.720639512	0.037029102	Ripples		0.254572308	Dunes		0.021925239	0.480716086	1.878539436	Ripples
108	10300		0.021683465	1.727140178	0.037450383	Ripples		0.256499516	Dunes		0.022016736	0.484736671	1.902614795	Ripples
109	10400		0.021847851	1.733674701	0.037877067	Ripples		0.258444087	Dunes		0.02210875	0.488796825	1.926927097	Ripples
110	10500		0.022013727	1.740243553	0.038309246	Ripples		0.260406274	Dunes		0.022201287	0.49289715	1.95147994	Ripples
111	10600		0.022181113	1.746847179	0.038747015	Ripples		0.262386328	Dunes		0.022294354	0.497038239	1.976276883	Ripples
112	10700		0.02235003	1.753486008	0.039190465	Ripples		0.264384497	Dunes		0.022387958	0.501220683	2.001321453	Ripples
113	10800		0.0225205	1.760160446	0.039639693	Ripples		0.266401025	Dunes		0.022482105	0.505445063	2.026617143	Ripples
114	10900		0.022692541	1.766870881	0.04009479	Ripples		0.268436151	Dunes		0.022576801	0.509711959	2.052167418	Ripples
115	11000		0.022866175	1.773617685	0.040555853	Ripples		0.270490114	Dunes		0.022672052	0.514021944	2.077975712	Ripples
116	11100		0.023041421	1.780401209	0.041022975	Ripples		0.272563148	Dunes		0.022767863	0.518375587	2.104045432	Ripples
117	11200		0.023218299	1.78722179	0.041496251	Ripples		0.274655486	Dunes		0.02286424	0.522773453	2.130379961	Ripples
118	11300		0.023396829	1.794079747	0.041975776	Ripples		0.276767355	Dunes		0.022961187	0.527216103	2.156982654	Ripples
119	11400		0.023577028	1.800975384	0.042461647	Ripples		0.278898983	Dunes		0.02305871	0.531704093	2.183856843	Ripples
120	11500		0.023758917	1.80790899	0.042953959	Ripples		0.281050592	Dunes		0.023156813	0.536237975	2.211005836	Ripples
121	11600		0.023942513	1.814880837	0.043452809	Ripples		0.283222405	Dunes		0.0232555	0.540818297	2.238432917	Ripples
122	11700		0.024127836	1.821891183	0.043958292	Ripples		0.285414639	Dunes		0.023354777	0.545445605	2.266141345	Ripples
123	11800		0.024314904	1.828940273	0.044470507	Ripples		0.28762751	Dunes		0.023454646	0.550120438	2.294134358	Ripples
124	11900		0.024503734	1.836028334	0.044989549	Ripples		0.289861232	Dunes		0.023555113	0.554843333	2.322415167	Ripples
125	12000		0.024694344	1.843155581	0.045515518	Ripples		0.292116015	Dunes		0.023656179	0.559614822	2.350986959	Ripples

Figure A-6. Bedform calculation for the Lower Nakdong River (8 to 12 km)

	A	Y	Z	AA	AB	AC	AD	AE	AF	AG	AH	AI	AJ	AK
1														
2			Simons and Richardson method					Bogardi method			Van Rijn method			
3	XS Distance		Shear stress	Velocity	Shear stress *	Bed form		Shield parameter	Bed form		Grain shear	Grain shear	T	Bed form
4	(m)		lb/ft^2	ft/s	Velocity						velocity	stress		
126	12100		0.024886753	1.850322215	0.046048511	Ripples		0.294392067	Dunes		0.02375785	0.564435434	2.379852895	Ripples
127	12200		0.025080977	1.857528421	0.046588627	Ripples		0.296689592	Dunes		0.023860128	0.569305691	2.409016112	Ripples
128	12300		0.025277033	1.864774372	0.047135963	Ripples		0.299008793	Dunes		0.023963016	0.574226113	2.438479716	Ripples
129	12400		0.025474938	1.872060224	0.047690618	Ripples		0.301349869	Dunes		0.024066516	0.579197213	2.468246787	Ripples
130	12500		0.025674709	1.87938612	0.048252693	Ripples		0.303713017	Dunes		0.024170633	0.584219503	2.498320375	Ripples
131	12600		0.025876363	1.88675219	0.048822284	Ripples		0.30609843	Dunes		0.024275368	0.589293484	2.528703498	Ripples
132	12700		0.026079915	1.894158548	0.049399493	Ripples		0.308506297	Dunes		0.024380723	0.594419656	2.55939914	Ripples
133	12800		0.02628538	1.901605293	0.049984418	Ripples		0.310936805	Dunes		0.024486701	0.599598512	2.590410253	Ripples
134	12900		0.026492775	1.909092511	0.050577159	Ripples		0.313390137	Dunes		0.024593303	0.604830538	2.621739749	Ripples
135	13000		0.026702115	1.916620271	0.051177815	Ripples		0.315866473	Dunes		0.024700531	0.610116214	2.653390505	Ripples
136	13100		0.026913414	1.924188629	0.051786485	Ripples		0.318365987	Dunes		0.024808386	0.615456014	2.685365353	Ripples
137	13200		0.027126687	1.931797623	0.05240327	Ripples		0.320888853	Dunes		0.02491687	0.620850403	2.717667084	Ripples
138	13300		0.027341949	1.939447277	0.053028268	Ripples		0.323435237	Dunes		0.025025983	0.62629984	2.750298444	Ripples
139	13400		0.027559212	1.9471376	0.053661578	Ripples		0.326005302	Dunes		0.025135727	0.631804775	2.783262128	Ripples
140	13500		0.02777849	1.954868584	0.054303298	Ripples		0.328599207	Dunes		0.025246102	0.63736565	2.816560781	Ripples
141	13600		0.027999797	1.962640204	0.054953528	Ripples		0.331217106	Dunes		0.025357107	0.642982898	2.850196995	Ripples
142	13700		0.028223145	1.970452418	0.055612365	Ripples		0.333859148	Dunes		0.025468744	0.648656941	2.884173302	Ripples
143	13800		0.028448546	1.978305169	0.056279906	Ripples		0.336525476	Dunes		0.025581012	0.654388194	2.918492178	Ripples
144	13900		0.028676012	1.98619838	0.056956249	Ripples		0.33921623	Dunes		0.025693911	0.660177057	2.953156031	Ripples
145	14000		0.028905554	1.994131958	0.057641489	Ripples		0.341931541	Dunes		0.025807439	0.666023923	2.988167204	Ripples
146	14100		0.029137182	2.002105792	0.058335721	Ripples		0.344671536	Dunes		0.025921597	0.671929171	3.023527969	Dunes
147	14200		0.029370908	2.010119751	0.059039042	Ripples		0.347436337	Dunes		0.026036382	0.677893167	3.059240524	Dunes
148	14300		0.02960674	2.018173687	0.059751543	Ripples		0.350226057	Dunes		0.026151793	0.683916267	3.095306989	Dunes
149	14400		0.029844687	2.026267431	0.060473318	Ripples		0.353040804	Dunes		0.026267828	0.68999881	3.1317294	Dunes
150	14500		0.030084759	2.034400795	0.061204458	Ripples		0.355880679	Dunes		0.026384486	0.696141121	3.16850971	Dunes
151	14600		0.030326963	2.042573573	0.061945054	Ripples		0.358745774	Dunes		0.026501764	0.702343513	3.205649778	Dunes
152	14700		0.030571306	2.050785534	0.062695193	Ripples		0.361636175	Dunes		0.02661966	0.708606279	3.24315137	Dunes
153	14800		0.030817795	2.059036431	0.063454964	Ripples		0.36455196	Dunes		0.026738169	0.714929698	3.281016154	Dunes
154	14900		0.031066436	2.067325993	0.064224451	Ripples		0.367493199	Dunes		0.02685729	0.72131403	3.319245691	Dunes
155	15000		0.031317234	2.075653927	0.06500374	Ripples		0.370459953	Dunes		0.026977018	0.72775952	3.357841437	Dunes
156	15100		0.031570193	2.084019919	0.065792911	Ripples		0.373452273	Dunes		0.02709735	0.73426639	3.396804731	Dunes
157	15200		0.031825317	2.092423632	0.066592046	Ripples		0.376470204	Dunes		0.027218281	0.740834845	3.436136797	Dunes
158	15300		0.032082609	2.100864707	0.067401221	Ripples		0.379513777	Dunes		0.027339807	0.747465068	3.475838733	Dunes
159	15400		0.032342071	2.109342758	0.068220512	Ripples		0.382583018	Dunes		0.027461923	0.754157222	3.515911511	Dunes
160	15500		0.032603703	2.117857379	0.069049993	Ripples		0.385677939	Dunes		0.027584623	0.760911447	3.556355968	Dunes
161	15600		0.032867507	2.126408139	0.069889734	Ripples		0.388798542	Dunes		0.027707902	0.767727858	3.597172802	Dunes
162	15700		0.033133481	2.13499458	0.070739802	Ripples		0.391944821	Dunes		0.027831754	0.774606549	3.638362567	Dunes
163	15800		0.033401624	2.143616221	0.071600262	Ripples		0.395116754	Dunes		0.027956173	0.781547586	3.679925667	Dunes
164	15900		0.033671933	2.152272555	0.072471176	Ripples		0.398314312	Dunes		0.02808115	0.788551013	3.721862351	Dunes
165	16000		0.033944404	2.160963048	0.073352603	Ripples		0.401537451	Dunes		0.028206681	0.795616842	3.764172705	Dunes

Figure A-7. Bedform calculation for the Lower Nakdong River (12 to 16 km)

	A	Y	Z	AA	AB	AC	AD	AE	AF	AG	AH	AI	AJ	AK
1														
2			Simons and Richardson method					Bogardi method			Van Rijn method			
3 / 4	XS Distance (m)		Shear stress lb/ft^2	Velocity ft/s	Shear stress * Velocity	Bed form		Shield parameter	Bed form		Grain shear velocity	Grain shear stress	T	Bed form
166	16100		0.034219033	2.16968714	0.074244597	Ripples		0.404786114	Dunes		0.028332756	0.802745061	3.806856651	Dunes
167	16200		0.034495815	2.178444244	0.075147209	Ripples		0.408060234	Dunes		0.028459368	0.809935627	3.849913937	Dunes
168	16300		0.034774741	2.187233748	0.076060487	Ripples		0.411359728	Dunes		0.028586509	0.81718847	3.893344133	Dunes
169	16400		0.035055804	2.196055009	0.076984475	Ripples		0.414684502	Dunes		0.028714169	0.824503486	3.937146624	Dunes
170	16500		0.035338996	2.204907358	0.077919211	Ripples		0.418034447	Dunes		0.028842339	0.831880541	3.981320608	Dunes
171	16600		0.035624304	2.213790098	0.078864731	Dunes		0.421409437	Dunes		0.028971011	0.839319469	4.025865083	Dunes
172	16700		0.035911718	2.222702501	0.079821066	Dunes		0.424809336	Dunes		0.029100173	0.846820068	4.070778848	Dunes
173	16800		0.036201225	2.231643814	0.08078824	Dunes		0.42823399	Dunes		0.029229815	0.854382103	4.116060495	Dunes
174	16900		0.03649281	2.240613252	0.081766274	Dunes		0.431683229	Dunes		0.029359927	0.862005303	4.1617084	Dunes
175	17000		0.036786458	2.24961	0.082755184	Dunes		0.43515687	Dunes		0.029490496	0.869689361	4.207720723	Dunes
176	17100		0.037082152	2.258633216	0.08375498	Dunes		0.438654711	Dunes		0.029621511	0.877433931	4.254095396	Dunes
177	17200		0.037379873	2.267682027	0.084765666	Dunes		0.442176535	Dunes		0.02975296	0.885238631	4.300830124	Dunes
178	17300		0.037679602	2.276755527	0.085787242	Dunes		0.445722107	Dunes		0.02988483	0.893103036	4.347922373	Dunes
179	17400		0.037981317	2.285852785	0.0868197	Dunes		0.449291177	Dunes		0.030017107	0.901026684	4.395369368	Dunes
180	17500		0.038284996	2.294972835	0.087863026	Dunes		0.452883475	Dunes		0.030149777	0.909009071	4.443168088	Dunes
181	17600		0.038590614	2.304114683	0.088917201	Dunes		0.456498715	Dunes		0.030282828	0.917049648	4.491315259	Dunes
182	17700		0.038898146	2.313277304	0.089982198	Dunes		0.46013659	Dunes		0.030416243	0.925147827	4.53980735	Dunes
183	17800		0.039207564	2.322459642	0.091057985	Dunes		0.463796779	Dunes		0.030550008	0.933302975	4.588640567	Dunes
184	17900		0.039518839	2.33166061	0.092144521	Dunes		0.467478938	Dunes		0.030684107	0.941514412	4.63781085	Dunes
185	18000		0.039831941	2.340879093	0.093241759	Dunes		0.471182706	Dunes		0.030818524	0.949781416	4.687313867	Dunes
186	18100		0.040146838	2.350113941	0.094349643	Dunes		0.474907703	Dunes		0.030953242	0.958103217	4.737145009	Dunes
187	18200		0.040463495	2.359363978	0.095468113	Dunes		0.478653529	Dunes		0.031088245	0.966478998	4.787299389	Dunes
188	18300		0.040781878	2.368627996	0.096597098	Dunes		0.482419764	Dunes		0.031223515	0.974907896	4.837771835	Dunes
189	18400		0.041101949	2.377904756	0.097736521	Dunes		0.48620597	Dunes		0.031359034	0.983389	4.888556887	Dunes
190	18500		0.04142367	2.387192993	0.098886294	Dunes		0.490011687	Dunes		0.031494783	0.991921349	4.939648797	Dunes
191	18600		0.041746999	2.396491408	0.100046324	Dunes		0.493836435	Dunes		0.031630743	1.000503934	4.991041522	Dunes
192	18700		0.042071895	2.405798677	0.101216509	Dunes		0.497679715	Dunes		0.031766896	1.009135697	5.042728722	Dunes
193	18800		0.042398313	2.415113445	0.102396736	Dunes		0.501541007	Dunes		0.031903221	1.017815528	5.094703761	Dunes
194	18900		0.042726209	2.42443433	0.103586887	Dunes		0.50541977	Dunes		0.032039698	1.02654227	5.146959702	Dunes
195	19000		0.043055534	2.433759922	0.104786832	Dunes		0.509315445	Dunes		0.032176307	1.035314714	5.199489307	Dunes
196	19100		0.043386239	2.443088784	0.105996435	Dunes		0.513227449	Dunes		0.032313025	1.044131601	5.252285037	Dunes
197	19200		0.043718274	2.452419454	0.107215547	Dunes		0.517155183	Dunes		0.032449832	1.052991621	5.30533905	Dunes
198	19300		0.044051587	2.461750442	0.108444013	Dunes		0.521098023	Dunes		0.032586706	1.061893414	5.3586432	Dunes
199	19400		0.044386122	2.471080236	0.109681669	Dunes		0.525055329	Dunes		0.032723624	1.07083557	5.412189042	Dunes
200	19500		0.044721824	2.480407298	0.110928339	Dunes		0.529026439	Dunes		0.032860563	1.079816627	5.465967827	Dunes
201	19600		0.045058635	2.489730068	0.11218384	Dunes		0.533010672	Dunes		0.032997501	1.088835075	5.519970511	Dunes
202	19700		0.045396497	2.499046961	0.113447978	Dunes		0.537007326	Dunes		0.033134413	1.097889354	5.574187748	Dunes
203	19800		0.045735348	2.508356376	0.114720551	Dunes		0.541015683	Dunes		0.033271277	1.106977854	5.628609902	Dunes
204	19900		0.046075125	2.517656686	0.116001347	Dunes		0.545035001	Dunes		0.033408067	1.116098916	5.683227044	Dunes
205	20000		0.046415765	2.52694625	0.117290144	Dunes		0.549064525	Dunes		0.033544759	1.125250836	5.738028957	Dunes

Figure A-8. Bedform calculation for the Lower Nakdong River (16 to 20 km)

	A	Y	Z	AA	AB	AC	AD	AE	AF	AG	AH	AI	AJ	AK
1														
2			Simons and Richardson method					Bogardi method			Van Rijn method			
3	XS Distance		Shear stress	Velocity	Shear stress *	Bed form		Shield parameter	Bed form		Grain shear	Grain shear	T	Bed form
4	(m)		lb/ft^2	ft/s	Velocity						velocity	stress		
206	20100		0.046757203	2.536223405	0.118586711	Dunes		0.553103477	Dunes		0.033681328	1.134431859	5.793005143	Dunes
207	20200		0.04709937	2.545486475	0.119890808	Dunes		0.557151064	Dunes		0.03381775	1.143640186	5.848144827	Dunes
208	20300		0.047442198	2.554733767	0.121202186	Dunes		0.561206474	Dunes		0.033953998	1.152873972	5.90343696	Dunes
209	20400		0.047785618	2.563963572	0.122520584	Dunes		0.565268881	Dunes		0.034090047	1.162131328	5.95887023	Dunes
210	20500		0.048129558	2.573174172	0.123845736	Dunes		0.569337439	Dunes		0.034225872	1.171410322	6.014433067	Dunes
211	20600		0.048473945	2.582363837	0.125177364	Dunes		0.573411289	Dunes		0.034361446	1.180708979	6.070113647	Dunes
212	20700		0.048818706	2.591530824	0.126515182	Dunes		0.577489555	Dunes		0.034496743	1.190025284	6.125899907	Dunes
213	20800		0.049163765	2.600673387	0.127858895	Dunes		0.581571349	Dunes		0.034631737	1.199357185	6.181779549	Dunes
214	20900		0.049509046	2.60978977	0.129208201	Dunes		0.585655768	Dunes		0.0347664	1.208702589	6.237740051	Dunes
215	21000		0.049854471	2.618878212	0.130562788	Dunes		0.589741895	Dunes		0.034900707	1.218059369	6.293768677	Dunes
216	21100		0.050199962	2.627936951	0.131922336	Dunes		0.593828803	Dunes		0.035034631	1.227425365	6.349852486	Dunes
217	21200		0.05054544	2.63696422	0.133286517	Dunes		0.597915553	Dunes		0.035168144	1.236798383	6.405978344	Dunes
218	21300		0.050890824	2.645958256	0.134654996	Dunes		0.602001194	Dunes		0.035301221	1.2461762	6.462132935	Dunes
219	21400		0.051236033	2.654917293	0.136027431	Dunes		0.606084767	Dunes		0.035433834	1.255556563	6.518302771	Dunes
220	21500		0.051580986	2.66383957	0.137403471	Dunes		0.610165303	Dunes		0.035565956	1.264937192	6.574474203	Dunes
221	21600		0.051925599	2.672723331	0.13878276	Dunes		0.614241826	Dunes		0.03569756	1.274315784	6.630633434	Dunes
222	21700		0.05226979	2.681566825	0.140164935	Dunes		0.618313351	Dunes		0.03582862	1.28369001	6.686766528	Dunes
223	21800		0.052613475	2.690368306	0.141549624	Dunes		0.622378888	Dunes		0.035959109	1.293057523	6.742859419	Dunes
224	21900		0.052956569	2.699126039	0.142936453	Dunes		0.62643744	Dunes		0.036089	1.302415953	6.798897925	Dunes
225	22000		0.053298988	2.707838296	0.14432504	Dunes		0.630488004	Dunes		0.036218268	1.311762915	6.854867752	Dunes
226	22100		0.053640646	2.71650336	0.145714995	Dunes		0.634529575	Dunes		0.036346884	1.321096003	6.910754509	Dunes
227	22200		0.053981459	2.725119525	0.147105928	Dunes		0.638561142	Dunes		0.036474824	1.3304128	6.966543715	Dunes
228	22300		0.05432134	2.733685097	0.148497439	Dunes		0.64258169	Dunes		0.036602061	1.339710875	7.02222081	Dunes
229	22400		0.054660204	2.742198394	0.149889125	Dunes		0.646590204	Dunes		0.036728569	1.348987785	7.077771167	Dunes
230	22500		0.054997965	2.750657752	0.151280579	Dunes		0.650585666	Dunes		0.036854322	1.358241078	7.13318011	Dunes
231	22600		0.055334536	2.759061522	0.15267139	Dunes		0.654567058	Dunes		0.036979296	1.367468299	7.188432927	Dunes
232	22700		0.055669833	2.767408077	0.154061145	Dunes		0.658533366	Dunes		0.037103463	1.376666989	7.243514902	Dunes
233	22800		0.056003768	2.775695814	0.155449424	Dunes		0.662483578	Dunes		0.037226801	1.385834694	7.298411341	Dunes
234	22900		0.056336258	2.783923156	0.156835812	Dunes		0.666416687	Dunes		0.037349283	1.39496897	7.353107605	Dunes
235	23000		0.056667217	2.792088565	0.15821989	Dunes		0.670331698	Dunes		0.037470887	1.40406739	7.407589159	Dunes
236	23100		0.056996564	2.800190539	0.159601239	Dunes		0.674227627	Dunes		0.037591589	1.413127549	7.461841613	Dunes
237	23200		0.057324216	2.808227622	0.160979446	Dunes		0.678103506	Dunes		0.037711365	1.422147078	7.515850769	Dunes
238	23300		0.057650092	2.816198412	0.162354098	Dunes		0.681958387	Dunes		0.037830195	1.431123645	7.569602667	Dunes
239	23400		0.057974115	2.82410156	0.163724789	Dunes		0.685791341	Dunes		0.037948056	1.440054965	7.623083621	Dunes
240	23500		0.058296208	2.831935775	0.165091117	Dunes		0.689601466	Dunes		0.038064929	1.448938801	7.676280244	Dunes
241	23600		0.058616297	2.839699823	0.166452687	Dunes		0.693387878	Dunes		0.038180793	1.457772969	7.729179457	Dunes
242	23700		0.058934308	2.847392527	0.167809108	Dunes		0.697149721	Dunes		0.038295631	1.466555336	7.781768481	Dunes
243	23800		0.059250172	2.855012758	0.169159996	Dunes		0.700886157	Transition		0.038409424	1.475283814	7.834034814	Dunes
244	23900		0.059563819	2.862559432	0.17050497	Dunes		0.704596369	Transition		0.038522154	1.483956354	7.885966191	Dunes
245	24000		0.05987518	2.870031502	0.171843654	Dunes		0.708279551	Transition		0.038633806	1.492570941	7.937550546	Dunes

Figure A-9. Bedform calculation for the Lower Nakdong River (20 to 24 km)

	A	Y	Z	AA	AB	AC	AD	AE	AF	AG	AH	AI	AJ	AK
1														
2			Simons and Richardson method					Bogardi method			Van Rijn method			
3	XS Distance		Shear stress	Velocity	Shear stress *	Bed form		Shield parameter	Bed form		Grain shear	Grain shear	T	Bed form
4	(m)		lb/ft^2	ft/s	Velocity						velocity	stress		
246	24100		0.06018419	2.877427952	0.173175672	Dunes		0.711934915	Transition		0.038744362	1.501125589	7.988775983	Dunes
247	24200		0.060490783	2.884747794	0.174500653	Dunes		0.715561681	Transition		0.038853807	1.509618336	8.039630756	Dunes
248	24300		0.060794893	2.89199007	0.175818228	Dunes		0.719159084	Transition		0.038962126	1.518047248	8.090103281	Dunes
249	24400		0.061096458	2.899153855	0.177128032	Dunes		0.722726374	Transition		0.039069303	1.526410424	8.140182179	Dunes
250	24500		0.061395415	2.906238269	0.178429705	Dunes		0.726262818	Transition		0.039175324	1.534706008	8.189856338	Dunes
251	24600		0.061691705	2.913242481	0.179722897	Dunes		0.729767712	Transition		0.039280176	1.542932203	8.239114991	Dunes
252	24700		0.061985271	2.920165725	0.181007264	Dunes		0.733240381	Transition		0.039383845	1.551087282	8.287947797	Dunes
253	24800		0.062276059	2.927007306	0.182282479	Dunes		0.736680186	Transition		0.039486322	1.559169597	8.336344895	Dunes
254	24900		0.062564017	2.933766596	0.183548223	Dunes		0.740086521	Transition		0.039587594	1.567177587	8.384296927	Dunes
255	25000		0.062849098	2.940443038	0.184804192	Dunes		0.743458819	Transition		0.039687653	1.575109769	8.431795022	Dunes
256	25100		0.063131256	2.947036133	0.186050092	Dunes		0.746796541	Transition		0.039786489	1.582964734	8.478830744	Dunes
257	25200		0.063410448	2.953545434	0.187285638	Dunes		0.750099175	Transition		0.039884096	1.590741137	8.525396028	Dunes
258	25300		0.063686632	2.95997053	0.188510554	Dunes		0.753366233	Transition		0.039980466	1.598437682	8.571483125	Dunes
259	25400		0.063959769	2.966311051	0.18972457	Dunes		0.756597245	Transition		0.040075593	1.606053123	8.617084568	Dunes
260	25500		0.064229821	2.972566661	0.190927425	Dunes		0.759791764	Transition		0.040169469	1.613586264	8.662193197	Dunes
261	25600		0.064496752	2.97873707	0.192118867	Dunes		0.762949366	Transition		0.040262091	1.621035968	8.706802204	Dunes
262	25700		0.06476053	2.984822042	0.193298657	Dunes		0.76606966	Transition		0.040353453	1.62840117	8.750905212	Dunes
263	25800		0.065021123	2.990821403	0.194466567	Dunes		0.769152287	Transition		0.040443552	1.635680889	8.794496339	Dunes
264	25900		0.065278505	2.996735044	0.195622384	Dunes		0.772196927	Transition		0.040532385	1.642874229	8.837570231	Dunes
265	26000		0.065532652	3.002562919	0.19676591	Dunes		0.775203295	Transition		0.040619951	1.649980381	8.880122044	Dunes
266	26100		0.065783541	3.008305036	0.197896958	Dunes		0.778171135	Transition		0.040706248	1.656998613	8.922147384	Dunes
267	26200		0.066031155	3.013961445	0.199015355	Dunes		0.781100222	Transition		0.040791277	1.663928254	8.96364224	Dunes
268	26300		0.066275475	3.019532233	0.200120932	Dunes		0.783990348	Transition		0.040875037	1.670768688	9.004602921	Dunes
269	26400		0.066516486	3.025017519	0.201213534	Dunes		0.786841331	Transition		0.040957531	1.677519351	9.045026053	Dunes
270	26500		0.066754174	3.030417459	0.202293014	Dunes		0.78965301	Transition		0.041038759	1.684179738	9.084908609	Dunes
271	26600		0.066988529	3.035732257	0.203359237	Dunes		0.792425253	Transition		0.041118723	1.690749411	9.124247972	Dunes
272	26700		0.067219541	3.040962168	0.204412081	Dunes		0.79515796	Transition		0.041197427	1.697228013	9.163041995	Dunes
273	26800		0.067447205	3.046107503	0.205451438	Dunes		0.797851065	Transition		0.041274875	1.703615266	9.201289015	Dunes
274	26900		0.067671519	3.051168621	0.206477216	Dunes		0.800504532	Transition		0.04135107	1.709910965	9.238987817	Dunes
275	27000		0.067892481	3.056145921	0.207489329	Dunes		0.803118351	Transition		0.041426018	1.716114973	9.276137561	Dunes
276	27100		0.068110092	3.061039832	0.208487706	Dunes		0.805692532	Transition		0.041499725	1.722227199	9.312737716	Dunes
277	27200		0.068324355	3.065850809	0.20947228	Dunes		0.808227104	Transition		0.041572197	1.7282476	9.348788027	Dunes
278	27300		0.068535274	3.070579332	0.210442995	Dunes		0.810722117	Transition		0.041643441	1.734176185	9.384288532	Dunes
279	27400		0.068742854	3.075225919	0.211399807	Dunes		0.813177641	Transition		0.041713463	1.740013016	9.419239619	Dunes
280	27500		0.068947105	3.079791128	0.212342682	Dunes		0.815593777	Transition		0.041782272	1.745758227	9.453642078	Dunes
281	27600		0.069148036	3.08427556	0.213271599	Dunes		0.81797065	Transition		0.041849875	1.751412016	9.487497105	Dunes
282	27700		0.069345662	3.088679851	0.214186548	Dunes		0.820308414	Transition		0.041916281	1.756974645	9.520806256	Dunes
283	27800		0.069539995	3.093004663	0.21508753	Dunes		0.822607236	Transition		0.041981501	1.76244642	9.553571376	Dunes
284	27900		0.069731052	3.097250677	0.21597455	Dunes		0.824867304	Transition		0.042045543	1.767827687	9.585794531	Dunes
285	28000		0.06991885	3.101418588	0.216847622	Dunes		0.827088814	Transition		0.042108418	1.773118826	9.617478	Dunes

Figure A-10. Bedform calculation for the Lower Nakdong River (24 to 28 km)

	A	Z	AA	AB	AC	AE	AF	AH	AI	AJ	AK
2		Simons and Richardson method				Bogardi method		Van Rijn method			
3/4	XS Distance (m)	Shear stress lb/ft^2	Velocity ft/s	Shear stress * Velocity	Bed form	Shield parameter	Bed form	Grain shear velocity	Grain shear stress	T	Bed form
286	28100	0.070103407	3.105509115	0.217706769	Dunes	0.829271982	Transition	0.042170135	1.778320261	9.648624316	Dunes
287	28200	0.070284742	3.109523002	0.218552022	Dunes	0.831417045	Transition	0.042230705	1.783432464	9.679236314	Dunes
288	28300	0.070462878	3.113461027	0.219383423	Dunes	0.833524258	Transition	0.04229014	1.788455966	9.709317159	Dunes
289	28400	0.070637837	3.117323995	0.220201024	Dunes	0.835593901	Transition	0.042348451	1.793391341	9.738870308	Dunes
290	28500	0.070809645	3.121112727	0.221004884	Dunes	0.837626262	Transition	0.042405651	1.798239206	9.767899437	Dunes
291	28600	0.070978327	3.124828052	0.221795066	Dunes	0.839621644	Transition	0.04246175	1.803000199	9.796408376	Dunes
292	28700	0.071143908	3.128470807	0.222571641	Dunes	0.841580356	Transition	0.042516761	1.807674983	9.824401095	Dunes
293	28800	0.071306418	3.132041842	0.223334683	Dunes	0.843502719	Transition	0.042570697	1.812264251	9.851881742	Dunes
294	28900	0.071465882	3.135542026	0.224084277	Dunes	0.845389069	Transition	0.04262357	1.816768734	9.878854695	Dunes
295	29000	0.071622332	3.138972248	0.224820514	Dunes	0.84723976	Transition	0.042675393	1.821189205	9.905324582	Dunes
296	29100	0.071775799	3.142333414	0.225543491	Dunes	0.849055155	Transition	0.04272618	1.82552647	9.931296227	Dunes
297	29200	0.071926313	3.145626435	0.226253312	Dunes	0.850835629	Transition	0.042775944	1.829781355	9.95677458	Dunes
298	29300	0.072073907	3.148852221	0.226950083	Dunes	0.852581559	Transition	0.042824697	1.833954698	9.98176466	Dunes
299	29400	0.072218613	3.152011683	0.227633913	Dunes	0.854293326	Transition	0.042872454	1.838047352	10.00627157	Dunes
300	29500	0.072360464	3.15510574	0.228304916	Dunes	0.85597132	Transition	0.042919229	1.842060192	10.03030055	Dunes
301	29600	0.072499494	3.158135324	0.228963214	Dunes	0.857615945	Transition	0.042965034	1.845994121	10.05385701	Dunes
302	29700	0.072635738	3.161101378	0.229608933	Dunes	0.859227611	Transition	0.043009883	1.84985007	10.07694653	Dunes
303	29800	0.072769231	3.164004847	0.230242201	Dunes	0.860806736	Transition	0.043053792	1.853628984	10.09957475	Dunes
304	29900	0.072900009	3.166846672	0.23086315	Dunes	0.862353737	Transition	0.043096773	1.857331812	10.12174738	Dunes
305	30000	0.073028106	3.169627783	0.231471914	Dunes	0.863869033	Transition	0.04313884	1.860959505	10.14347009	Dunes
306	30100	0.073153559	3.172349113	0.232068627	Dunes	0.865353044	Transition	0.043180007	1.864513024	10.16474865	Dunes
307	30200	0.073276403	3.175011602	0.232653429	Dunes	0.866806201	Transition	0.043220289	1.86799335	10.18558892	Dunes
308	30300	0.073396675	3.177616194	0.233226464	Dunes	0.868228937	Transition	0.043259698	1.871401481	10.20599689	Dunes
309	30400	0.073514413	3.18016383	0.233787878	Dunes	0.869621691	Transition	0.04329825	1.874738424	10.22597859	Dunes
310	30500	0.073629653	3.182655445	0.234337817	Dunes	0.870984898	Transition	0.043335957	1.87800518	10.24554	Dunes
311	30600	0.073742432	3.185091956	0.234876428	Dunes	0.872318989	Transition	0.043372834	1.881202745	10.26468709	Dunes
312	30700	0.073852786	3.18747428	0.235403857	Dunes	0.873624398	Transition	0.043408894	1.884332116	10.28342585	Dunes
313	30800	0.073960753	3.189803333	0.235920256	Dunes	0.874901561	Transition	0.043444152	1.887394305	10.30176231	Dunes
314	30900	0.074066368	3.192080035	0.236425776	Dunes	0.876150917	Transition	0.043478619	1.890390332	10.31970259	Dunes
315	31000	0.074169671	3.194305297	0.236920572	Dunes	0.877372907	Transition	0.043512311	1.893321216	10.33725279	Dunes
316	31100	0.074270696	3.196480016	0.237404796	Dunes	0.878567964	Transition	0.04354524	1.896187965	10.35441895	Dunes
317	31200	0.074369481	3.198605071	0.237878599	Dunes	0.879736516	Transition	0.04357742	1.898991574	10.37120703	Dunes
318	31300	0.074466061	3.20068134	0.238342133	Dunes	0.880878991	Transition	0.043608864	1.90173304	10.38762299	Dunes
319	31400	0.074560473	3.202709698	0.238795551	Dunes	0.881995818	Transition	0.043639585	1.904413365	10.40367285	Dunes
320	31500	0.074652754	3.204691016	0.23923901	Dunes	0.883087428	Transition	0.043669595	1.907033556	10.41936261	Dunes
321	31600	0.074742939	3.206626155	0.239672662	Dunes	0.884154247	Transition	0.043698909	1.909594607	10.43469825	Dunes
322	31700	0.074831063	3.208515954	0.240096659	Dunes	0.885196692	Transition	0.043727537	1.912097495	10.4496856	Dunes
323	31800	0.074917161	3.210361238	0.240511151	Dunes	0.886215175	Transition	0.043755493	1.914543184	10.46433044	Dunes
324	31900	0.075001269	3.21216283	0.240916289	Dunes	0.887210107	Transition	0.043782789	1.916932639	10.47863856	Dunes
325	32000	0.075083421	3.21392155	0.241312224	Dunes	0.888181902	Transition	0.043809438	1.919266828	10.49261574	Dunes

Figure A-11. Bedform calculation for the Lower Nakdong River (28 to 32 km)

	A	Y	Z	AA	AB	AC	AD	AE	AF	AG	AH	AI	AJ	AK
1														
2			Simons and Richardson method					Bogardi method			Van Rijn method			
3	XS Distance		Shear stress	Velocity	Shear stress *	Bed form		Shield parameter	Bed form		Grain shear	Grain shear	T	Bed form
4	(m)		lb/ft^2	ft/s	Velocity						velocity	stress		
326	32100		0.075163651	3.215638207	0.241699108	Dunes		0.889130968	Transition		0.04383545	1.921546714	10.50626775	Dunes
327	32200		0.075241994	3.217313593	0.242077089	Dunes		0.890057705	Transition		0.043860839	1.923773236	10.51960022	Dunes
328	32300		0.075318482	3.218948479	0.242446313	Dunes		0.890962505	Transition		0.043885616	1.925947315	10.53261866	Dunes
329	32400		0.075393149	3.220543628	0.242806924	Dunes		0.891845756	Transition		0.043909792	1.928069866	10.54532854	Dunes
330	32500		0.075466026	3.2220998	0.243159069	Dunes		0.892707847	Transition		0.043933379	1.930141805	10.55773536	Dunes
331	32600		0.075537148	3.223617749	0.243502891	Dunes		0.893549164	Transition		0.043956388	1.932164042	10.56984456	Dunes
332	32700		0.075606546	3.22509821	0.243838535	Dunes		0.894370085	Transition		0.04397883	1.93413747	10.5816615	Dunes
333	32800		0.07567425	3.226541897	0.244166138	Dunes		0.895170978	Transition		0.044000715	1.936062957	10.59319136	Dunes
334	32900		0.075740292	3.227949511	0.244485838	Dunes		0.895952205	Transition		0.044022055	1.937941356	10.60443926	Dunes
335	33000		0.075804702	3.229321751	0.244797772	Dunes		0.896714127	Transition		0.04404286	1.939773523	10.61541032	Dunes
336	33100		0.07586751	3.230659309	0.245102077	Dunes		0.897457104	Transition		0.04406314	1.941560311	10.62610965	Dunes
337	33200		0.075928747	3.231962863	0.245398889	Dunes		0.898181488	Transition		0.044082905	1.943302552	10.63654222	Dunes
338	33300		0.07598844	3.233233065	0.245688338	Dunes		0.89888762	Transition		0.044102166	1.945001052	10.64671289	Dunes
339	33400		0.076046619	3.234470555	0.245970551	Dunes		0.899575834	Transition		0.044120932	1.946656603	10.65662637	Dunes
340	33500		0.076103311	3.23567597	0.246245656	Dunes		0.900246462	Transition		0.044139212	1.948269995	10.66628739	Dunes
341	33600		0.076158545	3.236849942	0.246513783	Dunes		0.900899838	Transition		0.044157015	1.949842014	10.67570068	Dunes
342	33700		0.076212348	3.237993086	0.246775056	Dunes		0.901536284	Transition		0.044174353	1.95137343	10.68487084	Dunes
343	33800		0.076264746	3.239105995	0.247029595	Dunes		0.902156113	Transition		0.044191232	1.952864984	10.6938023	Dunes
344	33900		0.076315765	3.240189249	0.24727752	Dunes		0.902759629	Transition		0.044207662	1.9543174	10.7024994	Dunes
345	34000		0.07636543	3.241243422	0.247518949	Dunes		0.903347138	Transition		0.044223652	1.955731401	10.71096647	Dunes
346	34100		0.076413769	3.242269088	0.247754	Dunes		0.903918943	Transition		0.04423921	1.957107709	10.71920784	Dunes
347	34200		0.076460804	3.243266803	0.247982788	Dunes		0.904475338	Transition		0.044254345	1.958447027	10.72722771	Dunes
348	34300		0.076506561	3.244237099	0.248205423	Dunes		0.905016607	Transition		0.044269064	1.959750026	10.73503009	Dunes
349	34400		0.076551062	3.245180496	0.248422014	Dunes		0.905543026	Transition		0.044283376	1.961017363	10.74261894	Dunes
350	34500		0.076594332	3.246097513	0.24863267	Dunes		0.906054872	Transition		0.044297288	1.962249699	10.7499982	Dunes
351	34600		0.076636392	3.246988667	0.248837498	Dunes		0.90655242	Transition		0.044310808	1.96344769	10.7571718	Dunes
352	34700		0.076677267	3.247854454	0.249036603	Dunes		0.907035937	Transition		0.044323944	1.964611969	10.76414353	Dunes
353	34800		0.076716977	3.248695348	0.249230086	Dunes		0.907505674	Transition		0.044336702	1.96574314	10.77091701	Dunes
354	34900		0.076755543	3.249511814	0.249418043	Dunes		0.907961883	Transition		0.04434909	1.966841797	10.77749579	Dunes
355	35000		0.076792986	3.25030432	0.249600576	Dunes		0.908404813	Transition		0.044361115	1.967908538	10.78388346	Dunes
356	35100		0.076829329	3.251073328	0.249777781	Dunes		0.908834713	Transition		0.044372784	1.968943957	10.79008357	Dunes
357	35200		0.076864589	3.251819276	0.249949752	Dunes		0.909251818	Transition		0.044384103	1.969948616	10.7960995	Dunes
358	35300		0.076898787	3.252542583	0.250116579	Dunes		0.909656356	Transition		0.044395079	1.970923054	10.80193445	Dunes
359	35400		0.076931942	3.253243666	0.250278351	Dunes		0.91004855	Transition		0.044405718	1.971867806	10.80759165	Dunes
360	35500		0.076964072	3.253922944	0.250435159	Dunes		0.910428626	Transition		0.044416027	1.972783416	10.81307435	Dunes
361	35600		0.076995196	3.254580826	0.250587089	Dunes		0.910796806	Transition		0.044426011	1.97367041	10.81838569	Dunes
362	35700		0.077025333	3.255217695	0.250734226	Dunes		0.911153298	Transition		0.044435676	1.974529284	10.82352865	Dunes
363	35800		0.077054498	3.255833921	0.250876648	Dunes		0.911498301	Transition		0.044445028	1.975360517	10.82850609	Dunes
364	35900		0.077082709	3.256429879	0.251014437	Dunes		0.911832018	Transition		0.044454073	1.976164594	10.83332092	Dunes
365	36000		0.077109983	3.257005942	0.251147674	Dunes		0.912154653	Transition		0.044462816	1.976942003	10.83797606	Dunes

Figure A-12. Bedform calculation for the Lower Nakdong River (32 to 36 km)

	A	Y	Z	AA	AB	AC	AD	AE	AF	AG	AH	AI	AJ	AK
1														
2			Simons and Richardson method					Bogardi method			Van Rijn method			
3 / 4	XS Distance (m)		Shear stress lb/ft^2	Velocity ft/s	Shear stress * Velocity	Bed form		Shield parameter	Bed form		Grain shear velocity	Grain shear stress	T	Bed form
366	36100		0.077136337	3.257562466	0.251276436	Dunes		0.912466399	Transition		0.044471263	1.977693204	10.84247428	Dunes
367	36200		0.077161786	3.258099784	0.251400797	Dunes		0.912767437	Transition		0.044479418	1.978418631	10.84681815	Dunes
368	36300		0.077186344	3.258618225	0.251520828	Dunes		0.913057946	Transition		0.044487287	1.979118712	10.85101025	Dunes
369	36400		0.077210028	3.259118125	0.251636602	Dunes		0.91333811	Transition		0.044494875	1.979793887	10.85505322	Dunes
370	36500		0.077232853	3.259599815	0.251748192	Dunes		0.913608108	Transition		0.044502186	1.980444587	10.85894962	Dunes
371	36600		0.077254832	3.260063595	0.251855665	Dunes		0.913868105	Transition		0.044509226	1.981071207	10.86270184	Dunes
372	36700		0.077275979	3.260509758	0.251959084	Dunes		0.914118261	Transition		0.044515999	1.981674127	10.86631214	Dunes
373	36800		0.077296308	3.260938601	0.252058515	Dunes		0.914358738	Transition		0.044522508	1.982253738	10.86978286	Dunes
374	36900		0.077315833	3.261350425	0.252154024	Dunes		0.914589701	Transition		0.04452876	1.982810434	10.87311637	Dunes
375	37000		0.077334566	3.261745507	0.252245673	Dunes		0.914811303	Transition		0.044534757	1.983344582	10.87631486	Dunes
376	37100		0.07735252	3.262124107	0.25233352	Dunes		0.915023685	Transition		0.044540504	1.983856521	10.87938037	Dunes
377	37200		0.077369707	3.262486486	0.252417622	Dunes		0.91522699	Transition		0.044546005	1.984346594	10.88231493	Dunes
378	37300		0.077386138	3.262832913	0.25249804	Dunes		0.915421367	Transition		0.044551264	1.984815157	10.8851207	Dunes
379	37400		0.077401828	3.263163645	0.25257483	Dunes		0.915606957	Transition		0.044556285	1.98526255	10.8877997	Dunes
380	37500		0.077416785	3.263478916	0.252648044	Dunes		0.915783888	Transition		0.044561071	1.985689079	10.89035377	Dunes
381	37600		0.07743102	3.263778951	0.252717734	Dunes		0.915952285	Transition		0.044565626	1.986095043	10.89278469	Dunes
382	37700		0.077444546	3.264063991	0.252783953	Dunes		0.916112281	Transition		0.044569954	1.986480762	10.89509438	Dunes
383	37800		0.077457372	3.264334272	0.252846753	Dunes		0.916264004	Transition		0.044574057	1.986846545	10.8972847	Dunes
384	37900		0.077469508	3.264590003	0.252906183	Dunes		0.916407572	Transition		0.044577939	1.987192673	10.89935732	Dunes
385	38000		0.077480965	3.264831383	0.252962286	Dunes		0.916543093	Transition		0.044581604	1.987519408	10.90131382	Dunes
386	38100		0.077491751	3.265058624	0.25301511	Dunes		0.916670685	Transition		0.044585054	1.98782703	10.90315587	Dunes
387	38200		0.077501877	3.265271938	0.253064703	Dunes		0.916790466	Transition		0.044588292	1.988115824	10.90488517	Dunes
388	38300		0.077511351	3.265471517	0.253111109	Dunes		0.91690254	Transition		0.044591323	1.988386043	10.90650325	Dunes
389	38400		0.077520182	3.265657535	0.253154367	Dunes		0.917007006	Transition		0.044594147	1.988637921	10.9080115	Dunes
390	38500		0.077528379	3.265830177	0.253194519	Dunes		0.917103966	Transition		0.044596768	1.988871702	10.90941139	Dunes
391	38600		0.07753595	3.265989634	0.253231608	Dunes		0.917193525	Transition		0.044599189	1.989087642	10.91070444	Dunes
392	38700		0.077542903	3.266136079	0.253265674	Dunes		0.91727578	Transition		0.044601412	1.989285973	10.91189206	Dunes
393	38800		0.077549247	3.266269667	0.253296752	Dunes		0.917350816	Transition		0.04460344	1.989466902	10.91297546	Dunes
394	38900		0.077554987	3.26639056	0.253324878	Dunes		0.917418724	Transition		0.044605276	1.989630643	10.91395595	Dunes
395	39000		0.077560133	3.266498926	0.253350092	Dunes		0.917479598	Transition		0.044606921	1.989777425	10.91483488	Dunes
396	39100		0.077564692	3.266594922	0.253372429	Dunes		0.917533524	Transition		0.044608379	1.989907456	10.91561351	Dunes
397	39200		0.07756867	3.266678685	0.253391921	Dunes		0.917580581	Transition		0.044609651	1.990020922	10.91629295	Dunes
398	39300		0.077572074	3.266750357	0.2534086	Dunes		0.917620845	Transition		0.044610739	1.990118012	10.91687432	Dunes
399	39400		0.077574911	3.266810088	0.2534225	Dunes		0.917654402	Transition		0.044611646	1.990198927	10.91735884	Dunes
400	39500		0.077577187	3.266858014	0.253433654	Dunes		0.917681327	Transition		0.044612373	1.990263853	10.91774762	Dunes
401	39600		0.077578908	3.266894261	0.25344209	Dunes		0.917701691	Transition		0.044612924	1.990312957	10.91804166	Dunes
402	39700		0.077580081	3.266918954	0.253447837	Dunes		0.917715564	Transition		0.044613299	1.990346409	10.91824197	Dunes
403	39800		0.077580711	3.266932221	0.253450925	Dunes		0.917723018	Transition		0.0446135	1.990364383	10.9183496	Dunes
404	39900		0.077580804	3.266934181	0.253451381	Dunes		0.917724119	Transition		0.04461353	1.990367038	10.9183655	Dunes
405	40000		0.077581365	3.266945998	0.253454131	Dunes		0.917730758	Transition		0.044613709	1.990383047	10.91846136	Dunes

Figure A-13. Bedform calculation for the Lower Nakdong River (36 to 40 km)

APPENDIX B: BUREAU OF RECLAMATION AUTOMATED MODIFIED EINSTEIN PROCEDURE (BORAMEP) CALCULATION

The Bureau of Reclamation Automated Modified Einstein Procedure (BORAMEP) is a computer program to calculate total sediment load and an automated version of a revised Modified Einstein Procedure (Shah, 2006). It was developed by the US Bureau of Reclamation. In this dissertation, the BORAMEP was used to estimate total sediment load at the NREB using field data of 1995. Main screen figures, and input and output files used to estimate total sediment load at the NREB are presented in this section (Figures B-1 to B-5).

Figure B-1. BORAMEP Program Main Screen

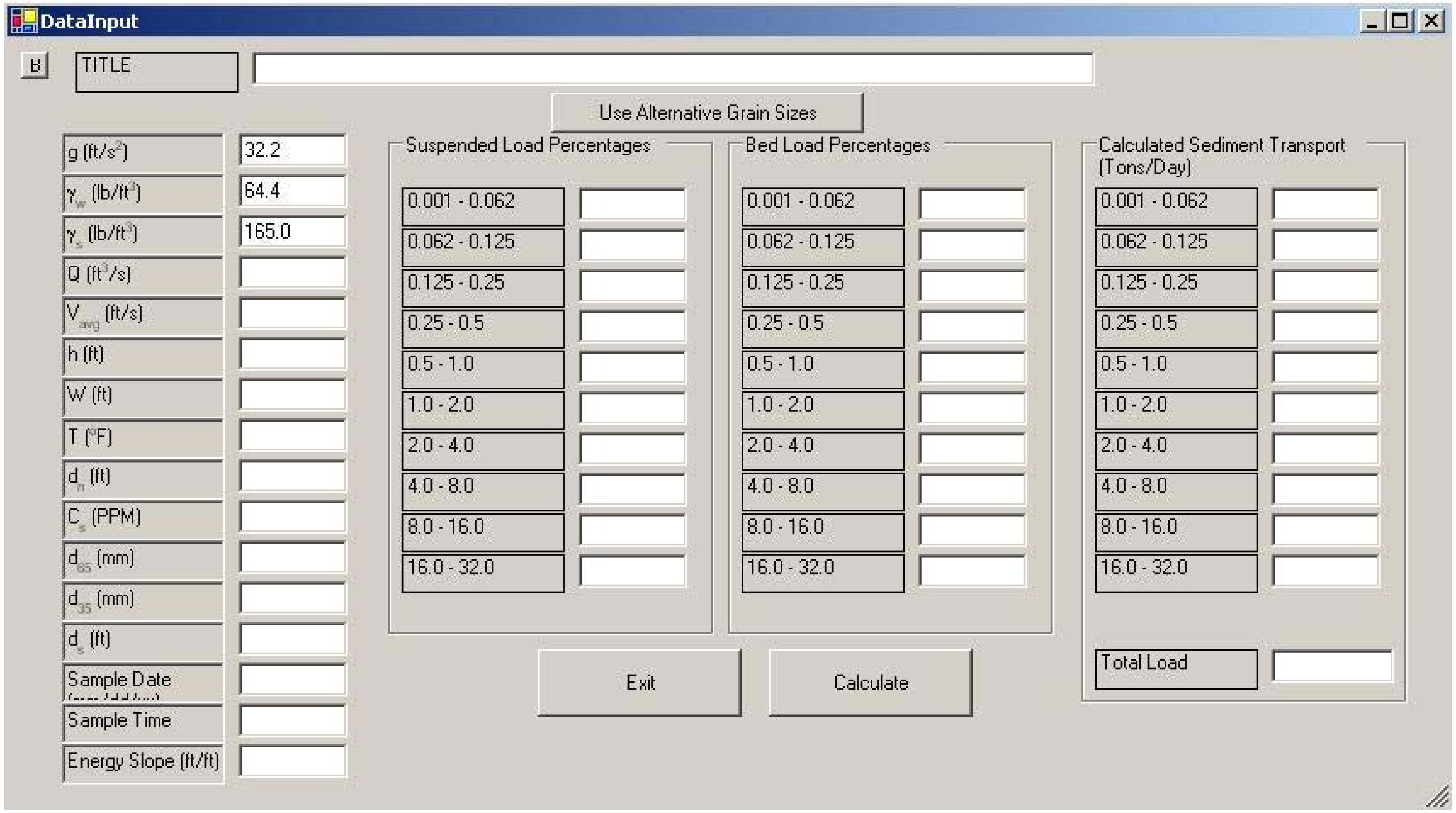

Figure B-2. Data Input Sheet for BORAMEP

Microsoft Excel - NREB_1995.csv

	A	B	C	D	E	F	G	H	I	J	K	L	M	N	O	P	Q
1	***	bin1		bin2		bin3		bin4		bin5		bin6		bin7		bin8	
2	16	0.0002	0.004	0.004	0.008	0.008	0.016	0.016	0.031	0.031	0.062	0.062	0.125	0.125	0.25	0.25	0.5
3	Input Varia	Title	Date	Time	S_energy	g (ft/s2)	gamma_w	gamma_s	Q (cfs)	Vavg (ft/s)	h (ft)	W (ft)	T (F)	dn (ft)	Cs (ppm)	d65 (mm)	d35 (mm)
4	###	Case 1	8/28/1995	1000	0.000246	32.2	62.4	165	23653.77	6.82	22.08	155.84	75	0.3	848	0.18	0.09
5	###	Case 2	8/30/1995	1000	0.000265	32.2	62.4	165	25161.7	7.15	22.51	155.84	75	0.3	288	0.18	0.09
6	###	Case 3	9/3/1995	1000	0.000645	32.2	62.4	165	37822.01	10.83	21.16	155.84	75	0.3	675	0.18	0.09
7	###	Case 4	9/4/1995	1000	0.00057	32.2	62.4	165	33548.94	10.17	21.16	155.84	75	0.3	1185	0.18	0.09

	R	S	T	U	V	W	X	Y	Z	AA	AB	AC	AD	AE	AF	AG	AH
1	bin9		bin10		bin11		bin12		bin13		bin14		bin15		bin16		
2	0.5	1	1	2	2	4	4	8	8	16	16	32	32	64	64	125	
3	ds (ft)	susbin1	susbin2	susbin3	susbin4	susbin5	susbin6	susbin7	susbin8	susbin9	susbin10	susbin11	susbin12	susbin13	susbin14	susbin15	susbin16
4	21.78	29.8	6.2	34	5	4	13.4	2.6	3	2	0	0	0	0	0	0	0
5	22.21	37	12.8	11.2	7	6.8	9.6	3.6	10	2	0	0	0	0	0	0	0
6	20.86	37.8	18.2	9.4	14.6	3	9	6	0.8	1.2	0	0	0	0	0	0	0
7	20.86	36.2	13.8	9.6	13	7.6	10	3.8	4	2	0	0	0	0	0	0	0

	AI	AJ	AK	AL	AM	AN	AO	AP	AQ	AR	AS	AT	AU	AV	AW	AX	AY
1																	
2																	
3	bedbin1	bedbin2	bedbin3	bedbin4	bedbin5	bedbin6	bedbin7	bedbin8	bedbin9	bedbin10	bedbin11	bedbin12	bedbin13	bedbin14	bedbin15	bedbin16	
4	0	4	4	7	9	24	32	16	3.5	0.5	0	0	0	0	0	0	
5	0	4	4	7	9	24	32	16	3.5	0.5	0	0	0	0	0	0	
6	0	4	4	7	9	24	32	16	3.5	0.5	0	0	0	0	0	0	
7	0	4	4	7	9	24	32	16	3.5	0.5	0	0	0	0	0	0	

Figure B-3. Input data summary file of BORAMEP for the NREB

NREB_1995.txt - Notepad

File Edit Format View Help

OUTPUT
Case 1

METHOD OF COMPUTATION MODIFIED EINSTEIN DATE OF COMPUTATION 7/12/2006
DATE OF SAMPLE 8/28/1995 TIME OF SAMPLE 1000 TEMPERATURE 75 SLOPE OF ENERGY GRADIENT 0.000246
D65 = 0.18 mm D35 = 0.09 mm
Velocity (ft/s) = 6.82 Width (ft) = 155.84 Depth (ft) = 22.08
Dn (ft) = 0.3 Ds (ft) = 21.78

SIZE FRACTION IN MILLIMETERS		PERCENT OF MATERIAL SUSPENDED	BED	IBQB T/D	QPRIME SUBS(T/D)	Z-VALUES COMPUTED	FITTED	COMPUTATIONAL FACTORS F(J)	F(I)+1	COMPUTED TOTAL LOAD
0.0002	0.004	29.8	0	-9999	16106.36	-9999	0.296	1.042	-9999	16787.15
0.004	0.008	6.2	4	0.260	3350.987	-9999	0.447	1.086	5858.71	3640.472
0.008	0.016	34	4	0.735	18376.38	-9999	0.523	1.122	1732.824	20618.11
0.016	0.031	5	7	3.550	2702.409	-9999	0.608	1.180	529.378	3187.49
0.031	0.062	4	9	12.607	2161.927	-9999	0.708	1.278	167.440	2763.899
0.062	0.125	13.4	24	95.664	7242.456	0.746	0.823	1.457	56.890	10554.25
0.125	0.25	2.6	32	362.952	1405.253	1.104	0.935	1.722	25.098	2420.242
0.25	0.5	3	16	323.110	1621.445	1.076	1.018	1.966	15.717	3187.608
0.5	1	2	3.5	94.842	1080.964	0.953	1.077	2.109	12.069	1144.658
1	2	0	0.5	15.847	0	-9999	1.127	-9999	10.078	159.708
2	4	0	0	-9999	0	-9999	1.175	-9999	-9999	0
4	8	0	0	-9999	0	-9999	1.222	-9999	-9999	0
8	16	0	0	-9999	0	-9999	1.271	-9999	-9999	0
16	32	0	0	-9999	0	-9999	1.322	-9999	-9999	0
32	64	0	0	-9999	0	-9999	1.374	-9999	-9999	0
64	125	0	0	-9999	0	-9999	1.428	-9999	-9999	0
TOTAL										64463.581

OUTPUT
Case 2

METHOD OF COMPUTATION MODIFIED EINSTEIN DATE OF COMPUTATION 7/12/2006
DATE OF SAMPLE 8/30/1995 TIME OF SAMPLE 1000 TEMPERATURE 75 SLOPE OF ENERGY GRADIENT 0.000265
D65 = 0.18 mm D35 = 0.09 mm
Velocity (ft/s) = 7.15 Width (ft) = 155.84 Depth (ft) = 22.51
Dn (ft) = 0.3 Ds (ft) = 22.21

SIZE FRACTION IN MILLIMETERS		PERCENT OF MATERIAL SUSPENDED	BED	IBQB T/D	QPRIME SUBS(T/D)	Z-VALUES COMPUTED	FITTED	COMPUTATIONAL FACTORS F(J)	F(I)+1	COMPUTED TOTAL LOAD
0.0002	0.004	37	0	-9999	7226.007	-9999	0.486	1.102	-9999	7962.569
0.004	0.008	12.8	4	0.285	2499.808	-9999	0.643	1.207	623.459	3018.335
0.008	0.016	11.2	4	0.806	2187.332	-9999	0.714	1.285	236.013	2810.233
0.016	0.031	7	7	3.896	1367.082	-9999	0.791	1.400	96.803	1913.838
0.031	0.062	6.8	9	13.835	1328.023	-9999	0.876	1.578	43.184	2096.068
0.062	0.125	9.6	24	104.978	1874.856	0.913	0.970	1.858	21.474	3484.405
0.125	0.25	3.6	32	398.287	703.071	1.210	1.057	2.205	13.206	1549.974
0.25	0.5	10	16	355.193	1952.975	1.064	1.119	2.452	10.239	4789.52
0.5	1	2	3.5	105.144	390.595	1.135	1.163	2.531	8.959	941.969
1	2	0	0.5	18.079	0	-9999	1.199	-9999	8.180	147.894
2	4	0	0	-9999	0	-9999	1.232	-9999	-9999	0
4	8	0	0	-9999	0	-9999	1.266	-9999	-9999	0
8	16	0	0	-9999	0	-9999	1.300	-9999	-9999	0
16	32	0	0	-9999	0	-9999	1.334	-9999	-9999	0
32	64	0	0	-9999	0	-9999	1.370	-9999	-9999	0
64	125	0	0	-9999	0	-9999	1.406	-9999	-9999	0
TOTAL										28714.804

Figure B-4. Output file of BORAMEP for the NREB (Case 1 and 2)

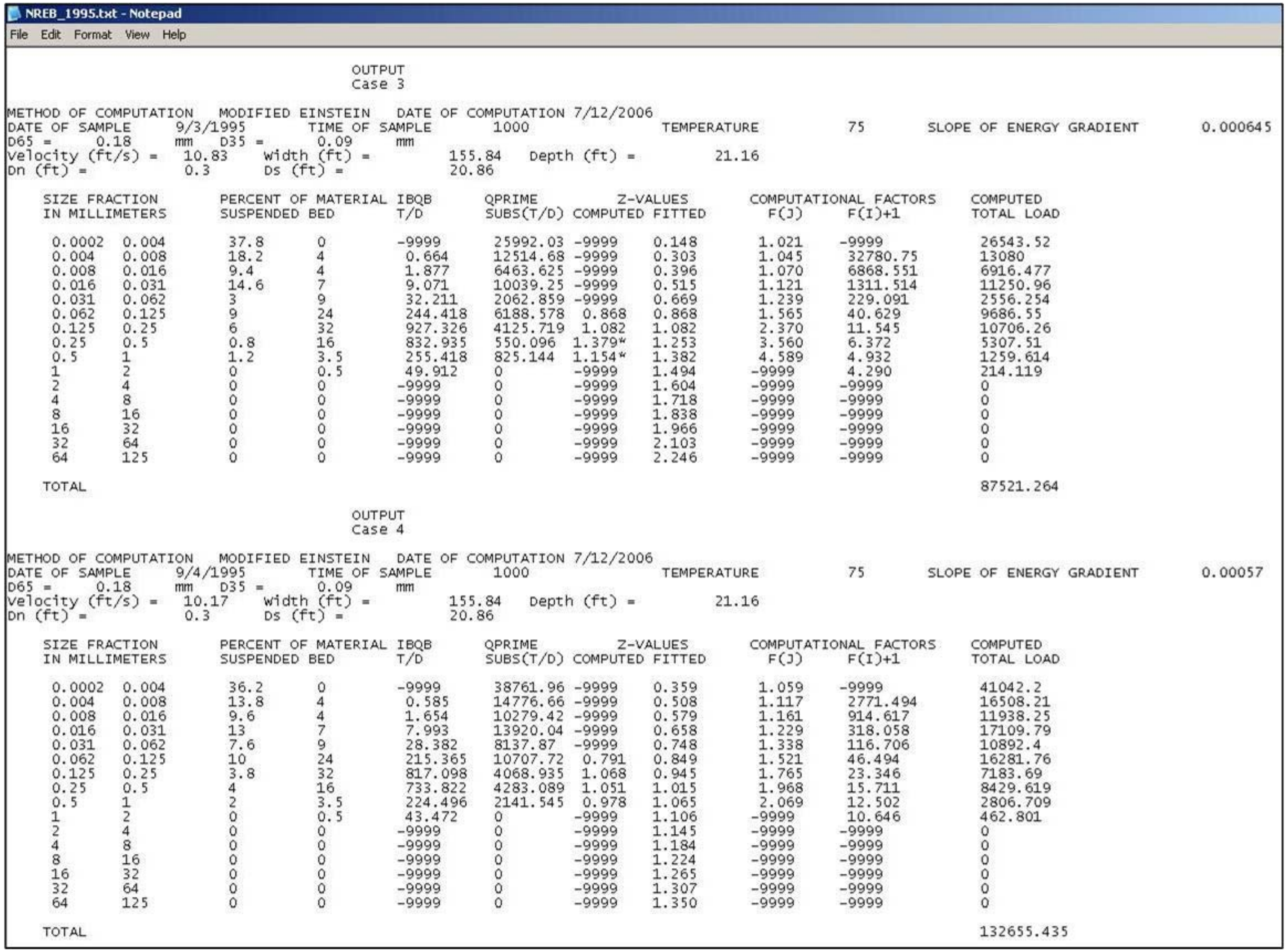
NREB_1995.txt - Notepad
File Edit Format View Help

```
                                          OUTPUT
                                          Case 3

METHOD OF COMPUTATION   MODIFIED EINSTEIN   DATE OF COMPUTATION 7/12/2006
DATE OF SAMPLE      9/3/1995       TIME OF SAMPLE      1000             TEMPERATURE          75      SLOPE OF ENERGY GRADIENT       0.000645
D65 =     0.18      mm   D35 =       0.09     mm
Velocity (ft/s) =   10.83     Width (ft) =         155.84   Depth (ft) =         21.16
Dn (ft) =           0.3       Ds (ft) =            20.86

    SIZE FRACTION        PERCENT OF MATERIAL IBQB      QPRIME       Z-VALUES       COMPUTATIONAL FACTORS    COMPUTED
    IN MILLIMETERS       SUSPENDED BED       T/D       SUBS(T/D) COMPUTED FITTED      F(J)      F(I)+1      TOTAL LOAD

     0.0002  0.004        37.8      0        -9999      25992.03 -9999    0.148       1.021     -9999        26543.52
     0.004   0.008        18.2      4         0.664     12514.68 -9999    0.303       1.045      32780.75    13080
     0.008   0.016        9.4       4         1.877     6463.625 -9999    0.396       1.070      6868.551    6916.477
     0.016   0.031        14.6      7         9.071     10039.25 -9999    0.515       1.121      1311.514    11250.96
     0.031   0.062        3         9         32.211    2062.859 -9999    0.669       1.239      229.091     2556.254
     0.062   0.125        9         24        244.418   6188.578  0.868   0.868       1.565      40.629      9686.55
     0.125   0.25         6         32        927.326   4125.719  1.082   1.082       2.370      11.545      10706.26
     0.25    0.5          0.8       16        832.935   550.096  1.379*   1.253       3.560      6.372       5307.51
     0.5     1            1.2       3.5       255.418   825.144  1.154*   1.382       4.589      4.932       1259.614
     1       2            0         0.5       49.912    0        -9999    1.494      -9999       4.290       214.119
     2       4            0         0        -9999      0        -9999    1.604      -9999      -9999        0
     4       8            0         0        -9999      0        -9999    1.718      -9999      -9999        0
     8       16           0         0        -9999      0        -9999    1.838      -9999      -9999        0
     16      32           0         0        -9999      0        -9999    1.966      -9999      -9999        0
     32      64           0         0        -9999      0        -9999    2.103      -9999      -9999        0
     64      125          0         0        -9999      0        -9999    2.246      -9999      -9999        0

    TOTAL                                                                                                  87521.264

                                          OUTPUT
                                          Case 4

METHOD OF COMPUTATION   MODIFIED EINSTEIN   DATE OF COMPUTATION 7/12/2006
DATE OF SAMPLE      9/4/1995       TIME OF SAMPLE      1000             TEMPERATURE          75      SLOPE OF ENERGY GRADIENT       0.00057
D65 =     0.18      mm   D35 =       0.09     mm
Velocity (ft/s) =   10.17     Width (ft) =         155.84   Depth (ft) =         21.16
Dn (ft) =           0.3       Ds (ft) =            20.86

    SIZE FRACTION        PERCENT OF MATERIAL IBQB      QPRIME       Z-VALUES       COMPUTATIONAL FACTORS    COMPUTED
    IN MILLIMETERS       SUSPENDED BED       T/D       SUBS(T/D) COMPUTED FITTED      F(J)      F(I)+1      TOTAL LOAD

     0.0002  0.004        36.2      0        -9999      38761.96 -9999    0.359       1.059     -9999        41042.2
     0.004   0.008        13.8      4         0.585     14776.66 -9999    0.508       1.117      2771.494    16508.21
     0.008   0.016        9.6       4         1.654     10279.42 -9999    0.579       1.161      914.617     11938.25
     0.016   0.031        13        7         7.993     13920.04 -9999    0.658       1.229      318.058     17109.79
     0.031   0.062        7.6       9         28.382    8137.87  -9999    0.748       1.338      116.706     10892.4
     0.062   0.125        10        24        215.365   10707.72  0.791   0.849       1.521      46.494      16281.76
     0.125   0.25         3.8       32        817.098   4068.935  1.068   0.945       1.765      23.346      7183.69
     0.25    0.5          4         16        733.822   4283.089  1.051   1.015       1.968      15.711      8429.619
     0.5     1            2         3.5       224.496   2141.545  0.978   1.065       2.069      12.502      2806.709
     1       2            0         0.5       43.472    0        -9999    1.106      -9999       10.646      462.801
     2       4            0         0        -9999      0        -9999    1.145      -9999      -9999        0
     4       8            0         0        -9999      0        -9999    1.184      -9999      -9999        0
     8       16           0         0        -9999      0        -9999    1.224      -9999      -9999        0
     16      32           0         0        -9999      0        -9999    1.265      -9999      -9999        0
     32      64           0         0        -9999      0        -9999    1.307      -9999      -9999        0
     64      125          0         0        -9999      0        -9999    1.350      -9999      -9999        0

    TOTAL                                                                                                  132655.435
```

Figure B-5. Output file of BORAMEP for the NREB (Case 3 and 4)

APPENDIX C: AT-A-STATION HYDRAULIC GEOMETRY RELATIONSHIP OF THE LOWER NAKDONG RIVER

The at-a-station hydraulic geometry relationship used to examine each term of the St. Venant equation was developed for the Nakdong River. At a given discharge, the hydraulic geometry and velocity were calculated using the cross section geometry of Jindong Station (Figure C-1 and Table C-1).

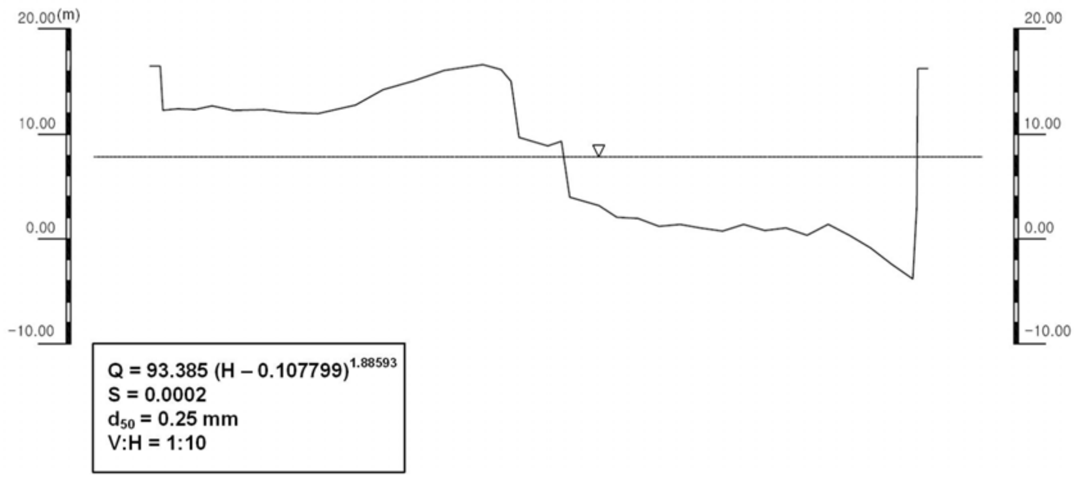

Figure C-1. Cross section of Jindong Station (Nakdong River)

Table C-1. Cross section coordinates of Jindong Station (Nakdong River)

X (m)	Y (m)	X (m)	Y (m)	X (m)	Y (m)
0	16.467	220.745	14.225	521.907	0.989
10	16.467	250.298	15.069	541.907	0.705
12.502	12.277	278.654	16.055	561.907	1.346
19.664	12.3496	315.214	16.598	581.907	0.759
26.825	12.415	332.546	16.122	601.907	1.004
34.835	12.3755	341.907	15.023	621.907	0.304
42.845	12.336	349.439	9.707	641.907	1.352
50.926	12.5155	376.607	8.897	661.907	0.305
59.006	12.695	389.507	9.338	681.907	-0.885
68.996	12.48	397.369	3.928	701.907	-2.432
78.985	12.265	425.086	3.128	721.907	-3.834
108.265	12.335	441.907	2.016	725.679	3.128
130.654	12.055	461.907	1.914	726.139	9.68
159.235	11.963	481.907	1.164	726.599	16.232
194.798	12.774	501.907	1.344	736.599	16.232

Figure C-2 presents the stage-discharge relationship and the regression equation is

$$Q = 70.1H^{2.09}$$

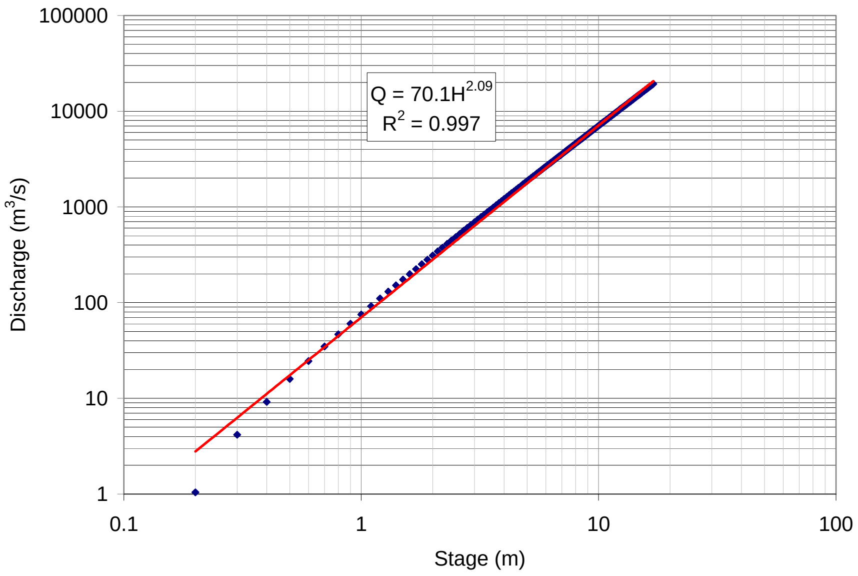

Figure C-2. At-a-station stage-discharge regression of the Nakdong River

Figure C-3 presents the width-discharge relationship and the regression equation is

$$T_w = 55.2H^{0.236}$$

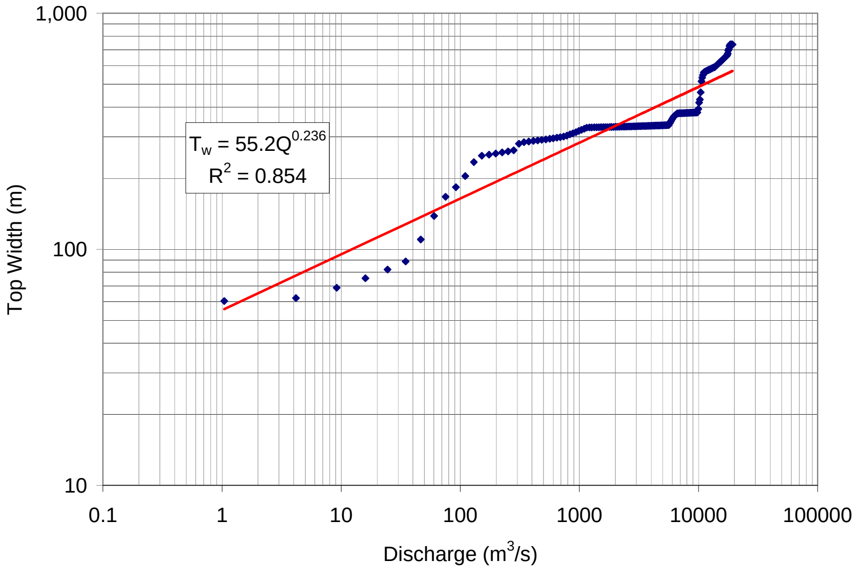

Figure C-3. At-a-station width-discharge regression of the Nakdong River

Figure C-4 presents the depth-discharge relationship and the regression equation is

$$h = 0.392Q^{0.324}$$

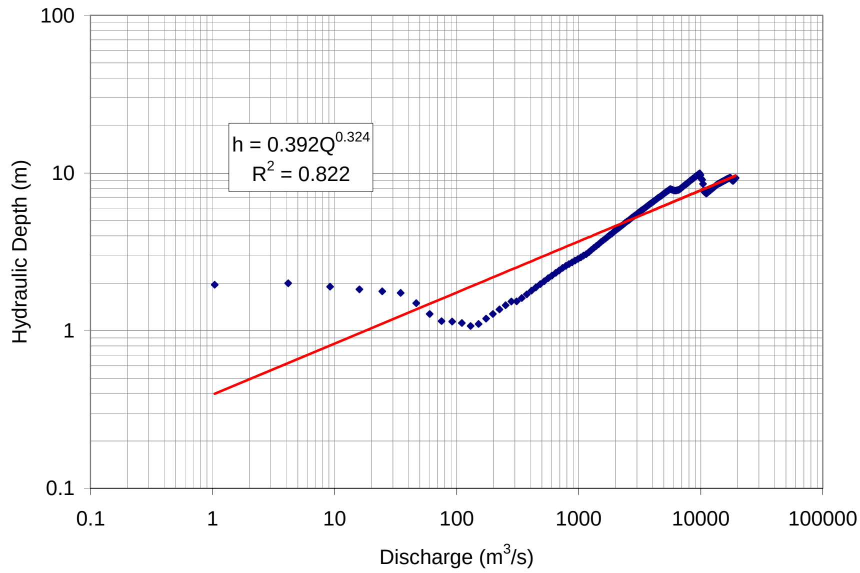

Figure C-4. At-a-station hydraulic depth-discharge regression of the Nakdong River

Figure C-5 presents the area-discharge relationship and the regression equation is

$$A = 10.3Q^{0.648}$$

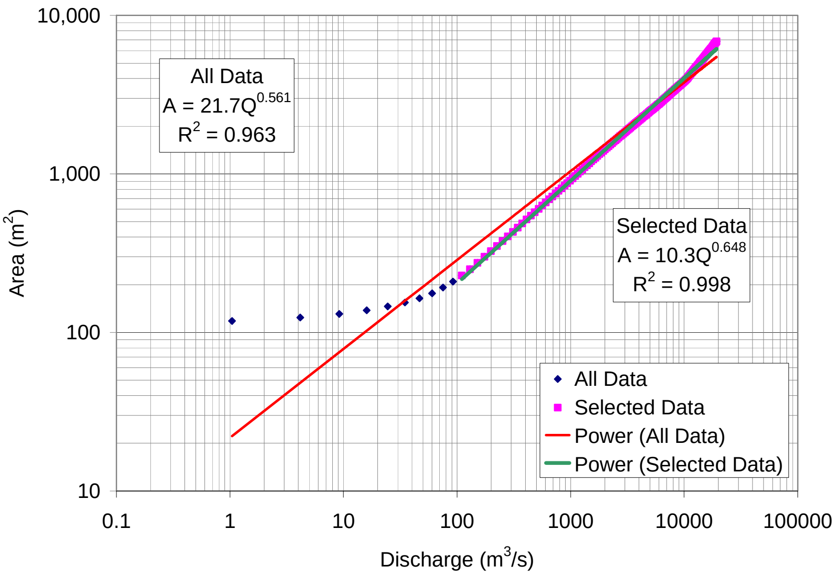

Figure C-5. At-a-station area-discharge regression of the Nakdong River

Figure C-6 presents the velocity-discharge relationship and the regression equation is

$$V = 0.0461Q^{0.439}$$

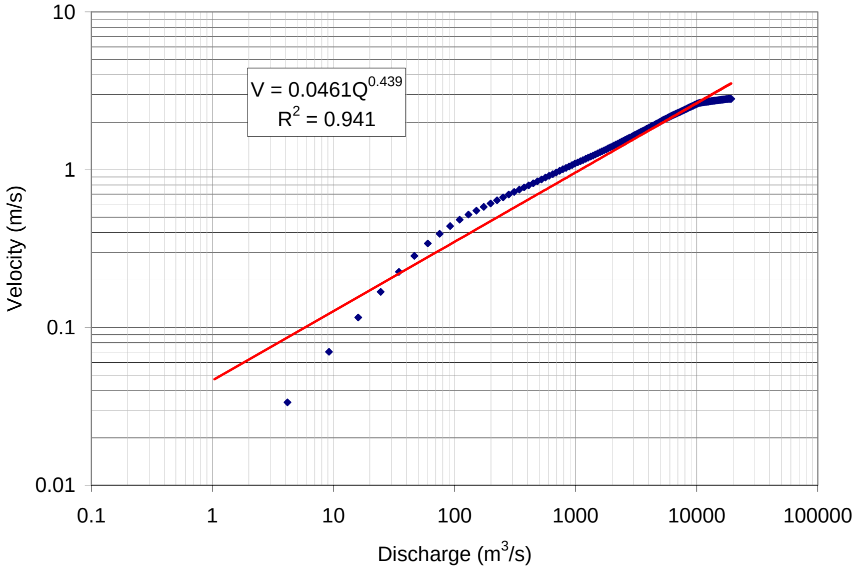

Figure C-6. At-a-station velocity-discharge regression of the Nakdong River

APPENDIX D: NUMERICAL MODEL PROGRAM

The numerical model program and the program codes are presented in this section.

Input data spread sheet

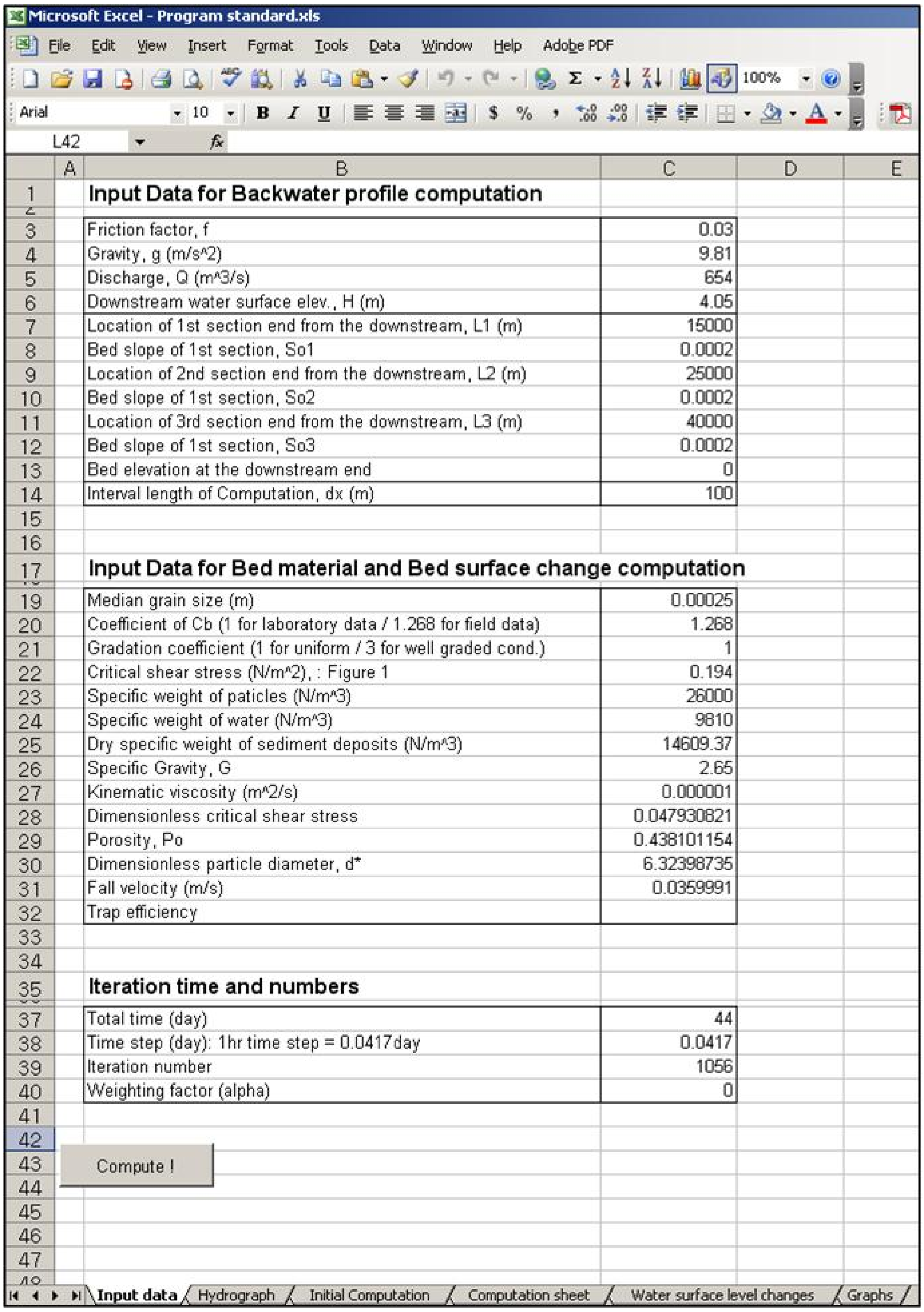

Row	B	C
1	**Input Data for Backwater profile computation**	
3	Friction factor, f	0.03
4	Gravity, g (m/s^2)	9.81
5	Discharge, Q (m^3/s)	654
6	Downstream water surface elev., H (m)	4.05
7	Location of 1st section end from the downstream, L1 (m)	15000
8	Bed slope of 1st section, So1	0.0002
9	Location of 2nd section end from the downstream, L2 (m)	25000
10	Bed slope of 1st section, So2	0.0002
11	Location of 3rd section end from the downstream, L3 (m)	40000
12	Bed slope of 1st section, So3	0.0002
13	Bed elevation at the downstream end	0
14	Interval length of Computation, dx (m)	100
17	**Input Data for Bed material and Bed surface change computation**	
19	Median grain size (m)	0.00025
20	Coefficient of Cb (1 for laboratory data / 1.268 for field data)	1.268
21	Gradation coefficient (1 for uniform / 3 for well graded cond.)	1
22	Critical shear stress (N/m^2), : Figure 1	0.194
23	Specific weight of paticles (N/m^3)	26000
24	Specific weight of water (N/m^3)	9810
25	Dry specific weight of sediment deposits (N/m^3)	14609.37
26	Specific Gravity, G	2.65
27	Kinematic viscosity (m^2/s)	0.000001
28	Dimensionless critical shear stress	0.047930821
29	Porosity, Po	0.438101154
30	Dimensionless particle diameter, d*	6.32398735
31	Fall velocity (m/s)	0.0359991
32	Trap efficiency	
35	**Iteration time and numbers**	
37	Total time (day)	44
38	Time step (day): 1hr time step = 0.0417day	0.0417
39	Iteration number	1056
40	Weighting factor (alpha)	0

Hydrograph and Downstream water level spread sheet

Hydrograph and Downstream water level

Time	NREB Upstream water level	NREB Downstream tide level	Differences	Gate operation	New upstream water level with gate operation	Upstream water level	Discharge (Samryangjin)
YYYY-MM-DD-HH	m	m	m	m	m	m (SMSL+H)	cms
2003-04-27-00	0	-0.32	0.32	-	-0.12	3.88	100
2003-04-27-01	0.02	-0.27	0.29	-	-0.07	3.93	100
2003-04-27-02	0.11	-0.18	0.29	-	0.02	4.02	100
2003-04-27-03	0.25	-0.06	0.31	-	0.14	4.14	100
2003-04-27-04	0.42	0.09	0.33	-	0.29	4.29	100
2003-04-27-05	0.59	0.22	0.37	-	0.42	4.42	100
2003-04-27-06	0.71	0.29	0.42	-	0.49	4.49	100
2003-04-27-07	0.72	0.27	0.45	-	0.47	4.47	100
2003-04-27-08	0.67	0.19	0.48	-	0.39	4.39	100
2003-04-27-09	0.52	0.04	0.48	-	0.24	4.24	100
2003-04-27-10	0.29	-0.16	0.45	-	0.04	4.04	100
2003-04-27-11	0.11	-0.33	0.44	-	-0.13	3.87	199
2003-04-27-12	-0.01	-0.45	0.44	-	-0.25	3.75	297
2003-04-27-13	-0.08	-0.47	0.39	-	-0.27	3.73	413
2003-04-27-14	-0.03	-0.38	0.35	-	-0.18	3.82	525
2003-04-27-15	0.16	-0.23	0.39	-	-0.03	3.97	760
2003-04-27-16	0.28	-0.04	0.32	-	0.16	4.16	843
2003-04-27-17	0.5	0.13	0.37	-	0.33	4.33	1,066
2003-04-27-18	0.67	0.24	0.43	-	0.44	4.44	1,199
2003-04-27-19	0.73	0.27	0.46	-	0.47	4.47	1,311
2003-04-27-20	0.68	0.21	0.47	-	0.41	4.41	1,418
2003-04-27-21	0.52	0.05	0.47	-	0.25	4.25	1,470
2003-04-27-22	0.33	-0.13	0.46	-	0.07	4.07	1,541
2003-04-27-23	0.13	-0.33	0.46	-	-0.13	3.87	1,613
2003-04-28-00	-0.03	-0.45	0.42	-	-0.25	3.75	1,659
2003-04-28-01	-0.08	-0.46	0.38	-	-0.26	3.74	1,724
2003-04-28-02	-0.03	-0.38	0.35	-	-0.18	3.82	1,799
2003-04-28-03	0.09	-0.24	0.33	-	-0.04	3.96	1,934
2003-04-28-04	0.27	-0.06	0.33	-	0.14	4.14	2,044
2003-04-28-05	0.45	0.09	0.36	-	0.29	4.29	2,125
2003-04-28-06	0.6	0.2	0.4	-	0.4	4.4	2,197
2003-04-28-07	0.69	0.25	0.44	-	0.45	4.45	2,291
2003-04-28-08	0.69	0.2	0.49	-	0.4	4.4	2,354
2003-04-28-09	0.56	0.08	0.48	-	0.28	4.28	2,419
2003-04-28-10	0.36	-0.13	0.49	-	0.07	4.07	2,462
2003-04-28-11	0.13	-0.35	0.48	-	-0.15	3.85	2,462
2003-04-28-12	-0.06	-0.52	0.46	-	-0.32	3.68	2,451
2003-04-28-13	-0.16	-0.61	0.45	-	-0.41	3.59	2,419

Initial computation spread sheet

Microsoft Excel - Program standard.xls

M38 =′Input data′!C$3/8*(′Initial Computation′!J38^2/(9.81*′Initial Computation′!G38))

Initial computation

XS Distance (m)	Bed slope So	Bed elev. z (m)	Channel Width W (m)	Unit Discharge q (m^2/s)	dh (m)	Water depth h (m)	Normal depth hn (m)	Critical depth hc (m)	Mean Velocity V (m/s)
0	0.000246151	0.221582	220	2.972727		3.828418	2.394180703	0.965784822	0.776489777
100	0.000246151	0.246127	220	2.972727	0.018898	3.809520	2.394180703	0.965784822	0.780341784
200	0.000247371	0.270812	220	2.972727	0.018905	3.790615	2.390237896	0.965784822	0.784233507
300	0.000248453	0.295602	220	2.972727	0.018929	3.771686	2.38676325	0.965784822	0.788169366
400	0.000249585	0.320503	220	2.972727	0.018952	3.752734	2.383148311	0.965784822	0.792149771
500	0.000250743	0.345519	220	2.972727	0.018976	3.733758	2.379476627	0.965784822	0.796175737
600	0.000251928	0.370652	220	2.972727	0.019001	3.714757	2.37573801	0.965784822	0.800248208
700	0.000253142	0.395904	220	2.972727	0.019027	3.695730	2.371934989	0.965784822	0.804368157
800	0.000254384	0.421280	220	2.972727	0.019053	3.676676	2.368069054	0.965784822	0.808536564
900	0.000255653	0.446781	220	2.972727	0.019080	3.657596	2.364142444	0.965784822	0.81275442
1000	0.00025695	0.472411	220	2.972727	0.019108	3.638488	2.360158052	0.965784822	0.817022715
1100	0.000258274	0.498171	220	2.972727	0.019136	3.619352	2.356119555	0.965784822	0.821342433
1200	0.000259623	0.524065	220	2.972727	0.019164	3.600188	2.352031545	0.965784822	0.825714547
1300	0.000260996	0.550096	220	2.972727	0.019193	3.580995	2.347899674	0.965784822	0.830140002
1400	0.000262391	0.576265	220	2.972727	0.019221	3.561775	2.343730814	0.965784822	0.834619711
1500	0.000263806	0.602574	220	2.972727	0.019248	3.542527	2.339533243	0.965784822	0.839154532
1600	0.000265238	0.629026	220	2.972727	0.019274	3.523252	2.335316847	0.965784822	0.843745254
1700	0.000266682	0.655621	220	2.972727	0.019300	3.503952	2.331093329	0.965784822	0.848392577
1800	0.000268134	0.682362	220	2.972727	0.019323	3.484630	2.326876452	0.965784822	0.853097082
1900	0.00026959	0.709248	220	2.972727	0.019344	3.465286	2.322682278	0.965784822	0.857859206
2000	0.000271041	0.736280	220	2.972727	0.019361	3.445924	2.318529419	0.965784822	0.862679206
2100	0.00027248	0.763456	220	2.972727	0.019375	3.426549	2.314439294	0.965784822	0.867557119
2200	0.000273899	0.790776	220	2.972727	0.019384	3.407166	2.310436366	0.965784822	0.872492719
2300	0.000275286	0.818236	220	2.972727	0.019386	3.387779	2.306548367	0.965784822	0.877485467
2400	0.000276631	0.845833	220	2.972727	0.019382	3.368398	2.302806479	0.965784822	0.882534457
2500	0.000277918	0.873562	220	2.972727	0.019368	3.349030	2.299245471	0.965784822	0.887638351
2600	0.000279133	0.901417	220	2.972727	0.019345	3.329685	2.295903762	0.965784822	0.89279532
2700	0.00028026	0.929389	220	2.972727	0.019309	3.310376	2.292823393	0.965784822	0.898002975
2800	0.000281279	0.957469	220	2.972727	0.019260	3.291115	2.290049891	0.965784822	0.903258295
2900	0.000282172	0.985645	220	2.972727	0.019196	3.271920	2.287631998	0.965784822	0.908557562
3000	0.000282917	1.013903	220	2.972727	0.019114	3.252806	2.285621263	0.965784822	0.913896294
3100	0.000283494	1.042228	220	2.972727	0.019012	3.233794	2.284071459	0.965784822	0.919269185
3200	0.000283879	1.070602	220	2.972727	0.018888	3.214906	2.283037845	0.965784822	0.924670057
3300	0.000284051	1.099004	220	2.972727	0.018741	3.196165	2.282576252	0.965784822	0.930091827
3400	0.000283989	1.127412	220	2.972727	0.018567	3.177598	2.28274201	0.965784822	0.935526486
3500	0.000283673	1.155802	220	2.972727	0.018366	3.159232	2.283588729	0.965784822	0.940965108
3600	0.000283086	1.184147	220	2.972727	0.018135	3.141097	2.285166968	0.965784822	0.946397883
3700	0.000282212	1.212419	220	2.972727	0.017874	3.123222	2.28752282	0.965784822	0.951814173
3800	0.000281041	1.240589	220	2.972727	0.017582	3.105641	2.29069647	0.965784822	0.957202607
3900	0.000279565	1.268627	220	2.972727	0.017257	3.088384	2.294720767	0.965784822	0.9625512
4000	0.000277782	1.296502	220	2.972727	0.016900	3.071483	2.299619876	0.965784822	0.967847504
4100	0.000275695	1.324184	220	2.972727	0.016512	3.054971	2.305408068	0.965784822	0.973078787
4200	0.000273312	1.351641	220	2.972727	0.016094	3.038877	2.312088701	0.965784822	0.978232228
4300	0.000270647	1.378846	220	2.972727	0.015647	3.023230	2.319653458	0.965784822	0.983295134
4400	0.000267718	1.405771	220	2.972727	0.015173	3.008056	2.328081874	0.965784822	0.988255153

Input data | Hydrograph | Initial Computation | Computation sheet | Water surface level changes | Graphs

Initial computation spread sheet (continued)

	K	L	M	N	O	P	Q	R	S	T
3	H.G.L	E.G.L	Friction Slope	Shear stress	Total head	Vc	Sed. Concentration	Sed. Concentration	Sed. Load	Sed. Discharge
4	(m)	(m)	Sf		H (m)	(m/s)	Cppm	Cmgl	metric tons/day	m^3/day
5	4.050000	4.080730702	6.02025E-05	2.2587066	3.859148487	0.229580999	43.26170952	43.26287487	2444.594702	922.4885669
6	4.055647	4.086683297	6.11029E-05	2.281172145	3.840555896	0.229102637	44.44715471	44.44838481	2511.582652	947.7670387
7	4.061427	4.092774085	6.20217E-05	2.303982224	3.821961668	0.228622739	45.66898812	45.67028678	2580.626956	973.821493
8	4.067288	4.098949641	6.29602E-05	2.327166399	3.803348014	0.22814083	46.92971297	46.93108431	2651.869078	1000.705312
9	4.073237	4.10521963	6.39189E-05	2.350731021	3.784716599	0.227656932	48.23065661	48.23210504	2725.384034	1028.446805
10	4.079276	4.111585042	6.48984E-05	2.374686117	3.766066335	0.227171	49.57339518	49.57492538	2801.260903	1057.079586
11	4.085408	4.118048114	6.58994E-05	2.399041478	3.74739657	0.226682995	50.95954636	50.96116333	2879.591111	1086.638155
12	4.091634	4.124610997	6.69224E-05	2.423807219	3.728706653	0.22619288	52.39080265	52.39251173	2960.470311	1117.158608
13	4.097956	4.131275928	6.79683E-05	2.448993686	3.709996003	0.225700618	53.86892901	53.87073589	3043.998254	1148.678586
14	4.104377	4.138045216	6.90375E-05	2.474611441	3.691264129	0.225206175	55.3957652	55.39767596	3130.278919	1181.237328
15	4.110899	4.144921245	7.01309E-05	2.500671233	3.67251065	0.224709519	56.97322697	56.97524811	3219.42058	1214.87569
16	4.117523	4.151906475	7.12492E-05	2.527183964	3.653735326	0.224210621	58.60330677	58.60544521	3311.535845	1249.636168
17	4.124253	4.159003448	7.23931E-05	2.554160636	3.634938086	0.223709455	60.28807352	60.29033669	3406.741649	1285.562886
18	4.131091	4.166214792	7.35633E-05	2.58161229	3.616119067	0.223206001	62.02967152	62.03206734	3505.159184	1322.701579
19	4.138039	4.173543219	7.47607E-05	2.609549926	3.597278663	0.222700246	63.83031786	63.8328548	3606.91376	1361.099532
20	4.145101	4.180991529	7.59859E-05	2.63798441	3.578417571	0.222192184	65.6922983	65.69498541	3712.134567	1400.805497
21	4.152278	4.188562615	7.72398E-05	2.66692635	3.559536852	0.221681819	67.61796106	67.62080802	3820.954329	1441.869558
22	4.159574	4.196259463	7.85232E-05	2.696385954	3.540638001	0.221169166	69.60970816	69.6127253	3933.508811	1484.342948
23	4.166992	4.204085151	7.98367E-05	2.726372856	3.521723024	0.220654256	71.66998369	71.67318208	4049.936158	1528.277795
24	4.174534	4.212042854	8.11812E-05	2.756895907	3.502794526	0.220137133	73.80125856	73.80465001	4170.376032	1573.726804
25	4.182204	4.220135836	8.25572E-05	2.787962935	3.483855808	0.219617865	76.00601096	76.00960808	4294.96851	1620.742834
26	4.190006	4.228367454	8.39656E-05	2.819580454	3.46491098	0.219096539	78.28670189	78.29051812	4423.852701	1669.378378
27	4.197942	4.23674115	8.54068E-05	2.851753338	3.445965074	0.218573272	80.64574502	80.64979472	4557.165041	1719.684921
28	4.206016	4.245260444	8.68814E-05	2.884484443	3.427024181	0.21804821	83.08547019	83.08976863	4695.03723	1771.712162
29	4.214231	4.253928927	8.83898E-05	2.917774181	3.408095579	0.217521534	85.60807975	85.61264317	4837.59377	1825.507083
30	4.222592	4.262750243	8.99322E-05	2.951620048	3.389187879	0.216993467	88.21559724	88.2204429	4984.949058	1881.112852
31	4.231102	4.271728078	9.15088E-05	2.986016106	3.370311168	0.216464274	90.90980795	90.91495412	5137.204032	1938.567559
32	4.239765	4.280866133	9.31195E-05	3.020952429	3.351477146	0.215934271	93.69219112	93.69765712	5294.442334	1997.902768
33	4.248584	4.290168099	9.47639E-05	3.056414511	3.332699258	0.215403828	96.563844	96.56965021	5456.726027	2059.141897
34	4.257564	4.299637628	9.64416E-05	3.092382671	3.313992809	0.214873373	99.52539839	99.53156622	5624.090868	2122.298441
35	4.266709	4.309278292	9.81517E-05	3.128831451	3.295375052	0.214343396	102.5769308	102.5834827	5796.54124	2187.374053
36	4.276022	4.319093541	9.98931E-05	3.165729043	3.27686525	0.213814453	105.7178683	105.7248276	5974.044816	2254.356534
37	4.285508	4.329086655	0.000101664	3.203036776	3.258484685	0.213287166	108.9468919	108.9542828	6156.527124	2323.217783
38	4.295169	4.339260692	0.000103463	3.240708678	3.240256628	0.212762224	112.2618425	112.26969	6343.866195	2393.911772
39	4.305010	4.349618433	0.000105287	3.278691166	3.222206239	0.212240381	115.659631	115.6679607	6535.887522	2466.37265
40	4.315034	4.360162321	0.000107134	3.31692289	3.204360407	0.211722454	119.1361601	119.1449982	6732.359609	2540.51306
41	4.325244	4.370894407	0.000109	3.355334763	3.186747519	0.211209315	122.6862611	122.6956338	6932.990406	2616.222795
42	4.335641	4.381816294	0.000110883	3.393850215	3.169397155	0.210701884	126.3036517	126.3135852	7137.424922	2693.367895
43	4.346230	4.392929086	0.000112777	3.432385684	3.152339718	0.210201119	129.98092	129.9914404	7345.244337	2771.790316
44	4.357011	4.404233346	0.000114678	3.470851362	3.135605998	0.209708005	133.7095402	133.7206729	7555.966852	2851.308246
45	4.367985	4.415729064	0.000116581	3.509152199	3.119226689	0.209223534	137.4799215	137.4916909	7769.050489	2931.717166
46	4.379155	4.427415635	0.000118482	3.54718914	3.103231869	0.208748697	141.2814949	141.2939242	7983.897961	3012.791683
47	4.390518	4.439291849	0.000120374	3.584860577	3.087650463	0.20828446	145.1028355	145.1159463	8199.863615	3094.288157
48	4.402076	4.451355899	0.000122253	3.622063969	3.072509705	0.207831751	148.9318207	148.9456326	8416.262337	3175.948052
49	4.413827	4.4636054	0.000124112	3.658697565	3.057834633	0.207391445	152.7558181	152.7703484	8632.380197	3257.501961

Input data | Hydrograph | Initial Computation | Computation sheet | Water surface level changes | Graphs

Initial computation spread sheet (continued)

Microsoft Excel - Program standard.xls

	U	V	W	X	Y	Z	AA	AB	AC
1									
2									
3	**Trap Efficiency**	**(1-Te) delta Qs**	**New Sed. Discharge**				**Bed elev. Changes**	**New Bed elev.**	**New Bed slpoe**
4	**Te**		**m^3/day/m**	**dAs**	**alpha * dAs**	**(1-alpha) * dAs**	**dz(i) (m)**	**(m)**	**So**
5	0.702094483	10.86915484	933.3577217			0.01901038	0.0000864108	0.2216686260	0.0002462
6	0.702094483	11.20677008	958.9738087	0.01901038	0.00000000	0.01960087	0.0000890949	0.2462164957	0.0002462
7	0.702094483	11.56408384	985.3855768	0.01960087	0.00000000	0.02022582	0.0000919356	0.2709043522	0.0002474
8	0.702094483	11.9341386	1012.639451	0.02022582	0.00000000	0.02087305	0.0000948775	0.2956965043	0.0002485
9	0.702094483	12.31865318	1040.765459	0.02087305	0.00000000	0.02154558	0.0000979344	0.3206009652	0.0002496
10	0.702094483	12.71809214	1069.797678	0.02154558	0.00000000	0.02224421	0.0001011100	0.3456198175	0.0002508
11	0.702094483	13.13312838	1099.771283	0.02224421	0.00000000	0.02297011	0.0001044096	0.3707559535	0.0002520
12	0.702094483	13.56442508	1130.723033	0.02297011	0.00000000	0.02372446	0.0001078385	0.3960121829	0.0002532
13	0.702094483	14.01266283	1162.691249	0.02372446	0.00000000	0.02450844	0.0001114020	0.4213913277	0.0002544
14	0.702094483	14.47853056	1195.715858	0.02450844	0.00000000	0.02532325	0.0001151057	0.4468961934	0.0002557
15	0.702094483	14.96271974	1229.83841	0.02532325	0.00000000	0.02617011	0.0001189550	0.4725295493	0.0002570
16	0.702094483	15.46591601	1265.102084	0.02617011	0.00000000	0.02705021	0.0001229555	0.4982941038	0.0002583
17	0.702094483	15.98878861	1301.551675	0.02705021	0.00000000	0.02796472	0.0001271124	0.5241924751	0.0002597
18	0.702094483	16.5319771	1339.233556	0.02796472	0.00000000	0.02891477	0.0001314308	0.5502271557	0.0002610
19	0.702094483	17.09607483	1378.195607	0.02891477	0.00000000	0.02990139	0.0001359154	0.5764004707	0.0002624
20	0.702094483	17.68160871	1418.487106	0.02990139	0.00000000	0.03092550	0.0001405704	0.6027145282	0.0002639
21	0.702094483	18.28901453	1460.158573	0.03092550	0.00000000	0.03198786	0.0001453994	0.6291711625	0.0002653
22	0.702094483	18.91860742	1503.261555	0.03198786	0.00000000	0.03308903	0.0001504047	0.6557718664	0.0002667
23	0.702094483	19.5705468	1547.848342	0.03308903	0.00000000	0.03422929	0.0001555877	0.6825177148	0.0002682
24	0.702094483	20.24479529	1593.9716	0.03422929	0.00000000	0.03540856	0.0001609480	0.7094092758	0.0002696
25	0.702094483	20.94107127	1641.683905	0.03540856	0.00000000	0.03662637	0.0001664835	0.7364465110	0.0002711
26	0.702094483	21.65879486	1691.037173	0.03662637	0.00000000	0.03788168	0.0001721894	0.7636286637	0.0002725
27	0.702094483	22.39702754	1742.081948	0.03788168	0.00000000	0.03917286	0.0001780585	0.7909541340	0.0002740
28	0.702094483	23.15440598	1794.866568	0.03917286	0.00000000	0.04049753	0.0001840797	0.8184203431	0.0002753
29	0.702094483	23.92907115	1849.436154	0.04049753	0.00000000	0.04185244	0.0001902384	0.8460235865	0.0002767
30	0.702094483	24.71859466	1905.831447	0.04185244	0.00000000	0.04323333	0.0001965151	0.8737588793	0.0002780
31	0.702094483	25.5199049	1964.087464	0.04323333	0.00000000	0.04463484	0.0002028856	0.9016197954	0.0002792
32	0.702094483	26.32921657	2024.231984	0.04463484	0.00000000	0.04605034	0.0002093197	0.9295983061	0.0002803
33	0.702094483	27.1419682	2086.283865	0.04605034	0.00000000	0.04747186	0.0002157812	0.9576846220	0.0002813
34	0.702094483	27.95277305	2150.251214	0.04747186	0.00000000	0.04888998	0.0002222272	0.9858670465	0.0002822
35	0.702094483	28.7553896	2216.129442	0.04888998	0.00000000	0.05029377	0.0002286080	1.0141318477	0.0002830
36	0.702094483	29.54271849	2283.899253	0.05029377	0.00000000	0.05167082	0.0002348674	1.0424631581	0.0002836
37	0.702094483	30.30683262	2353.524615	0.05167082	0.00000000	0.05300728	0.0002409422	1.0708429116	0.0002839
38	0.702094483	31.03904663	2424.950818	0.05300728	0.00000000	0.05428793	0.0002467633	1.0992508275	0.0002841
39	0.702094483	31.73003098	2498.102681	0.05428793	0.00000000	0.05549648	0.0002522567	1.1276644509	0.0002840
40	0.702094483	32.36997341	2572.883034	0.05549648	0.00000000	0.05661575	0.0002573443	1.1560592585	0.0002837
41	0.702094483	32.94878822	2649.171583	0.05661575	0.00000000	0.05762811	0.0002619460	1.1844088344	0.0002831
42	0.702094483	33.45636984	2726.824265	0.05762811	0.00000000	0.05851588	0.0002659813	1.2126851203	0.0002822
43	0.702094483	33.88288366	2805.6732	0.05851588	0.00000000	0.05926186	0.0002693721	1.2408587402	0.0002811
44	0.702094483	34.21908284	2885.527329	0.05926186	0.00000000	0.05984988	0.0002720449	1.2688993935	0.0002796
45	0.702094483	34.45663626	2966.173802	0.05984988	0.00000000	0.06026537	0.0002739335	1.2967763091	0.0002778
46	0.702094483	34.58844995	3047.380133	0.06026537	0.00000000	0.06049591	0.0002749814	1.3244587471	0.0002757
47	0.702094483	34.60896281	3128.897119	0.06049591	0.00000000	0.06053179	0.0002751445	1.3519165302	0.0002733
48	0.702094483	34.51439767	3210.462449	0.06053179	0.00000000	0.06036639	0.0002743927	1.3791205862	0.0002706
49	0.702094483	34.30295032	3291.804911	0.06036639	0.00000000	0.05999657	0.0002727117	1.4060434789	0.0002677

Input data / Hydrograph / **Initial Computation** / Computation sheet / Water surface level changes / Graphs

Main computation spread sheet

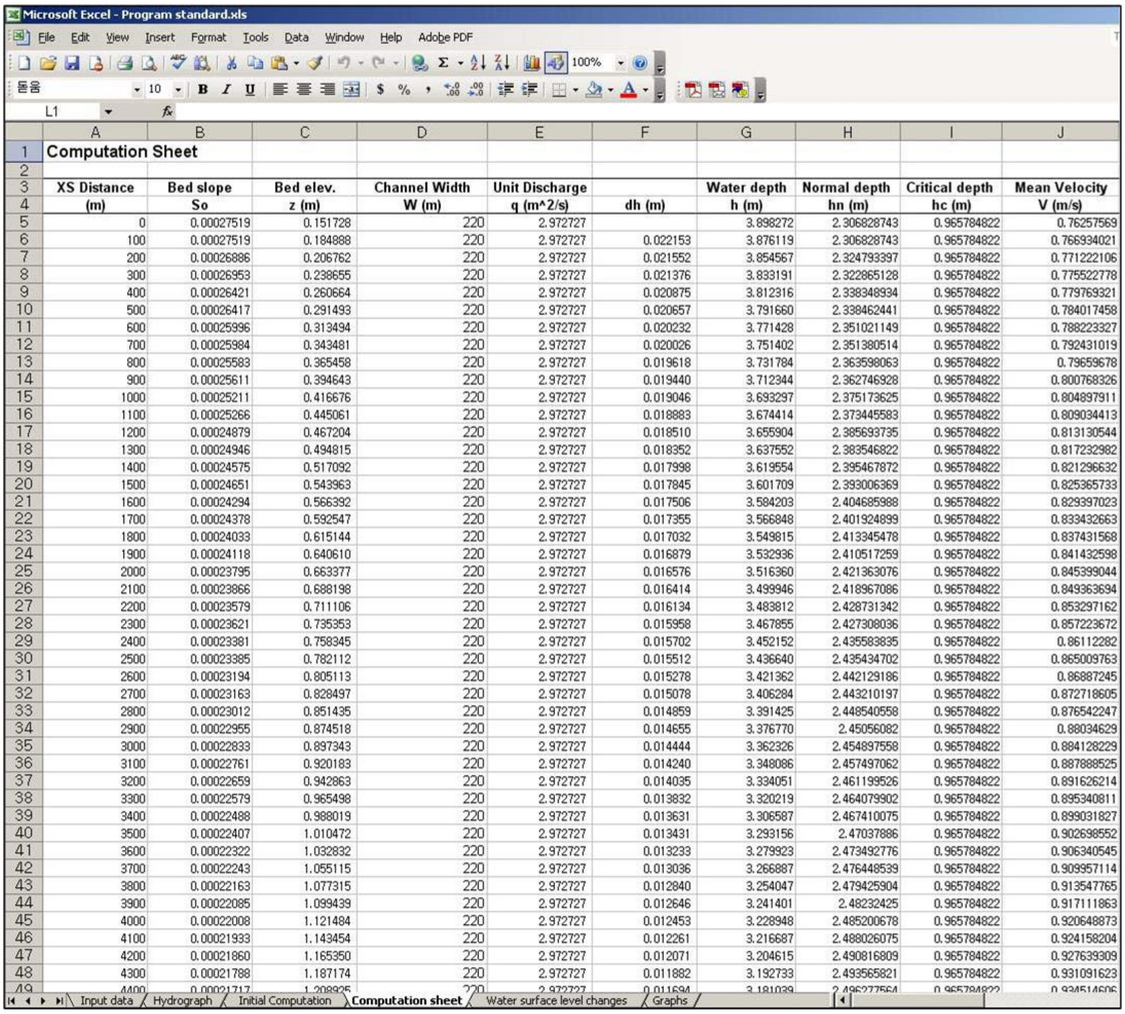

Computation Sheet

	XS Distance (m)	Bed slope So	Bed elev. z (m)	Channel Width W (m)	Unit Discharge q (m^2/s)	dh (m)	Water depth h (m)	Normal depth hn (m)	Critical depth hc (m)	Mean Velocity V (m/s)
5	0	0.00027519	0.151728	220	2.972727		3.898272	2.306828743	0.965784822	0.76257569
6	100	0.00027519	0.184888	220	2.972727	0.022153	3.876119	2.306828743	0.965784822	0.766934021
7	200	0.00026886	0.206762	220	2.972727	0.021552	3.854567	2.324793397	0.965784822	0.771222106
8	300	0.00026953	0.238655	220	2.972727	0.021376	3.833191	2.322865128	0.965784822	0.775522778
9	400	0.00026421	0.260664	220	2.972727	0.020875	3.812316	2.338348934	0.965784822	0.779769321
10	500	0.00026417	0.291493	220	2.972727	0.020657	3.791660	2.338462441	0.965784822	0.784017458
11	600	0.00025996	0.313494	220	2.972727	0.020232	3.771428	2.351021149	0.965784822	0.788223327
12	700	0.00025984	0.343481	220	2.972727	0.020026	3.751402	2.351380514	0.965784822	0.792431019
13	800	0.00025583	0.365458	220	2.972727	0.019618	3.731784	2.363598063	0.965784822	0.79659678
14	900	0.00025611	0.394643	220	2.972727	0.019440	3.712344	2.362746928	0.965784822	0.800768326
15	1000	0.00025211	0.416676	220	2.972727	0.019046	3.693297	2.375173625	0.965784822	0.804897911
16	1100	0.00025266	0.445061	220	2.972727	0.018883	3.674414	2.373445583	0.965784822	0.809034413
17	1200	0.00024879	0.467204	220	2.972727	0.018510	3.655904	2.385693735	0.965784822	0.813130544
18	1300	0.00024946	0.494815	220	2.972727	0.018352	3.637552	2.383546822	0.965784822	0.817232982
19	1400	0.00024575	0.517092	220	2.972727	0.017998	3.619554	2.395467872	0.965784822	0.821296632
20	1500	0.00024651	0.543963	220	2.972727	0.017845	3.601709	2.393006369	0.965784822	0.825365733
21	1600	0.00024294	0.566392	220	2.972727	0.017506	3.584203	2.404685988	0.965784822	0.829397023
22	1700	0.00024378	0.592547	220	2.972727	0.017355	3.566848	2.401924899	0.965784822	0.833432663
23	1800	0.00024033	0.615144	220	2.972727	0.017032	3.549815	2.413345478	0.965784822	0.837431568
24	1900	0.00024118	0.640610	220	2.972727	0.016879	3.532936	2.410517259	0.965784822	0.841432598
25	2000	0.00023795	0.663377	220	2.972727	0.016576	3.516360	2.421363076	0.965784822	0.845399044
26	2100	0.00023866	0.688198	220	2.972727	0.016414	3.499946	2.418967086	0.965784822	0.849363694
27	2200	0.00023579	0.711106	220	2.972727	0.016134	3.483812	2.428731342	0.965784822	0.853297162
28	2300	0.00023621	0.735353	220	2.972727	0.015958	3.467855	2.427308036	0.965784822	0.857223672
29	2400	0.00023381	0.758345	220	2.972727	0.015702	3.452152	2.435583835	0.965784822	0.86112282
30	2500	0.00023385	0.782112	220	2.972727	0.015512	3.436640	2.435434702	0.965784822	0.865009763
31	2600	0.00023194	0.805113	220	2.972727	0.015278	3.421362	2.442129186	0.965784822	0.86887245
32	2700	0.00023163	0.828497	220	2.972727	0.015078	3.406284	2.443210197	0.965784822	0.872718605
33	2800	0.00023012	0.851435	220	2.972727	0.014859	3.391425	2.448540558	0.965784822	0.876542247
34	2900	0.00022955	0.874518	220	2.972727	0.014655	3.376770	2.45056082	0.965784822	0.88034629
35	3000	0.00022833	0.897343	220	2.972727	0.014444	3.362326	2.454897558	0.965784822	0.884128229
36	3100	0.00022761	0.920183	220	2.972727	0.014240	3.348086	2.457497062	0.965784822	0.887888525
37	3200	0.00022659	0.942863	220	2.972727	0.014035	3.334051	2.461199526	0.965784822	0.891626214
38	3300	0.00022579	0.965498	220	2.972727	0.013832	3.320219	2.464079902	0.965784822	0.895340811
39	3400	0.00022488	0.988019	220	2.972727	0.013631	3.306587	2.467410075	0.965784822	0.899031827
40	3500	0.00022407	1.010472	220	2.972727	0.013431	3.293156	2.47037886	0.965784822	0.902698552
41	3600	0.00022322	1.032832	220	2.972727	0.013233	3.279923	2.473492776	0.965784822	0.906340545
42	3700	0.00022243	1.055115	220	2.972727	0.013036	3.266887	2.476448539	0.965784822	0.909957114
43	3800	0.00022163	1.077315	220	2.972727	0.012840	3.254047	2.479425904	0.965784822	0.913547765
44	3900	0.00022085	1.099439	220	2.972727	0.012646	3.241401	2.48232425	0.965784822	0.917111863
45	4000	0.00022008	1.121484	220	2.972727	0.012453	3.228948	2.485200678	0.965784822	0.920648873
46	4100	0.00021933	1.143454	220	2.972727	0.012261	3.216687	2.488026075	0.965784822	0.924158204
47	4200	0.00021860	1.165350	220	2.972727	0.012071	3.204615	2.490816809	0.965784822	0.927639309
48	4300	0.00021788	1.187174	220	2.972727	0.011882	3.192733	2.493565821	0.965784822	0.931091623
49	4400	0.00021717	1.208925	220	2.972727	0.011694	3.181039	2.496277564	0.965784822	0.934514606

Water surface level and sediment concentration changes spread sheet

Microsoft Excel - Program standard.xls

	A	B	C	D	E	F	G	H	I	J
1	**Water surface level changes**									
2										
3	**Time**	**NREB**	**5km**	**10km**	**12.5km**	**20km**	**30km**	**Samryangjin**		**Cppm NREB**
4	2003-04-27-00	3.88	3.894848346	3.962635781	4.054827613	5.015203036	6.85031275	8.747364271		0
5	2003-04-27-01	3.93	3.944094008	4.006957853	4.090771223	5.016176524	6.850314628	8.747363963		0
6	2003-04-27-02	4.02	4.032861486	4.088018604	4.158792614	5.018501289	6.850316148	8.747363856		0
7	2003-04-27-03	4.14	4.151434383	4.19820996	4.25505402	5.023285734	6.850318561	8.74736375		0
8	2003-04-27-04	4.29	4.299935799	4.338561022	4.382315164	5.033558785	6.850323099	8.747363643		0
9	2003-04-27-05	4.42	4.428844409	4.461967316	4.497258556	5.048571979	6.850329858	8.747363536		0
10	2003-04-27-06	4.49	4.498323302	4.528950814	4.560529452	5.059972519	6.850335576	8.747363427		0
11	2003-04-27-07	4.47	4.47846785	4.509778929	4.542366276	5.056452504	6.850334828	8.747363316		0
12	2003-04-27-08	4.39	4.399081287	4.433366848	4.470417035	5.044498814	6.850330555	8.747363204		0
13	2003-04-27-09	4.24	4.250404125	4.291503358	4.339171419	5.029521242	6.850325453	8.74736309		0
14	2003-04-27-10	4.04	4.052607531	4.106230409	4.174431725	5.019245766	6.850322448	8.747362976		0
15	2003-04-27-11	3.87	3.927992898	4.143788291	4.360426815	5.466599247	7.287257769	9.182013105		0
16	2003-04-27-12	3.75	3.890827875	4.31675254	4.637175119	5.837802624	7.651600907	9.543499035		0.713568595
17	2003-04-27-13	3.73	3.991358867	4.605593011	4.98267716	6.227245355	8.034878944	9.923005552		7.852746422
18	2003-04-27-14	3.82	4.18495571	4.903166932	5.304846137	6.569528755	8.372561458	10.2569162		22.70920927
19	2003-04-27-15	3.97	4.564092072	5.454575566	5.89745428	7.208119906	9.011717125	10.88947422		91.13751184
20	2003-04-27-16	4.16	4.772430691	5.664179672	6.107687334	7.419767242	9.221494893	11.09685016		107.6855029
21	2003-04-27-17	4.33	5.121396943	6.11683556	6.58764369	7.939363918	9.750595602	11.62286825		219.1370505
22	2003-04-27-18	4.44	5.326759568	6.370972154	6.85526771	8.228685308	10.04731983	11.91894078		301.531945
23	2003-04-27-19	4.47	5.466191324	6.564193663	7.062882692	8.459422388	10.28726565	12.15954117		407.2557839
24	2003-04-27-20	4.41	5.561805013	6.728387504	7.244498641	8.668653152	10.50841859	12.38259915		581.8603688
25	2003-04-27-21	4.25	5.563180046	6.788869751	7.318635856	8.763461689	10.61233368	12.48853245		795.9144721
26	2003-04-27-22	4.07	5.426394208	6.664774858	7.194950235	8.636701118	10.48265486	12.35860776		1026.878676
27	2003-04-27-23	3.87	5.455494365	6.754020431	7.297546306	8.759827545	10.61497203	12.49285091		1542.483398
28	2003-04-28-00	3.75	5.481766766	6.812429205	7.363394721	8.837587779	10.69836463	12.57751542		1974.401319
29	2003-04-28-01	3.74	5.554870699	6.906687355	7.463740158	8.948968017	10.81551037	12.69595689		2267.253103
30	2003-04-28-02	3.82	5.655794418	7.019783601	7.581656246	9.076777116	10.94899294	12.83078471		2347.908982
31	2003-04-28-03	3.96	5.836357066	7.220430838	7.790299603	9.302067353	11.18420952	13.0686127		2516.273976
32	2003-04-28-04	4.14	5.386320887	6.596362492	7.121718497	8.558080942	10.40275293	12.27887167		811.0725358
33	2003-04-28-05	4.29	5.510952387	6.708822965	7.233058248	8.6700336	10.51562504	12.39144716		786.2288651
34	2003-04-28-06	4.4	5.608749483	6.802596305	7.327283408	8.766919179	10.61431683	12.4902093		785.2174315
35	2003-04-28-07	4.45	5.699933731	6.909778095	7.439420432	8.888361954	10.7405339	12.61725835		865.4817707
36	2003-04-28-08	4.4	5.7303235	6.968476691	7.50513238	8.965480034	10.82314224	12.70114712		1007.9763
37	2003-04-28-09	4.28	5.741704959	7.020734453	7.566911114	9.042152829	10.90688345	12.78669042		1268.618499
38	2003-04-28-10	4.07	5.717177611	7.042838208	7.599036128	9.089215077	10.96084772	12.84255228		1715.029651
39	2003-04-28-11	3.85	5.664804808	7.022733647	7.585174418	9.083958783	10.9593095	12.84212029		2223.251617
40	2003-04-28-12	3.68	5.618982364	6.996936544	7.563048003	9.066662412	10.94400465	12.82743971		2680.978929
41	2003-04-28-13	3.59	5.56993534	6.953966458	7.520774905	9.024664603	10.90182465	12.7852988		2825.151374
42	2003-04-28-14	3.63	5.523435603	6.894554306	7.458244296	8.956780319	10.83118363	12.71402345		2428.078648
43	2003-04-28-15	3.77	5.502021132	6.844244316	7.401973488	8.891534462	10.76181159	12.64366285		1853.731533
44	2003-04-28-16	3.99	5.509752557	6.804142652	7.352269147	8.828129785	10.6924904	12.57290474		1300.820355
45	2003-04-28-17	4.22	5.53799892	6.773005851	7.308809105	8.767302436	10.62437687	12.5030352		917.3261574
46	2003-04-28-18	4.4	5.571729805	6.752927351	7.277008657	8.718960167	10.56921148	12.44624811		702.0091603
47	2003-04-28-19	4.51	5.594916761	6.738819234	7.254395787	8.684248712	10.52955666	12.40544584		593.5788196
48	2003-04-28-20	4.49	5.571100721	6.712725877	7.227515426	8.655954558	10.50065303	12.37650762		585.752781
49	2003-04-28-21	4.36	5.510247603	6.680349594	7.201177924	8.637708451	10.48562984	12.36239202		663.9909077

Input data / Hydrograph / Initial Computation / Computation sheet / **Water surface level changes** / Graphs

Graphs

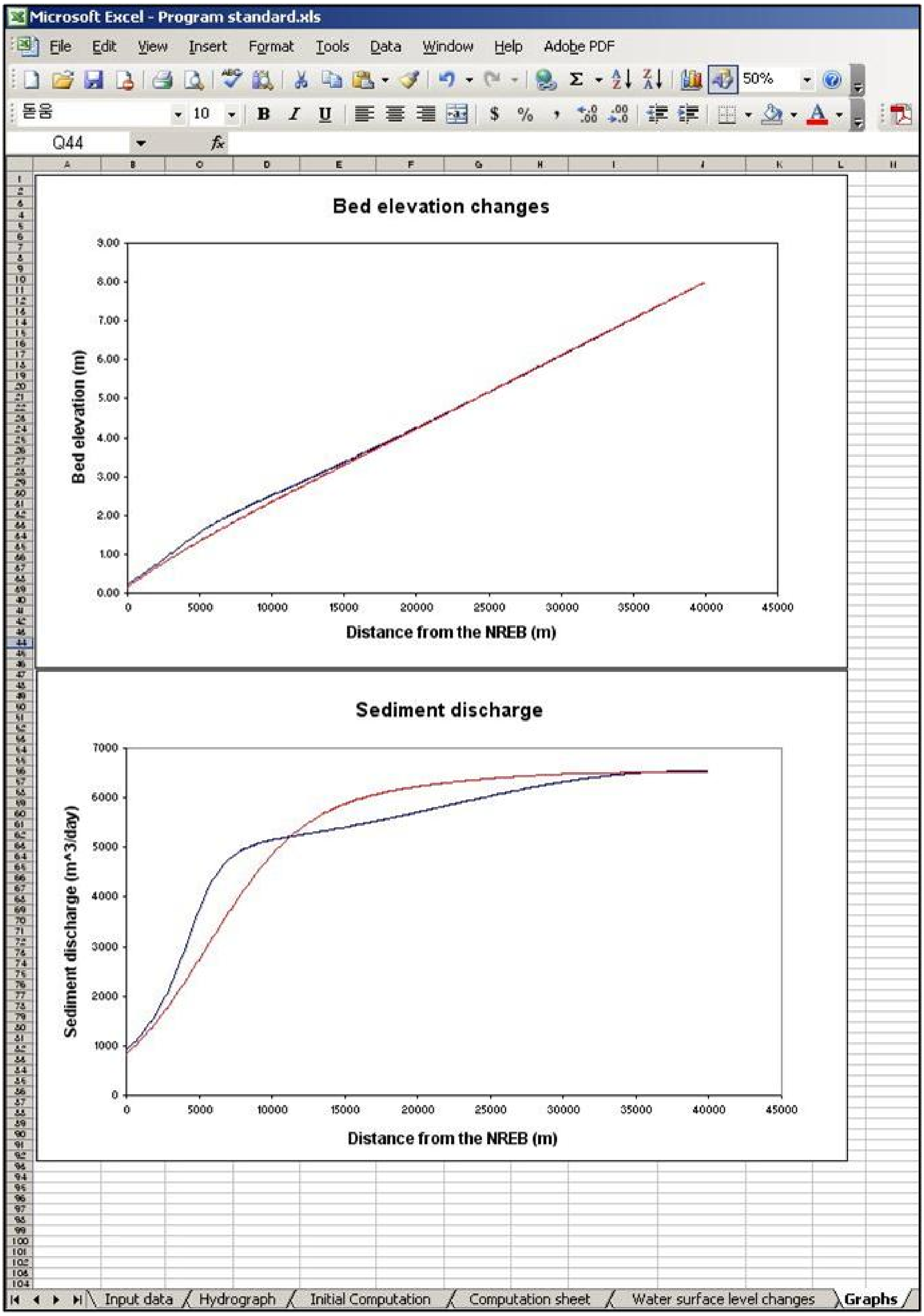

Microsoft Excel - Program standard.xls
File Edit View Insert Format Tools Data Window Help Adobe PDF
Q44
Bed elevation changes
Bed elevation (m)
Distance from the NREB (m)
Sediment discharge
Sediment discharge (m^3/day)
Distance from the NREB (m)
Input data
Hydrograph
Initial Computation
Computation sheet
Water surface level changes
Graphs

Program code I: Excel with Visual Basic Application

```
Private Sub Computation_Click()

Application.ScreenUpdating = False
    Call Macro1
Application.ScreenUpdating = True

End Sub


Sub Macro1()
'
' Macro1 Macro
' Macro recorded 1/25/2005 by Un Ji
'
' CE717 River Mechanics : Computer Modeling
' Keyboard Shortcut: Ctrl+q
'


Dim Sheet1 As String    ' The sheet for Input data
Dim Sheet2 As String    ' The sheet for Output data

Dim f As Double        ' friction factor
Dim g As Double        ' gravity (m/s^2)
Dim q As Double        ' unit discharge (m^2/s)
Dim z As Double        ' bed elevation (m)
Dim z1 As Double       ' bed elevation of upstream
Dim z2 As Double       ' bed elevation of downstream
Dim H As Double        ' water surface elevation at the dam (m)
Dim L1 As Double       ' reach length of the first section (m)
Dim L2 As Double       ' reach length of the second section (m)
Dim L3 As Double       ' reach length of the third section (m)
Dim L As Double        ' reach length from the downstream (m)
Dim So1 As Double      ' bed slope of the first section
Dim So2 As Double      ' bed slope of the second section
Dim So3 As Double      ' bed slope of the third section
Dim dx As Double       ' interval length of the computation (m)
Dim dL As Double       ' reach length from the downstream end (m)
Dim c As Double        ' Chezy coefficient
Dim hc As Double       ' critical depth (m)
Dim hn As Double       ' normal depth (m)
Dim V As Double        ' mean velocity of the section (m/s)
Dim Sf As Double       ' friction slope
Dim T As Double        ' shear stress
Dim tH As Double       ' total head (energy) (m)
Dim dh As Double       ' differences of water depth (m)

Dim Cppm As Double     ' Sediment Concentration
Dim Cb As Double       ' Coefficient of Brownlie's equation lab=1 field=1.268
```

```
Dim sg As Double       ' specific gravity 2.65
Dim Gg As Double       ' Gradation Coefficient uniform=1 well graded=3
Dim ds As Double       ' median grain size (mm)
Dim TstarC As Double   ' Shield dimensionless critical shear stress
Dim TC As Double       ' critical shear stress (Pa = N/m^2 = kg/m*s^2)
Dim Vc As Double       ' critical velocity of Brownlie's equation
Dim rs As Double       ' specific weight of solid particles 26000 N/m^3
Dim r As Double        ' specific weight of water 9810 n/m^3
Dim W As Double
Dim Cmgl As Double     ' Sediment Concentration
Dim qs As Double       ' unit sediment load (metric tons/day/m)
Dim qsv As Double      ' unit sediment discharge (m^3/day/m)


Dim dz As Double       ' bed elevation change (m)
Dim TE As Double       ' Trap efficiency
Dim WV As Double       ' settling velocity (m/s)
Dim Po As Double       ' porosity
Dim rmdl As Double     ' dry specific weight for sand 14609.37 N/m^3 = 93 lb/ft^3
Dim dstar As Double    ' dimensionless particle diameter
Dim vm As Double       ' kinematic viscosity (m^2/s)

Dim dt As Double       ' time step
Dim I As Double
Dim IT As Double       ' Number of Iterations
Dim qs1 As Double      ' qs(i)
Dim qs2 As Double      ' qs(i+1)
Dim a As Double        ' weighting factor
Dim dz1 As Double      ' dz(i)
Dim dz2 As Double      ' dz(i+1)
Dim dzt As Double      ' total bed elevation changes (m)
Dim E1 As Double
Dim E As Double
Dim H1 As Double
Dim V1 As Double
Dim tH1 As Double
Dim Sf1 As Double



''''''''''''''''''''''''''''''''''''''''''''''''''''''''''''''''''''''''''''''''''''''''''''''''''''''''''''''''''''''''''''''''''''''''''''''''
'Input data

Sheets("Input data").Select

f = Cells(3, 3)
g = Cells(4, 3)
q = Cells(5, 3)
H = Cells(6, 3)
L1 = Cells(7, 3)
So1 = Cells(8, 3)
```

```
L2 = Cells(9, 3)
So2 = Cells(10, 3)
L3 = Cells(11, 3)
So3 = Cells(12, 3)
dx = Cells(13, 3)

ds = Cells(18, 3)     'Brownlie's equation and aggradation and degradation input data
Cb = Cells(19, 3)
Gg = Cells(20, 3)
TC = Cells(21, 3)
rs = Cells(22, 3)
r = Cells(23, 3)
rmdl = Cells(24, 3)
sg = Cells(25, 3)
vm = Cells(26, 3)


TstarC = TC / ((rs - r) * (ds / 1000))
Po = 1 - (rmdl / rs)
dstar = (ds / 1000) * ((sg - 1) * g / vm ^ 2) ^ (1 / 3)
WV = 8 * vm / (ds / 1000) * ((1 + 0.0139 * dstar ^ 3) ^ 0.5 - 1)
TE = 1 - Exp(-1 * WV * dx / q)


''''''''''''''''''''''''''''''''''''''''''''''''''''''''''''''''''''''''''''''''''''''''
'Initial Computation
Row1 = 5
Row = Row1

z = 0
dL = 0
L = L1

here:

Do Until dL > L3    'Start the computation

If dL <= L Then

c = (8 * g / f) ^ 0.5
hc = (q ^ 2 / g) ^ (1 / 3)
hn = (q ^ 2 / (c ^ 2 * So1)) ^ (1 / 3)
V = q / H
Sf = f / 8 * (V ^ 2 / (g * H))
T = 9800 * H * Sf
tH = H + V ^ 2 / (2 * g)

W = ((sg - 1) * g * ds / 1000) ^ 0.5     'bed material computation
Vc = 4.596 * TstarC ^ 0.529 * Sf ^ (-0.1405) * Gg ^ (-0.1606) * W

If Vc >= V Then
```

```
Cppm = 0
Cmgl = 0
qs = 0
qsv = 0
ElseIf Vc < V Then
Cppm = 7115 * Cb * ((V - Vc) / W) ^ 1.978 * Sf ^ 0.6601 * (H / (ds / 1000)) ^ (-0.3301)
Cmgl = 1 * sg * Cppm / (sg + (1 - sg) * 10 ^ (-6) * Cppm)
qs = 0.0864 * Cmgl * q
qsv = qs * 1000 / 2650
End If

Sheets("Computation sheet").Select
Cells(Row, 1) = dL
Cells(Row, 2) = z
Cells(Row, 3) = So1
Cells(Row, 4) = H
Cells(Row, 5) = hn
Cells(Row, 6) = hc
Cells(Row, 7) = V
Cells(Row, 8) = Sf
Cells(Row, 9) = T
Cells(Row, 10) = tH
Cells(Row, 11) = Cppm
Cells(Row, 12) = qs
Cells(Row, 13) = qsv

z = z + dx * So1
dL = dL + dx

dh = So1 * (1 - (hn / H) ^ 3) / (1 - (hc / H) ^ 3) * dx
H = H - dh
Row = Row + 1

ElseIf dL = L1 + dx Then
z = So1 * L1 + dx * So2
L = L2
So1 = So2
GoTo here
ElseIf dL = L2 + dx Then
z = So1 * L1 + So2 * L2 + dx * So3
L = L3
So1 = So3
GoTo here
ElseIf dL = L3 + dx Then

End If

Loop    'End the computation

there:
```

```
NRow = Row - 1

''''''''''''''''''''''''''''''''''''''''''''''''''''''''''''''''''''''''''''''''''''
'Bed aggradation and degradation computation
I = 1
IT = 100
dt = 0.01
a = 0

Do Until I > IT

''''''''''''''''''''''''''''''''''''''''''''''''''
Row = Row1 + 1

Do Until Row > NRow   'Calculation of bed elevation changes

Sheets("Computation sheet").Select
qs1 = Cells(Row, 13)
qs2 = Cells(Row - 1, 13)

dz = -1 * TE / (1 - Po) * (qs2 - qs1) / dx * dt

dz1 = a * dz
dz2 = (1 - a) * dz

Sheets("Computation sheet").Select
Cells(Row, 14) = dz1
Cells(Row - 1, 15) = dz2

Row = Row + 1

Loop  'End the computation

Row = Row1

Do Until Row > NRow     'Start the computation

Sheets("Computation sheet").Select
dz1 = Cells(Row, 14)
dz2 = Cells(Row, 15)

dzt = dz1 + dz2

Sheets("Computation sheet").Select
Cells(Row, 16) = dzt

Row = Row + 1

Loop   'End the computation

''''''''''''''''''''''''''''''''''''''''''''''''''
```

```
Row = Row1

Do Until Row > NRow   'Calculation of new bed elevation

Sheets("Computation sheet").Select
z = Cells(Row, 2)
dzt = Cells(Row, 16)

z = z + dzt

Sheets("Computation sheet").Select
Cells(Row, 2) = z

Row = Row + 1

Loop    'End the computation

''''''''''''''''''''''''''''''''''''''''''''''''''
Row = Row1 + 1

Do Until Row > NRow - 1  'Calculation of new bed slope

If Row = Row1 Then
Sheets("Computation sheet").Select
So1 = Cells(8, 3)
Sheets("Computation sheet").Select
Cells(Row, 3) = So1

ElseIf Row > Row1 Then
Sheets("Computation sheet").Select
z1 = Cells(Row - 1, 2) 'down
z2 = Cells(Row + 1, 2) 'up
So1 = (z2 - z1) / (2 * dx)
Sheets("Computation sheet").Select
Cells(Row, 3) = So1

ElseIf Row = NRow - 1 Then
z1 = Cells(Row - 1, 2) 'down
z2 = Cells(Row, 2) 'up
So1 = (z2 - z1) / (2 * dx)
Sheets("Computation sheet").Select
Cells(Row, 3) = So1
End If

Row = Row + 1

Loop    'End the computation
''''''''''''''''''''''''''''''''''''''''''''''
Row = Row1

Sheets("Input data").Select
```

```
H = Cells(6, 3)
So1 = Cells(8, 3)

dL = 0
L = L3
Sf = f / 8 * ((q / H) ^ 2 / (g * H))

Do Until dL > L3    'Start the computation

Sheets("Computation sheet").Select

z1 = Cells(Row + 1, 2)
z2 = Cells(Row, 2)
So1 = Cells(Row, 3)

c = (8 * g / f) ^ 0.5
hc = (q ^ 2 / g) ^ (1 / 3)
hn = (q ^ 2 / (c ^ 2 * So1)) ^ (1 / 3)
V = q / H
T = 9800 * H * Sf
tH = H + V ^ 2 / (2 * g)
E = z2 + tH

W = ((sg - 1) * g * (ds / 1000)) ^ 0.5     'bed material computation
Vc = 4.596 * TstarC ^ 0.529 * Sf ^ (-0.1405) * Gg ^ (-0.1606) * W

If Vc >= V Then
Cppm = 0
Cmgl = 0
qs = 0
qsv = 0
ElseIf Vc < V Then
Cppm = 7115 * Cb * ((V - Vc) / W) ^ 1.978 * Sf ^ 0.6601 * (H / (ds / 1000)) ^ (-0.3301)
Cmgl = 1 * sg * Cppm / (sg + (1 - sg) * 10 ^ (-6) * Cppm)
qs = 0.0864 * Cmgl * q
qsv = qs * 1000 / 2650
End If

Sheets("Computation sheet").Select
Cells(Row, 1) = dL
'Cells(Row, 2) = z
Cells(Row, 4) = H
Cells(Row, 5) = hn
Cells(Row, 6) = hc
Cells(Row, 7) = V
Cells(Row, 8) = Sf
Cells(Row, 9) = T
Cells(Row, 10) = tH
Cells(Row, 11) = Cppm
Cells(Row, 12) = qs
Cells(Row, 13) = qsv
```

```
dL = dL + dx
dh = So1 * (1 - (hn / H) ^ 3) / (1 - (hc / H) ^ 3) * dx
H1 = H - dh
V1 = q / H1
tH1 = H1 + V1 ^ 2 / (2 * g)
E1 = z1 + tH1
Sf1 = (E1 - E) / dx

H = H1
Sf = Sf1

Row = Row + 1

Loop

I = I + 1

Loop

End Sub
```

Program code II: Excel spread sheet with Visual Basic Application

```
Private Sub Computation_Click()

Application.ScreenUpdating = False
    Call Macro1
Application.ScreenUpdating = True

End Sub


Sub Macro1()
'
' Macro1 Macro
' Macro recorded 1/25/2005 by Un Ji
'
' CE717 River Mechanics : Computer Modeling
' Keyboard Shortcut: Ctrl+q
'

Dim Sheet1 As String    ' The sheet for Input data
Dim Sheet2 As String    ' The sheet for Initial condition data
Dim Sheet3 As String    ' The sheet for Computation data
Dim Sheet4 As String    ' The sheet for Graph
Dim Sheet5 As String    ' The sheet for Hydrograph data for unsteady state simulation
Dim Sheet6 As String    ' The sheet for Water surface level changes by the time


Dim INUM As Double      ' Iteration numbers
Dim I As Double         ' Iteration start


''''''Copy of the initial H and Q''''''''''''''''''''''
I = 1

Sheets("Hydrograph").Select

Cells(I + 4, 7).Select
Selection.Copy

Sheets("Input data").Select

Cells(6, 3).Select
Selection.PasteSpecial Paste:=xlPasteValues, Operation:=xlNone, SkipBlanks _
        :=False, Transpose:=False


Sheets("Hydrograph").Select

Cells(I + 4, 8).Select
```

```
Selection.Copy

Sheets("Input data").Select

Cells(5, 3).Select
Selection.PasteSpecial Paste:=xlPasteValues, Operation:=xlNone, SkipBlanks _
        :=False, Transpose:=False

''''''''''''''''''''''''''''''''''''''''''''''''''''''''''''''''''''''''''


"""Print of the initial calculation of water surface level result""""""

Sheets("Initial Computation").Select """""""""""""""""NREB

Cells(5, 11).Select
Selection.Copy

Sheets("Water surface level changes").Select

Cells(I + 3, 2).Select
Selection.PasteSpecial Paste:=xlPasteValues, Operation:=xlNone, SkipBlanks _
        :=False, Transpose:=False

Sheets("Initial Computation").Select """""""""""""""""5km

Cells(55, 11).Select
Selection.Copy

Sheets("Water surface level changes").Select

Cells(I + 3, 3).Select
Selection.PasteSpecial Paste:=xlPasteValues, Operation:=xlNone, SkipBlanks _
        :=False, Transpose:=False

Sheets("Initial Computation").Select """""""""""""""""10km

Cells(105, 11).Select
Selection.Copy

Sheets("Water surface level changes").Select

Cells(I + 3, 4).Select
Selection.PasteSpecial Paste:=xlPasteValues, Operation:=xlNone, SkipBlanks _
        :=False, Transpose:=False

Sheets("Initial Computation").Select """""""""""""""""12.5km Gupo Bridge

Cells(130, 11).Select
Selection.Copy
```

```
Sheets("Water surface level changes").Select

Cells(I + 3, 5).Select
Selection.PasteSpecial Paste:=xlPasteValues, Operation:=xlNone, SkipBlanks _
        :=False, Transpose:=False

Sheets("Initial Computation").Select """""""""""""""20km

Cells(205, 11).Select
Selection.Copy

Sheets("Water surface level changes").Select

Cells(I + 3, 6).Select
Selection.PasteSpecial Paste:=xlPasteValues, Operation:=xlNone, SkipBlanks _
        :=False, Transpose:=False

Sheets("Initial Computation").Select """""""""""""""30km

Cells(305, 11).Select
Selection.Copy

Sheets("Water surface level changes").Select

Cells(I + 3, 7).Select
Selection.PasteSpecial Paste:=xlPasteValues, Operation:=xlNone, SkipBlanks _
        :=False, Transpose:=False

Sheets("Initial Computation").Select """""""""""""""Samryangjin

Cells(405, 11).Select
Selection.Copy

Sheets("Water surface level changes").Select

Cells(I + 3, 8).Select
Selection.PasteSpecial Paste:=xlPasteValues, Operation:=xlNone, SkipBlanks _
        :=False, Transpose:=False
"""""""""""""""""""""""""""""""""""


"""Print of the initial calculation of Cppm (NREB) result""""""

Sheets("Initial Computation").Select """""""""""""""NREB

Cells(5, 17).Select
Selection.Copy

Sheets("Water surface level changes").Select

Cells(I + 3, 10).Select
```

```
Selection.PasteSpecial Paste:=xlPasteValues, Operation:=xlNone, SkipBlanks _
        :=False, Transpose:=False

""""""""""""""""""""""""""""""""""""""""""""""""""""""""""""""""""""""""""""""""



""""""Copy of the initial computation"""""""""""""
 ''' Copy of Bed elevation '''
    Sheets("Initial Computation").Select
    Range("AB5:AB405").Select
    Selection.Copy
    Sheets("Computation sheet").Select
    Range("C5:C405").Select
    Selection.PasteSpecial Paste:=xlPasteValues, Operation:=xlNone, SkipBlanks _
        :=False, Transpose:=False
 ''' Copy of Bed slope '''
    Sheets("Initial Computation").Select
    Range("AC5:AC405").Select
    Selection.Copy
    Sheets("Computation sheet").Select
    Range("B5:B405").Select
    Selection.PasteSpecial Paste:=xlPasteValues, Operation:=xlNone, SkipBlanks _
        :=False, Transpose:=False
""""""""""""""""""""""""""""""""""""""""""""""""""""""




""""""""""""""""""""""""""""""""""""""""""""""""""""""
I = 2

Sheets("Input data").Select
INUM = Cells(39, 3)

Do Until I > INUM


 ''' Copy of Bed elevation '''
    Sheets("Computation sheet").Select
    Range("AB5:AB405").Select
    Selection.Copy
    Sheets("Computation sheet").Select
    Range("C5:C405").Select
    Selection.PasteSpecial Paste:=xlPasteValues, Operation:=xlNone, SkipBlanks _
        :=False, Transpose:=False
 ''' Copy of Bed slope '''
    Sheets("Computation sheet").Select
    Range("AC5:AC405").Select
    Selection.Copy
    Sheets("Computation sheet").Select
    Range("B5:B405").Select
    Selection.PasteSpecial Paste:=xlPasteValues, Operation:=xlNone, SkipBlanks _
```

```
        :=False, Transpose:=False


''' Copy of H and Q ''''''''''''''''''''''''''''''''''

Sheets("Hydrograph").Select

Cells(I + 4, 7).Select
Selection.Copy

Sheets("Input data").Select

Cells(6, 3).Select
Selection.PasteSpecial Paste:=xlPasteValues, Operation:=xlNone, SkipBlanks _
        :=False, Transpose:=False


Sheets("Hydrograph").Select

Cells(I + 4, 8).Select
Selection.Copy

Sheets("Input data").Select

Cells(5, 3).Select
Selection.PasteSpecial Paste:=xlPasteValues, Operation:=xlNone, SkipBlanks _
        :=False, Transpose:=False


''''''Print of the calculation results of water surface level result''''''''''''''

Sheets("Computation sheet").Select ''''''''''''''''''''''''''''''''''''''NREB

Cells(5, 11).Select
Selection.Copy

Sheets("Water surface level changes").Select

Cells(I + 3, 2).Select
Selection.PasteSpecial Paste:=xlPasteValues, Operation:=xlNone, SkipBlanks _
        :=False, Transpose:=False

Sheets("Computation sheet").Select ''''''''''''''''''''''''''''''''''''''5km

Cells(55, 11).Select
Selection.Copy

Sheets("Water surface level changes").Select

Cells(I + 3, 3).Select
Selection.PasteSpecial Paste:=xlPasteValues, Operation:=xlNone, SkipBlanks _
```

```
        :=False, Transpose:=False

Sheets("Computation sheet").Select """""""""""""""10km

Cells(105, 11).Select
Selection.Copy

Sheets("Water surface level changes").Select

Cells(I + 3, 4).Select
Selection.PasteSpecial Paste:=xlPasteValues, Operation:=xlNone, SkipBlanks _
        :=False, Transpose:=False

Sheets("Computation sheet").Select """""""""""""""12.5km Gupo Bridge

Cells(130, 11).Select
Selection.Copy

Sheets("Water surface level changes").Select

Cells(I + 3, 5).Select
Selection.PasteSpecial Paste:=xlPasteValues, Operation:=xlNone, SkipBlanks _
        :=False, Transpose:=False

Sheets("Computation sheet").Select """""""""""""""20km

Cells(205, 11).Select
Selection.Copy

Sheets("Water surface level changes").Select

Cells(I + 3, 6).Select
Selection.PasteSpecial Paste:=xlPasteValues, Operation:=xlNone, SkipBlanks _
        :=False, Transpose:=False

Sheets("Computation sheet").Select """""""""""""""30km

Cells(305, 11).Select
Selection.Copy

Sheets("Water surface level changes").Select

Cells(I + 3, 7).Select
Selection.PasteSpecial Paste:=xlPasteValues, Operation:=xlNone, SkipBlanks _
        :=False, Transpose:=False

Sheets("Computation sheet").Select """""""""""""""Samryangjin

Cells(405, 11).Select
Selection.Copy
```

```
Sheets("Water surface level changes").Select

Cells(I + 3, 8).Select
Selection.PasteSpecial Paste:=xlPasteValues, Operation:=xlNone, SkipBlanks _
        :=False, Transpose:=False
''''''''''''''''''''''''''''''''''''''''''''''''''''''''''''''''''''''''''''''''''''''


'''''Print of the calculation of Cppm (NREB) result''''''''''''

Sheets("Computation sheet").Select ''''''''''''''''''''''''''''''''''''''''NREB

Cells(5, 17).Select
Selection.Copy

Sheets("Water surface level changes").Select

Cells(I + 3, 10).Select
Selection.PasteSpecial Paste:=xlPasteValues, Operation:=xlNone, SkipBlanks _
        :=False, Transpose:=False

'''''''''''''''''''''''''''''''''''''''''''''''''''''''''''''''''''''''''''''''

I = I + 1
Loop


Sheets("Hydrograph").Select ''''''''''''''''''''''''''''''''''''''''Date copy

    Range("A5:A10000").Select
    Selection.Copy
    Sheets("Water surface level changes").Select
    Range("A4:A9999").Select
    Selection.PasteSpecial Paste:=xlPasteValues, Operation:=xlNone, SkipBlanks _
        :=False, Transpose:=False
''''''''''''''''''''''''''''''''''''''''''''''''''''''''''''''''''''''''''''''''''''''


End Sub
```

APPENDIX E: DISCHARGE HYDROGRAPH AT SAMRYANGJIN STATION FROM 1998 TO 2003

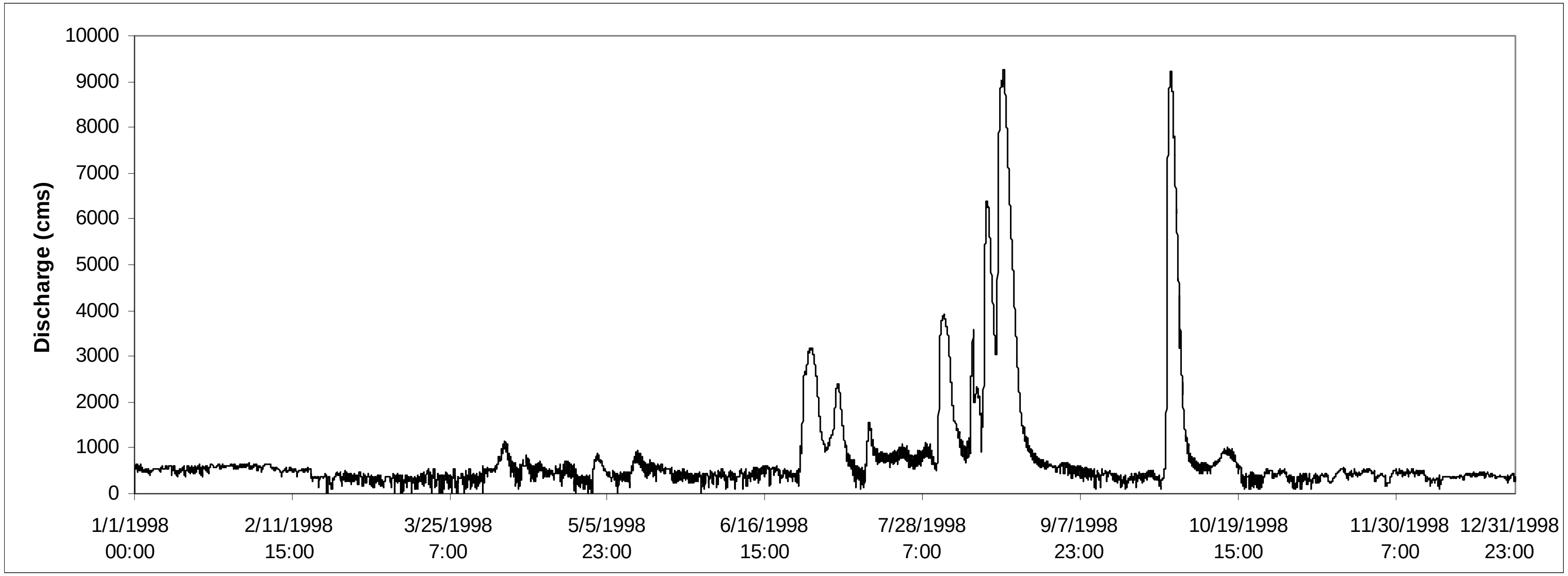

Figure E-1. Discharge hydrograph at Samryangjin Station in 1998

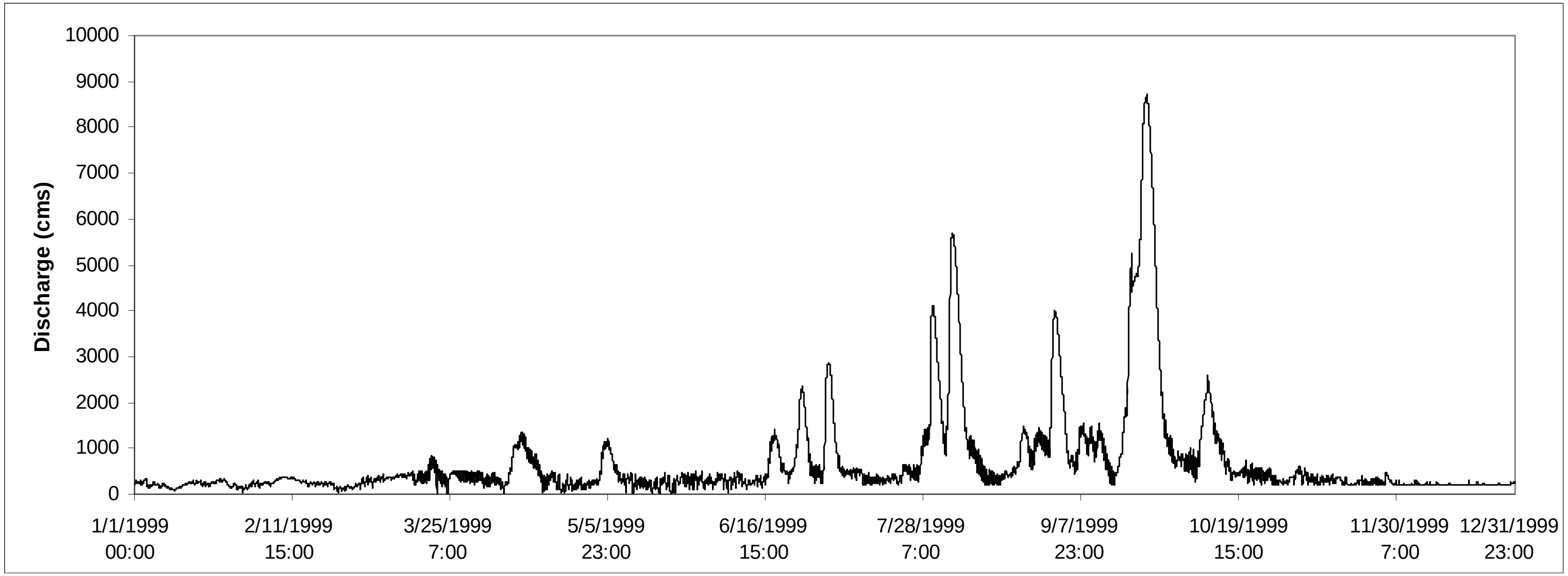

Figure E-2. Discharge hydrograph at Samryangjin Station in 1999

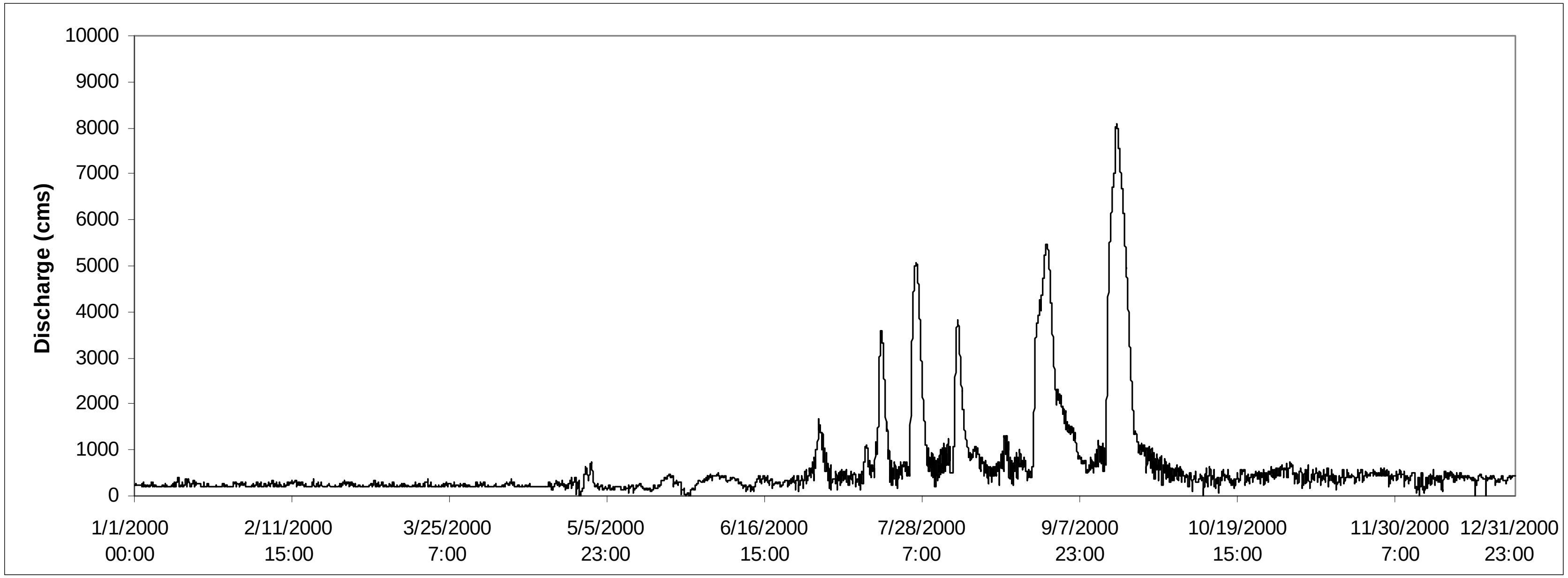

Figure E-3. Discharge hydrograph at Samryangjin Station in 2000

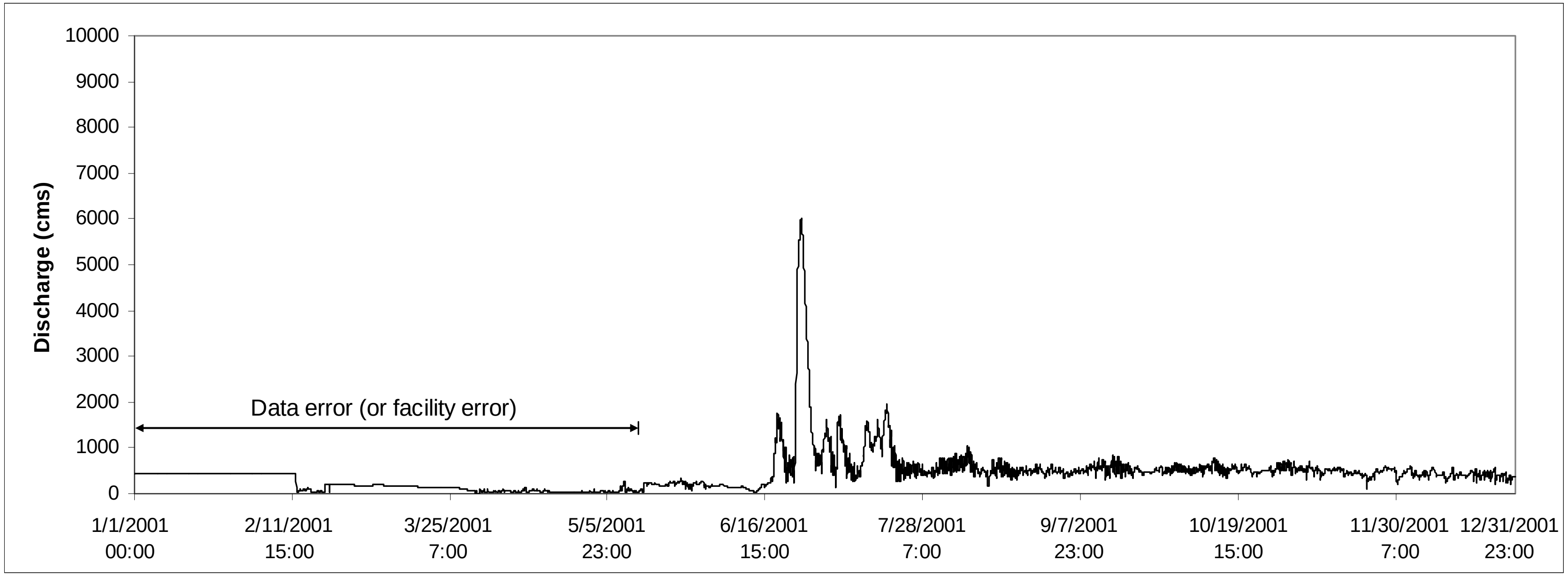

Figure E-4. Discharge hydrograph at Samryangjin Station in 2001

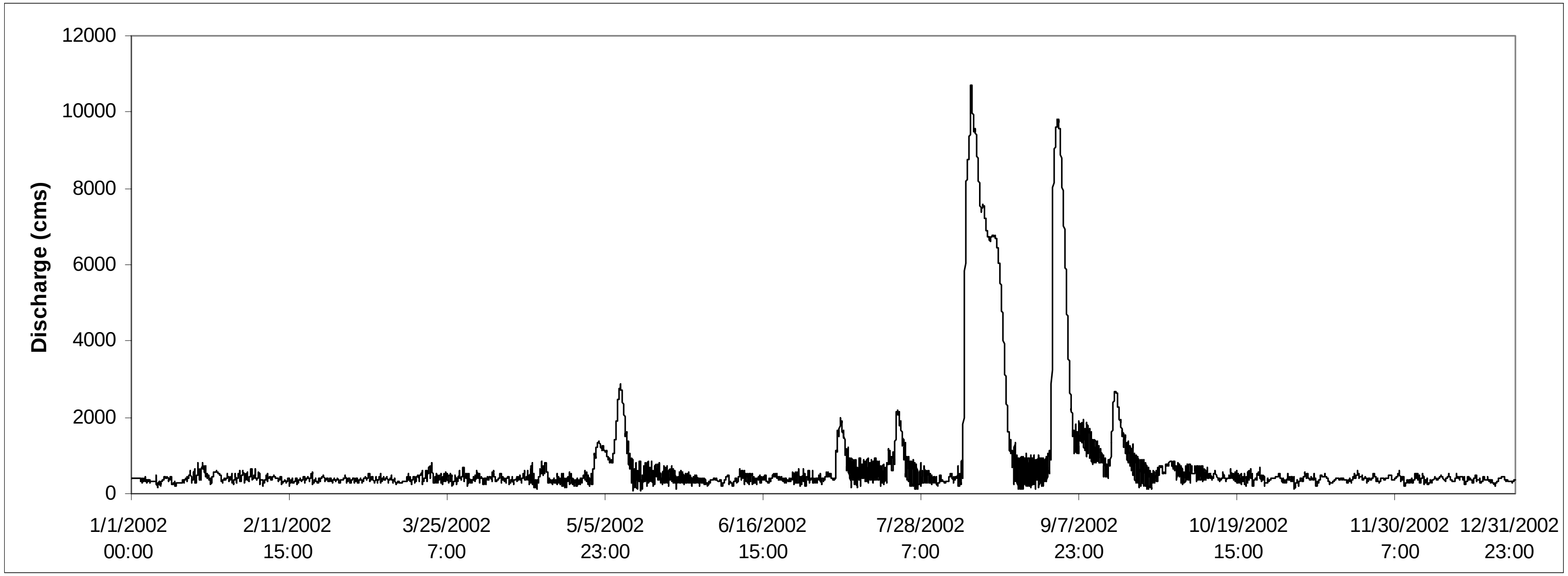

Figure E-5. Discharge hydrograph at Samryangjin Station in 2002

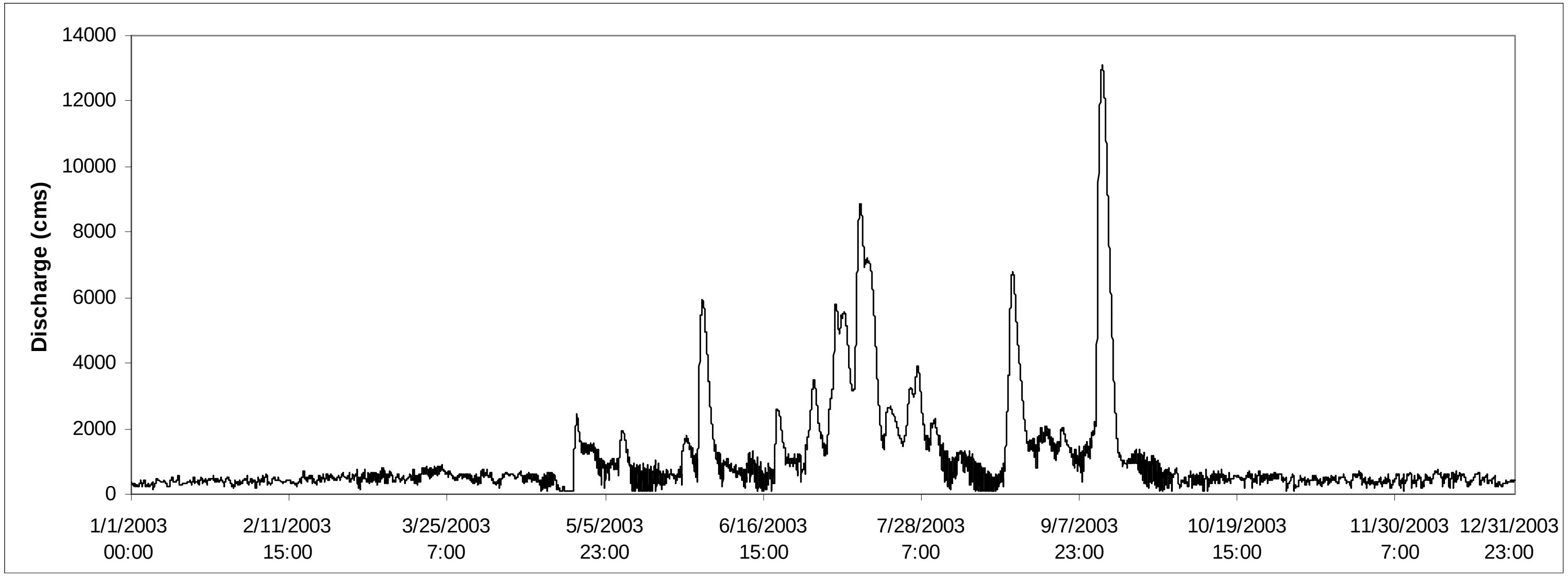

Figure E-6. Discharge hydrograph at Samryangjin Station in 2003